Defining the link between epidermal patterning and auxin responsiveness in the *Arabidopsis thaliana* root

Ashlea Luddington

Submitted in accordance with the requirements for the degree of Doctor of Philosophy.

The University of Leeds

School of Biology

September 2014

The candidate confirms that the work submitted is her own and that appropriate credit has been given where reference has been made to the work of others.

Acknowledgements

I would like to thank all members of the Kepinski lab, for their support and advice over the past four years. I would like to thank Dr Stefan Kepinski for his supervision and Dr Martin Kieffer who has worked closely with me on this project. I would particularly like to thank Amy Burrow and Sigurd Ramans Harborough for being my lab bench buddies and putting up with my endless chatter about PCR issues and Barry the chinchilla.

I would also like to thank Professor Claire Grierson and Professor Richard Napier for supervising me during two lab rotations. I thoroughly enjoyed the opportunity to explore two different and interesting areas of science.

Personally special thanks goes to Jane Tillson and Amy Burrow for helping to proof reading this thesis. Bella, Bobby, Maizy, Alfie and Tilly who regularly suffered as my lab talk practice audience and the never ending support of my parents. The last and most important thanks go to Ash Homer, for his love, patience and guidance throughout both this PhD and life in general.

Abstract

The aim of this project was to define the link between developmental patterning and auxin response in the *Arabidopsis thaliana* root epidermis. The root epidermis was used as a model to understand the interaction of patterning mechanisms, such as those that define the hair and non-hair producing epidermal cells, and auxin. According to data published before this project began the epidermal patterning mechanism and the auxin response network are two independent aspects of plant growth. However the results detailed within this thesis have highlighted that this view is too simplistic, and they actually interact at multiple levels

Having established the presence of a repressive auxin response regime in the non-hair cells of the root epidermis, analysis of the *gl2-1* mutant allowed us to further understand the functional significance of this. Results were consistent with *ARF10* and/or *ARF16* functioning to restrict root hair growth. In order to place the spatial control of auxin response in the current knowledge of the epidermal patterning mechanism, analysis of mutant and marker line crosses was carried out. These indicated that members of both pathways were involved in promoting and inhibiting the expression of components of the other pathway, thereby indicating the presence of multiple interactions, with both positive and negative feedback loops existing between the two. Specifically the non-hair promoting components *WER* and *MYB23* were observed to promote the expression of the repressive ARF, *ARF10.* In turn *ARF10* was observed to promote the expression of *WER* and *GL2,* but inhibit the expression of *MYB23.* Finally analysis of constructs that blocked the down-regulation of *MYB23* by auxin highlighted the possibility that auxin mediated root hair elongation may function via the down-regulation of the epidermal patterning component *MYB23,* thus indicating a potentially novel role for an epidermal patterning component that has previously been considered to be somewhat insignificant.

Contents Page

1 : GENERAL INTRODUCTION 15

1.1 AUXIN 17
1.2 AUXIN TRANSPORT 18
1.3 AUXIN SIGNALLING 20
1.3.1 AUXIN RECEPTORS 20
1.3.2 AUX/IAAS 22
1.3.3 AUXIN RESPONSE FACTORS 24
1.4 ROOT DEVELOPMENT 27
1.4.1 ARABIDOPSIS ROOT MORPHOLOGY 27
1.4.2 ROOT HAIRS 31
1.5 ROOT EPIDERMAL PATTERNING 34
1.5.1 POSITIONAL SIGNALLING 34
1.5.2 LATERAL INHIBITION 36
1.5.3 KEY ROOT EPIDERMAL PATTERNING COMPONENTS 38
1.6 AUXIN RESPONSE IN THE ROOT EPIDERMIS 41
1.7 PROJECT AIMS 47

2 : MATERIALS AND METHODS 48

2.1 PLANT LINES AND SOURCES 49
2.2 PLANT GROWTH CONDITIONS 57
2.2.1 GROWTH ROOMS 57
2.2.2 WALK-INS 57
2.2.3 GREENHOUSES 57
2.3 SEED STERILISATION METHODS AND PLANT GROWTH MEDIA 58
2.3.1 GAS STERILISATION 58
2.3.2 LIQUID STERILISATION 58
2.3.3 STERILE GROWTH MEDIA 58
2.4 ROOT DATA COLLECTION TECHNIQUES 60
2.4.1 ROOT HAIR LENGTH AND DENSITY MEASUREMENTS 60
2.4.2 ECTOPIC ROOT HAIRS 60
2.4.3 PRIMARY ROOT LENGTH 61
2.4.4 ROOT GRAVITROPIC RESPONSE MEASUREMENTS (OVER 24 HOURS) 61
2.4.5 ROOT GRAVITROPIC RESPONSE MEASUREMENTS (CONTINUOUS) 62
2.4.6 CONFOCAL MICROSCOPY 62
2.5 CROSSING TECHNIQUES 64
2.5.1 CROSSING 64
2.5.2 SELECTION OF AN F1 GENERATION 64
2.5.3 SELECTION OF AN F2 GENERATION 65
2.5.4 SELECTION OF AN F3 GENERATION 65
2.5.5 BASTA SELECTION 66
2.6 DNA EXTRACTION AND AMPLIFICATION 67

2.6.1 EDWARDS PREP DNA EXTRACTION FROM LEAF TISSUE 67
2.6.2 POLYMERASE CHAIN REACTION (PCR) 67
2.6.3 AGAROSE GEL ELECTROPHORESIS 69
2.6.4 RESTRICTION DIGESTS 69
2.6.5 PRIMERS 69
2.7 CLONING 74
2.7.1 INVITROGEN® GATEWAY® VECTORS 74
2.7.2 INVITROGEN® GATEWAY® BP REACTION 77
2.7.3 INVITROGEN® GATEWAY®, LR REACTION 78
2.7.4 CLASSICAL CLONING VECTORS 79
2.7.5 CLASSICAL CLONING CONSTRUCT GENERATION 80
2.7.6 LIGATION REACTIONS 81
2.7.7 ESTIMATION OF DNA CONCENTRATIONS 81
2.7.8 PLASMID MINIPREP - ALKALINE LYSIS METHOD 81
2.7.9 PLASMID MINIPREP - QIAPREP SPIN MINIPREP KIT (QIAGEN) 82
2.7.10 QIAEX II GEL EXTRACTION (QIAGEN) 82
2.7.11 QIAQUICK PCR PURIFICATION KIT 83
2.7.12 BACTERIAL STRAINS AND GROWTH CONDITIONS 83
2.7.13 TRANSFORMATION OF BIOLINE DH5A COMPETENT CELLS 84
2.7.14 PREPARATION AND TRANSFORMATION OF COMPETENT AGROBACTERIUM TUMEFACIENS CELLS 84
2.7.15 FLORAL DIPPING TRANSFORMATION 85
2.8 CHROMATIN IMMUNOPRECIPITATION (CHIP) 87
2.9 BUFFER SUMMARY 91
2.9.1 ARABIDOPSIS THALIANA SALTS 91
2.9.2 EDWARDS PREP EXTRACTION BUFFER 91
2.9.3 TE BUFFER 91
2.9.4 ALKALINE LYSIS MINI PREP SOLUTION 1 92
2.9.5 ALKALINE LYSIS MINI PREP SOLUTION 2 92
2.9.6 ALKALINE LYSIS MINI PREP SOLUTION 3 92
2.9.7 LYSOGENY BROTH 92
2.9.8 FLORAL DIPPING SOLUTION 93
2.9.9 CHIP MC BUFFER 93
2.9.10 CHIP M1 BUFFER 93
2.9.11 CHIP M2 BUFFER 94
2.9.12 CHIP M3 BUFFER 94
2.9.13 CHIP SONIC BUFFER 94
2.9.14 CHIP IP BUFFER 95
2.9.15 CHIP HIGH SALT BUFFER 95
2.9.16 CHIP LICL BUFFER 95
2.9.17 CHIP ELUTION BUFFER 96

3 : ESTABLISHING THE FUNCTIONAL SIGNIFICANCE OF THE APPARENT NON-HAIR REPRESSIVE AUXIN RESPONSE REGIME 97

3.1 INTRODUCTION 98
3.2 EPIDERMAL PATTERNING MUTANTS 100
3.3 ANALYSIS OF THE AUXIN RESPONSE REGIME IN THE *GL2-1* MUTANT BACKGROUND 102
3.4 ANALYSIS OF THE ROOT HAIRS IN THE *GL2-1* MUTANT 105

3.5 DOES THE LOSS OF AUX1 IN THE *GL2-1* MUTANT INFLUENCE THE SHORT ROOT HAIR PHENOTYPE? 108
3.6 ARE THESE SHORTER ROOT HAIRS LESS RESPONSIVE TO AUXIN? 112
3.7 ARE THESE SHORTER ROOT HAIRS THOSE PRODUCED BY THE NON-HAIR CELLS? 114
3.8 DOES REMOVING THE REPRESSIVE ARFS, *ARF10* AND *ARF16,* RESTORE THE ECTOPIC ROOT HAIR LENGTH? 117
3.9 DISCUSSION 119

4 : PLACING SPATIAL CONTROL OF AUXIN RESPONSE IN CURRENT KNOWLEDGE OF THE EPIDERMAL PATTERNING MECHANISM 121

4.1 INTRODUCTION 122
4.1.1 THE EPIDERMAL PATTERNING MECHANISM 122
4.1.2 THE AUXIN RESPONSE NETWORK 123
4.2 IS *WEREWOLF* PATTERNING AUXIN RESPONSE IN THE ROOT EPIDERMIS? 125
4.3 DOES AUX1 PATTERN EXPRESSION OF THE AUXIN RESPONSE COMPONENTS IN THE ROOT EPIDERMIS? 131
4.4 HOW IS AUXIN RESPONSE PATTERNED IN A *WER-1 MYB23-1* DOUBLE MUTANT? 137
4.5 IS *MYB23* PATTERNING AUXIN RESPONSE IN THE ROOT EPIDERMIS? 142
4.6 IS *CAPRICE* PATTERNING AUXIN RESPONSE IN THE ROOT EPIDERMIS? 147
4.7 HOW IS AUXIN RESPONSE PATTERNED IN THE *CPC-1 TRY-82* DOUBLE MUTANT? 152
4.8 DISCUSSION 156
4.8.1 AUXIN SIGNALLING OUTPUT 156
4.8.2 IAA17 EXPRESSION 158
4.8.3 *ARF10* EXPRESSION *160*
4.8.4 CELL SIZE 163
4.8.5 SUMMARY 165

5 : ESTABLISHING FEEDBACK LOOPS AND DIRECT LINKS BETWEEN THE EPIDERMAL PATTERNING MECHANISM AND THE AUXIN RESPONSE NETWORK 167

5.1 INTRODUCTION 168
5.2 DOES WER OR MYB23 BIND TO THE *ARF10* PROMOTER? 168
5.2.1 CHROMATIN IMMUNOPRECIPITATION 174
5.2.2 ARF10 PROMOTER TRUNCATIONS 177
5.3 DO FEEDBACK LOOPS EXIST BETWEEN THE EPIDERMAL PATTERNING MECHANISM AND THE AUXIN RESPONSE NETWORK? 179
5.3.1 DO ARF10 AND/OR ARF16 REGULATE *WER* EXPRESSION? *180*
5.3.3 DO ARF10 AND/OR ARF16 REGULATE *GL2* EXPRESSION? *184*
5.3.4 DO ARF10 AND/OR ARF16 REGULATE *MYB23* EXPRESSION? *184*
5.4 DOES ARF10 DIRECTLY BIND TO THE *MYB23* PROMOTER? 187
5.5 DISCUSSION 189

6 : THE ROLE OF THE AUXIN MEDIATED DOWN-REGULATION OF *GL2* AND *MYB23* ON ROOT HAIR GROWTH 191

6.1 INTRODUCTION 192
6.2 FURTHER CLARIFICATION OF AUXIN DOWN-REGULATION OF EPIDERMAL PATTERNING COMPONENTS 192
6.2.1 DOES AUXIN DOWN-REGULATE GL2 AND MYB23 INDEPENDENTLY OF ONE ANOTHER? 193
6.3 DOES *MYB23* AND/OR *GL2* DOWN-REGULATION BY AUXIN AFFECT ROOT HAIR INITIATION? 197
6.3.1 *DOES AUXIN DOWN-REGULATION OF MYB23 IN THE GL2-1* MUTANT HAVE AN EFFECT ON ROOT HAIR INITIATION? *199*
6.3.2 ROOT HAIR INITIATION IN THE MYB23-1 GL2-1 DOUBLE MUTANT 202
6.4 DOES *MYB23* AND/OR *GL2* DOWN-REGULATION BY AUXIN AFFECT ROOT HAIR ELONGATION? 204
6.4.1 DOES BLOCKING DOWN-REGULATION OF MYB23 BY AUXIN HAVE AN IMPACT ON ROOT HAIR ELONGATION? 206
6.4.2 IS THE ECTOPIC EXPRESSION OF MYB23 IN THE HAIR CELLS AFFECTING ROOT HAIR ELONGATION IN RESPONSE TO AUXIN? 208
6.5 DISCUSSION 211
6.5.1 THE ROLE OF MYB23 ON ROOT HAIR INITIATION 211
6.5.2 ROOT HAIR ELONGATION 212
6.5.3 THE ROLE OF MYB23 ON ROOT HAIR ELONGATION *213*

7 : GENERAL DISCUSSION 217

7.1.1 THE FUNCTIONAL SIGNIFICANCE OF THE REPRESSIVE AUXIN RESPONSE REGIME IN THE NON-HAIR CELLS 218
7.1.2 SPATIAL CONTROL OF AUXIN RESPONSE IN THE EPIDERMAL PATTERNING MECHANISM 221
7.1.3 FEEDBACK LOOPS AND DIRECT LINKS BETWEEN THE EPIDERMAL PATTERNING MECHANISM AND THE AUXIN RESPONSE NETWORK 224
7.1.4 AUXIN MEDIATED DOWN-REGULATION OF GL2 AND MYB23 227
7.2 CONCLUSIONS 230

8 : REFERENCES 236

9 : SUPPLEMENTARY DATA 248

Table of Figures

Chapter 1

Figure 1-1: The chemical structure of synthetic and naturally occurring auxins. 17
Figure 1-2: A schematic representation of the auxin response network. 21
Figure 1-3: A schematic representation of Aux/IAA and ARF protein structures. 23
Figure 1-4: A simplified representation of the *Arabidopsis thaliana* root. 28
Figure 1-5: Zonal classification of the developing *Arabidopsis thaliana* root. 30
Figure 1-6: Patterning of root hair cells in different species. 35
Figure 1-7: A schematic representation of the epidermal patterning mechanism. 37
Figure 1-8: *pGL2::GUS* expression in the *myb23-1* in comparison to the wild-type. 40
Figure 1-9: Expression of the *pDR5::GFP* marker in the root epidermis. 42
Figure 1-10: Expression of the *pIAA17::GFP* marker in the root epidermis. 44
Figure 1-11: Expression of the *pARF10::GFP* marker in the root epidermis 45

Chapter 2

Figure 2-1: Vector pDONR 207. Image produced by Invitrogen Life Technologies. 74
Figure 2-2: Vector pDONR 221. Image produced by Invitrogen Life Technologies. 75
Figure 2-3: Vector pFP101. Figured adapted from (Bensmihen et al., 2004) 76
Figure 2-4: Vector map for pJTG01. 76
Figure 2-5: Generation of the Gateway Entry Clone 77
Figure 2-6: Generation of the Gateway Expression Clone 78
Figure 2-7: Vector pGreen0029, Image produced by snapgene. 79
Figure 2-8: Construction of the pMYB23::MYB23-GFP marker line using classical cloning methods. 80
Figure 2-9: A schematic representation of the chromatin immunoprecipitation technique. 88

Chapter 3

Figure 3-1: Mutant phenotypes of epidermal patterning mutants used during this project. 101
Figure 3-2: Markers for *IAA17*, *ARF10* and *pDR5::GFP* in the *gl2-1* mutant. 104
Figure 3-3: Analysis of the *gl2-1* mutant root hair length. 107
Figure 3-4: Analysis of the *gl2-1* mutant in comparison to the *aux1-7* and *aux1-22* mutants. 110
Figure 3-5 : Treatment of the *gl2-1* mutant with NAA. 111
Figure 3-6: Treatment of the *gl2-1* mutant with IAA. 113
Figure 3-7 : Expression of the *pGL2::GFP* marker in the *gl2-1* mutant. 116
Figure 3-8: Analysis of the *gl2-1 arf10-3 arf16-2* triple mutant. 118
Figure 3-10: ARF10 and/or ARF16 inhibit root hair growth. 120

Chapter 4

Figure 4-1: Markers for auxin response in the *wer-1* mutant background. 127
Figure 4-2: Markers for auxin response in the wer-1 background. 129
Figure 4-3: *WER* promotes the expression of *ARF10* and *IAA17* in the non-hair cells. 130
Figure 4-4: *pIAA17::IAA17-GFP* expression in the *wer-1* mutant when treated with NAA. 133
Figure 4-5: *IAA17* markers in the *AUX1* mutant backgrounds. 134
Figure 4-6: *ARF10* markers in the *AUX1* mutant backgrounds. 135
Figure 4-7: The translational *ARF10* marker in the *AUX1* mutant backgrounds. 136
Figure 4-8: The *pDR5::GFP* and *ARF10* transcriptional and translational markers in the *wer-1 myb23-1* mutant background. 140
Figure 4-9: Transcriptional and Translational markers for IAA17 in the *wer-1 myb23-1* double mutant background. 141
Figure 4-10: Markers for auxin response in the *myb23-1* mutant background. 144
Figure 4-11: Transcriptional marker for *IAA17* in the *myb23-1* mutant background. ..145
Figure 4-12: *MYB23* positively regulates the expression of *ARF10.* 146
Figure 4-13: Markers for auxin response crossed into the *cpc-1* mutant background.149
Figure 4-14: Transcriptional and translational markers for IAA17 in the *cpc-1* mutant. 150
Figure 4-15: *CPC* inhibits the expression of *ARF10* and *IAA17.* 151
Figure 4-16: Markers of auxin response in the *cpc-1 try-82* mutant. 154
Figure 4-17: *CPC* and *TRY* act redundantly to inhibit the expression of *ARF10* and *IAA17*....155
Figure 4-18: A summary of the patterning of auxin signalling output, as indicated by the *pDR5::GFP* marker, in a range of epidermal patterning mutants. 157
Figure 4-19: A summary of the patterning of *IAA17* in the root epidermis....159
Figure 4-20: A summary of the patterning of negative auxin response, as indicated by the pARF10::GFP marker in a range of epidermal patterning mutants. 161
Figure 4-21: Cell size differences between hair and non-hair cells in epidermal patterning mutants. 164
Figure 4-22: A summary of interactions brought about by the crossing of these epidermal mutants with markers of auxin response. 166

Chapter 5

Figure 5-1: Published WER binding sites. 170
Figure 5-2: Promoter truncation analysis. 171
Figure 5-3: Potential MYB binding sites within the *ARF10* promoter. 173
Figure 5-4: Primer location for ChIP analysis of the *ARF10* promoter. 175
Figure 5-5: ChIP analysis of the *ARF10* promoter. 176
Figure 5-6: *ARF10* promoter truncation analysis. 178
Figure 5-7: Expression of the transcriptional marker for *WER* in the *arf10-3 arf16-2* mutant background. 181
Figure 5-8: *ARF10* and/or *ARF16* promote the expression of *WER.* 182
Figure 5-9: The translational marker for WER in the *arf10-3 arf16-2* background. 183
Figure 5-10: Expression of *pGL2::GFP* in the *arf10-3 arf16-2* mutant background. ...185

Figure 5-11: *ARF10* and/or *ARF16* promote the expression of *GL2* and inhibit the expression of *MYB23.* 186
Figure 5-12: ChIP analysis of the *MYB23* promoter 188
Figure 5-13: Interactions identified during this chapter. 190

Chapter 6

Figure 6-1: *pGL2::GFP* expression when treated with IAA and PEO. 194
Figure 6-2: Analysis of the *pGL2::GFP* marker in the *myb23-1* background. 195
Figure 6-3: Auxin down-regulates *MYB23* and *GL2.* 196
Figure 6-4: Analysis of root hairs in the *cpc*-1 and *cpc-1 try-82* mutants. 198
Figure 6-5: Root hair density in the *gl2-1* mutant. 200
Figure 6-6: Changes in *ARF10* and *IAA17* expression in the *gl2-1* mutant when treated with auxin. 201
Figure 6-7: Analysis of root hairs in the *gl2-1 myb23-1* double mutant. 203
Figure 6-8: Root hair elongation in response to auxin treatment. 205
Figure 6-9: Analysis of the *pWER::MYB23 wer-1* construct. 207
Figure 6-10: Root hair phenotypes in the pCOBL9::MYB23 and pEXP7::MYB23 constructs. 210
Figure 6-11: Analysis of the *cpc-1 myb23-1* double mutant 215
Figure 6-12: Analysis of root hair length in the *gl2-1 myb23-1* double mutant. 216

Chapter 7

Figure 7-1: A summary of the interactions identified between the epidermal patterning mechanism and the auxin response network during this project. 220
Figure 7-2: A summary of the current published knowledge of the epidermal patterning mechanism in conjunction with the additional interactions identified during this project 233

Chapter 9

Figure 9-1: Root hair density in the *gl2-1* single mutant. 249
Figure 9-2: Analysis of the *pAUX1::AUX1-YFP* marker in the *gl2-1* background. 250
Figure 9-3: *pARF10::GFP* expression in ectopic root hairs. 251
Figure 9-4: Primary root length analysis of epidermal patterning mutants when treated with auxin. 252
Figure 9-5: RT-qPCR analysis. 253
Figure 9-6: Analysis of root hairs in the *pCOBL9::ARF10 construct.* 254
Figure 9-7: Analysis of root hair density and ectopic root hairs in the *arf10-2,arf16-2,gl2-1* mutant in comparison to the wild-type and single mutants. 255
Figure 9-8: Root hair density in the *pEXP7::MYB23* construct. 256
Figure 9-9: Ectopic root hairs in the *pEXP7::MYB23* construct. 257
Figure 9-10: Root hair length frequencies in the *pEXP7::MYB23* construct. 258
Figure 9-11: Changes in expression level of putative *MYB23* target genes in *pEXP7::MYB23* plants. 259

Table of Tables

Table 2-1: *Arabidopsis thaliana* lines used in this project and the source from whence they were acquired. 56
Table 2-2: Variations in ATS growth media. 59
Table 2-3: PCR mixture components with different DNA polymerases. 68
Table 2-4: PCR reaction cycles. 68
Table 2-5: Primers during this project. Bold highlights indicate the Gateway *attB* flanking sequences used. 73
Table 2-6: Antibiotic selection conditions and concentrations. 84

Abbreviations

2,4-D - 2,4-DICHLOROPHENOXYACETIC ACID

3S5 – CALIFLOWER MOSAIC VIRUS PROMOTER

ABCB – B-TYPE ATP-BINDING CASSETTE

ARF – AUXIN RESPONSE FACTOR

ARF- – REPRESING AUXIN RESPONSE FACTOR

ARF+ – ACTIVATING AUXIN RESPONSE FACTOR

ATS – ARABIDOPSIS THALIANA SALTS

AUX1 – AUXIN RESISTANT 1

AUXRE – AUXIN RESPONSE ELEMENTS

BASTA – D-PHOSPHINOTHRICIN, MELFORD ®

CHIP – CHROMATIN IMMUNOPRECIPITATION

COBL9 – COBRA LIKE 9

COL – COLUMBIA (ARABIDOPSIS WILD-TYPE)

CPC – CAPRICE

CTD – C-TERMINAL DOMAIN

DBD – DNA BINDING DOMAIN

DMSO – DIMETHYL SULFOXIDE

DNA – DEOXYRIBONUCLEIC ACID

E.COLI – ESCHERICHIA COLI

EGL3 – ENHANCER OF GLABRA3

ETC1 – ENHANCER OF TRIPTYCHON1

EXP – EXPANSIN

GFP – GREEN FLUORESCENT PROTEIN

GL2 – GLABRA2

GL3 – GLABRA3

HCL – HYDROCHLORIC ACID

IAA – INDOLE-3-ACETIC ACID

JDK – JACKDAW

LAX – LIKE AUXIN RESISTANT 1

LB – LYSOGENY BROTH

LER – LANDSBERG ERECTA (ARABIDOPSIS WILD-TYPE)

LRL3 – LJRHL-I-LIKE 3

MR – MIDDLE REGION

NAA - 1-NAPTHALENEACETIC ACID

NEB – NEW ENGLAND BIOLABS

PCR – POLYMERASE CHAIN REACTION

PGP – PHOSPHOGLYCOPROTEINS

PGS – PLANT GROWTH SUIT

PIN – PIN-FORMED

RHD6 – ROOT HAIR DEFECTIVE6

RNA – RIBONUCLEIC ACID

RSL4 – ROOT HAIR DEFECTIVE 6 LIKE 4

SCF – SKP1-CULLIN1-F-BOX

SCM – SCRAMBLED

SE – STANDARD ERROR

SRDX – SUPERMAN REPRESSOR DOMAIN

TIR1/ARF - TRANSPORT INHIBITOR RESPONSE 1 / AUXIN RELATED F-BOX

TPL – TOPLESS

TPR – TOPLESS-RELATED

TRY – TRIPTYCHON

TTG1 – TRASPARENT TESTA GLABRA1

WER – WEREWOLF

WS – WASSILEWSKIJA (ARABIDOPSIS WILD-TYPE)

1 : General Introduction

1.1 Auxin

The phytohormone auxin is a versatile regulator of many growth and developmental processes (Chapman and Estelle, 2009; Del Bianco and Kepinski, 2011; Goh *et al*., 2014). Auxin is the term given for a class of structurally diverse small molecules, which elicit a qualitatively similar response in plants, to that observed as a result of treatment with the naturally occurring auxin indole-3-acetic acid (IAA) (Del Bianco and Kepinski, 2011; Ljung, 2014). IAA is a weak acid derivative of tryptophan, a carboxylic acid in which the carboxyl group is attached through a methylene group to the C3 position of an indole ring (Figure 1-1) (Robert and Friml, 2009; Abel and Theologis, 2010; Tromas and Perrot-Rechenmann, 2010). Several synthetic auxins are also used both scientifically and commercially. These include 1-naphthaleneacetic acid (NAA) which, in contrast to IAA can enter cells without the involvement of auxin influx transporters and 2,4-Dichlorophenoxyacetic acid (2,4-D), which can be readily transported into, but not out of, cells (Delbarre, 1994; Walsh *et al*,2006; Grossmann, 2007).

A combination of homeostatic mechanisms including, coordinated and directional transport, de novo synthesis, degradation and reversible conjugation create the patterns of auxin distribution throughout the plant that regulate numerous, diverse aspects of development (Del Bianco and Kepinski, 2011; Overvoorde *et al*., 2010; Kieffer *et al*., 2010; Pencík *et al.*, 2013). An important component of auxin's versatility as a developmental regulator arises from the existence of context-specific responses to auxin. For example, the generation of an auxin maximum in the root tip positions and maintains the stem cell niche, whilst auxin accumulation in xylem-pole pericycle cells initiates lateral root growth (Péret *et al*., 2009; Tromas and Perrot-Rechenmann, 2010). It has been suggested that these context-dependent responses to auxin arise from cell and tissue-specific patterns of expression of auxin signalling components, although this hypothesis remains to be substantiated (Del Bianco and Kepinski, 2011).

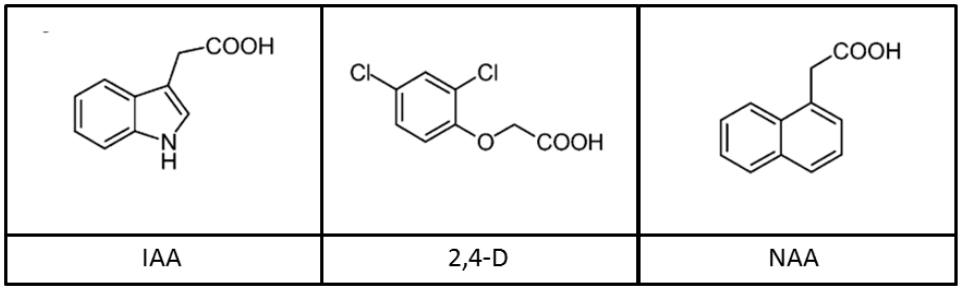

IAA	2,4-D	NAA

Figure 1-1: The chemical structure of synthetic and naturally occurring auxins.

(Adapted from Walsh *et al*., 2006, Figure 6). Auxins are a variety of structurally diverse molecules. This figure indicates the chemical structure of the naturally occurring IAA and two synthetic auxins 2,4-Dichlorophenoxyacetic Acid (2,4-D) and 1-napthaleneacetic acid (NAA).

1.2 Auxin transport

The coordinated and directional manner in which IAA is transported is one of the primary reasons auxin is such a remarkable regulator of growth and development (Tromas and Perrot-Rechenmann, 2010). Unique intercellular and directional transport systems enable differential IAA distribution and result in reliable establishments of auxin gradients and maxima (Robert and Friml, 2009; Peer *et al*., 2014; Eckardt, 2014). IAA is transported via two methods, long distance via the phloem and short distance via the highly regulated polar cell-to-cell system (Robert and Friml, 2009; Tromas and Perrot-Rechenmann, 2010).

A significant amount of IAA is transported via the phloem, allowing the bulk movement of IAA in a root-ward direction. Although this transport route is efficient and reasonably rapid, achieving speeds of up 7 cm per hour, it can not be finely regulated (Overvoorde *et al*., 2010). Despite the polar cell-to-cell IAA transport method being much slower, only achieving a speed of up to 10 mm per hour, it is able to be finely regulated by the coordinated activities of auxin influx and efflux transporters (Overvoorde *et al*., 2010).

The short-distance cell-to-cell movement of IAA is described by the chemiosmotic model (Robert and Friml, 2009). Due to the acidic pH (5.5) of the apoplast, extracellular IAA is partially protonated. The lipophilic characteristics and small size of protonated IAA means that it can diffuse across the plasma membrane into the cell (Robert and Friml, 2009). Once inside the cell the neutral pH of the cytoplasm means that IAA is almost completely deprotonated and therefore unable to diffuse out of the cell passively (Jones *et al*., 2009; Tromas and Perrot-Rechenmann, 2010). Despite efficient passive transport of protonated IAA into cells, the auxin influx transporters AUXIN RESISTANT 1 (AUX1) and three LIKE AUXIN RESISTANT1 (LAX) proteins also play an important role in cellular

homeostasis because they allow the uptake of deprotonated IAA (Robert and Friml, 2009; Tromas and Perrot-Rechenmann, 2010).

The active transport of auxin out of cells is mediated by two families of membrane proteins, the *PIN-FORMED (PIN)* and *B-type ATP-BINDING CASSETTE (ABCB)* families of auxin efflux transporters (Robert and Friml, 2009). The *ABCB* family consists of phosphoglycoproteins (PGP), PGP1,4 and 19 have been identified as mediating auxin efflux and have been shown to exhibit complex interactions with PIN proteins (Robert and Friml, 2009). PINs are known for their importance in facilitating the directionality of auxin transport via their coordinated expression and asymmetric localisation in the plasma membrane (Jones *et al*., 2009). In the root, due to this dynamic coordinated expression and orientation of the pin proteins, IAA is transported in a root-ward direction in the stele and a shoot-ward direction in the epidermis and lateral root cap (Robert and Friml, 2009; Jones *et al*., 2009). It is hypothesised that the ABCB/PGP proteins influence how much auxin is available for the PIN directed transport, however PIN and ABCB/PGP proteins have been observed to act in both a synergistic and antagonistic manner, thus allowing for the fine tuning of auxin distribution in many developmental processes (Cho *et al*., 2007; Robert and Friml, 2009). Using the root hair as a model for auxin response, in 2007 Cho *et al* highlighted the importance of auxin transporters in influencing auxin related phenotypes, overexpression of PGP4 resulted in shorter root hairs whilst overexpression of AUX1 resulted in longer root hairs.

.

1.3 Auxin signalling

In *Arabidopsis thaliana* (hereafter referred to as *Arabidopsis*) three protein families form part of a dynamic interaction network that brings about a transcriptional response to auxin. These are the TRANSPORT INHIBITOR RESPONSE1/ AUXIN RELTED F-BOX ($SCF^{TIR1/AFB}$) family of auxin receptors, and two families of transcription factors, the Aux/IAA's and the AUXIN RESPONSE FACTORS (ARFs) (Lokerse and Weijers, 2009; Tromas and Perrot-Rechenmann, 2010). ARFs bind to AUXIN RESPONSE ELEMENTS (AuxRE) located in the promoter region of auxin response genes (Guilfoyle and Hagen, 2007). Once bound the ARF can either activate or repress the transcription of the targeted gene. ARFs also form dimers with the Aux/IAA repressor proteins, which in turn recruit members of the TOPLESS (TPL) co-repressor protein family, to bring about a repressed chromtain state at the targeted locus (Szemenyei *et al*., 2008). Auxin affects transcrptional activity at ARF-targeted loci by facilitating the interaction between Aux/IAA repressor proteins and the auxin receptor complex $SCF^{TIR1/AFB}$, thereby promoting the ubiquitination and proteolysis of Aux/IAAs and the derepression of ARF-regulated genes (Figure 1-2) (Del Bianco and Kepinski, 2011).

1.3.1 Auxin receptors

There are six members of the $SCF^{TIR1/AFB}$ auxin receptor family, *TIR1* and *AFB1-5* (Del Bianco and Kepinski, 2011). TIR1 and the AFBs are F-Box proteins, which are subunits of the SKP1-CULLIN1-F-BOX ubiquitin ligase complex (Lokerse and Weijers, 2009; Tromas and Perrot-Rechenmann, 2010; Kieffer *et al*., 2010). The F-Box protein components are responsible for the specific recruitment of Aux/IAAs for polyubiquitination by the core catalytic components of the SCF complex (Kepinski, 2007; Lokerse and Weijers, 2009; Tromas and Perrot-Rechenmann, 2010; Kieffer *et al*., 2010).

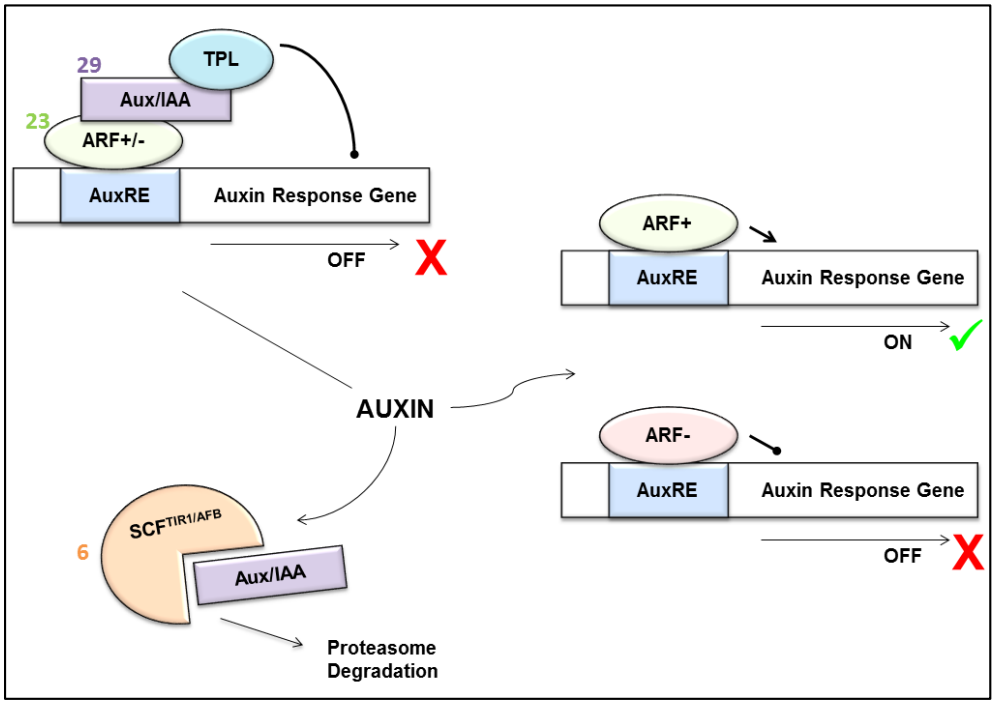

Figure 1-2: A schematic representation of the auxin response network.

Three key protein families form part of a dynamic interaction network that brings about a transcriptional response to auxin. When auxin interacts with the $SCF^{TIR1/AFB}$ receptors the Aux/IAA proteins are recurited away from interacting with ARFs and co-repressors like TOPLESS (TPL), this results in proteasomal degradation of the Aux/IAAs, thus leaving the ARFs free to activate or repress auxin response gene expression. In *Arabidopsis* there are 29 Aux/IAAs, 23 ARFs and 6 TIR1/AFB receptors.

Auxin binding the complex acts to stabilise the association between $SCF^{TIR1/AFB}$ and the Aux/IAA, thereby promoting the polyubiquitination and subsequent proteolysis of the Aux/IAA in the 26s proteasome (Lokerse and Weijers, 2009; Tromas and Perrot-Rechenmann, 2010; Hua and Vierstra, 2011). Differences have been observed between these F-box proteins, for example, AFB4 and AFB5 have long amino-terminal extensions and whilst a loss of function in TIR1 and AFB1-3 results in resistance to exogenous auxin, the same mutation in AFB5 results in slight hypersensitivity to exogenous auxin (Yu et al., 2013).

1.3.2 Aux/IAAs

In *Arabidopsis* the Aux/IAA family of repressor proteins consists of 29 members, IAA1-20 and IAA26-34 (Tiwari *et al*., 2004; Guilfoyle and Hagen, 2007; Overvoorde *et al*., 2010). The *Aux/IAA* genes encode 18- to 35- kD proteins that are localised in the nuclei and have short half-lives (Tromas and Perrot-Rechenmann, 2010). The transcription of most of these *Aux/IAA*s is up-regulated by auxin, resulting in a feedback loop that facilitates tight regulation of auxin response (Kieffer *et al*., 2010).

Most of the Aux/IAAs have four domains with individual functions (Figure 1-3) (Lokerse and Weijers, 2009; Tromas and Perrot-Rechenmann, 2010; Overvoorde *et al*., 2010). Domain I facilitates transcriptional repression by recruiting co-repressors like TPL and TOPLESS-RELATED (TRP) (Szemenyei *et al*., 2008; Tiwari *et al*., 2001). These transcriptional co-repressors do not bind DNA directly, but are recruited via associations with DNA binding transcription factors (Szemenyei *et al*., 2008). Within Domain I conserved leucine residues have been shown to be important for effective Aux/IAA repression (Tiwari *et al*., 2004).

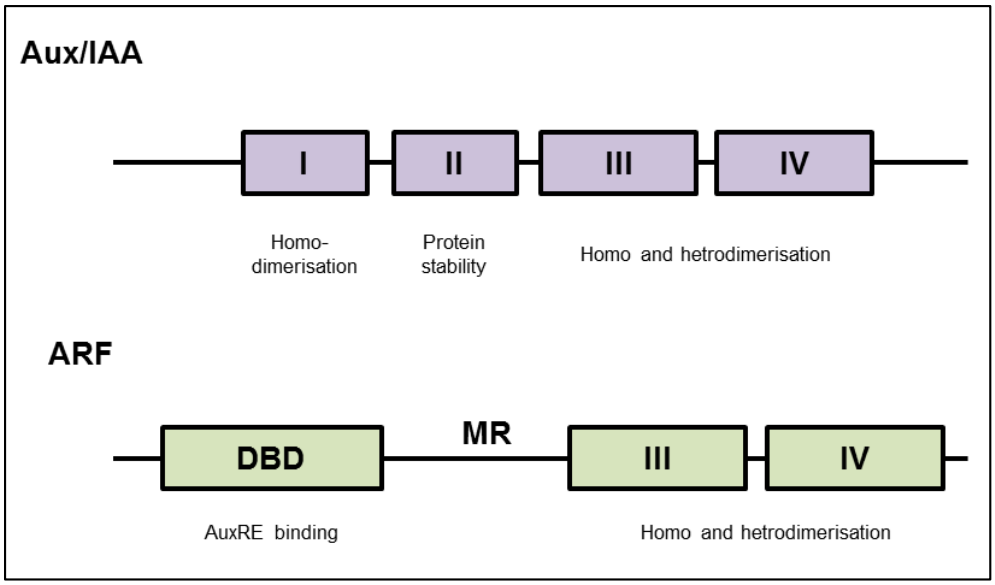

Figure 1-3: A schematic representation of Aux/IAA and ARF protein structures.

(Re-drawn from Kepinski and Leyser, 2002, Figure 2.) The shared homology in the C-terminal Domains III and IV of the ARFs and Aux/IAAs mediates homo and heterodimeristion. The ARFs have an N-terminal DNA binding domain (DBD) which binds to AuxRE's in the promoter regions of auxin response genes, whilst the composition of the middle region determines if the ARF is activating or repressing. Protein stability of the Aux/IAAs is determined by Domain II.

Domain II is required for the Aux/IAAs characteristic instability, it contains the residues that interact with the $SCF^{TIR1/AFB}$ receptor complex, thus acting as a so-called degron motif (Kepinski and Leyser, 2002). This results in a range of half-lives from a little as 6 minutes to in excess of 80 minutes (Kepinski and Leyser, 2002). Mutations in Domain II result in accumulation of the Aux/IAA protein, interestingly these mutants exhibit varying phenotypes, in *IAA7* mutants gravitropic defects are observed whereas the same mutation in *IAA14* results in the loss of lateral root development (Tiwari *et al*., 2001; Tromas and Perrot-Rechenmann, 2010; Overvoorde *et al*., 2010).

Domains III and IV are within the Aux/IAAs C-terminal region, and are also known as the C-terminal interaction domain (CTD) (Lokerse and Weijers, 2009). The CTD mediates homotypic and heterotypic interactions between the Aux/IAAs and the ARFs (Lokerse and Weijers, 2009; Tromas and Perrot-Rechenmann, 2010). In some of the Aux/IAAs a mutation in Domain III has resulted in a reversal of the repression of auxin response genes (Rouse, 1998; Tiwari *et al*., 2001).

There are three non-canonical Aux/IAAs that do not exhibit this four domain structure (Dreher *et al*., 2006). IAA20, 30 and 31 all either completely or partially lack a Domain II meaning they exhibit little or no degradation in response to auxin (Dreher *et al*., 2006).

1.3.3 Auxin response factors

AUXIN RESPONSE FACTORS (ARFs) bind to auxin response elements (AuxREs) in the promoter regions of auxin response genes (Overvoorde *et al*., 2010). In *Arabidopsis* there are 23 members of the *ARF* family (Tromas and Perrot-Rechenmann, 2010). Unlike the *Aux/IAAs* they are not generally induced by auxin and are relatively stable proteins that have a three domain structure

(Figure 1-3) (Guilfoyle and Hagen, 2007; Tromas and Perrot-Rechenmann, 2010; Kieffer *et al*., 2010). The majority of the ARFs have a DNA-binding domain (DBD), a middle region (MR) and a C-terminal dimerization domain (CTD), which is structurally similar to the Aux/IAA CTD (Tiwari *et al*., 2003, Guilfoyle and Hagen, 2007).

The ARFs CTD enables a variety of hetero and homo-dimer formations with both other ARFs and Aux/IAAs, whilst the DBD binds to AuxREs in the promoter regions of auxin response genes (Del Bianco and Kepinski, 2011). AuxREs are generally characterised by a TGTCNC sequence (Tiwari *et al*., 2003; Guilfoyle and Hagen, 2007; Tromas and Perrot-Rechenmann, 2010). Tromas *et al* 2009 hypothesised that the distribution and sequence context of the AuxREs may regulate the degree of response to auxin at that locus, and could therefore function as the first level of complexity in the transcriptional regulation of auxin response genes.

When ARFs interact with these AuxREs they can be either activators or repressors of gene expression, a characteristic that is determined by the MR composition (Guilfoyle and Hagen, 2007). Generally ARFs with a glutamine, serine and/or leucine rich MR are activators, whilst those with a serine, proline and/or glycine rich MR are repressors (Tiwari *et al*., 2003; Guilfoyle and Hagen, 2007). Within the *ARF* family *ARFs5-8* and *19* are activators (ARF+) whilst the remaining 18 are repressors (ARF-) (Del Bianco and Kepinski, 2011). Although interactions between Aux/IAAs and ARF- may appear insignificant, they have been observed in both in vivo and in vitro assays, however they have appeared to be fewer and weaker that Aux/IAA-ARF+ interactions (Tromas and Perrot-Rechenmann, 2010; Overvoorde *et al*., 2010; Del Bianco and Kepinski, 2011). Hypotheses for ARF- function currently include competition between ARF+ and ARF- for AuxRE binding sites, and the idea that some ARF+ may function better as dimers, the formation of which may be blocked by ARF- interactions (Tromas and Perrot-Rechenmann, 2010; Overvoorde *et al*., 2010; Del Bianco and Kepinski, 2011).

The *Arabidopsis* ARF family consists of 22 full length ARFs and one putative partial length pseudogene, *ARF23*, which has a stop codon in its binding domain (Guilfoyle and Hagen, 2007). Phylogenetic analysis of this family has established that the ARFs fall into related pairs and one triplet (Guilfoyle and Hagen, 2007). These are *ARFs 1* and *2, ARFs 3* and *4, ARFs 6* and *8, ARFs 7* and *19, ARFs 11* and *18* and *ARFs 10, 16* and *17* (Guilfoyle and Hagen, 2007). The roles in these related pairs are likely to be redundant as double mutants of both pair members usually have much stronger phenotypes than a single mutant (Guilfoyle and Hagen, 2007).

Thus the auxin response network is a complex system that enables the capacity for fine control. Differential expression of the pathway components, specific interactions between certain members and protein characteristics may all contribute to the versatility of auxin response in multiple developmental contexts (Knox *et al*., 2003; Overvoorde *et al*., 2010).

1.4 Root development

1.4.1 Arabidopsis root morphology

In *Arabidopsis* the root structure is highly uniform with radial organisation (Figure 1-4) (Yu *et al*., 2010). In the centre is the stele, which contains the xylem and phloem. Adjacent to this is the endodermis and cortex layer and on the outer side is the epidermal layer (Schiefelbein *et al*., 2009; Overvoorde *et al*., 2010). The epidermal layer is composed of two cell types trichoblasts (hereafter referred to as hair cells) and atrichoblasts (hereafter referred to as non-hair cells) (Schiefelbein *et al*., 2009). The tissues in the root arise from a repetitive process of cell division and expansion of four types of stem cell initials, which are adjacent to the quiescent centre (Overvoorde *et al*., 2010). The collumella initials give rise to the central area of the root cap and the epidermal / lateral root cap initials produce to the lateral root cap and the epidermis (Overvoorde *et al*., 2010). The cortex / endodermal initials support the formation of the ground tissue, whilst the vascular initials sustain the vascular tissue and pericycle (Overvoorde *et al.*, 2010).

The root can be divided into a series of distinct developmental zones along its length (Figure 1-5) (Ishikawa and Evans, 1995; van den Berg *et al*., 1995). From the tip these consist of the meristematic zone, the elongation zone and the differentiation zone (Overvoorde *et al*., 2010). At the convergence of the meristematic and elongation zones is the transition zone which has, in the past, also been referred to as the ‘distal elongation zone’ (Baluska *et al*., 2010; Overvoorde *et al*., 2010).

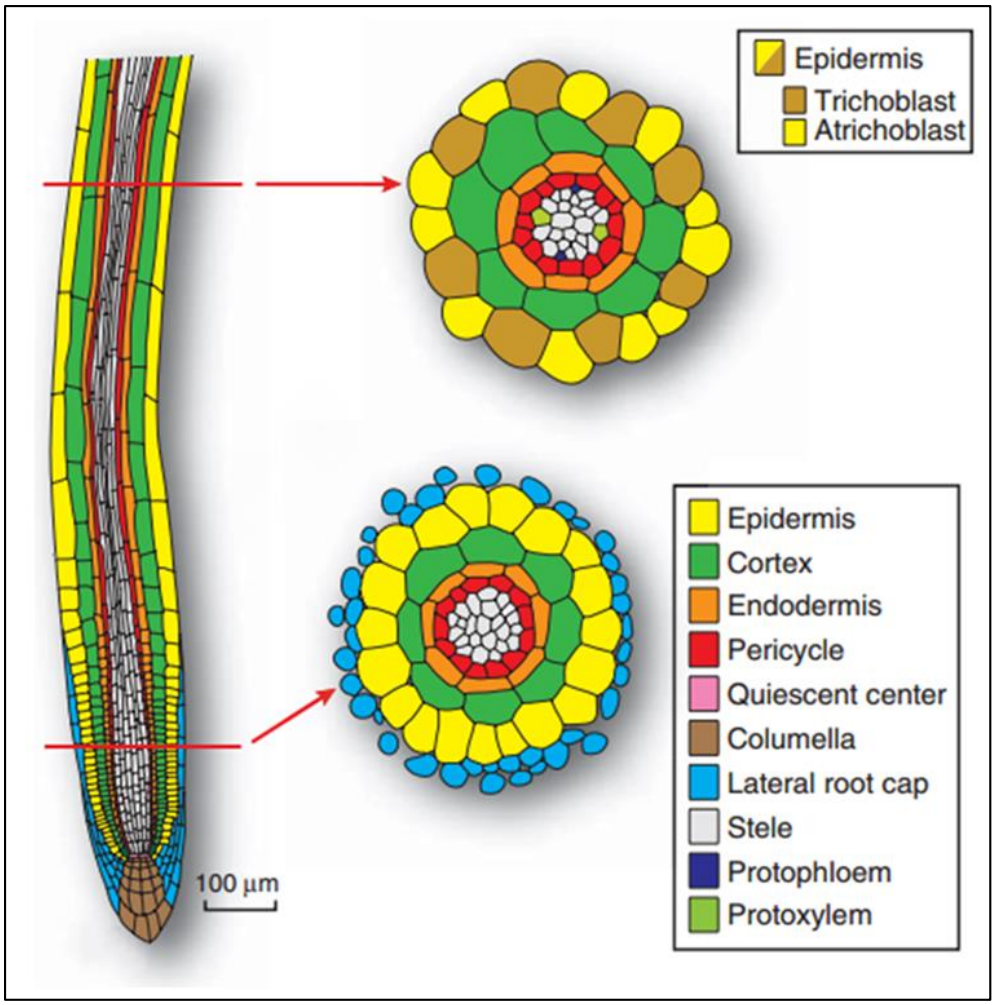

Figure 1-4: A simplified representation of the *Arabidopsis* root.

Figure taken from (Overvoorde *et al*., 2010, Figure 1). Many tissue layers combine to form the *Arabidopsis* root. Here two cross sections highlight the circumferential and radial organisation of the root and the position dependent formation of hair (trichoblast) and non-hair (atrichoblast) epidermal cells.

The meristematic zone contains the four types of initial cells and the dividing cells of the root, in this zone random cell division occurs (Hayashi *et al*., 2013). In the elongation zone endoreduplication occurs and the cells elongate substantially (Hayashi *et al*., 2013). From the basal half of the meristem the increase of cell size is gradual but this rapidly increases once cells enter the elongation zone (Hayashi *et al*., 2013). The concept of a transition zone arose from the fact that cells leaving the meristematic zone needed a transitional stage of cyto-architectural rearrangement in order to be able to perform the rapid cell elongation required in the elongation zone (Baluška *et al*., 1990; Baluska *et al*., 1996; Baluska *et al*., 1997). Cells in the transition zone have important sensorial and functional properties, Darwin himself identified that in *Zea mays* 1.0-1.5 mm from the tip was the most sensitive zone of the root apex with respect to reaction to stimuli, this position corresponds with the location of the transition zone in this species (Baluska *et al*., 2010). Apart from tip growing cells like root hairs, the transition zone cells have the highest rate of vesicle recycling and in addition to this their auxin transport shows the highest degree of activity (Tian and Reed, 1999; Růzicka *et al*., 2007). In the differentiation zone elongated cells mature and root hairs are initiated (Foreman, 2001). During this project the transition zone was defined as the point where the cells began to elongate. Auxin plays an important role in root morphology, including the auxin transport dependent positioning of the stem cell niche and the maintenance of the meristematic zone (Del Bianco and Kepinski, 2011). Within the root the principal flow of auxin is located within the central vascular tissues, moving root-ward towards the root tip and then out through the root cap and back up in a shoot-ward direction through the epidermal layer (Jones *et al*., 2009). At the transition zone a proportion of the auxin flow is refluxed laterally, back into the central root-ward flow, thus reinforcing a high auxin concentration in the meristematic zone (Del Bianco and Kepinski, 2011).

Auxin also plays a role in gravitropic and cell elongation responses (Marchant *et al*., 1999) . Treatment with high concentrations of exogenous auxin results in significantly shorter primary roots and in addition to other responses PIN

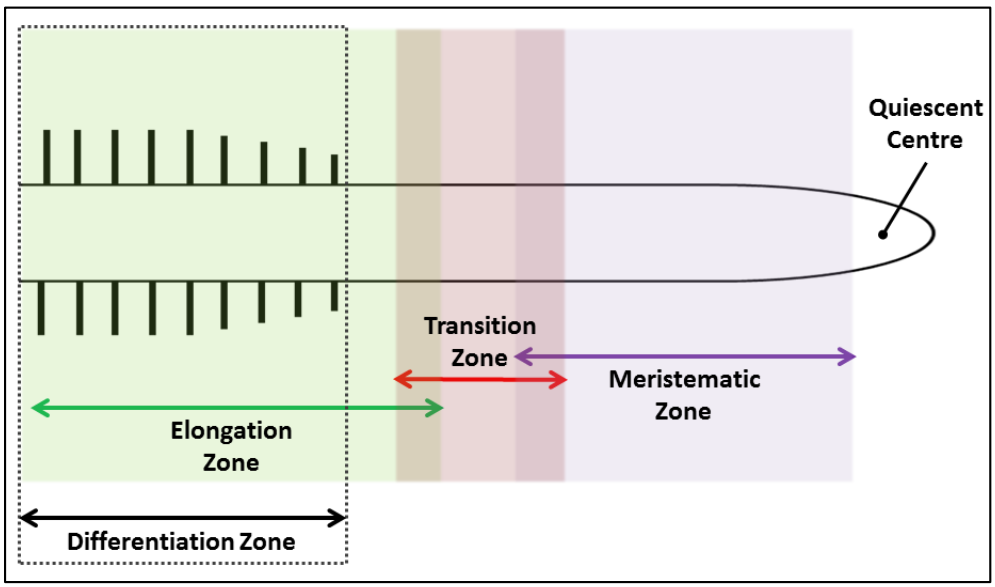

Figure 1-5: Zonal classification of the developing *Arabidopsis* root.

The developing *Arabidopsis* root can be classified into distinct zones. Beyond the quiescent centre in the root tip is the meristematic zone, a shift from this zone to the elongation zone is covered by the transition zone. Shortly after the elongation begins the differentiation zone is apparent and root hairs are initiated. During this project the transition zone was defined as the point where the cells began to elongate.

proteins have been observed to relocate due to a change in gravity (Scott and Allen, 1999; Kleine-Vehn *et al*., 2010).

1.4.2 Root hairs

Root hairs are tip growing tubular shaped extensions produced by the hair cells in the root epidermis (Datta *et al*., 2011; Park and Nebenführ, 2013; Ketelaar, 2014). They function to increase root surface area, nutrient uptake and plant anchorage (Datta *et al*., 2011; Ichikawa *et al*., 2014; Zhao *et al*., 2014). In crop species higher root hair densities are considered an advantage (Datta *et al*., 2011; Müller and Bartelheimer, 2013)**.**

There are two main stages to root hair growth, initiation and elongation (Datta *et al*., 2011). In *Arabidopsis* root hairs emerge toward the basal end of the hair cells (here the basal end of the cell is defined as the one closest to the root tip), the precise positioning being affected by auxin (Foreman, 2001; Grebe *et al*., 2002; Cho, 2002). In the *ROOT HAIR DEFECTIVE6* mutant (*rhd6)* root hairs arise in a more apical position, but this can be partially rescued with exogenous auxin treatment (Masucci and Schiefelbein, 1994). In addition to this a reduced response to auxin in the *axr2-1* mutant also results in an apical shift in root hair position and the formation of more than one hair per root hair cell (Fischer *et al*., 2007). It is hypothesised that root hair position is orientated towards the auxin concentration maximum in the root tip, when this is disrupted in *AUX1* mutants an apical shift is also observed (Fischer *et al.*, 2007).

Once the site of root hair initiation has been established a bulge forms, this coincides with a decrease in pH, which is thought to be associated with the production of *EXPANSINs* (Ikeda *et al*., 2009; Datta *et al*., 2011). Both

EXPANSIN 7 and *EXPANSIN 8* are up-regulated by auxin treatment, and both are involved in root hair elongation (Cho, 2002).

Root hair elongation occurs via tip growth, once this process has begun the nucleus relocates to the root hair where it remains at a constant distance from the growing tip, if the nucleus moves away from this point elongation is blocked (Ketelaar, 2002). At the tip of the elongating root hair is dense cytoplasm and a large number of secretory vesicles that contain cell wall and membrane components (Datta *et al*., 2011). Next to this is an organelle rich area containing the golgi body, mitochondria and endoplasmic reticulum, these synthesise and transport the macromolecules required in the growing tip (Datta *et al*., 2011). The basal region of the root hair cell is vacuolated (Datta *et al*., 2011).

Downstream of *RHD6,* several genes promote hair elongation, these include, *ROOT HAIR DEFECTIVE 6 LIKE 4 (RSL4)* and *LJRHL-I-LIKE 3 (LRL3)* (Datta *et al*., 2011). *RSL4* in particular is interesting because whilst loss-of-function mutants result in shorter root hairs, over expression mutants result in root hairs that grow continuously (Yi *et al*., 2010). In addition to root hair initiation auxin also plays a role in root hair elongation (Pitts *et al*., 1998). Treatment with exogenous auxin results in significant root hair elongation, whilst auxin signalling mutants like *axr3-1* result in short or glabrous root hair phenotypes (Pitts *et al*., 1998). Auxin also positively regulates the expression of *RSL4* and in addition to this, *RSL4* is required for auxin-stimulated root hair growth (Yi *et al*., 2010; Datta *et al*., 2011).

Interestingly, mutations in different components of the auxin response network result in different root hair phenotypes. Whilst semi-dominant Domain II stabilising mutations in *IAA17* result in a greatly reduced number of root hairs, the same mutation in *IAA2* results in an increase in root hair length (Knox *et al*., 2003). In addition to this when driven by the same inducible promoter, *IAA17* still blocks root hair production whilst *IAA2* results in much longer root hairs, indicating that

these Aux/IAAs are likely to be interacting with different ARFs, which in turn may be targeting distinct auxin response genes (Del Bianco and Kepinski, 2011).

Nutrient and water uptake are two of the most important functions of root hairs. Root hairs have influx channels and transporters for a vast array of substances including; phosphate, sulphate, peptides, calcium, urea, ammonium, water and potassium (Datta *et al*., 2011). In addition to enhancing acquisition of these compounds, root hair development is affected by nutrient availability; deficiencies in phosphate, nitrate, potassium and iron all result in various forms of increased root hair growth. For example, under phosphate deficient conditions root hair density is increased and they can reach up to three times their normal length (Datta *et al*., 2011).

Root hairs are also required for secretion and plant anchorage (Datta *et al*., 2011). They have been shown to modify the rhizosphere by exuding organic compounds like organic acids that function to aid various processes, including nutrient mobilisation and growth inhibition of pathogens and/or neighbouring plants (Gahoonia and Nielsen, 2003; Yan *et al*., 2004; Datta *et al*., 2011).

1.5 Root epidermal patterning

The root epidermis is made of two cell types, hair cells and non-hair cells (Schiefelbein *et al*., 2009). In *Arabidopsis* these arise in a position dependent manner in relation to the underlying cortex cells thereby resulting in an alternating pattern of hair and non-hair files that transverse the length of the root (Figure 1-6) (Schiefelbein *et al*., 2009; Datta *et al*., 2011). The positional signalling that results in this arrangement is hypothesised to provide continuous input, as late changes in a cell position often also result in a change of cell fate (Costa and Shaw, 2006; Costa and Shaw, 2007; Schiefelbein *et al*., 2009). In addition to producing or not-producing a root hair these two cell types also differ in size, cell division, vacuolation and cytoplasmic density (Kwak and Schiefelbein, 2007; Schiefelbein *et al*., 2009).

In different species root epidermal cells are patterned differently. For example, in some species any cell can develop as a hair, whilst in others they develop in an alternating manner along the length of the root (Figure 1-6) (Datta et al., 2011).

1.5.1 Positional signalling

One benefit of using the root epidermis to study the relationship between developmental patterning and auxin response is these two cell types, another is that the genetic network which patterns this tissue is well characterised

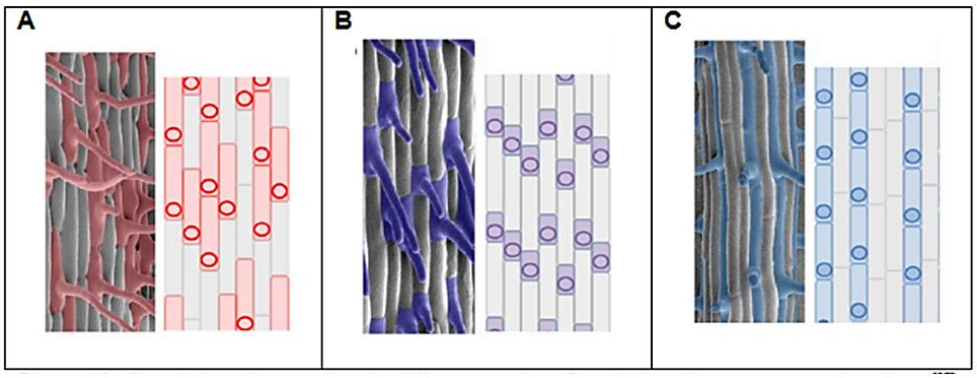

Figure 1-6: Root epidermal cell patterning in different species

Adapted from Datta *et al*., 2011, a combination of scanning electron microscope images (left) and schematic diagrams (right) indicate the epidermal cell arrangement in different species. A: Any cell can develop as a hair cell i.e. *Oryza sativa*. B: Hair and non-hair cells develop alternately along a cell file i.e. *Brachypodium distachyon.* C: Hair cells develop according to the underlying cortex cells i.e. *Arabidopsis*.

(Figure 1-7). The location of hair and non-hair cells is determined by positional signalling. Hair cells arise over the junction between two underlying cortical cells while non-hair cells occur where there is not a junction. In the cortex layer *JACKDAW (JDK)* promotes the expression of *SCRAMBLED (SCM)* in the space between two cortex cells (Figure 1-7) (Hassan *et al*., 2010). In this position *SCM* then inhibits the expression of *WEREWOLF (WER)*. Thus in cells with no underlying cortical cell junction, the expression of WER is not inhibited and a non-hair cell is formed (Kwak and Schiefelbein, 2008; Kang *et al*., 2009).

1.5.2 Lateral inhibition

A further method to reinforce the correct positioning of hair and non-hair cells is lateral inhibition. Several components of the epidermal patterning mechanism are produced in either the hair or non-hair cells and then move across into the adjacent cell of a different type (Figure 1-7) (Schiefelbein *et al*., 2009; Kang *et al*., 2009). For example although the expression of *CAPRICE (CPC)* is promoted in the non-hair cells it then moves across into the hair cells where it functions by inhibiting the formation of the non-hair promoting complex (Kurata *et al*., 2005). This results in very ordered and regulated patterning of the root epidermis, so much so that if *SCM* gene function is lost in a knock out mutant, hair and non-hair cells often continue to develop in an alternating pattern (Kwak and Schiefelbein, 2007). Indicating that root epidermal cell patterning is dependent on the mutual support of both cell types, in particular the movement of CPC and GL3 has been highlighted as important (Savage *et al*., 2008).

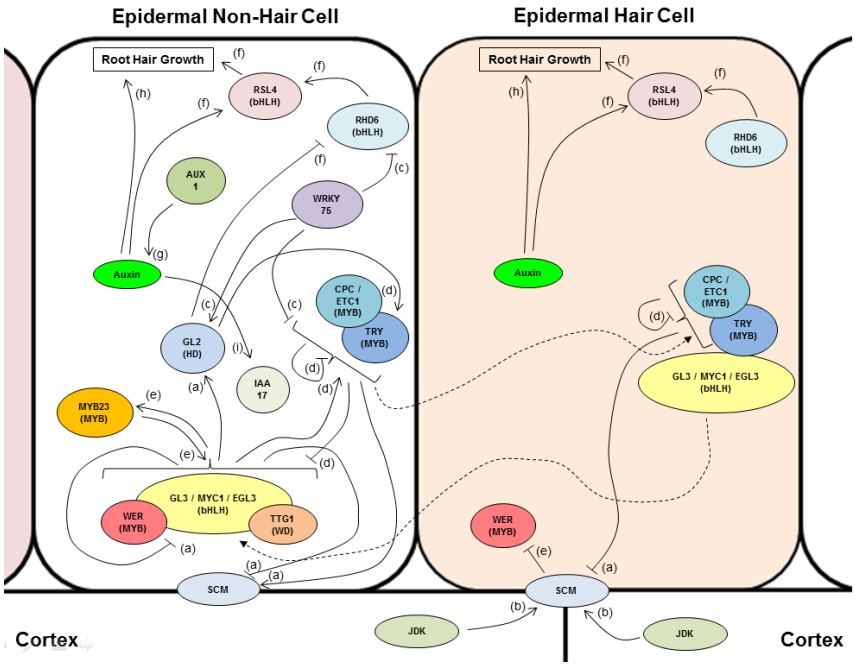

Figure 1-7: A schematic representation of the epidermal patterning mechanism.

The epidermal patterning mechanism according to the most recently published data. Regulation of the development of a hair or non-hair cell starts in the underlying cortex layer. The strength of signal from *JDK* promotes the expression of *SCM* in the gap between two cortex cells. In this position SCM inhibits the expression of *WER* and thereby promoting the formation of a hair cell. In the cells where there is not an underlying cortical cell junction *WER* expression is not inhibited and WER works in conjunction with GL3, EGL3, MYC1 and TTG1 to promote the expression of *MYB23, GL2, CPC, ETC1* and *TRY.* Whilst *MYB23* and *GL2* both promote the non-hair cell fate, CPC, ETC1 and TRY move into adjacent hair cells and promote the hair cell fate by inhibiting formation of the non-hair promoting complex. Downstream of *GL2 RLS4* and *RHD6* promote root hair production. Recently described *WRKY75*, functions to both inhibit and promote components of the epidermal patterning mechanism and the hair promoting component *RHD6*. It is worth remembering that this schematic representation doesn't indicate the different developmental time points in which these genes are expressed, and therefore relative amounts of the genes indicated here may vary depending on the stage of root development. Solid lines indicate promotion (arrow head) or inhibition (flat head), dashed lines indicate movement in the direction of the arrow head. Letters next to the arrows indicate the published source of the interaction. (a) (Kwak and Schiefelbein, 2008) (b) (Hassan et al., 2010) (c) (Rishmawi et al., 2014) (d) (Simon et al., 2007) (e) (Kang et al., 2009) (f) (Yi et al., 2010) (g) (Jones et al., 2009) (h) (Masucci and Schiefelbein, 1996) (i) Tromas and Perrot-Rechenmann 2010.

1.5.3 Key root epidermal patterning components

As detailed previously in the hair cells SCM inhibits the expression of the MYB type transcription factor *WEREWOLF (WER)* (Kwak and Schiefelbein, 2007; Kwak and Schiefelbein, 2008). In epidermal cells that are not positioned over a cortical cell junction *WER* transcription is not inhibited leading to the formation of a non-hair cell. In the non-hair cells WER interacts with TRANSPARENT TESTA GLABRA1 (TTG1), GLABRA3 (GL3), MYC1 and ENHANCER OF GLABRA3 (EGL3) to form a key non-hair promoting transcription factor complex (Ohashi *et al*., 2003; Schiefelbein *et al*., 2009). This complex promotes the non-hair cell fate via the positive regulation of *GLABRA2 (GL2)*, which in turn represses the transcription of root hair promoting genes such as *RHD6* (Masucci and Schiefelbein, 1994). This complex also positively regulates the expression of *MYB23,* which undergoes a positive feedback loop with itself and *WER*, thus reinforcing the non-hair cell fate (Kang *et al*., 2009). In *myb23-1* mutants the epidermal cells are less likely to adopt the correct cell fate in positional changes that occur later in the root development, this is clearest when a T-Junction occurs (Kang et al., 2009). A T-Junction is observed when a longitudinal anticlinal cell division occurs and a change in position can result in a change of cell fate, known as transdifferentiation (Costa and Shaw, 2006; Costa and Shaw, 2007; Schiefelbein *et al*., 2009). Under wild-type circumstances cells quickly and reliably adopt the correct new epidermal cell identity, however in a *myb23-1* mutant the cell identity is often incorrect (Figure 1-8) (Kang *et al*., 2009).

In addition to promoting the non-hair cell fate the non-hair promoting complex also promotes the expression of several one repeat MYB genes that promote the hair cell specification, these are *CAPRICE (CPC), TRIPTYCHON (TRY)* and *ENHANCER OF TRIPTYCHON1 (ETC1)* (Ryu *et al*., 2005*;* Schiefelbein *et al*., 2009; Pesch *et al*., 2013). Despite being produced in the non-hair cells these proteins relocate to the adjacent hair cells, where they function to repress the

non-hair complex formation and thereby promote the hair cell fate (Savage *et al*., 2008).

It is likely that a similar patterning mechanism plays a role throughout the entire plant. With the exception of *SCM*, the majority of the root epidermal patterning components also affect patterning in other areas of the plant (Schiefelbein *et al*., 2009). For example, in a *cpc-1 try-82* double mutant excessive trichome production is observed, whilst *GL2* and *TTG1* are also known to affect trichome formation (Schiefelbein *et al*., 2009; Kang *et al*., 2009; Seo *et al*., 2011). In addition to this recently published findings have indicated that *WER* has a role in floral development (Schiefelbein *et al.*, 2009; Kang *et al*., 2009; Seo *et al*., 2011).

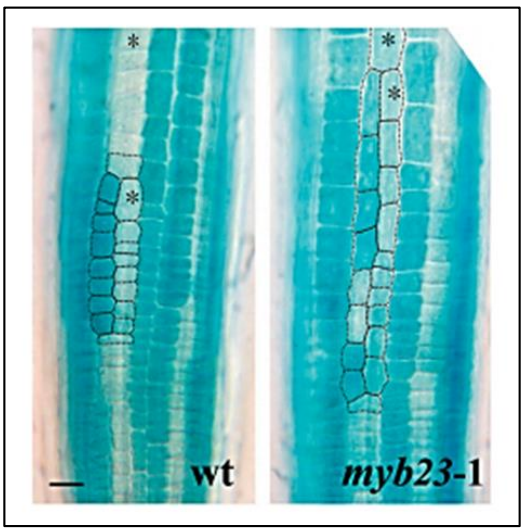

Figure 1-8: *pGL2::GUS* expression in the *myb23-1* in comparison to the wild-type.

Figure adapted from Kang *et al.,* 2009, Figure 8. *pGL2::GUS* highlights non-hair files. Expression in wild-type and *myb23-1* mutant roots indicates altered cell patterning in a *myb23-1* mutant when a T-junction occurs. Instead of the tightly controlled differentiation into a hair or non-hair file, as is observed in the wild-type, the cell identity appears more random. Asterisks indicate the hair cell files. Scale bar represents 20 µm.

1.6 Auxin response in the root epidermis

The concept of a differential auxin response between the hair and non-hair files of the root epidermis is apparent in both published and unpublished data. In 2009 Jones *et al* investigated the expression of the *pDR5::GFP* marker in the root epidermis. *pDR5::GFP* consists of 7 AuxREs driving a green fluorescent protein (GFP) and is a reporter of auxin signalling output. In 2009 Jones *et al* described a higher level of *pDR5::GFP* signal in the non-hair files of the root epidermis (Jones *et al*., 2009). This was consistent with an interesting pattern of expression of the auxin influx carrier AUX1, Jones *et al* found that a translational *pAUX1::AUX1-YFP* reporter was expressed almost exclusively in the non-hair cells (Jones *et al*., 2009). Because auxin is known to affect root hair growth and therefore, ultimately, hair cells, *pDR5::GFP* expression in the root epidermis was investigated further (Figure 1-9). This unpublished analysis carried out by Dr Martin Kieffer indicated that whilst *pDR5::GFP* expression was initially higher in the non-hair cells, at the transition zone expression equalises between all of the files and after this point it persists with greater strength in the hair files as they transit the elongation and differentiation zone.

In order to consider the impact of the differential AUX1 expression on these results the *pDR5::GFP* marker was treated with the synthetic auxin 2,4-D. Jones *et al*, predicted that due to the preferential localisation of AUX1 in the non-hair files the auxin concentration in these cells maybe up to ten fold of that present in the hair cells (Jones *et al*., 2009). Treatment with 2,4-D was informative because whilst 2,4-D is efficiently transported into cells via auxin influx proteins, it is a poor substrate for the auxin efflux carriers (Delbarre, 1994). Thus 2,4-D treatment of *pDR5::GFP* plants would be predicted to result in higher GFP signal in non-hair cells relative to hair cells. The fact that higher levels of GFP signal were observed in hair cells compared to neighbouring non-

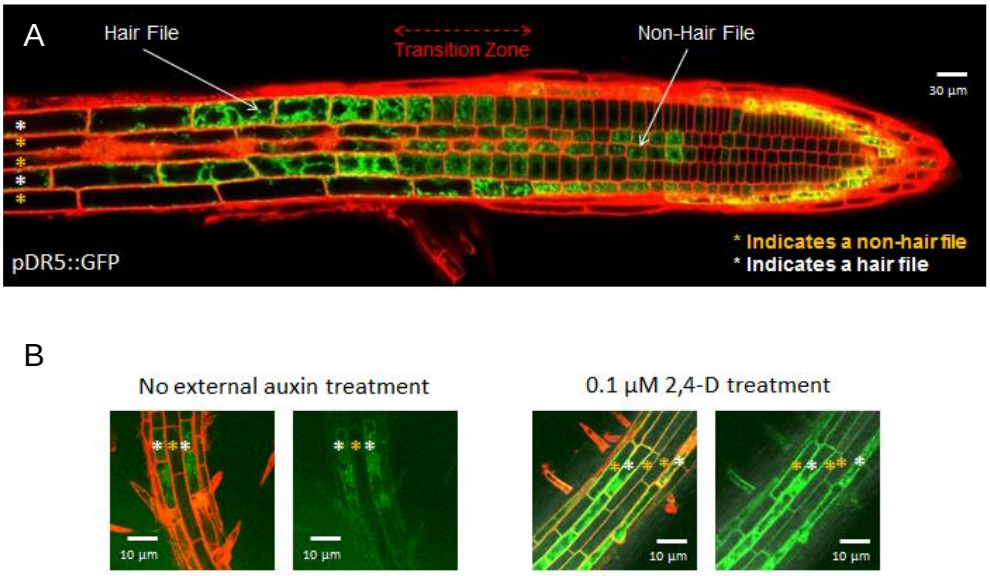

Figure 1-9: Expression of the *pDR5::GFP* marker in the root epidermis.

The *pDR5::GFP* marker indicates auxin signalling output. A: In the root epidermis *pDR5::GFP* expression is initially higher in the non-hair cells, at the transition zone this differential expression is lost and after this point it persists with greater strength in the hair cells. B: To investigate the effect of auxin concentration on this differential expression roots were treated with the synthetic auxin 2,4-D. 2,4-D is unable to leave epidermal cells therefore over a period of prolonged treatment the level of auxin in the root epidermis equalises. The differential expression of *pDR5::GFP* was still apparent after 2,4-D treatment indicating that the hair and non-hair cells in the root epidermis have a different capacity to respond to auxin. Images and analysis courtesy of Dr Martin Kieffer. Scale bars are labelled accordingly. White * indicate hair files whilst Orange * indicate non-hair files.

hair cells indicates that these two cell types of the root epidermis have a different inherent capacity to respond to auxin.

In addition to this, unpublished transcriptomic data of Dr Matrin Kieffer's also indicated that some components of the auxin response network were expressed differentially between the hair and non-hair cells. Two key genes displaying significant differences in expression levels between hair and non-hair cells were the Aux/IAA repressor protein *IAA17* and the repressing ARF, *ARF10.* In order to confirm this differential expression, GFP transcriptional and translational marker lines for both genes were produced and analysed.

Analysis of the *IAA17* marker by Dr Martin Kieffer indicated that *IAA17* expression begins earlier and stronger in the non-hair files of the root epidermis (Figure 1-10). Around eight cells later expression reaches a similar level in the hair files. *ARF10* expression was found to be consistently stronger in the non-hair files from the root tip (Figure 1-11). Taken in conjunction with the high DR5 expression in the hair files after the transition zone these data indicated the potential of a repressive auxin response regime in the non-hair files of the root epidermis.

How these differences in auxin response in the root epidermis are patterned remains poorly understood. In addition, the functional significance of these are unclear. Although both the epidermal patterning mechanism and the auxin response network are well characterised in has long be accepted that auxin acts downstream of the epidermal patterning mechanism. In 1996 a paper published by Masucci *et al* first looked the concept of these two pathways working together. One of their primary experiments used the *rhd6, ttg1-1* and *gl2*-1 mutants. Whilst the *rhd6* mutant exhibits significantly fewer root hairs this can be rescued by exogenous auxin treatment but the *gl2*-1 and *ttg1-1* mutants produce root hairs from every root epidermal cell (Masucci and Schiefelbein, 1996). In order to establish the relationship between these two pathways they

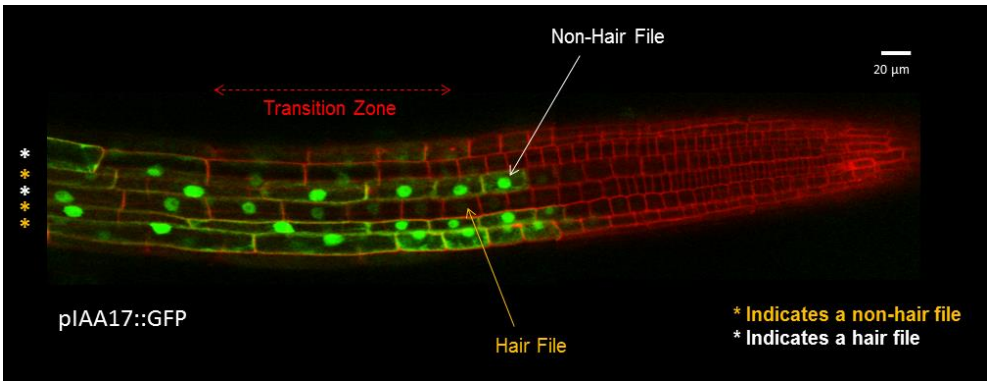

Figure 1-10: Expression of the *pIAA17::GFP* marker in the root epidermis.

The *pIAA17::GFP* transcriptional maker indicates differential expression of *IAA17* in the hair and non-hair files of the root epidermis. *IAA17* expression begins around the start of the transition zone in the non-hair cells and then approximately eight cells later it reaches a smilar fluorescence level in the hair files. Scale bars are labelled accordingly. White * indicate hair files whilst Orange * indicate non-hair files.

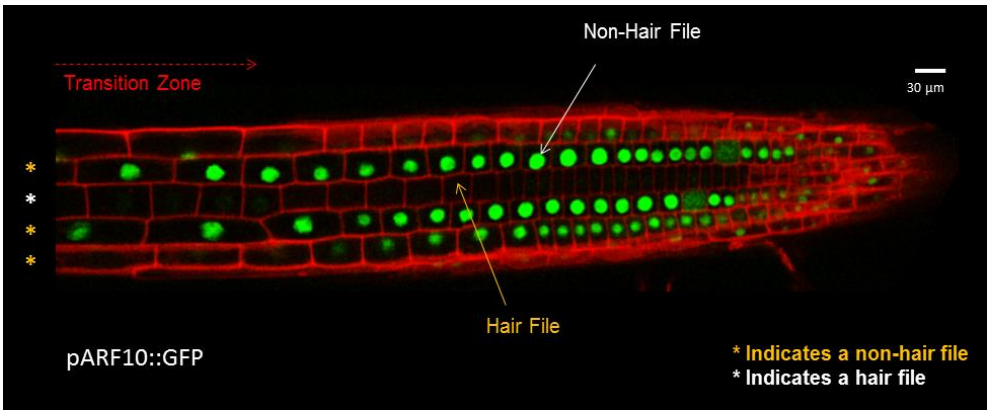

Figure 1-11: Expression of the *pARF10::GFP* marker in the root epidermis

The *pARF10::GFP* transcriptional maker indicates differential expression of *ARF10* in the hair and non-hair files of the root epidermis. Strong *ARF10* expression in the non-hair cells is apparent from the tip. Scale bars are labelled accordingly. White * indicate hair files whilst Orange * indicate non-hair files.

generated double *ttg1-1 rhd6* and *gl2-1 rhd6* mutants (Masucci and Schiefelbein, 1996). As auxin was able to rescue the *rhd6* mutant phenotype in these double mutants they concluded that auxin did not act through a pathway that required the *GL2* or *TTG1* gene products and therefore must act downstream of this epidermal patterning mechanism (Masucci and Schiefelbein, 1996). Since 1996 understanding of the epidermal patterning mechanism and the auxin response network has increased, however this proposed separate method of action has remained consistent.

In addition to the apparent repressive auxin response regime in the non-hair files, unpublished microarray data generated in the Kepinski lab before this project began indicated that auxin down-regulated both *MYB23* and *GL2.* This preliminary data indicated that the relationship between the epidermal patterning mechanism and the auxin response network in the root epidermis had the potential to be more complex than was currently accepted.

1.7 Project aims

Against the background detailed, the overall aim of this project was to define the links between epidermal patterning and auxin responsiveness in the root epidermis of *Arabidopsis.* In order to do this the following objectives were considered:

1) To establish the functional significance of the apparent repressive auxin response regime in the non-hair cells of the root epidermis.

2) To place the spatial control of auxin response in the current knowledge of the epidermal patterning mechanism.

3) To investigate feedback loops and direct links between components of the epidermal patterning mechanism and the auxin response network.

4) To investigate the role of auxin-mediated down-regulation of *GL2* and *MYB23*.

2 : Materials and Methods

2.1 Plant lines and sources

Various *Arabidopsis* lines were used during this project (Table 2-1). Some were acquired from the National Arabidopsis Stock Centre (NASC) and the Leeds University Plant Growth Suite (PGS), the majority were produced during this project.

Arabidopsis Line	Source
Col, WT	PGS
Ler, WT	Dr Josh Neve Kepinski Lab Member
Ws-0,WT	NASC (National Arabidopsis Stock Centre)
cpc-1-1 try-82, pWER-1::GFP	Professor Claire Grierson, Bristol University
gl2-1, pWER-1::GFP	Professor Claire Grierson, Bristol University
cpc-1-1 try-82	Professor Claire Grierson, Bristol University
gl2-1-1	Dr Martin Kieffer Kepinski Lab Member
cpc-1-1	Dr Martin Kieffer Kepinski Lab Member
wer-1-1	Dr Martin Kieffer Kepinski Lab Member
ttg1-1	NASC
gl3-1 egl3-1	NASC
myb23-1-1	NASC
wer-1-1 myb23-1-1	Produced During This Project
pARF10::ARF10-GFP	Dr Martin Kieffer Kepinski Lab
pIAA17::IAA17-GFP	Dr Martin Kieffer Kepinski Lab
pARF10::GFP	Dr Martin Kieffer Kepinski Lab Member
pAUX1::AUX1-YFP	Professor Claire Grierson, Bristol University

pIAA17::GFP	Dr Martin Kieffer Kepinski Lab Member
pDR5::GFP	Dr Martin Kieffer Kepinski Lab Member
arf10-3 arf016-2	Dr Mata Del Bianco Kepinski Lab Member
gl2-1,DR5::GFP (L3-2)	Produced During This Project
WT,DR5::GFP (CTRL7-2)	Produced During This Project
cpc-1,DR5::GFP (L2-2)	Produced During This Project
WT,DR5::GFP (CTRL4-3)	Produced During This Project
gl2-1,pARF10::GFP (X1)	Produced During This Project
WT,pARF10::GFP (CTRL1)	Produced During This Project
cpc-1,pARF10::GFP (L1-8)	Produced During This Project
WT,pARF10::GFP (CTRL12)	Produced During This Project
Col WS	Produced During This Project
WS Ler	Produced During This Project
Ler Col	Produced During This Project
myb23-1,DR5::GFP (X5)	Produced During This Project
WT,DR5::GFP (CTRL8)	Produced During This Project
myb23-1,pIAA17::GFP(C1-2)	Produced During This Project
WT,pIAA17::GFP(CTRL)	Produced During This Project
myb23-1,pAUX1::AUX1-YFP()	Produced During This Project
WT,pAUX1::AUX1-YFP (CTRL1)	Produced During This Project
myb23-1,pARF10::GFP (C3-1)	Produced During This Project
WT,pARF10::GFP (CTRL)	Produced During This Project

cpc-1,pIAA17::IAA17-GFP(X4)	Produced During This Project
WT,pIAA17::IAA17-GFP(CTRL5)	Produced During This Project
gl2-1,pIAA17::IAA17-GFP(X6)	Produced During This Project
WT,pIAA17::IAA17-GFP(CTRL12)	Produced During This Project
wer-1,pIAA17::IAA17-GFP(X8)	Produced During This Project
WT,pIAA17::IAA17-GFP(CTRL1)	Produced During This Project
aux1-22,pIAA17::IAA17-GFP(X6)	Produced During This Project
WT,pIAA17::IAA17-GFP(CTRL9)	Produced During This Project
aux1-7,pIAA17::IAA17-GFP(X4)	Produced During This Project
WT,pIAA17::IAA17-GFP(CTRL6)	Produced During This Project
myb23-1,pARF10::ARF10-GFP(x8-2)	Produced During This Project
WT,pARF10::ARF10-GFP(CTRL)	Produced During This Project
cpc-1,pARF10::ARF10-GFP(X7)	Produced During This Project
WT,pARF10::ARF10-GFP(CTRL2)	Produced During This Project
cpc-1 try-82,pARF10::ARF10-GFP(X9)	Produced During This Project
WT,pARF10::ARF10-GFP(CTRL9)	Produced During This Project
gl2-1,pARF10::ARF10-GFP(X4)	Produced During This Project
WT,pARF10::ARF10-GFP(CTRL5)	Produced During This Project
wer-1,pARF10::ARF10-GFP(X22)	Produced During This Project
(WT),pARF10::ARF10-GFP(CTRL16)	Produced During This Project
aux1-22,pARF10::ARF10-GFP(X4)	Produced During This Project
(WT),pARF10::ARF10-GFP(CTRL5)	Produced During This Project
aux1-7,pARF10::ARF10-GFP(X5)	Produced During This Project
(WT),pARF10::ARF10-GFP(CTRL12)	Produced During This Project

pGL2::GFP,arf10-3 arf16-2 (X1)	Produced During This Project
pGL2::GFP,WT (CTRL11)	Produced During This Project
pWER::GFP,arf10-3 arf16-2 (X1)	Produced During This Project
pWER::GFP,WT (CTRL4)	Produced During This Project
pWER::WER-GFP,arf10-3 arf16-2 (X3-2)	Produced During This Project
pWER-1::WER-1-GFP,WT(CTRL11)	Produced During This Project
myb23-1 gl2-1 (5)	Produced During This Project
WT (CTRL3)	Produced During This Project
myb23-1 arf10-3 arf16-2 (x8-4)	Produced During This Project
WT (CTRL)	Produced During This Project
wer-1 myb23-1,pIAA17::IAA17-GFP(x6)	Produced During This Project
WT,pIAA17::IAA17-GFP(CTRL6)	Produced During This Project
gl2-1 axr3-10	Produced During This Project
WT (CTRL 11)	Produced During This Project
DR5::GFP,arf10-3 arf16-2 (x1)	Produced During This Project
DR5::GFP,(WT) (CTRL5)	Produced During This Project
axr3-10,DR5::GFP(6)	Produced During This Project
WT,DR5::GFP (CTRL9)	Produced During This Project
aux1-104,pARF10::GFP (X1)	Produced During This Project
(WT),pARF10::GFP (CTRL3)	Produced During This Project
aux1-21,pARF10::GFP(X5)	Produced During This Project
aux1-21,pARF10::GFP(CTRL4)	Produced During This Project
aux1-104,pARF10::ARF10-GFP(X1)	Produced During This Project

aux1-104,pARF10::ARF10-GFP(CTRL10)	Produced During This Project
aux1-21,pARF10::ARF10-GFP(X1)	Produced During This Project
aux1-104,pARF10::ARF10-GFP(CTRL6)	Produced During This Project
wer-1 myb23-1, pDR5::GFP (x2)	Produced During This Project
(WT),DR5::GFP (CTRL2-5)	Produced During This Project
wer-1 myb23-1,pARF10::GFP (x6)	Produced During This Project
(WT),pARF10::GFP (CTRL)	Produced During This Project
wer-1 myb23-1,pIAA17::GFP (x1-6)	Produced During This Project
(WT),pIAA17::GFP (CTRL7-6)	Produced During This Project
wer-1 myb23-1,pARF10::ARF10-GFP(x1)	Produced During This Project
(WT),pARF10::ARF10-GFP(CTRL1)	Produced During This Project
cpc-1 try-82,DR5::GFP (X2)	Produced During This Project
(WT),DR5::GFP (CTRL1)	Produced During This Project
aux1-22,DR5::GFP(X3)	Produced During This Project
(WT),DR5::GFP (CTRL5)	Produced During This Project
cpc-1 myb23-1 (x3-1)	Produced During This Project
WT (CTRL4)	Produced During This Project
gl2-1 arf10-3 arf16-2 (x3)	Produced During This Project
WT(CTRL7-12)	Produced During This Project
pWER-1::MYB23-1,wer-1	Professor John Schiefelbein, University of Michigan
pWER-1::MYB23-1,cpc-1	Produced During This Project
pWER-1::MYB23-1,gl2-1	Produced During This Project

pWER-1::MYB23-1,myb23-1	Produced During This Project
aux1-7,DR5::GFP (X5)	Produced During This Project
WT,DR5::GFP (CTRL11)	Produced During This Project
gl2-1,pIAA17::GFP(X1)	Produced During This Project
(WT),pIAA17::GFP (CTRL2)	Produced During This Project
cpc-1,pIAA17::GFP(X1)	Produced During This Project
(WT),pIAA17::GFP(CTRL5)	Produced During This Project
cpc-1 try-82,pIAA17::GFP(X2)	Produced During This Project
(WT),pIAA17::GFP(ctrl6)	Produced During This Project
aux1-22,pIAA17::GFP(X2-10)	Produced During This Project
(WT),pIAA17::GFP(CTRL2-4)	Produced During This Project
aux1-7,pIAA17::GFP(X3)	Produced During This Project
(WT),pIAA17::GFP(CTRL1)	Produced During This Project
cpc-1 try-82,pAUX1::AUX1-YFP(X1)	Produced During This Project
(WT),pAUX1::AUX1-YFP(CTRL4)	Produced During This Project
wer-1,pARF10::GFP (X2)	Produced During This Project
(WT),pARF10::GFP (CTRL9-1)	Produced During This Project
cpc-1 try-82,pARF10::GFP (X2)	Produced During This Project
(WT),pARF10::GFP (CTRLC4)	Produced During This Project
aux1-22,pARF10::GFP (X8-2)	Produced During This Project
(WT),pARF10::GFP (CTRL4-2)	Produced During This Project
aux1-7,pARF10::GFP (X5)	Produced During This Project
(WT),pARF10::GFP (CTRL3)	Produced During This Project
wer-1,DR5::GFP(X2)	Produced During This Project

(WT),DR5::GFP (CTRL5-1)	Produced During This Project
wer-1,pIAA17::GFP (X2)	Produced During This Project
(WT),pIAA17::GFP (CTRL2)	Produced During This Project
wer-1,pAUX1::AUX1-YFP (X4)	Produced During This Project
(WT),pAUX1::AUX1-YFP (CTRL3)	Produced During This Project
pARF10F1 Promoter Truncation	Produced During This Project
pARF10F2 Promoter Truncation	Produced During This Project
pARF10F3 Promoter Truncation	Produced During This Project
pEXP7::MYB23-1	Produced During This Project
pCOBL9::MYB23-1	Produced During This Project
pMYB23-1::MYB23-1-GFP	Produced During This Project
pGL2-1::GFP,gl2-1 (x3)	Produced During This Project
pGL2-1::GFP,WT (C1)	Produced During This Project
pGL2-1::GFP	NASC
pWER-1::MYB23-1 wer-1 (Segregating)	Professor John Schieflebein University of Michigan
pWER-1::MYB23-1,wer-1(8)	Homozygote line selected during this project.

Table 2-1: *Arabidopsis thaliana* lines used in this project and the source from whence they were acquired.

2.2 Plant growth conditions

Plants were grown under long day conditions (16 hours light / 8 hours dark) at a temperature of 20-22 °C. Variations in these conditions included the following:

2.2.1 Growth rooms

Sterile seeds were sown on circular Sarstedt 92 x 16 mm petri dishes with 30 ml of growth media or square Greiner Bio-One 120 x 120 x 17 mm petri dishes with 50 ml of growth media. Plates were sealed with two layers of micro porous tape.

2.2.2 Walk-ins

Plants were grown in a controlled light intensity of 200 µmol m-2 s-1 on circular Sarstedt 92 x 16 mm petri dishes with 30 ml of growth media or square Greiner Bio-One 120 x 120 x 17 mm petri dishes with 50 ml of growth media. Plates were sealed with two layers of micro porous tape.

2.2.3 Greenhouses

Plants were grown in a 3:1 soil to sand mix. They were planted in trays with 12 individual cells measuring 55 x 50 x 55 mm or individual plastic plant pots measuring 90 x 90 x 95 mm. Unsterilised seeds were sown on damp soil and covered with a propagator hood with aluminium foil and cold treated for 1-3 days at 4 °C. They were then relocated to the greenhouses and the aluminium foil and propagator hoods were removed.

2.3 Seed sterilisation methods and plant growth media

Seeds were sterilised using various methods and grown on different media depending on the particular requirement of the different assays.

2.3.1 Gas sterilisation

Cleaned seeds were placed in open 0.5 ml eppendorfs. They were sterilised with chlorine gas, which was created by adding 3 ml of Hydrochloric Acid (HCL) to 100 ml of household bleach in a sealed glass container. Seeds were left in these conditions for 3 hours before being put onto growth media and cold treated at 4 °C overnight or ventilated for 1 hour and stored at room temperature until required.

2.3.2 Liquid sterilisation

For liquid sterilisation the cleaned seeds were immersed in 70 % ethanol for 2 minutes, followed by 10 % bleach at room temperature for 30 minutes. After washing with sterile water at least 5 times, the seeds were either put onto growth media or kept at 4 °C in sterile water for up to one week.

2.3.3 Sterile growth media

Plants were grown on Arabidopsis Thaliana Salts (ATS) growth media; 5 mM KNO_3, 2.5 mM KH_2PO4, 2 mM $MgSO_4$, 2 mM $Ca(NO_3)_2$, 20 mM FE-EDTA, 1 ml/L of Micronutrients (70 mM H_3BO_3, 14 mM $MnCL_2$, 0.5 mM $CuS0_4$, 1 mM $ZnSO_4$, 0.2 mM $NaMoO_4$, 10 mM NaCl, 0.01 mM $CoCL_2$), 0.8 % plant agar and 1 % sucrose. The ATS was autoclaved and cooled to approximately 60 °C before

being poured into plates under sterile conditions in the PGS laminar flow hoods. The media was allowed to ‘dry’ for approximately 20 minutes before seeds were sown. Seeds were either sown individually using autoclaved cocktail sticks or suspended in autoclaved water and pipetted in dense lines. If the media was not required immediately it was stored for up to two weeks at 4°C. Occasionally variations to this basic ATS media were used, Table 2-2.

Variations	Method Alterations
With IAA	Preparation method as above with IAA was added before pouring. If not used immediately these plates were stored at 4 °C for a maximum of 48 hours before seeds were added.
With 2,4D	Preparation method as above with 2,4D was added before pouring. If not used immediately these plates were stored at 4 °C for a maximum of 48 hours before seeds were added.
High/Low Phosphorus	Prepared as detailed above with 0.8% phytagel instead of agar. The low phosphate media contained 0.2% of the KH_2PO4 with the remaining volume (99.8%) added in the form of KCL. Plates were used immediately.
Phytagel	Phytagel was in assays designed to measure root hair length. 0.6% phytagel was added instead of plant agar whilst the liquid was in motion.

Table 2-2: Variations in ATS growth media.

2.4 Root data collection techniques

2.4.1 Root hair length and density measurements

Plants were grown on sterile ATS (with phytagel) in PGS walk-in's for a period of 6-8 days. Plates (with lids removed) were then analysed using a Lecia M165C microscope. Images were taken and used to measure root hair length and density using Media Cybernetics Image-Pro Plus computer software.

A minimum of three plates were used for each assay, with controls and the lines of interest grown on the same plates. Roots were selected randomly across all of the plates and a minimum of 30 root hairs measured for each individual root. These 30 (or more) measurements were then averaged and an overall average from all of the roots analysed was generated.

When measuring root hair data the plants were grown on phytagel and in the walk-in's under low light conditions to minimise stress. Each assay was repeated at least three times before any conclusions were drawn.

2.4.2 Ectopic root hairs

Plants were grown on sterile ATS (with phytagel) in PGS walk-in's for a period of 6-8 days. Plates (with lids removed) were then analysed using a Lecia M165C microscope.

A minimum of three plates were used for each assay, with controls and the lines of interest grown on the same plates. Roots were selected randomly across all of the plates and a minimum of 100 root hairs were counted for each individual root.

These 100 (or more) measurements were then averaged and an overall average from all of the roots analysed was generated.

In order to assess the number of ectopic root hairs the number of hairs that appeared in a file next to another hair would be counted as 1 ectopic hair. Measurements started at the tip and 100 root hairs or bumps were counted up the root from that point.

2.4.3 Primary root length

Plants were grown on sterile ATS (with phytagel) in PGS walk-ins under strict light control (200 µmol m-2 s-1) for a period of 6-8 days. Root hair lengths were then measured using a transparent ruler through the media whilst the plates remained sealed. Plants were grown across a minimum of three plates and all of the roots were measured.

2.4.4 Root gravitropic response measurements (over 24 hours)

Plants were grown on sterile ATS (with phytagel) in PGS growth rooms for a period of 5 days, on day 5 the plates were rotated by 135 °. After 24 hours the plates were scanned using a HP Scanjet G4050 scanner, the images were increased by 200% and printed using a HP Laserjet 1320n. A transparent protractor was used to measure the angle change as a result of the 135 ° rotation.

2.4.5 Root gravitropic response measurements (continuous)

Plants were grown on sterile ATS (with phytagel) in PGS growth rooms for a period of 5 days, on day 5 a constant mark was placed next to the plant root on the media and the plates were rotated by 90°. Using the Lecia M165C microscope in conjunction with the Media Cybernetics Image-Pro Plus computer software a photograph was taken of the root at regular intervals (length depended on assay and ranged from every 10 to 30 minutes) up until a period of approximately 10 hours. The angle change of the root in these images was then calculated using Image J computer software.

2.4.6 Confocal microscopy

Confocal microscopy was used to observe fluorescence levels in the root epidermis. The analysis was carried out using an Upright Zeiss LSM 510 META Axioplan 2 Microscope, with Argon (477 nm) and HeNe1 (543 nm) lasers. Propidium Iodide (1 mg/ml) was used to stain the cell walls of the root epidermis and images were captured using both the 20 x (dry) and 40 x (oil) lenses. Different confocal settings were used for different marker lines, these were as follows:

- *pARF10::GFP, pIAA17::IAA17::GFP* and *pIAA17::GFP* (Master gain FITC Ch2 633 / Rhod Ch3 676, Digital gain FITC Ch2 1.00 / Rhod Ch3 1.00, Digital Offset FITC Ch2 0.00 / Rhod Ch3 0.00.)
- *pDR5::GFP* and *pARF10::ARF10-GFP* (Master gain FITC Ch2 1119 / Rhod Ch3 766, Digital gain FITC Ch2 1.00 / Rhod Ch3 1.00, Digital Offset FITC Ch2 0.00 / Rhod Ch3 -0.14.)
- *pGL2::GFP* (Master gain FITC Ch2 1081 / Rhod Ch3 896, Digital gain FITC Ch2 1.00 / Rhod Ch3 1.00, Digital Offset FITC Ch2 0.00 / Rhod Ch3 0.00.)
- *pWER::GFP* and *pWER::WER-GFP* (Master gain FITC Ch2 1081 / Rhod Ch3 766, Digital gain FITC Ch2 1.00 / Rhod Ch3 1.00, Digital Offset FITC Ch2 0.00 / Rhod Ch3 0.00.)

- pARF10::GFP promoter truncation lines (Master gain FITC Ch2 782 / Rhod Ch3 706, Digital gain FITC Ch2 1.00 / Rhod Ch3 1.00, Digital Offset FITC Ch2 0.00 / Rhod Ch3 -0.07.)

Images presented during this thesis are raw unless otherwise stated in figure legends.

2.5 Crossing techniques

2.5.1 Crossing

Arabidopsis lines were crossed soon after the plants had first bolted. When crosses consisted of a fluorescent marker line being crossed with a non-fluorescent mutant line, the non-fluorescent line was always used as the female line. When two mutant lines were crossed then the male and female line were chosen at random.

In the female line buds were selected just before they were about to open and the sepals, petals and stamens were removed using a MEIJI EMT 2248 microscope and Ideal-tek 5.SA forceps. Approximately 4 or 5 buds would be prepared in this way and the rest of the flowers and siliques removed. From the male line an open flower would be chosen and the stamen removed using the Ideal-tek 5.SA forceps, these would then be used to brush pollen onto the prepared female line using the MEIJI EMT 2248 microscope to ensure accurate pollen transfer. This would be repeated the following day, the stigma's would then be left to develop into a mature siliques.

2.5.2 Selection of an F1 generation

If a fluorescent marker was used seedlings were sown on sterile plates and checked for fluorescent expression using an Olympus SZX12 GFP Microscope. Those with fluorescent expression were selected and transferred to soil to self-fertilise and produce the F_2 generation.

If no fluorescent marker was used F1 seeds would be chosen at random and sown on soil to produce an F_2 generation.

2.5.3 Selection of an F2 generation

If the lines crossed had a visible phenotype or fluorescent expression they were sown on sterile plates and selected for 12 of the best cross and 12 of the best control candidates. These were then transferred to soil to produce the F3 generation.

If there were no easily identifiable phenotypes F2 seeds were sown directly onto soil in preparation for genotyping. The numbers sown would be determined by the chance of getting a perfect homozygote line, i.e. in a triple mutant this would be 1/64. These were then genotyped using the Edwards Prep DNA extraction method and PCR.

If every case it was necessary to select not only for a homozygote cross but also a homozygote control. This was essential for accurate analysis as it ensured that different backgrounds were not influencing fluorescence expressions or phenotypes.

2.5.4 Selection of an F3 generation

Lines that were selected on the basis of phenotypes were sown on sterile plates and analysed for homozygote lines. For example, in the *gl2-1*,*pDR5::GFP* cross I would need a homozygote line in which every plant carried the *gl2-1* mutation and *pDR5::GFP* marker and a homozygote control line in which every plant was wild-type but also carried the *pDR5::GFP* marker.

If a homozygote line was not apparent at this point plants from the F2 generation would be reselected or F3 plants self-fertilised to produce an F4 generation if a partial line was present, i.e. homozygote for one mutation but segregating the second.

2.5.5 BASTA selection

BASTA selection was used under various circumstances. Some lines supplied to me by other research groups and Kepinski lab members were BASTA (D-phosphinothricin, Melford ®) resistant. In order to establish homozygote lines seeds were grown on ATS with BASTA included in the media at a concentration of 10 µg/ml.

BASTA was also used as a selection during the making of constructs in which the fluorescent seed coat marker could not be used. In this instance BASTA was sprayed onto the plants at a concentration of 100 mg/L just after the seeds germinated and then again after possible positives have been selected.

2.6 DNA extraction and amplification

DNA extraction, amplification and analysis were used at many points throughout this project. These included genotyping for mutations where no visible phenotype was apparent and generating fragments for cloning.

2.6.1 Edwards prep DNA extraction from leaf tissue

Plant material was collected using a 1.5 ml eppendorf cap. 400 µl of extraction buffer (200 mM Tris-HCL pH 7.5, 250 mM NaCl, 25 mM EDTA,0.5 % SDS) was added and the sample ground for 15 seconds. A phenol extract (one volume of phenol:chloroform:isoamyalchohol 24:24:1) was performed and the supernatant transferred to a fresh tube. The sample was then precipitated with 300 µl isopropanol and centrifuged for 20 minutes. After the supernatant was discarded the pellet was then washed with 100 µl of 70% ethanol, centrifuged for 1 minute and the supernatant removed. The pellet was re-suspended in 20 µl TE Buffer (10Mm Tris-Cl, pH7.5, 1mM EDTA) and RNAase A (20 mg/ml).

2.6.2 Polymerase chain reaction (PCR)

PCR conditions varied depending on which DNA polymerase was used. The typical reaction components and cycle conditions are detailed in Table 2-3 and Table 2-4.

Additional Components	Polymerase		
	Phusion 1 µl	**Velocity 0.5 µl**	**Red Taq 2 µl**
(20-50 ng) Genomic DNA	1 µl	1 µl	2 µl
10 µM Forward Primer	5 µl	5 µl	5 µl
10 µM Reverse Primer	5 µl	5 µl	5 µl
Buffer	20 µl	20 µl	10 µl
2 mM dNTP	10 µl	10 µl	10 µl
Sterile Water	58 µl	58.5 µl	63 µl
50 mM $MgCl_2$	2-4 µl if not working	2-4 µl if not working	3µl
DMSO	3-10 µl if not working	3-10 µl if not working	-

Table 2-3: PCR mixture components with different DNA polymerases.

Cycle	Polymerase		
	Phusion	**Velocity**	**Red Taq**
Initial Denaturation	98 °C 2’	98 °C 2’	95 °C 3’
Denaturation	98 °C 30’’	98 °C 30’’	95 °C 1’
Primer Annealing	Primer Dependant Temperature 30’’	Primer Dependant Temperature 30’’	Primer Dependant Temperature 30’’
Elongation	72 °C (30’’/KB)	72 °C (15’’/KB)	72 °C (30’’/KB)
Final Elongation	72 °C3’	72 °C3’	72 °C3’
Cycle End	10 °C5’	10 °C5’	10 °C5’

Table 2-4: PCR reaction cycles.

2.6.3 Agarose gel electrophoresis

Gels were used at various concentrations depending on the specific requirements. These concentrations ranged from 1.1-3.5% and were made by dissolving agarose in 1xTE buffer (10 mM Tris-Cl, pH 7.5, 1 mM EDTA) once cooled ethidium bromide (1 µl/100 ml) or SYBR safe (5 µl/100 ml) was added.

Samples were loaded with orange 6x loading dye (0.08 g Orange G, 12 ml 100% Glycerol, 4.8 ml 0.5 M EDTA, 22.12 ml H_2O) and a 1 Kb Invitrogen DNA ladder was used. Samples were run at 70-90 V for 20-40 minutes in 1 x TE buffer in Bio-Rad gel tanks and bands were visualised using a UV Transilluminator.

2.6.4 Restriction digests

Diagnostic digests were carried out to check for the presence of a particular mutation and for cloning purposes.

To check for mutations 2-10 µl of DNA was added to 2 µl of 10 x NEB Restriction Enzyme Buffer, 1 µl of NEB Restriction Enzyme and made up to total volume of 20 µl with sterile water. Digests were incubated at 37 °C for 60 – 90 minutes.

Digests that were carried out for cloning were done at slightly different volumes. 30 µl of Column Purified PCR was added to, 1 µl of NEB Restriction Enzyme, 1 µl of NEB Restriction Enzyme 2, 5 µl of 10X NEB Restriction Enzyme Buffer and made up to a total volume of 50 µl with sterile water. Digests were incubated at 37 °C for 60 – 120 minutes.

2.6.5 Primers

Various primers were used throughout this project to identify mutations and create new constructs (Table 2-5).

Primer	Sequence	Details
pAUX1-22F	CAGGGATTATTCTTTGCATCTTAACCC	Mt band (300 bp) WT band(334 bp)
pAUX1-22R	TGCCATTTAGCTTTAACTTAAATAGTAATTCAAC	
pAux1-7F	TGGCTAGATTGCCTGTGGTC	1021 bp band when point mutation present
pAux1-7R	ACATTGGTAACACTTGGCAAAGAGAT	
pAux1 (WT)R	ACATTGGTAACACTTGGCAAAGAGAC	1021 bp band when WT
gl2mtF	TCAAGGTAATGTATATCTTACG	Mt band (295 bp) WT band (310 bp)
gl2mtR	TGAAGCCTGCAGGGGTAG	
aux1-22F	CTTGGAATGACCACTTACACCG	Mt band (323 bp) WT band (357 bp)
aux1-22R	AATGTTTCACACCTTCCGC	
wer-1FW	TAGGTTTAAAGAGATGTGGAAAG	Sau3A1 Digest Mt bands (bp) (247/95/92/27) WT bands (bp) (339/95/27)
wer-1Re	ACCATTGCTCTGTTTGG	
myb23-1F	TGTGTTTTGTTGTTCGGTG	WT band (744 bp)
myb23-1R	CTAAATATTAAAAGAATTTACGATGTTAG	
ARF16.2F	CCTCGGCGTCACCTTCTTACA	WT band (884 bp)
ARF16.2R	TCCGCTACTGCTTCTACTCTAACC	
LBA1	ATGGTTCACGTAGTGGGCCATC	MT band (1000 bp)
ARF10.3F	ACTATGGCATGCTTGTGCAGGATC	WT band (798 bp)
ARF10.3R	TCCGCTACTGCTTCTACTCTAACC	
GabiTDNA	GTGGATTGATGTGATATCTCC	MT band (500 bp)

B1pARF10 F1	**GGGGACAAGTTTGTACAAAAAAGCAGGCT**AAAACTTAGGCCTTAGATGGAAATCTT	Promoter Truncation Band (2078 bp)
B1pARF10 F2	**GGGGACAAGTTTGTACAAAAAAGCAGGCT**ATTTACCATGGGTTTAACCTATTTCTTG	Promoter Truncation Band (850 bp)
B1pARF10 F3	**GGGGACAAGTTTGTACAAAAAAGCAGGCT**GGTTTGTATCTGGTCAAGCATGG	Promoter Truncation Band (710 bp)
pARF10rb2	**GGGGACCACTTTGTACAAGAAAGCTGGGTA**CTAGACGAAGTTGTGTAACCCCCAAATTCT	
attB5MYB23F	**GGGGACAACTTTGTATACAAAAGTTG**AACAATGAGAATGACAAGAGATGG	Coding Region For MYB23 Constructs (1679 bp)
attB2MYB23R	**GGGGACCACTTTGTACAAGAAAGCTGGGTA**TCAAAGGCAATACCCATTAGTAAAATC	
IAA17A3	AGAAAGATTCAATAACAGTAATAGAGTAATAAC	WT Band (1000 bp)
Seq17R2	TGGAAAAGAGCTGAACATGTCGG	
Da5'la	ACGGTCGGGAAACTAGCTCTAC	Mt Band (600 bp)
QpARF10 F8	TTCTGATTAGTTGGGTGGGAAT	qPCR, ARF10 Section A
QpARF10 R7	CCTACCACGAGATTGTTGAATTG	qPCR, ARF10 Section A
QpARF10 F9	ATGTCAGTATATTTGATGTAGATGAGC	qPCR, ARF10 Section B
QpARF10 R8	TTGATTATGTTTGGACTTTTGAGC	qPCR, ARF10 Section B
QpARF10 F6	TAATGCAAGACAACCCACCA	qPCR, ARF10 Section C
QpARF10 R5	TTGACATGGCTAGAAAGAAGCA	qPCR, ARF10 Section C
QpARF10 F10	ACTGAAAACCCATGTAAAGCTG	qPCR, ARF10 Section D

QpARF10 R9	GATTCGCAAAACAGATTAGTCACA	qPCR, ARF10 Section D
QpARF10 F2	CACTCCAATCTCCACAATCC	qPCR, ARF10 Section E
QpARF10 R2	GGTTGACCCGAGAGATGAAA	qPCR, ARF10 Section E
QpARF10 F5	AAATGAGGTGAAATGAGGGAAT	qPCR, ARF10 Section F
QpARF10 R4	AAATTTGACGTTATGCCTCACC	qPCR, ARF10 Section F
QpARF10 F1	TACGATGGTCTTGTCCGTACC	qPCR, ARF10 Section G
QpARF10 R1	GAAGAAGAGAGAGATAGAGAGAGATGC	qPCR, ARF10 Section G
QARF10 F2	GCAACTAAACGGCTAACAATCA	qPCR, ARF10 Control (H)
QARF10 R2	ATCCACGTCCTATGCAAACC	qPCR, ARF10 Control (H)
QpGL2 F	CAAGCAATTTAGGGTTCCATGT	qPCR, GL2 Positive Control
QpGL2 R	GGGACTCTGGGAGAAGCATA	qPCR, GL2 Positive Control
QGL2 F2	CGTATGAGTCGGTGGTGGTA	qPCR, GL2 Control
QGL2 R2	AGCTGTGTCGTGTTTATATCTACGG	qPCR, GL2 Control
QpMYB23 F4	CTAGTTGGGTTGATCTGAAAGTAAG	qPCR, MYB23 Section A
QpMYB23 R4	AGATTATAGCTTCCACTTGATTTAGC	qPCR, MYB23 Section A
QpMYB23 F3	TTGACATATCTTAGCTGGATGAGC	qPCR, MYB23 Section B

QpMYB23 R3	CCCTTGGGATAGACAGTAGGC	qPCR, MYB23 Section B
QpMYB23 F2	CCACAACGTCCTCCTCTCAT	qPCR, MYB23 Section C
QpMYB23 R2	TGGTTTGAGTTTGGATTCGTC	qPCR, MYB23 Section C
QpMYB23 F1	AAGAATGTAGGGATTGACTTTACCAT	qPCR, MYB23 Section D
QpMYB23 R1	TGTTTGCTGTTGTCTCTCCAA	qPCR, MYB23 Section D
QMYB23 F1	ATTGAATTAAGAGACCAC	qPCR, MYB23 Control (E)
QMYB23 R1	TTTCTTGCTGAGATGTGT	qPCR, MYB23 Control (E)

Table 2-5: Primers during this project. Bold highlights indicate the Gateway *attB* flanking sequences used.

2.7 Cloning

Constructs produced during this project were generated using both the classical cloning method and the Invitrogen® GATEWAY® system.

2.7.1 Invitrogen® GATEWAY® vectors

Various vectors were used during this project: pDONR207 (Figure 2-1) pDONR221 (Figure 2-2), pFP101 (Figure 2-3), and pJTG01 (Figure 2-4) were used for GAREWAY cloning. pDONR207 contains the *attL1* and *attR1* recombination sites for incorporation of DNA sequences. It contains gentamycin resistance for positive selection and the *ccdB* gene, toxic to bacteria, which is excised upon recombination (Figure 2-1)

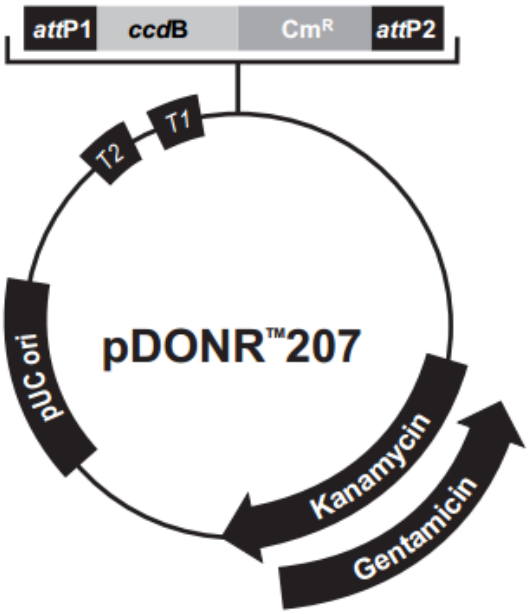

Figure 2-1: Vector pDONR 207. Image produced by Invitrogen Life Technologies.

pDONR221 contains the *attP5* and *attP2* recombination sites for incorporation of DNA sequences. It contains kanamycin resistance for positive selection and the *ccdB* gene, toxic to bacteria, which is excised upon recombination (Figure 2-2).

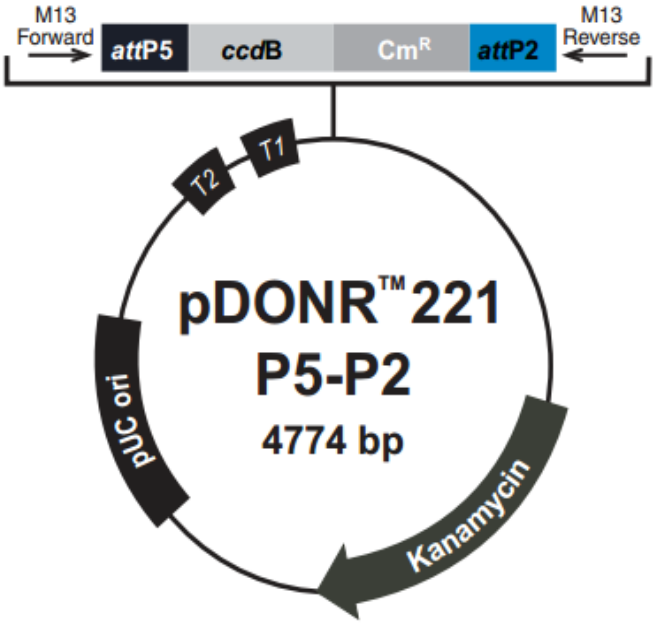

Figure 2-2: Vector pDONR 221. Image produced by Invitrogen Life Technologies.

The pFP101 vector was first described by Bensmihen et al., 2004. The original pFP100 vector was generated using the At2S3 promoter and a GFP sequence with a 35S terminator in pZP200 (Bensmihen et al., 2004). To generate pFP101 a double enhanced 35S promoter-NOS terminator cassette was inserted in pFP100 (Bensmihen et al., 2004) (Figure 2-3). This vector allows selection based on GFP fluorescence. The vector contains the coding sequence of an endoplasmic reticulum targeted GFP under the control of the *At2S3* promoter (Bensmihen et al., 2004). The GATEWAY® recombination cassette allows insertion of cDNAs in frame with a triple HA tag and VP16-AD (Bensmihen et al., 2004).

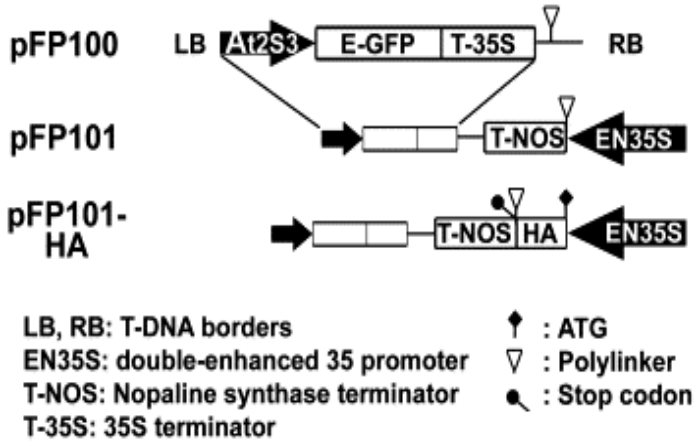

Figure 2-3: Vector pFP101. Figured adapted from (Bensmihen et al., 2004)

The pJTG01 vector was used as a destination vector to make ARF10 promoter truncations. The GATEWAY® recombination cassette allows insertion of cDNAs and the GFP sequences enable visualisation of the truncations in root epidermis. This vector contains kanamycin resistance for positive selection and the *ccdB* gene, toxic to bacteria, which is excised upon recombination (Figure 2-4). This vector allows selection based on BASTA resistance.

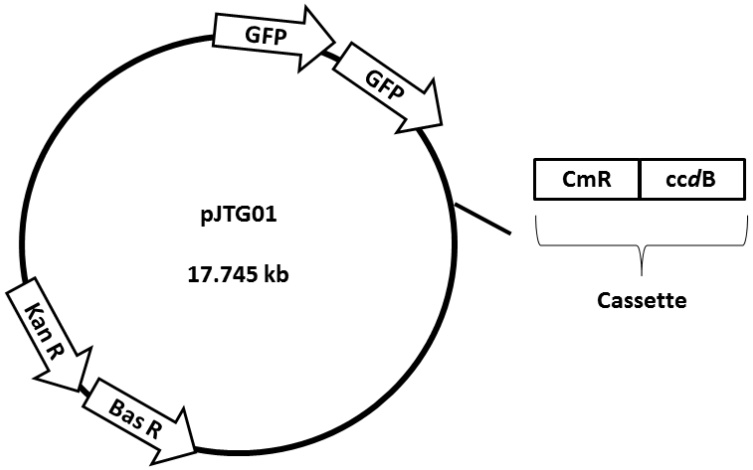

Figure 2-4: Vector map for pJTG01.

2.7.2 Invitrogen® GATEWAY® BP reaction

In the Invitrogen GATEWAY system the BP reaction generates the gateway entry clone using a destination vector and your region of interest amplified with appropriate gateway *attB* extensions (Figure 5-2).

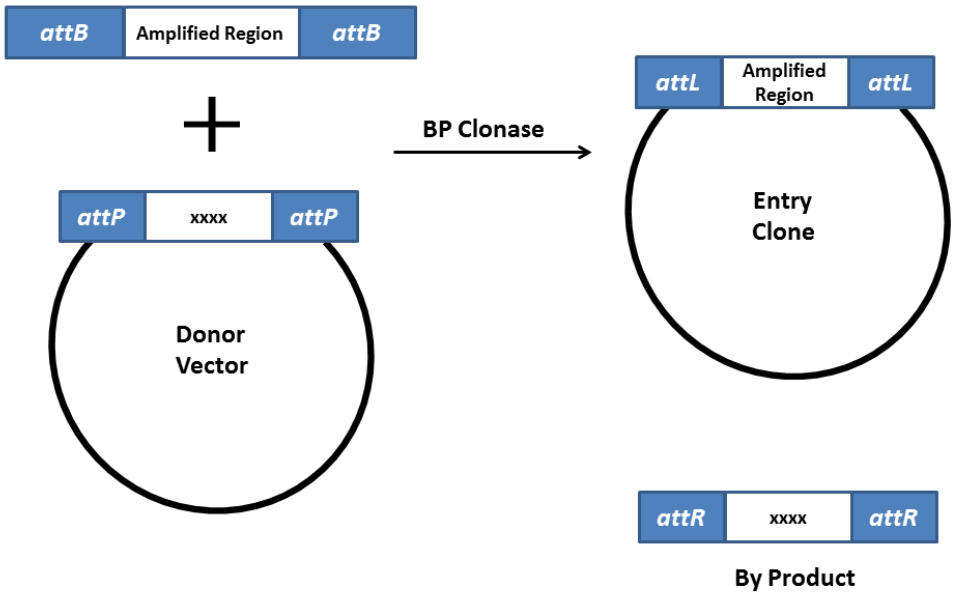

Figure 2-5: Generation of the Gateway Entry Clone

In a 1.5 ml eppendorf *att*B-PCR product (≥10 ng/ul), donor vector (150 ng/µl) and TE buffer (10Mm Tris-Cl, pH7.5, 1mM EDTA, pH 8.0) were added to a total volume of 8 µl. BP Clonase II Enzyme Mix was thawed on ice and 2 µl was added to each sample. Samples were then briefly vortexed and the reactions incubated at 25 °C for 1 hour. 1 µl of Proteinase K solution was then added to each sample to terminate the reaction. Samples were vortexed briefly and incubated at 37 °C for 10 minutes.

2.7.3 Invitrogen® GATEWAY®, LR reaction

The LR reaction generates the gateway expression clone from your previously generated entry clone and a destination vector (Figure 2-6).

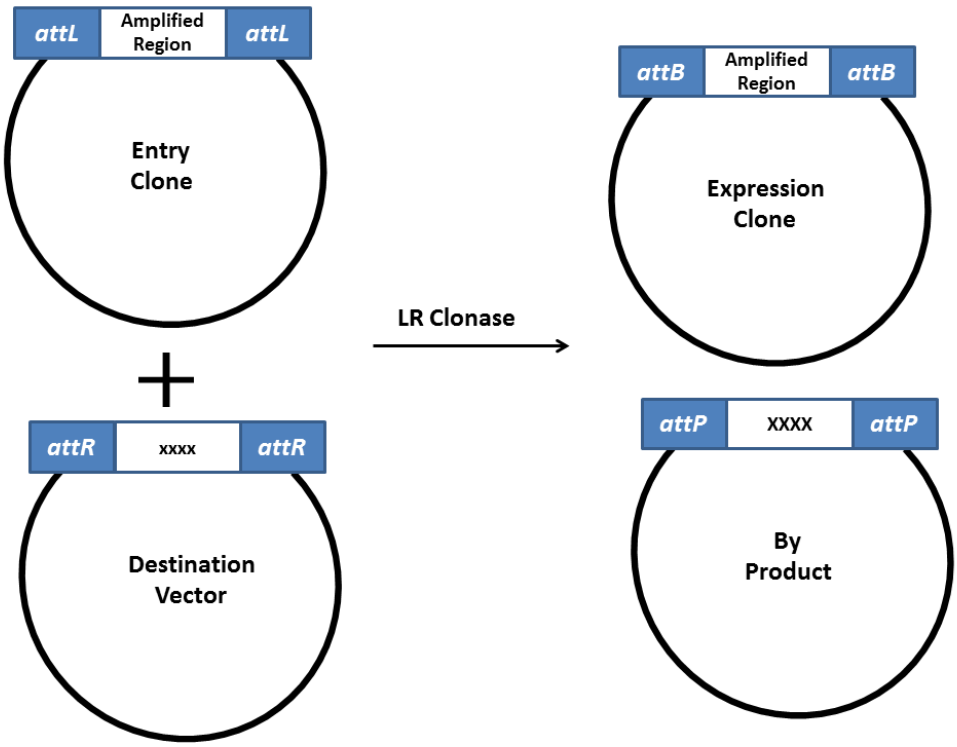

Figure 2-6: Generation of the Gateway Expression Clone

In a 1.5 ml eppendorf entry clone (50-150 ng), destination vector (150 ng/µl) and TE buffer, pH 8.0 were added to a total volume of 8 µl. LR Clonase II Enzyme Mix was thawed on ice and 2 µl was added to each sample. Samples were then briefly vortexed and the reactions incubated at 25 °C for 1 hour. 1 µl of Proteinase K solution was then added to each sample to terminate the reaction. Samples were vortexed briefly and incubated at 37 °C for 10 minutes.

2.7.4 Classical cloning vectors

The pGreen0029 vector (Figure 2-7) was used with classical cloning methods to generate the pMYB23::MYB23-GFP construct. pGreen0029 is a compact agrobacterium binary vector, it has kanamycin resistance genes for bacterial and plant transformation.

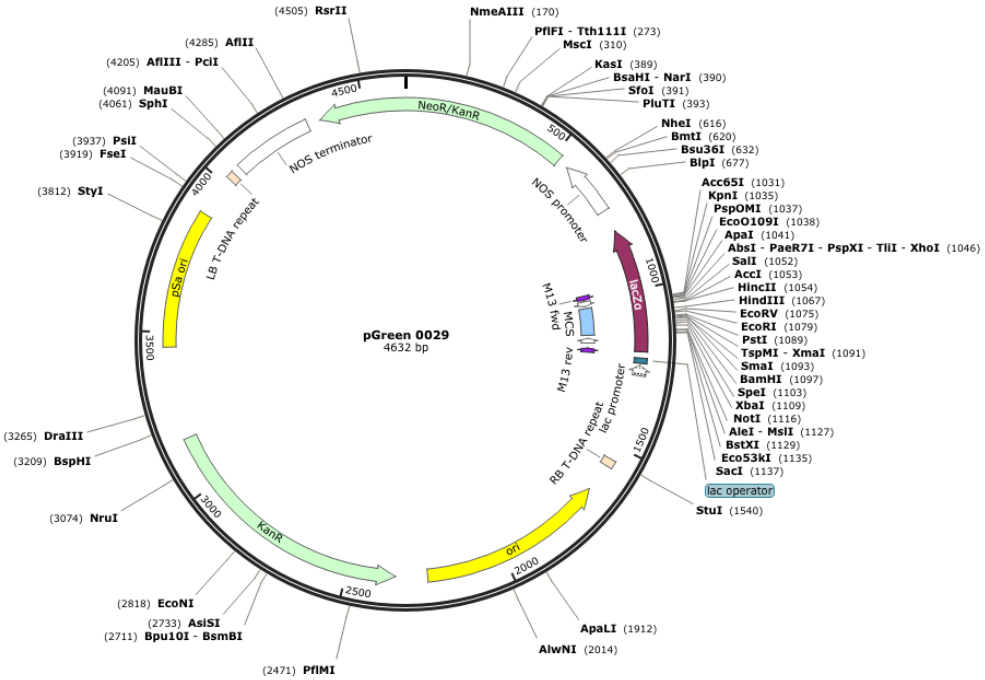

Figure 2-7: Vector pGreen0029, Image produced by snapgene.

2.7.5 Classical cloning construct generation

The pMYB23::MYB23-GFP line was generated using classical cloning methods. Three fragments were generated using PCR, appropriate restriction sites were added via primer sequences (Figure 2-8). The first fragment was 4.7 kb long and consisted of the MYB23 promoter and genomic DNA, it was flanked by KPN1 and EcoRV restriction sites. The second fragment was 717 bp long and consisted of the green fluorescent protein (GFP), this fragment was flanked by EcoRV and Not1 restriction sites. The final fragment was 1kb long and consisted of the MYB23 3' sequence, flanked by two Not1 restriction sites.

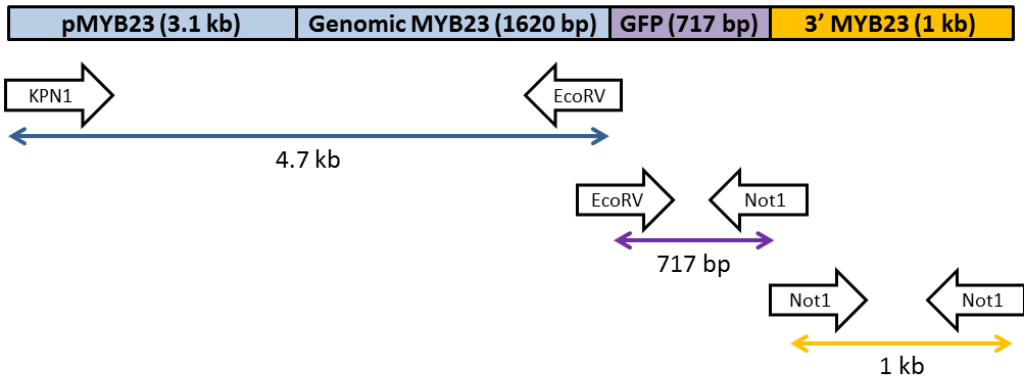

Figure 2-8: Construction of the pMYB23::MYB23-GFP marker line using classical cloning methods.

In order to construct this line the pGreen0029 vector was digested with appropriate restriction sites and then three successive ligations were performed with the fragments detailed above. The construct was checked with sequencing before being transformed into *Agrobacterium* for plant transformation.

2.7.6 Ligation reactions

For ligation reactions 1.5 µl of linearised vector (50 ng/µl) was added to 3 µl of 10 x NEB T4 Buffer, 1.5 µl of NEB T4 DNA Ligase and the fragment added at a ratio of 3:1 (see equation below for further details). The reaction was made up to a total volume of 10 µl with sterile water and incubated overnight at 16 or 4°C, depending on if the restriction sites are blunt or sticky ends.

Fragment to be inserted at 3:1 ratio to vector,

$$\frac{\text{(fragment size (bp) x 50(conc. of vector) x3}}{\text{Vector size bp}}$$

2.7.7 Estimation of DNA concentrations

DNA concentrations were estimated using a Nano Drop ND-1000, with 1 µl at a wavelength of 260 nm.

2.7.8 Plasmid miniprep - alkaline lysis method

A culture from a single colony was grown o/n in 5 ml LB with appropriate antibiotic selection. 1.5 ml of this was transferred to an eppendorf and centrifuged for 1 minute. The pellet was then re-suspended in 150 µl of solution 1 (50 mM glucose, 10 mM EDTA, 25 mM Tris pH 8, stored at 4 °C) and 200 µl of freshly made solution 2 (0.2 M NaOH, 1 % SDS). The solution was mixed gently and left to stand for 5 minutes. 150 µl of solution 3 (3 M KaC, pH4.4, stored at 4 °C) was then added and mixed to allow the formation of a precipitate. The sample was then centrifuged for 10 minutes and the supernatant transferred to a fresh tube.

A phenol extract (one volume of phenol:chloroform:isoamyalchohol 24:24:1) was performed and the aqueous phase recovered. Two volumes of ethanol were added and the sample centrifuged for 20 minutes. The supernatant was removed and the pellet washed with 150 µl of 70 % ethanol and centrifuged for 3 minutes. The supernatant was removed and the pellet allowed to dry before being re-suspended in 50 µl of sterile water with 0.5 µl of RNAase A (20mg/ml).

2.7.9 Plasmid miniprep - QIAprep spin miniprep kit (QIAGEN)

Pelleted bacterial cells were re-suspended in 205 µl of Buffer PI and transferred to a micro centrifuge tube. 200 µl of buffer P2 was added and the solution mixed thoroughly by inverting the tube 6 times. 350 µl buffer N3 was added and the solution mixed immediately and thoroughly by inverting the tube 4-6 times. The sample was then centrifuged for 10 minutes at 13,000 rpm and the supernatant applied to the QIA spin column. This was then centrifuged for 30-60 seconds and the flow through discarded. The QIA spin column was washed by adding 0.75 ml buffer PE and centrifuged for 30-60 seconds. The flow through was discarded flow and the column centrifuged for an additional minute. To elute the DNA, the QIA spin column was placed in a clean 1.5 ml micro centrifuge tube and 50 µl of Elution Buffer was added. This was then left to stand for 1 minute and then centrifuged for 1 minute.

2.7.10 QIAEX II gel extraction (QIAGEN)

When the PCR product was confirmed bands were cut from agarose electrophoresis gel and purified by adding Buffer QX1 (volume was dependant on fragment size and band size). The QIAEX II beads were resuspended by vortexing for 30 seconds and 10 µl added to the solution. This was then incubated for 10 minutes at 50 °C, whilst vortexing every 2 minutes to keep the QIAEX II beads in suspension. The sample was then centrifuged for 30 seconds and the

supernatant removed with a pipette and the pellet washed with 500 µl of Buffer QX1. After the pellet had been resuspended it was centrifuged for 30 seconds and the supernatant removed. The pellet was then washed twice with 500 µl of Buffer PE and then air-dried for 10-15 minutes until it became white. To elute the DNA 20 µl of TE Buffer (10Mm Tris-Cl, pH7.5, 1mM EDTA) was added and the pellet resuspended by vortexing. The solution was then incubated between 5 and 10 minutes (temperature and length dependant on fragment size) and the centrifuged for 30 seconds. The supernatant now contained the DNA and was extracted carefully and stored in a fresh tube.

2.7.11 QIAquick PCR purification kit

5 volumes of Buffer PB was added to 1 volume of the PCR (or ChIP) solution and mixed. The solution was then placed in a 2 ml column that was in a collection tube and centrifuged for 30 seconds. 750 µl of Buffer PE was then added to the column and it was once again centrifuged for 30 seconds. The column was then placed in a clean eppendorf and 50 µl of Elution Buffer added. The column was centrifuged for 60 seconds and then discarded. The eluted solution was stored at -20 °C until required.

2.7.12 Bacterial strains and growth conditions

For the propagation of plasmid DNA the *E.coli* strain DH5α was used. The *Agrobacterium tumefaciens* strain GV3101 was used for Arabidopsis transformation. *E.coli* was grown at 37 °C on solid or liquid LB media (10 mM NaCl, 2 % Tryptome, 0.5 % Yeast (± 2 % agar)) whilst the *Agrobacterium* was grown on the same medium at 28 °C. When grown on liquid media the cultures were grown whilst shaking at 200 rpm. Appropriate antibiotic selections were used where necessary (Table 2-6: Antibiotic

Antibiotic	Solvent	Concentration
Kanamycin	Water	40 µg/ml
Gentamycin	Water	10 µg/ml
Rifampicin	DMSO	100 µg/ml
Spectinomycin	Water	40 µg/ml

Table 2-6: Antibiotic selection conditions and concentrations.

2.7.13 Transformation of bioline DH5α competent cells

A 50 µl aliquot of Bioline α-Select Chemically Competent Cells was thawed on wet ice. DNA was added to the (≤5 µl per 50 µl cells) cell suspension and the mixture was gently swirled then incubated on ice for 30 minutes. The samples were then placed in a 42 °C water bath for 30 to 45 seconds and then replaced on ice for 2 minutes. They were then diluted by making up to 1 ml with liquid LB (10 mM NaCl, 2 % Tryptome, 0.5 % Yeast) and the tubes shaken at ~200 rpm for 60 minutes at 37 °C. The samples were then spread on LB agar (as above with 2 % agar) plates containing appropriate antibiotic and incubate over night at 37°C.

2.7.14 Preparation and transformation of competent agrobacterium tumefaciens cells

LB agar plates were prepared with rifampicin as detailed in Table 2-6. The cells were then streaked from a glycerol stock onto these and incubated for two days at 28 °C. A single colony was selected and used to inoculate 50 ml of liquid LB. This culture was grown until an optical density (OD) of 0.5-1 was reached at 600 nm. At this point the culture was transferred to a pre-chilled 50 ml falcon tube and spun at 3500 rpm for 20 minutes, 4 °C. The supernatant was removed and the pellet re-suspended in 1 ml of 20 mM $CaCl_2$. This was then dispensed into 100 µl aliquots and frozen in liquid nitrogen. These were then stored at -80 °C.

For Agrobacterium transformation 1 µg of plasmid DNA was added to one of the frozen 100 µl aliquots. These were then incubated at 37 °C for 5 minutes. Liquid LB was added up to a volume of 1 ml and shaken at 28 °C for 2-4 hours. This was then spread on LB agar plates containing suitable antibiotics and incubated at 28 °C for two days.

2.7.15 Floral dipping transformation

Seven seedlings were grown in square 6 cm pots until inflorescence meristems became visible. A minimum of three 6 cm pots were used per construct. Three days before floral dipping was scheduled the stems of the plants were cut therefore allowing new stems to grow.

A single *Agrobacterium* colony containing the appropriate construct was used to inoculate a 5 ml liquid LB culture with appropriate selection. This culture was grown overnight and then 2 ml of this was used to inoculate a 2 L flask with 500 ml LB plus antibiotics. This was also grown overnight and then centrifuged for 12 minutes at 12,000 rpm at room temperature. The pellet was re-suspended in 250 ml of floral dipping solution (5 % w/v sucrose, 10 mM $MgCl_2.6H_2O$, 25 µl Silwett ® Vac-in stuff ®).

Each pot of seedlings was dipped into the transformation solution for 2 to 3 minutes. The plants were then enclosed in an autoclave bag overnight to maintain a high level of humidity. The following day the bag was removed and the siliques allowed to mature. Plants were then bagged as normal and the seeds collected.

Homozygote lines were selected using a florescent seed coat marker or BASTA resistance depending upon which destination vector was used. BASTA was sprayed onto the plants at a concentration of 80 mg/L just after the seeds had germinated and then again after possible positives had been selected. For constructs with a fluorescent seed coat marker initially fluorescent seeds were

selected from the T1 generation using an Olympus SZX12 GFP Microscope. The T2 generation was then analysed for lines which exhibited a 3:1 fluorescent to non-fluorescent ratio to check for multiple inserts and then reselected again at the T3 generation for a homozygote line.

2.8 Chromatin immunoprecipitation (ChIP)

ChIP was used to look for a direct interaction between ARF10, WEREWOLF and MYB23. Using two marker lines and qPCR, ChIP enabled us to look for an interaction between pWER::WER-GFP and pMYB23::MYB23-GFP and the ARF10 promoter region. ChIP works by initially crosslinking proteins and DNA and then shearing the DNA, with the proteins still attached, via sonication. Using the GFP antibody the proteins are then immunoprecipitated and the associated DNA is isolated. The cross link is then reversed and the DNA analysed (Figure 2-9). The ChIP protocol took place over several days. Initially plants were grown in dense lines on ATS covered with autoclaved mesh (13 square plates per line, 4 rows per plate, grown for 5-6 days).

When the plants reached an appropriate age MC Buffer was freshly prepared (10 mM Sodium Phosphate pH7, 50 mM NaCl, 0.1 M Sucrose) and a scalpel blade was used to cut away the section of root required. These sections were collected in a 50 ml falcon tube (with a small amount of MC Buffer in to prevent it freezing) kept on ice. In a flow hood the falcon tube was filled with 25 ml MC Buffer and 1 % Formaldehyde was added. This was then vacuum infiltrated for 4 minutes, after this 2.5 ml of 1.25 % glycine was added to stop the reaction.

The root material was then washed three times with MC buffer and ground into a fine powder using liquid nitrogen. The powder was stored overnight at -80 °C.

The following day buffers were freshly prepared as follows:

- M1 buffer (10 mM Sodium Phosphate, pH7, 0.1 M NaCl, 1 M 2-methyl-2.4-pentanediol, 10 mM 2-mercaptoethanol, complete protease inhibitor cocktail (roche)).

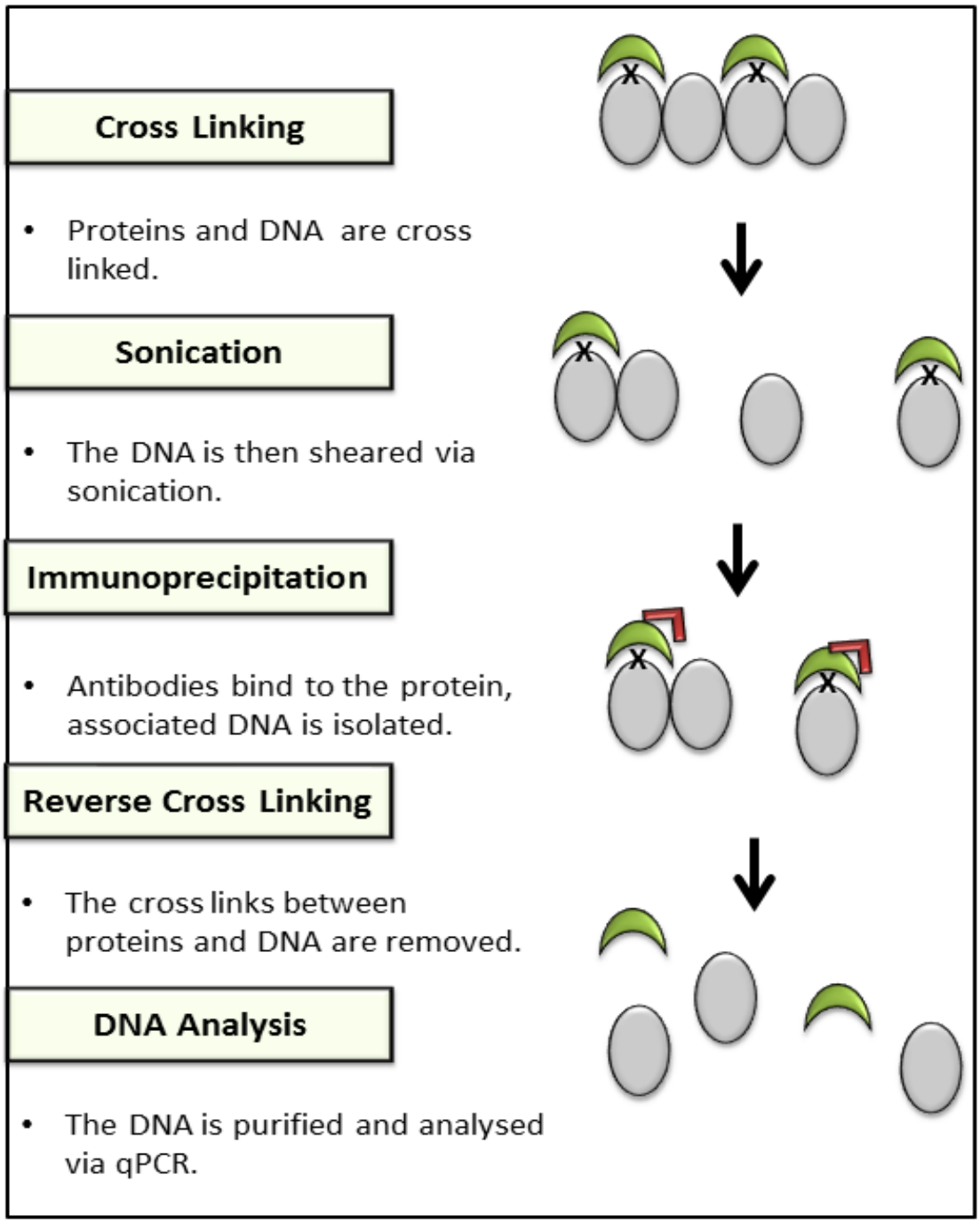

Figure 2-9: A schematic representation of the chromatin immunoprecipitation technique.

Chromatin Immunoprecipitation was used to look for an interaction between ARF10 and WEREWOLF and/or MYB23. It works by cross linking the proteins and DNA then immunoprecipiating the proteins, thus allowing the associated DNA to be analysed.

- M2 buffer (10 mM Sodium Phosphate, pH7, 0.1 M NaCl, 1 M 2-methyl-2.4-pentanediol, 10 mM 2-mercaptoethanol, 10 mM $MgCl_2$, 0.5% Triton-x-100, complete protease inhibitor cocktail (roche)).
- M3 buffer (10 mM Sodium Phosphate, pH7, 0.1 M NaCl, 10mM 2-mercaptoethanol, complete protease inhibitor cocktail (roche)).

20 ml of M1 buffer was added to the root powder and the slurry filtered through a 50 µm fabric mesh and centrifuged for 20 minutes at 1000 g, 4 °C. The pellet was then washed five times with 5 ml of buffer M2 and once with 5 ml of buffer M3. After every wash the solution was centrifuged for 10 minutes.

After the final wash the pellet was resuspended in 1 ml of sonic buffer (10 mM Sodium Phosphate, pH7, 0.1 M NaCl, 0.5 % Sarkozyl, 10 mM EDTA, Complete protease inhibitor cocktail) and 42 µl of 25 x protease inhibitor. This was then sonicated for 14 minutes with 15 seconds of sonication interspersed with 45 seconds of cooling until the DNA was sheared to approximately 300-500 bp. An agarose electrophoresis gel was run to check this.

After sonication the solution was centrifuged three times for ten minutes at 4 °C to remove any debris. At this stage a 100 µl input sample was taken. To the remaining solution 1 ml of IP Buffer (50 mM Hepes, pH7.5, 150 mM NaCl, 5 mM $MgCl_2$, 10 µM $ZnSO_4$, 1 % Triton- x -100, 0.05 % SDS) was added along with 50 µl of Miltenyi paramagnetic GFP beads. The solution was the incubated for an hour on a rotating device at 4 °C.

The columns containing the paramagnetic beads were placed in the magnetic field and 200 µl of IP Buffer was applied. The solution that had been incubated at

4 °C was then applied to the column and the lysate allowed to run through. Multiple washes were then applied to the column as follows:

- Three times 400 µl IP Buffer,
- One times 200 µl IP Buffer,
- Two times 200 µl High Salt Buffer (500 mM NaCl, 0.1% SDS, 1% Triton – x-100, 2 mM EDTA, 20 mM Tris-HCL pH8),
- Two times 200 µl LiCl Buffer (10 mM Tris-HCL pH8, 1Mm EDTA, 1 % NP-40, 1 % sodium deoxychelate (Sigma D-6750), 0.25 M LiCl)
- Two times 200 µl TE Buffer (10 mM Tris-Cl, pH7.5, 1 mM EDTA)

After these washes were complete 20 µl of hot (95 °C) Elution Buffer (1 % SDS, 50 mM Tris-HCL pH8, 10 mM EDTA, 50 mM DTT) was added to the column and left to incubate for 5 minutes. 3 x 50 µl of hot elution buffer was then added to the column and the eluted solution collected in a clean eppendorf. 100 µl of TE Buffer (10 mM Tris-Cl, pH7.5, 1 mM EDTA) and 11.25 µl of Proteinase K (20 mg/ml) was added to the eppendorf and the solution was incubated overnight at 37 °C. 150 µl of TE and 11.25 µl of Proteinase K was also added to the previously taken input sample and this was also incubated overnight at 37 °C.

The following day 11.25 µl of Proteinase K was added to both the input and immunoprecipitated sample and they were incubated at 65 °C for 6 hours. After this time they were removed from the heat, allowed to cool and then transferred to ice. The samples were then ethanol precipitated (2.5 vol EtOH, 1/10 vol 3 M Sodium Acetate, 3 µl Glycogen (5 mg/ml, Ambion) and incubated overnight at -20 °C.

The following day both samples were centrifuged for 30 minutes at full speed and the pellet was then resuspended in 100 µl of ultrapure water. The samples were then purified using a QIAquick kit (as detailed previously) and eluted in 50 µl of Elution Buffer. Samples were then stored at -20 °C until RT- qPCR was carried out.

2.9 Buffer summary

2.9.1 Arabidopsis thaliana salts

5 mM KNO_3

2.5 mM KH_2PO4

2 mM $MgSO_4$

2 mM $Ca(NO_3)_2$

20 mM FE-EDTA

1 ml/L of Micronutrients (70 mM H_3BO_3, 14 mM $MnCL_2$, 0.5 mM $CuS0_4$, 1 mM $ZnSO_4$, 0.2 mM $NaMoO_4$, 10 mM NaCl, 0.01 mM $CoCL_2$)

0.8 % plant agar

1 % sucrose

2.9.2 Edwards prep extraction buffer

200 mM Tris-HCL pH 7.5

250 mM NaCl

25 mM EDTA

0.5 % SDS

2.9.3 TE buffer

10 mM Tris-Cl, pH7.5,

1 mM EDTA

2.9.4 Alkaline lysis mini prep solution 1

50 mM glucose

10 mM EDTA,

25 mM Tris pH 8

2.9.5 Alkaline lysis mini prep solution 2

0.2 M NaOH,

1 % SDS

2.9.6 Alkaline lysis mini prep solution 3

3 M KaC pH4.4

2.9.7 Lysogeny broth

10 mM NaCl

2 % Tryptome

0.5 % Yeast

± 2 % agar

2.9.8 Floral dipping solution

5 % w/v sucrose

10 mM $MgCl_2.6H_2O$

25 µl Silwett ® Vac-in stuff ®

2.9.9 ChIP MC buffer

10 mM Sodium Phosphate pH7

50 mM NaCl

0.1 M Sucrose

2.9.10 ChIP M1 buffer

10 mM Sodium Phosphate, pH7,

0.1 M NaCl,

1 M 2-methyl-2.4-pentanediol,

10 mM 2-mercaptoethanol,

Complete protease inhibitor cocktail (roche)

2.9.11 ChIP M2 buffer

10 mM Sodium Phosphate, pH7

0.1 M NaCl

1 M 2-methyl-2.4-pentanediol

10 mM 2-mercaptoethanol

10 mM $MgCl_2$

0.5 % Triton-x-100

Complete protease inhibitor cocktail (roche)

2.9.12 ChIP M3 buffer

10 mM Sodium Phosphate, pH7

0.1 M NaCl

10 mM 2-mercaptoethanol

Complete protease inhibitor cocktail (roche)

2.9.13 ChIP sonic buffer

10 mM Sodium Phosphate, pH7

0.1 M NaCl

0.5 % Sarkozyl

10 mM EDTA

Complete protease inhibitor cocktail (roche)

2.9.14 ChIP IP buffer

50 mM Hepes, pH7.5

150 mM NaCl

5 mM $MgCl_2$

10 µM $ZnSO_4$

1 % Triton- x -100

0.05 % SDS

2.9.15 ChIP high salt buffer

500 mM NaCl

0.1% SDS

1% Triton –x-100

2 mM EDTA

20 mM Tris-HCL pH8

2.9.16 ChIP LiCl buffer

10 mM Tris-HCL pH8

1 mM EDTA

1 % NP-40

1 % sodium deoxychelate (Sigma D-6750)

0.25 M LiCl

2.9.17 ChIP elution buffer

1 % SDS

50 mM Tris-HCL pH8

10 mM EDTA

50 mM DTT

3 : Establishing the Functional Significance of the Apparent Non-Hair Repressive Auxin Response Regime

3.1 Introduction

The phytohormone auxin is a remarkably versatile regulator of many developmental and growth processes, including lateral root production and root hair growth (Del Bianco and Kepinski, 2011). In this work the root epidermis in *Arabidopsis thaliana* was used as a model to understand the interaction of patterning mechanisms, such as those that define hair and non-hair producing epidermal cells, and auxin. An advantage of using this particular tissue is that it is made up of just two cell types, cells that produce root hairs (hair cells) and cells that do not (non-hair cells) (Ishida *et al*., 2008). In addition to this the location of these two cell types is governed by a well characterised patterning mechanism resulting in the production of files of distinct hair and non-hair cells along the length of the root (Figure 1-7).

Data published by Jones et al in 2009, indicated that the auxin influx transporter AUX1 is expressed in a highly specific pattern, it is almost exclusively confined to the non-hair cells, which results in a predicted 10 fold increase in the auxin concentration in the non-hair files (Jones *et al*., 2009). In conjunction with this, their analysis of the *pDR5::GFP* marker indicated a higher level of auxin signalling output in the non-hair cells (Jones *et al*., 2009). However because the root hair growth response to auxin must ultimately occur within hair cells rather than non-hair cells, before this research project began the expression pattern of the *pDR5::GFP* marker was examined in greater detail. This analysis showed that although the expression is indeed initially higher in the non-hair cells, at the transition zone, where root hairs begin to initiate, the GFP expression equalises between the two cell types and then persists with greater strength in the hair files (Figure 1-9). Treatment with the synthetic auxin 2,4D, which is readily transported into cells, but can not be exported, results in the proposed differences in auxin concentration being removed. The fact that the *pDR5::GFP* differential expression pattern persisted after this treatment (Figure 1-9), indicated that the hair and non-hair cells have an underlying difference in their capacity to respond to auxin.

Transcriptomic data generated by Dr Martin Kieffer before this work began, indicated that some auxin response network components were expressed differentially in the hair and non-hair files. In particular the transcription of two components that have been shown to be negative regulators of auxin response, *ARF10* and *IAA17*, were present in higher abundance in the non-hair files. These expression differences were further confirmed with the analysis of transcriptional and translational GFP marker lines for these two genes (Figure 1-10/11). Taken in conjunction with the *pDR5::GFP* data these results were consistent with there being a lower or reduced auxin response in the non-hair files.

The functional significance of this contrasting auxin response regime between hair and non-hair files was not known. Two non-mutually exclusive hypotheses were considered, firstly that this repressive auxin response was part of the mechanism that restricted hair growth, and secondly that it may facilitate an auxin transport superhighway via the non-hair cells, to enabled a sustained and reliable delivery of auxin to the hair cells, as was first described by Jones *et al* in 2009.

3.2 Epidermal patterning mutants

In addition to there only being two cell types, another advantage of using the root epidermis to study the developmental patterning of auxin responsiveness, is that the root epidermal patterning mechanism is well characterised and therefore mutants for the majority of the components are readily available (Figure 3-1) (Koornneef, 1981*;* Tanaka *et al*., 2014). Given the apparent differences in auxin response between the hair and non-hair files, the existence of an extensive genetic framework is a distinct advantage.

In order to investigate if the apparent repressive auxin response regime functions to prevent the growth of root hairs in the non-hair cells, the *GLABRA 2* loss-of-function mutant, *gl2-1* was utilised (Koornneef, 1981). Within the root epidermal patterning mechanism GL2 functions primarily in the non-hair cells and inhibits the production of root hairs (Ohashi *et al*., 2003). Within this mechanism the expression of *GL2* is promoted by an upstream non-hair cell complex which encompasses WER, TTG1, GL3, MYC1 and EGL3 (Kang *et al*., 2009). In addition to its root epidermal function the *GL2* gene, which encodes a homeodomain-containing protein, has been shown to be required for trichome formation and seed mucilage production (Koornneef, 1981; Rerie *et al*., 1994; Masucci *et al*., 1996). The *GL2* mutant utilised during this study was the *gl2-1* mutant, which is in the *Landsberg erecta* background and is a fast neutron induced mutant allele that results in a 19 base pair deletion (Koornneef *et al*., 1982; Masucci *et al.*, 1996). Approximately 50% of its non-hair cells produce root hairs, but other cellular differences between the hair and non-hair cells, for example cell size and cytoplasmic density, remain unaffected, (Masucci *et al*., 1996). In the shoot the number of trichomes is reduced (Masucci *et al*., 1996). In this instance the fact that approximately 50% of the *gl2-1* mutants non-hair cells also produce root hairs makes it particularly useful, since these ectopically produced hairs facilitate a direct means of investigating how the repressive auxin response regime may be influencing root hair growth.

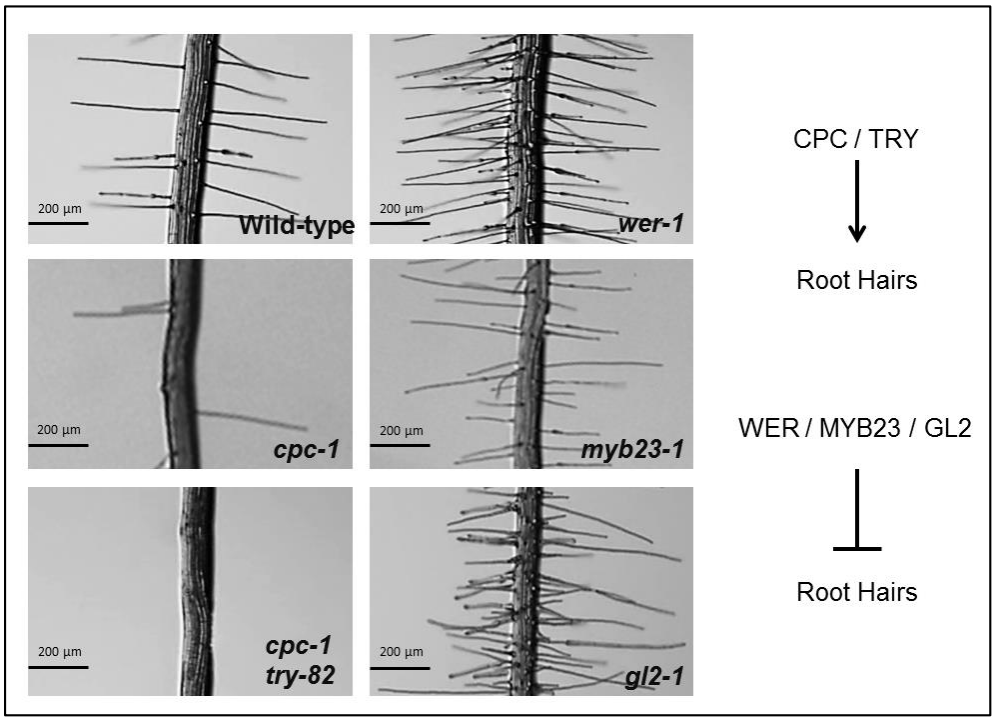

Figure 3-1: Mutant phenotypes of epidermal patterning mutants used during this project.

The root epidermal patterning mechanism is well characterised with multiple mutant lines available for many of the patterning components. These give a range of phenotypes from roots that produce no root hairs to roots that produce hairs from every epidermal cell. There are also intermediate phenotypes like *gl2-1* and *myb23-1* that have approximately 50% and 5% ectopic root hairs respectively. Generally *CAPRICE* and *TRIPTYCHON* promote the production of root hairs whilst *WEREWOLF, GLABRA 2* and *MYB23* inhibit the production of root hairs. Photographs Sharpened 50%, Brightness +20%, Contrast +40%.

3.3 Analysis of the auxin response regime in the *gl2-1* mutant background

In order to examine if the patterning of auxin response was affected by the loss of *GL2* function, the *gl2-1* mutant was crossed with the aforementioned *ARF10* and *IAA17* transcriptional and translational markers for *ARF10* and *IAA17*: *pIAA17::GFP,* pIAA17::IAA17-GFP, *pARF10::GFP*, pARF10::ARF10-GFP and the *pDR5::GFP* auxin signalling output reporter (Figure 3-2).

In the *gl2-1* mutant background the transcriptional and translational markers for the repressive *ARF*, *ARF10*, indicate that as is observed in the wild-type the gene is expressed strongly in the non-hair cells from the root tip and at a much lower level in the hair cell files (Figure 3-2 B). Thus indicating that *ARF10* is still highly expressed in the non-hair files despite approximately 50% of the cells producing root hairs (Masucci *et al.*, 1996).

Other markers used to indicate a repressed response to auxin were the transcriptional and translational GFP markers for the Aux/IAA repressor *IAA17*. In the root epidermis *IAA17* expression as indicated by both the transcriptional *pIAA17::GFP* and translational pIAA17::IAA17-GFP markers begins around the transition zone in the non-hair files and approximately eight cells later in the hair files (Figure 1-10). When these markers were crossed into the *gl2-1* mutant background they both retained this distinct expression pattern (Figure 3-2 A). Thus indicating that this aspect of the repressive auxin response regime is also still apparent in the non-hair files of the *gl2-1* mutant.

The final marker looked at was *pDR5::GFP* auxin signalling output marker. As described previously the expression in this marker indicates a high level of auxin response in the non-hair files near the root tip, but at the transition zone this evens out across all of the files and then becomes stronger in the hair files from this

point forward (Figure 1-9). In the *gl2-1* mutant background this expression pattern persists, (Figure 3-2 C), indicating that the overall auxin response in the hair and non-hair files remains unaltered from that of the wild-type.

As the expression pattern of all of these markers in the *gl2-1* mutant background was the same as that observed in the wild-type controls, this indicated that any ectopic root hairs produced by the non-hair cells in the *gl2-1* mutant would be subject to the repressive auxin response regime observed there. These data are consistent with the hypothesis that despite some of the cells in the non-hair files producing root hairs, in terms of location in relation to the underlying cortex and cell characteristics in terms of cell size, the non-hair cell identity is maintained (Masucci *et al*., 1996). Therefore by analysing these ectopic root hairs further the hypothesis that this repressive auxin response regime is functioning to prevent the growth of root hairs could be considered.

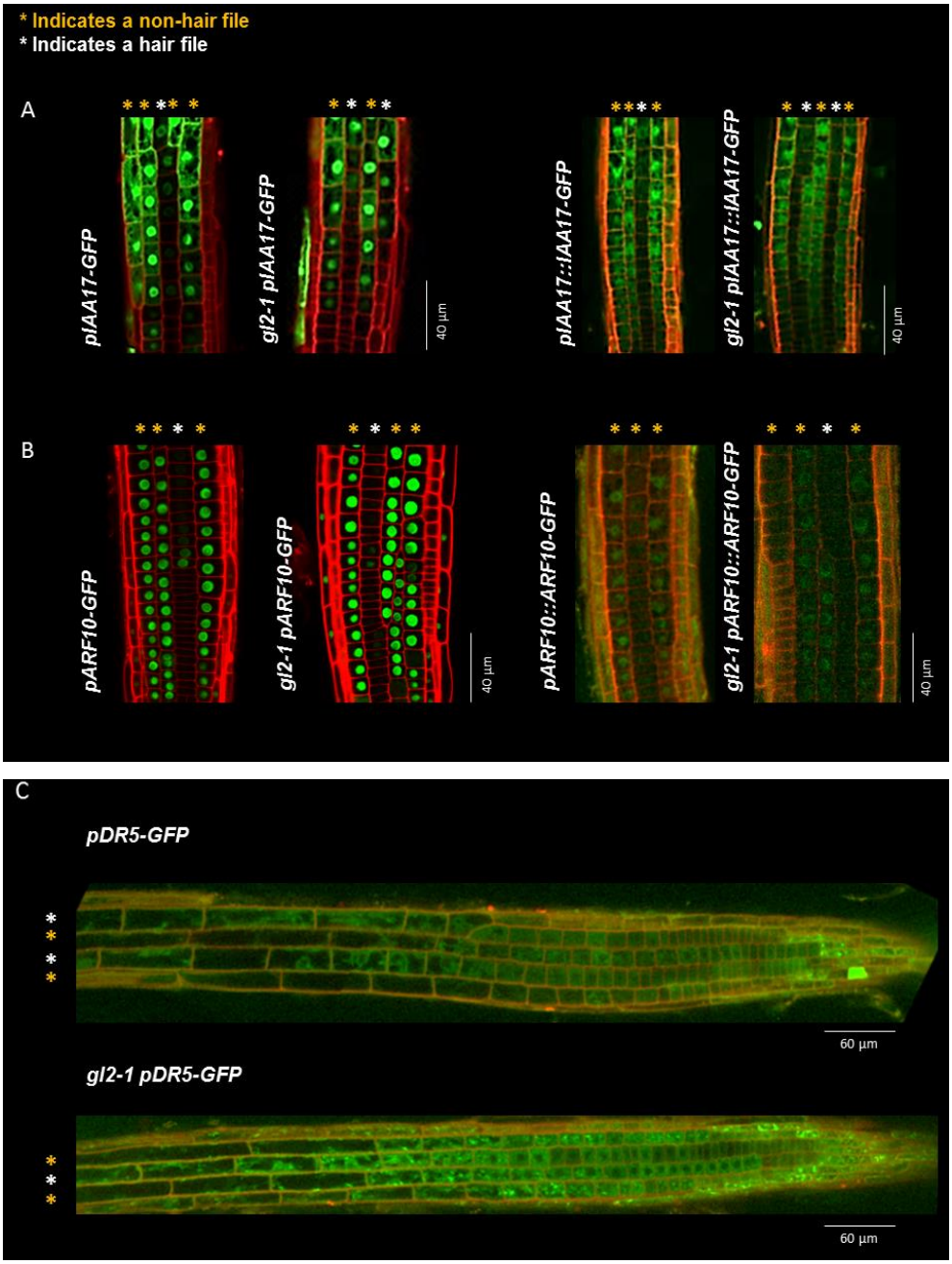

Figure 3-2: Markers for *IAA17*, *ARF10* and *pDR5::GFP* in the *gl2-1* mutant.

A: *pIAA17::GFP* and pIAA17::IAA17-GFP markers in the *gl2-1* mutant and wild-type control backgrounds. B: *pARF10::GFP* and pARF10::ARF10-GFP markers in the *gl2-1* mutant and wild-type control backgrounds. C: *pDR5::GFP* marker in the *gl2-1* mutant and wild-type control backgrounds. Photographs: Sharpened 50%, Brightness +20%, Contrast -20%. See 2.4 Confocal Microscopy for microscope settings.

3.4 Analysis of the root hairs in the *gl2-1* mutant

The *gl2-1* mutant produces root hairs in approximately 50% of its non-hair cells (Masucci *et al*., 1996). In order to begin to explore the significance of the apparent repressive auxin response regime in the non-hair cells, the root hair length profile of this mutant was characterised. It was hypothesised that if a repressive auxin response regime was affecting root hair growth in these mutants, it should be detectable in root hair length data, owing to the large number of ectopic root hairs in this background.

Root hairs in the *gl2-1* mutant were compared to the wild-type line *Landsberg erecta (*Figure 3-3). The root hair phenotype of the *gl2-1* mutant corroborated published data, in that the density of root hairs was significantly higher than the wild-type (Supplementary Data Figure 9-1). In addition to this whereas the wild-type root hairs were more uniform in length the root hair lengths in the *gl2-1* mutant appeared to be more variable (Figure 3-3 A).

Preliminary root hair data was measured from plants grown across several plates to account for any variability in environmental conditions (e.g. humidity), and the average root hair lengths were compared (Figure 3-3 B). The wild-type consistently and reproducibly had a significantly longer ($P<0.005$, T-Test) root hair length average than the *gl2-1* mutant (Figure 3-3 B).

In order to establish if the *gl2-1* mutant root hair length average was lower because of a uniform reduction in root hair length, or because some of the root hairs were unusually short and therefore bringing the average value down, the root hair length frequency profile was analysed. To do this root hairs were measured using the same methods and techniques that were used to assess the average root hair length, but instead of averaging the data the root hair lengths

were grouped into root hair length categories and the overall root hair length profile was assessed (Figure 3-3 C).

The root hair length frequency profile comparison indicated that the shorter average root hair length observed in the *gl2-1* mutant was due to the fact that the mutant had significantly more ($P<0.005$, ANOVA) shorter root hairs than the wild-type line *Landsberg erecta*.

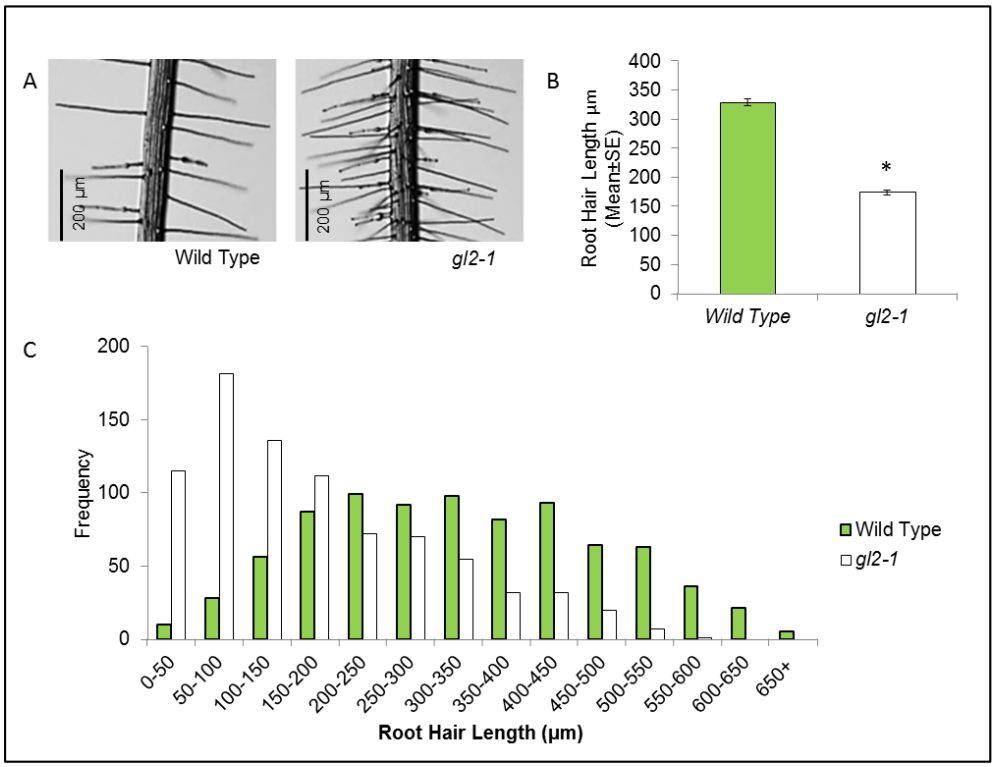

Figure 3-3: Analysis of the *gl2-1* mutant root hair length.

A: Root hairs in the *gl2-1* mutant are noticeably less uniform in length and much denser than the wild-type *Landsberg erecta*. B: The average root hair length of the *gl2-1* mutant is significantly shorter ($P<0.005$, T-Test) than that of the wild-type. C: Root hair length frequency analysis indicates that the *gl2-1* mutant has a significantly higher (ANOVA, $P<0.005$) number of shorter root hairs (less than 150 µm) than the wild-type. All root hair analysis was carried out on roots taken from several plates to account for differences in conditions, e.g. humidity, in addition to this all assays were repeated a minimum of three times before conclusions were drawn. Error bars represent standard error values.

3.5 Does the loss of aux1 in the *gl2-1* mutant influence the short root hair phenotype?

One hypothesis to account for these short root hairs was that they may be those produced ectopically by the non-hair cells. However before this could be explored further it was necessary to consider AUX1 expression. A previous cross produced in the Kepinski lab, *gl2-1,pAUX1::AUX1-YFP* indicated that AUX1 expression was lost in a *gl2-1* mutant (Supplementary Data Figure 9-2). This is consistent with previous results discussed in the Jones *et al* 2009 paper, whereby pAUX1::AUX1-YFP expression was lost in the *wer-1 myb23-1* double mutant. Both WER and MYB23 promote the expression of *GL2* (Kang *et al.*, 2009; Schiefelbein *et al*., 2009). In addition to this, published data has indicated that auxin transport in the root is important for successful root hair elongation (Jones *et al.*, 2009). In order to evaluate if the short root hairs in the *gl2-1* mutant were a consequence of the loss of AUX1, the root hair profile of the *gl2-1* mutant was compared to that of two AUX1 knockout mutants, *aux1-7* and *aux1-22 (*Figure 3-4).

The *aux1-7* mutant produces a missense protein that is translated and transported but is not functionally active, whereas as *aux1-22* is a null mutation whereby the protein is subject to nonsense mediated degradation (Marchant and Bennett, 1998; Swarup *et al.*, 2004; Ugartechea-Chirino *et al*., 2010). In previous publications missense and null mutations in AUX1 have elicited different responses, therefore both mutants were compared during this assay in order to account for that possibility (Marchant and Bennett, 1998; Swarup *et al*., 2004; Ugartechea-Chirino *et al*., 2010).

In comparison to both the *aux1-7* and *aux1-22* mutant lines the *gl2-1* mutant exhibited significantly more ($P<0.005$, ANOVA) shorter root hairs (Figure 3-4). This indicates that whilst the disruption of auxin influx transport in the non-hair

cells of the *gl2-1* mutant may result in more shorter root hairs, the loss of *AUX1* function in the *gl2-1* background is not the principal cause of the higher frequency of shorter root hairs observed.

In order to confirm this further the *gl2-1* mutant was treated with the synthetic NAA (Figure 3-5). NAA is particularly useful in this instance as it is a synthetic auxin that does not require AUX1 influx transporters in order to enter cells (Delbarre, 1994). Therefore any phenotype due to the loss of AUX1 should be negated during these assays.

The *gl2-1* root hair length frequency profiles indicated that after treatment with 0.1 µM NAA a population of short root hairs was still apparent (Figure 3-5 B). These data indicated that restoring effective auxin transport by circumventing the requirement for AUX1 did not rescue the *gl2-1* short root hair phenotype. Further confirming that other factors are influencing the lack of root hair elongation in the *gl2-1* mutant.

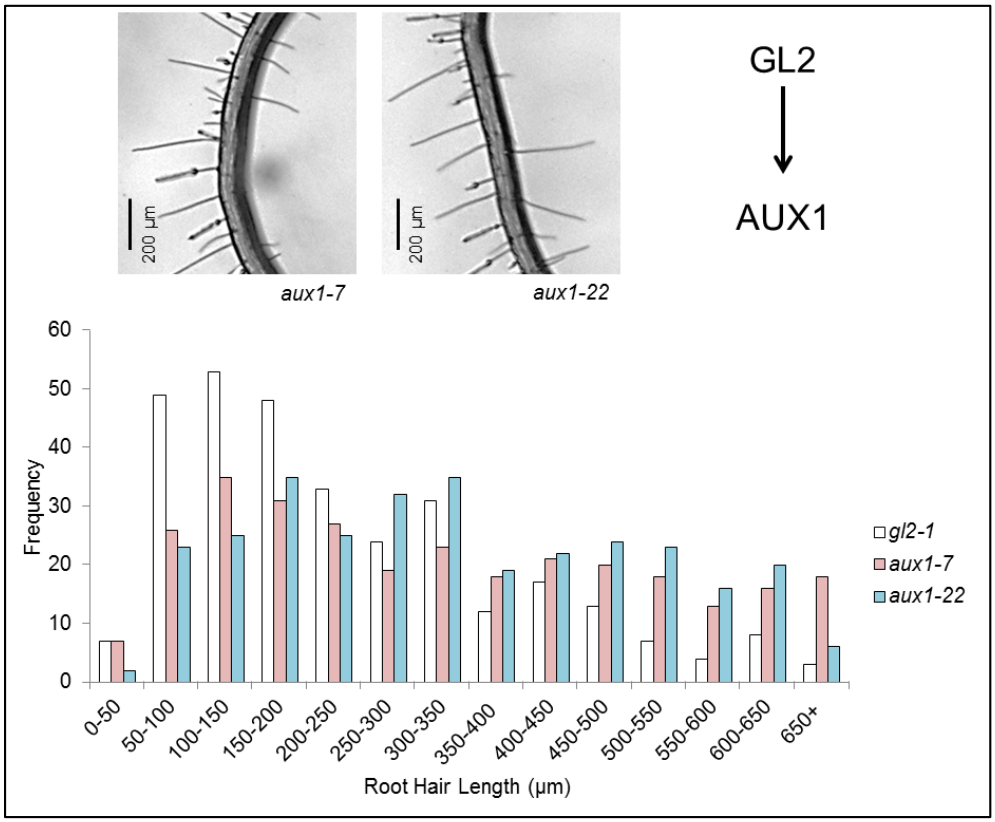

Figure 3-4: Analysis of the *gl2-1* mutant in comparison to the *aux1-7* and *aux1-22* mutants.

In a *gl2-1* background AUX1 is lost in the root epidermis. Both the *aux1-7* and *aux1-22* mutants have been characterised to have shorter root hairs. To establish that the shorter root hairs observed in the *gl2-1* background were not solely due to the loss of AUX1 the root hair length profiles of all the mutants were compared. This frequency data indicated that whilst *aux1-22* and *aux1-7* did have a higher number of shorter root hairs (less than 150 µm), the *gl2-1* mutant had signficantly more (ANOVA, $P<0.005$). Photographs: Sharpened 50%, Brightness +40%, Contrast -20%.

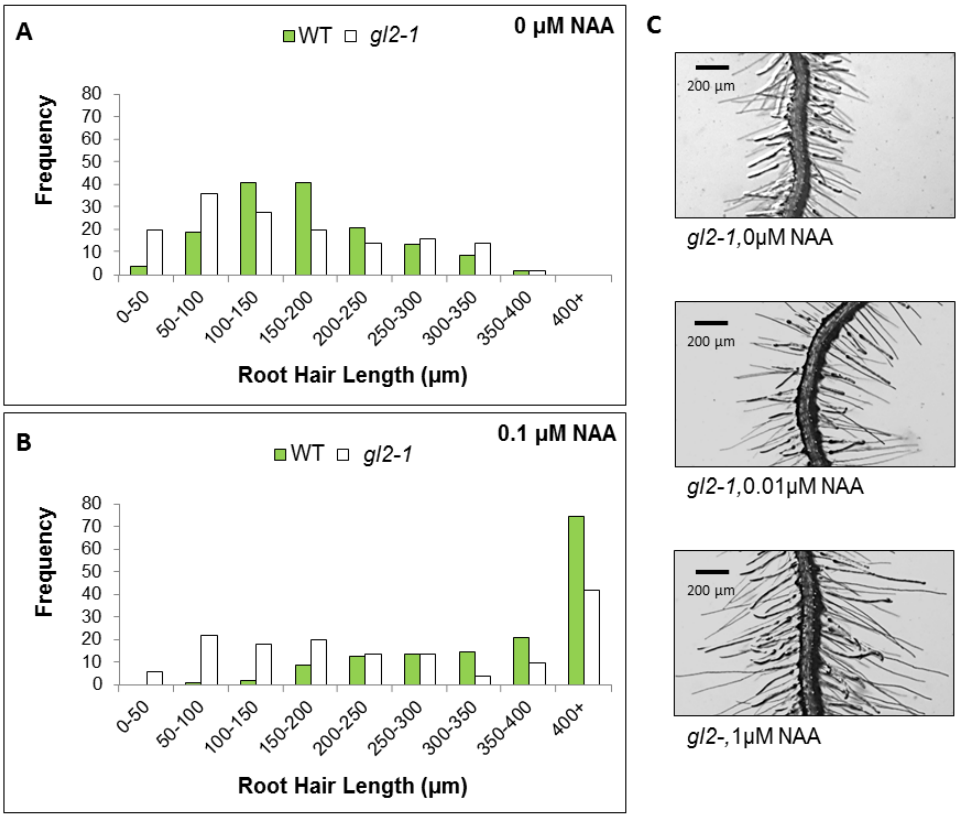

Figure 3-5 : Treatment of the *gl2-1* mutant with NAA.

After treatment with NAA, which does not require the AUX1 influx transporter to enter cells, the *gl2-1* short root hair profile persisted. Photographs: Sharpened 50%.

3.6 Are these shorter root hairs less responsive to auxin?

The NAA treatment assay highlighted the fact that rather than all, or none of the root hairs in the *gl2-1* mutant elongating in response to treatment with NAA, two distinct populations were apparent. Whilst the majority of the root hairs elongated normally like the wild-type to more than double their original length, a population of shorter root hairs, which had not elongated as much were still clearly apparent. Whilst these results were consistent with the hypothesis that the short root hairs in the *gl2-1* mutant were not due to the loss of AUX1, they also indicated that these shorter root hairs may in fact be less responsive to auxin in terms of root hair elongation. To check that this was not just a phenomenon of NAA treatment the assay was repeated with the naturally occurring form of auxin, IAA (Figure 3-6).

When treated with IAA a population of shorter root hairs in the *gl2-1* mutant was still apparent; however these do appear to have elongated slightly more than was seen with NAA treatment.

These results were consistent with the *gl2-1* mutant having a larger population of shorter root hairs than the wild-type due to factors other than the loss of *AUX1.* In addition to this the *gl2-1* mutant has a population of root hairs, potentially these shorter root hairs, which elongate significantly less than root hairs in the wild-type when treated with auxin.

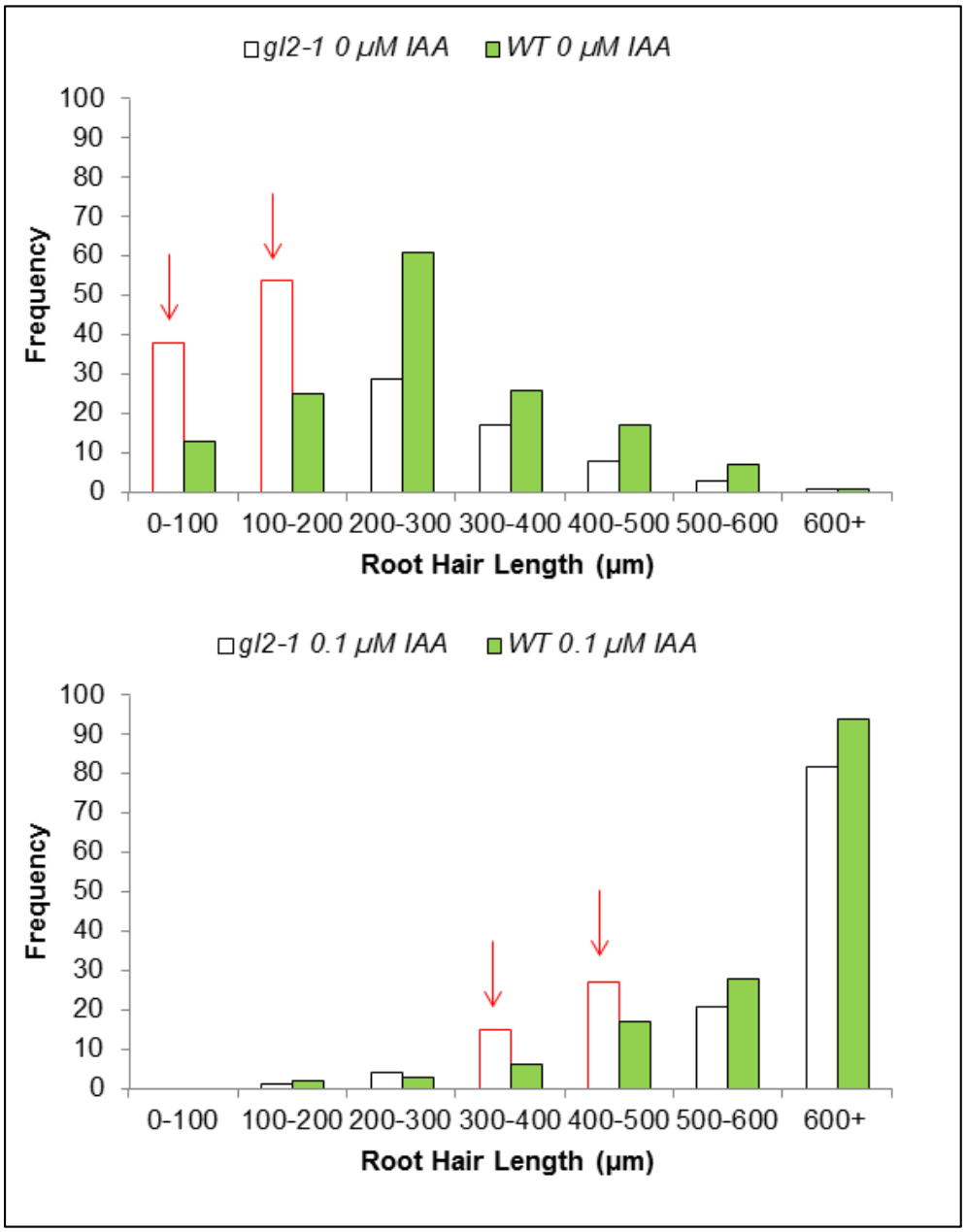

Figure 3-6: Treatment of the *gl2-1* mutant with IAA.

Treatment with the naturally occurring auxin Indole-3 Acetic Acid corroborated the phenomenon observed with NAA. A population of shorter root hairs, which appear to respond less to auxin are highlighted in red.

3.7 Are these shorter root hairs those produced by the non-hair cells?

In order to establish if this short root hair population were the root hairs produced by the non-hair cells, and therefore subject to the repressive auxin response regime present there, it was necessary to develop a method of individually identifying the hairs that were being produced by the non-hair and hair cells respectively.

In order to identify the ectopic root hairs, initially the *pARF10::GFP gl2-1* cross was analysed further. As the *ARF10* marker is nuclear localised and brighter in the non-hair cells it was hypothesised that identification of fluorescent nuclei in root hairs would indicate ectopically produced root hairs. However, although this worked in practice on the confocal microscope (Supplementary Data Figure 9-3) to measure enough root hairs to get any meaningful data whole root imaging was required on the less powerful Olympus SZX12 GFP Microscope. Unfortunately due to the small size of the nuclei it was difficult to tell if they were present in the root hairs. Typically you would expect nuclei to be at the tip of the root hair and false positives were common due to the root tip touching the growth media creating a root tip “glowing effect”.

Therefore in order to investigate this more reliably a new line was produced by crossing the *gl2-1* mutant with the *pGL2::GFP* marker line. The *pGL2::GFP* marker was a better choice because like *ARF10* it is preferentially expressed in the non-hair files, but unlike *ARF10* the fluorescence is expressed throughout the cytoplasm and at a very strong level (Kang et al., 2009) (Figure 3-7 A).

Although the GL2 protein is not functional in the *gl2-1* mutant background the *pGL2::GFP* marker is still active as only *GL2* promoter activity is required. In

addition to that, in the *gl2-1* background the *pGL2::GFP* marker appears to undergo some form of additional positive feedback, or lack of negative feedback, which results in the GFP level being higher than the wild-type.

The *pGL2::GFP* fluorescence in the *gl2-1* mutant background successfully marked the ectopic root hairs and therefore made it possible to measure their length in comparison to the non-fluorescent root hairs that were produced by the hair cells (Figure 3-7 B/C). The root hairs produced by the non-hair cells, and thus subject to the repressive auxin response regime were significantly shorter ($P<0.005$, T-Test) than those produced by hair cells.

These results were consistent with the hypothesis that the negative auxin response regime in the non-hair cells may be functioning to repress root hair growth in the non-hair position.

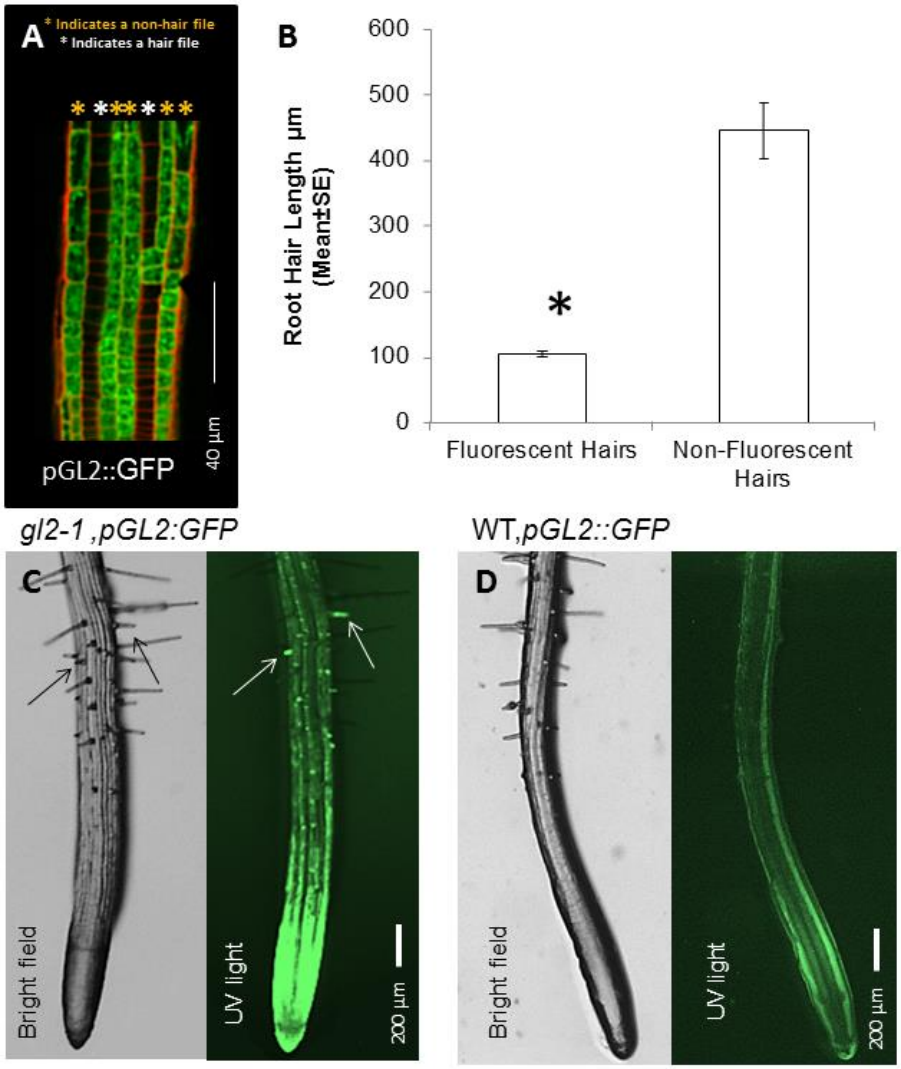

Figure 3-7 : Expression of the *pGL2::GFP* marker in the *gl2-1* mutant.

A: The *pGL2::GFP* marker is preferentially expressed in the non-hair cells. C-D: By crossing the *pGL2::GFP* marker into the *gl2-1* mutant ectopically produced root hairs were visible. B: Measurement of fluorscent root hairs indicated that those produced ectopically by the non-hair cells (fluorescent) were significantly shorter (T-TEST, $P<0.005$) than those produced by the hair cells (non-fluorescent). Photographs: Brightness +40%, Contrast -20%. See 2.4 Confocal Microscopy for microscope settings. Error bars represent standard error values.

3.8 Does removing the repressive ARFs, *ARF10* and *ARF16*, restore the ectopic root hair length?

In order to further confirm if the repressive auxin response regime in the non-hair cells was affecting root hair elongation, the *gl2-1* mutant was crossed with the *arf10-3 arf16-2* double mutant. The *arf10-3 arf16-2* double mutant knocks out two repressing ARFs within the same clade (Finet *et al*., 2013). In this clade *ARF10* and *ARF16*, along with *ARF17* all share high amino acid sequence similarities, and all contain an additional stretch of amino acids in the DNA binding domain (Wang *et al*., 2005). The double *arf10-3 arf16-2* mutant was used in this study because the high sequence similarities, coupled with overlapping expression patterns between *ARF10* and *ARF16* imply a functional redundancy (Wang *et al*., 2005). Both the *arf10-3* and *arf16-2* mutants carry a T-DNA insertion and as a double mutant the plants exhibit a severely agravitropic phenotype (Wang *et al*., 2005). In addition to this a high number of ectopic root hairs are observed. The *gl2-1 arf10-3 arf16-2* triple mutant was produced to assess if the removal of the function of these ARFs, which elicit a repressive auxin response, resulted in the loss of the shorter and the less responsive root hairs observed in the *gl2-1* mutant.

Analysis of the triple *gl2-1 arf10-3 arf16-2* mutant indicated that in comparison to the high frequency of short root hairs observed in the *gl2-1* mutant, the triple mutant did not exhibit significantly more shorter root hairs than the wild-type (Figure 3-8 C/D). In addition to this when the triple mutant was treated with auxin all of the root hairs elongated significantly (Figure 3-8 B). In contrast to *gl2-1,* the root hairs in the triple mutant elongated significantly more than the wild-type at a concentration of 0.1 μM IAA. This was also observed in the *arf10-3 arf16-2* double mutant (Figure 3-8 C/D).

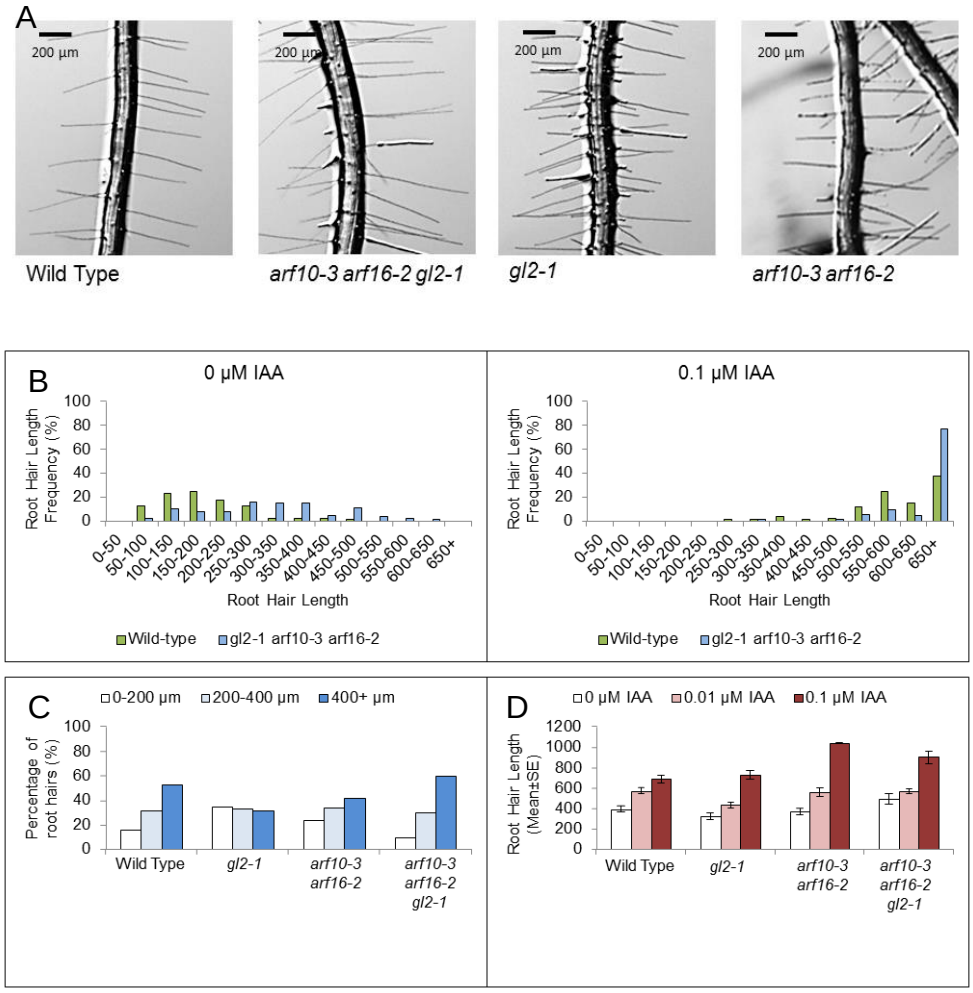

Figure 3-8: Analysis of the *gl2-1 arf10-3 arf16-2* triple mutant.

A: The root hairs of the *arf10-3 arf16-2 gl2-1* triple mutant in comparison to associated mutants and wild-types. B: When the *gl2-1 arf10-3 arf16-2* triple mutant was treated with 0.1 µM IAA all of the root hair population elongated. C/D: Without auxin treatment the *gl2-1 arf10-3 arf16-2* triple mutant did not exhibit the significantly higher percentage of short root hairs seen in the *gl2-1* mutant. Compared to the wild-type the *arf10-3 arf16-3 gl2-1* triple mutant has fewer short (less than 150 µm) root hairs. Photographs: Sharpened 50%, Brightness +20%, Contrast +20%. Error bars represent standard error values.

3.9 Discussion

To investigate the functional significance of the apparent repressive auxin response regime in the non-hair cells, two non-mutually exclusive hypotheses were considered. Firstly that the repressive auxin response is part of the mechanism that restricts root hair growth and secondly that it may facilitate an auxin superhighway via the non-hair cells, to enable a reliable and sustained delivery of auxin to the hair cells. In order to investigate this the *gl2-1* loss of function mutant was used (Koornneef, 1981; Ohashi *et al.*, 2003). By crossing this mutant with markers for *ARF10* and *IAA17* confirmation that the repressive auxin response was still apparent in the non-hair cells was achieved, despite up to 50% of them producing root hairs (Masucci *et al*., 1996). Subsequent analysis of these ectopic root hairs indicated that the *gl2-1* mutant had significantly more shorter root hairs, analysis of the *pGL2::GFP* marker confirmed that these shorter root hairs were those produced by the non-hair cells. To discount the effect of the loss of *AUX1* on the *gl2-1* mutant root hair length, comparisons with *AUX1* null and missense mutants, and treatment with the synthetic auxin NAA was tested. The NAA assays also highlighted that the *gl2-1* mutant has a population of root hairs that were less responsive to auxin, a phenomenon that was later additionally confirmed with IAA assays.

To assess if these short root hairs were lost when some of the repressive auxin response components were removed, the *arf10-3 arf16-2 gl2-1* triple mutant was produced and analysed. In this mutant the shorter root hairs typical of the *gl2-1* mutation were lost, in addition to this all of the root hairs elongated significantly when treated with auxin. These results were consistent with the repressive auxin response regime in the non-hair cells functioning as part of the mechanism that restricts root hair growth (Figure 3-9). It also highlighted the possibility that *ARF10* and/or *ARF16* may play a role in root hair elongation, knocking out both of these repressing ARFs resulted in significantly more root hair elongation in response to auxin treatment in comparison to the wild-type.

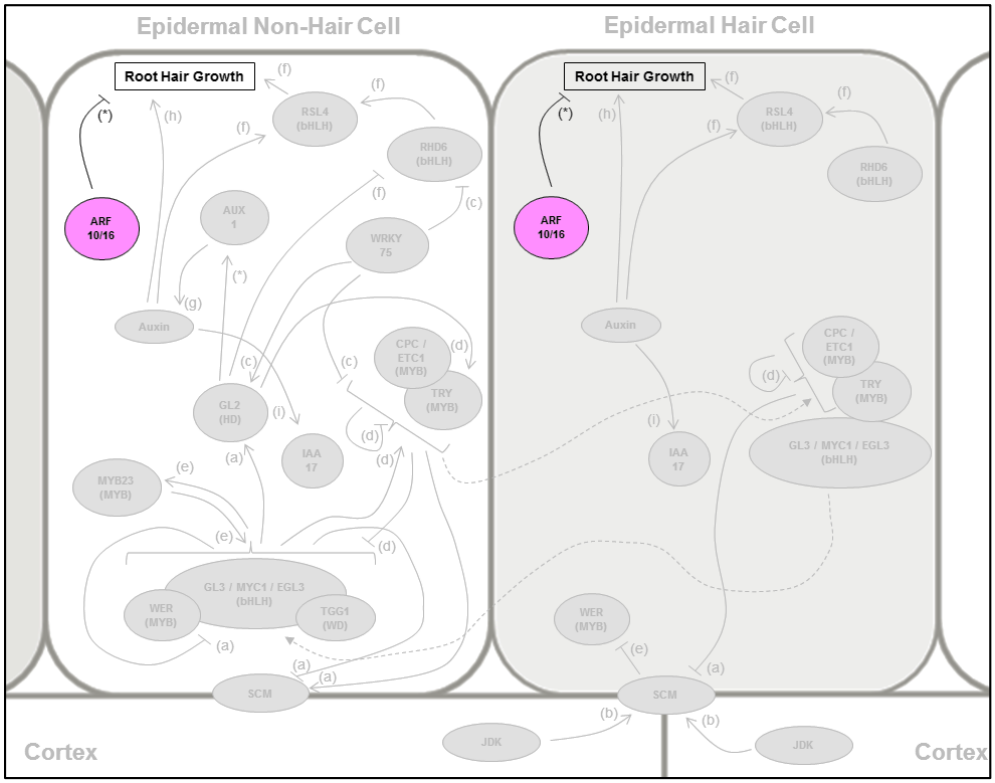

Figure 3-9: ARF10 and/or ARF16 inhibit root hair growth.

Analysis of the short ectopic root hairs in the *gl2-1* mutant and the subsequent lack of them in the *arf10-3 arf16-2 gl2-1* triple mutant indicated that *ARF10* and/or *ARF16* may play a role in inhibiting root hair growth. Solid lines indicate promotion (arrow head) or inhibition (flat head), dashed lines indicate movement in the direction of the arrow head. Letters next to the arrows indicate the published source of the interaction. (a) (Kwak and Schiefelbein, 2008) (b) (Hassan et al., 2010) (c) (Rishmawi et al., 2014) (d) (Simon et al., 2007) (e) (Kang et al., 2009) (f) (Yi et al., 2010) (g) (Jones et al., 2009) (h) (Masucci and Schiefelbein, 1996) (i) Tromas and Perrot-Rechenmann 2010. (*) indicates interactions identified during this project.

4 : Placing Spatial Control of Auxin Response in Current Knowledge of the Epidermal Patterning Mechanism

4.1 Introduction

Two well characterised pathways within plant growth are the auxin response network and the root epidermal patterning mechanism. In 1996 a paper by Masucci *et al* first looked the concept of these two pathways working together. As auxin was able to rescue the *rhd6* mutant phenotype in double *gl2-1 rhd6* and *ttg1-1 rhd6* mutants, they concluded that auxin did not act through a pathway that requires the *GL2* or *TTG1* gene products, and therefore must act downstream of this epidermal patterning mechanism (Masucci and Schiefelbein, 1996).

4.1.1 The epidermal patterning mechanism

Since this data was published, understanding of the epidermal patterning mechanism has progressed. Via a complex but well characterised mechanism it is now understood that in *Arabidopsis* hair and non-hair cells arise in a position dependent manner, whereby hair cells are produced over the anticlinal wall of two underlying cortical cells, and non-hair cells are produced over the periclinal wall (Kwak and Schiefelbein, 2007a; Schiefelbein *et al*., 2009).

In the hair cells SCM inhibits the expression of a MYB type transcription factor WER (Figure 1-7) (Kwak and Schiefelbein, 2007a). In epidermal cells that are not positioned over a cortical cell junction WER transcription is not inhibited (Kwak and Schiefelbein, 2008). WER interacts with TTG1, GL3, MYC1 and EGL3 to form a key non-hair promoting transcription factor complex (Ohashi *et al.*, 2003; Schiefelbein *et al*., 2009). This complex promotes the non-hair cell fate via the positive regulation of *GL2*, which in turn represses the transcription of root hair promoting genes like *RHD6* (Masucci and Schiefelbein, 1994). It also positively

regulates the expression of *MYB23,* which undergoes a positive feedback loop with itself and *WER*, thus reinforcing the non-hair cell fate (Kang et al., 2009).

In addition to promoting the non-hair cell fate this complex also promotes the expression of several one repeat MYB genes that promote the hair cell specification, these are *CPC, TRY* and *ETC1* (Ryu *et al*., 2005; Schiefelbein *et al*., 2009). Despite being produced in the non-hair cells these proteins relocate to adjacent hair cells, where they function to repress the non-hair complex formation, thereby promoting the hair cell fate (Savage *et al*., 2008). In a *scm-1* mutant, hair and non-hair cells often continue to develop in an alternating manner due to this lateral inhibition (Savage *et al*., 2008).

4.1.2 The auxin response network

The auxin response network is made up of three key protein families that form part of a dynamic interaction network (Figure 1-2) (Del Bianco and Kepinski, 2011). This network brings about a transcriptional response to auxin, as the repression of auxin response gene expression is reduced (Del Bianco and Kepinski, 2011). These three families consist of the $SCF^{TIR1/AFB}$ family of auxin receptors and two families of transcription factors, the Aux/IAA's and the *ARFs* (Tromas and Perrot-Rechenmann, 2010).

Auxin promotes the proteasomal degradation of the Aux/IAA repressor proteins, thus allowing the ARFs to activate or repress the auxin response genes they are interacting with (Figure 1-2) (Tiwari *et al*., 2001; Tiwari *et al.*, 2004; Del Bianco and Kepinski, 2011). Although the majority of ARFs are considered to be activating, five members are also thought to be repressing, these are hypothesised to function by competing with activating ARFs for auxin response elements in the promoter regions of auxin response genes (Lokerse and Weijers, 2009; Tromas and Perrot-Rechenmann, 2010).

Although understanding of the epidermal patterning mechanism and the auxin response network has increased since the Masucci *et al* data was originally published, the concept of auxin acting downstream of the epidermal patterning mechanism has remained consistent. Unpublished microarray data obtained in the Kepinski lab before this project began highlighted that auxin treatment down regulates the expression of two epidermal patterning components *MYB23* and *GL2* (Supplementary Data Figure 9-5), indicating that this view is too simplistic and the relationship between these two important aspects of plant growth may be more complex. Therefore in order to place the spatial control of auxin response in the current knowledge of the epidermal patterning mechanism, markers of auxin response were crossed into epidermal patterning mutants.

4.2 Is *WEREWOLF* patterning auxin response in the root epidermis?

WER expression is regulated in a position dependent manner due to inhibition by *SCM*, resulting in higher *WER* expression in the non-hair cells (Ryu *et al*., 2005). This asymmetric localisation of *WER* results in the formation of a non-hair transcription factor complex and the promotion of the non-hair cell fate (Masucci *et al*., 1996; Ohashi *et al*., 2003).

The *WER* gene encodes a MYB-related protein containing R2 and R3 repeats (Lee and Schiefelbein, 1999; Ryu *et al*., 2005; Ishida *et al*., 2007; Wang *et al*., 2008). The MYB transcription factor family is one of the largest known transcription factor families in the *Arabidopsis* genome (Riechmann *et al*., 2000). This *Arabidopsis* family has around 339 MYB genes, which encode one to three repeats of the MYB domain (Rosinski and Atchley, 1998). The MYB domain is approximately 50 amino acids in length and exhibits regularly spaces tryptophan residues, these are DNA biding domains that form helix-turn-helix structures and are associated with transcriptional regulation (Rosinski and Atchley, 1998; Lee and Schiefelbein, 1999). The WER amino acid sequence reveals a 203 residue protein, 23.5 kDa in size, with two MYB domains in its N-terminal region (Lee and Schiefelbein, 1999).

There are three WER mutants characterised: *wer-1, wer-2* and *wer-3* (Lee and Schiefelbein, 1999). These differ in their wild-type *Arabidopsis* backgrounds but all contain a single base substitution resulting in a non-sense mutation within the second MYB domain (Lee and Schiefelbein, 1999). The product from each of these mutants is a truncated WER protein that is non-functional (Lee and Schiefelbein, 1999). All of these mutants produce an excessively hairy root phenotype.

Many of the genetic components involved in the root epidermal pattering mechanism are also involved in the patterning of trichomes in the shoot (Wang *et al.*, 2007). Studying the interaction between the root epidermal patterning mechanism and auxin response also enables us to consider the link between epidermal patterning and auxin response more broadly. To some extent *WER* is an exception to this as it is primarily expressed in the roots, however there is another R2R3 MYB-type transcription factor involved in trichome production, *GLABRA1*, with which *WER* is functionally interchangeable (Kellogg, 2001; Wang *et al*., 2007). In addition to this, recently published data has also indicated that *WER* is expressed in aerial parts of the plant and may play an important role in the regulation of flowering time (Seo *et al.*, 2011). Whilst the patterning of root hairs and trichomes essentially shares the same 'genetic tool kit,' providing good evidence that trichomes and root hairs are evolutionary homologous this new data indicates a functional divergence in *WER* activity (Seo *et al*., 2011).

In order to establish if *WER* is patterning auxin response in the root epidermis, auxin response markers were crossed into the *wer-1* mutant (Figure 4-1). To ensure reliable comparisons control lines were selected alongside every cross produced during this project. Homozygote lines were established via genetic and phenotypic analysis. The fluorescent marker was always crossed into the mutant background.

In the wild-type and control backgrounds the *pDR5::GFP* marker of auxin signalling output is initially observed at a higher level in the non-hair files, this then evens out across all of the files at the transition zone and proceeds to be stronger in the hair files from that point forward (Figure 1-9). In the *wer-1* mutant all of the cells produce root hairs and every file exhibits *pDR5::GFP* expression that mirrors that of a typical hair file (Figure 4-1 A). These results were consistent with *WER* inhibiting auxin responsiveness in the hair files after the

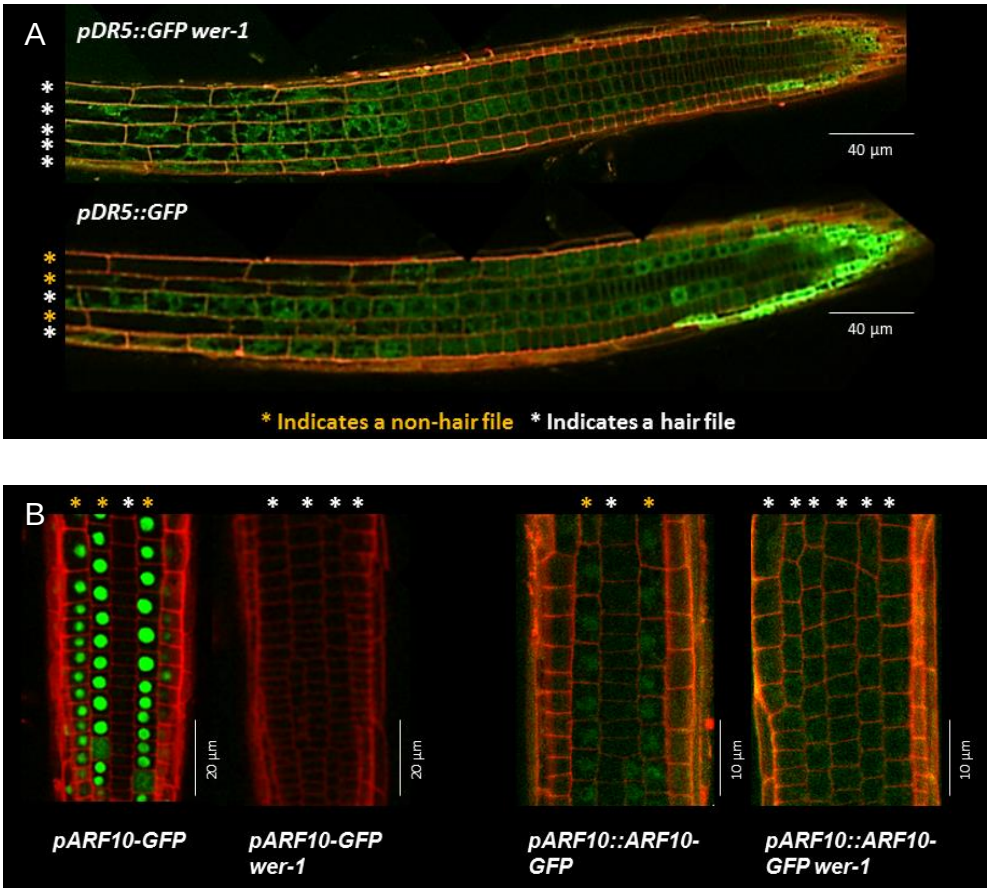

Figure 4-1: Markers for auxin response in the *wer-1* mutant background.

A: The *pDR5::GFP* marker of auxin signalling output in the *wer-1* mutant background. B: Transcriptional and translational markers for repressing auxin response factor *ARF10* in the *wer-1* mutant background. Scale bars are labelled accordingly. White * indicate hair files whilst Orange * indicate non-hair files. Photographs: Sharpened 50%, Brightness +40%. See 2.4 Confocal Microscopy for microscope settings.

transition zone, and support the hypothesis that *WER* plays a role in patterning auxin response in the root epidermis.

The *wer-1* mutant was also crossed with both the transcriptional and translational markers for the repressing auxin response factor, *ARF10*. In the wild-type and control backgrounds *ARF10* is preferentially expressed in the non-hair files from the root tip (Figure 1-11). In the *wer-1* mutant *ARF10* expression is almost entirely lost in the root epidermis, this occurs with both the translational and transcriptional markers (Figure 4-1 B).

The final markers analysed in the *wer*-1 background were the transcriptional and translational markers for the Aux/IAA repressor *IAA17*. In the control and wild-type backgrounds both the translational and transcriptional markers indicate that *IAA17* expression in the root epidermis begins around the transition zone in the non-hair cells and approximately eight cells later in the hair files (Figure 1-10). In the *wer-1* mutant the differential start of *IAA17* expression is lost, and expression begins in all of the files at the same time, at a position in the root epidermis that mirrors the eight cell delay typical of the hair files (Figure 4-2).

Results from the analysis of auxin response markers in the *wer-1* mutant background were consistent with *WER* promoting the repressive auxin response regime in the root epidermis. Specifically that *WER* promotes both the expression of *ARF10* and the early expression of *IAA17* (Figure 4-3).

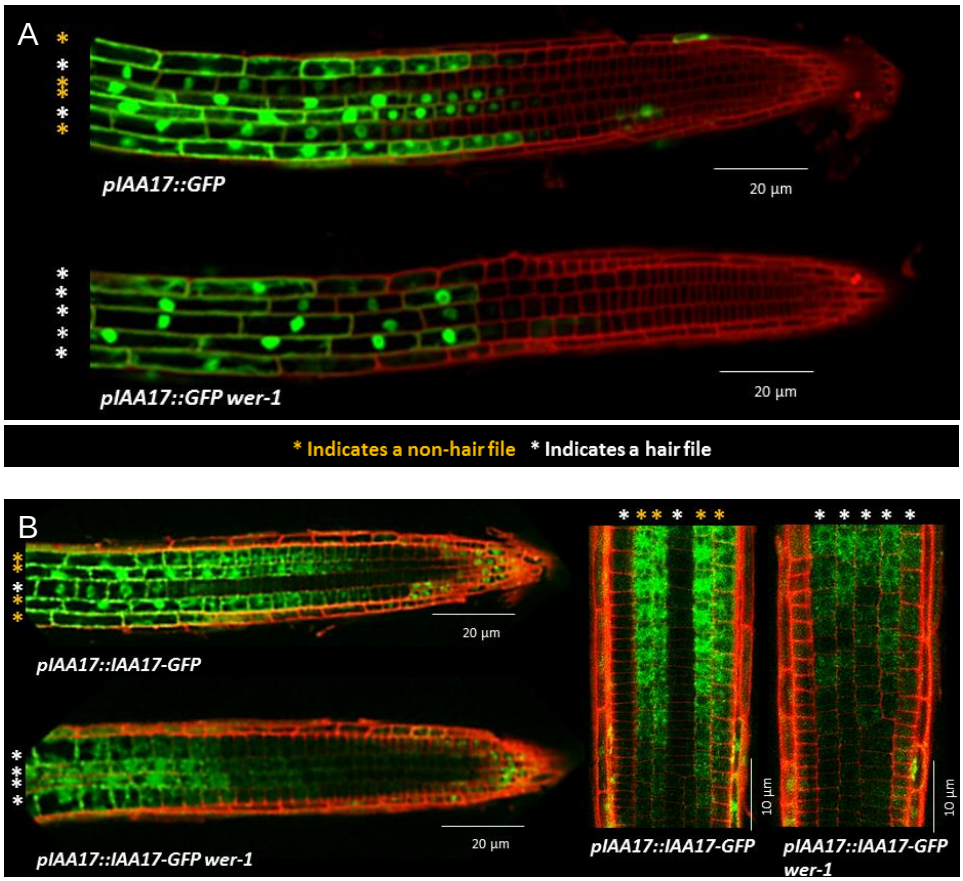

Figure 4-2: Markers for auxin response in the wer-1 background.

A: The transcriptional marker for the Aux/IAA repressor protein in the *wer-1* mutant background. B: The translational marker for the Aux/IAA repressor protein in the *wer-1* mutant background. Scale bars are labelled accordingly. White * indicate hair files whilst Orange * indicate non-hair files. Photographs: Sharpened 50%, Brightness +40%, Contrast +20%. See 2.4 Confocal Microscopy for microscope settings.

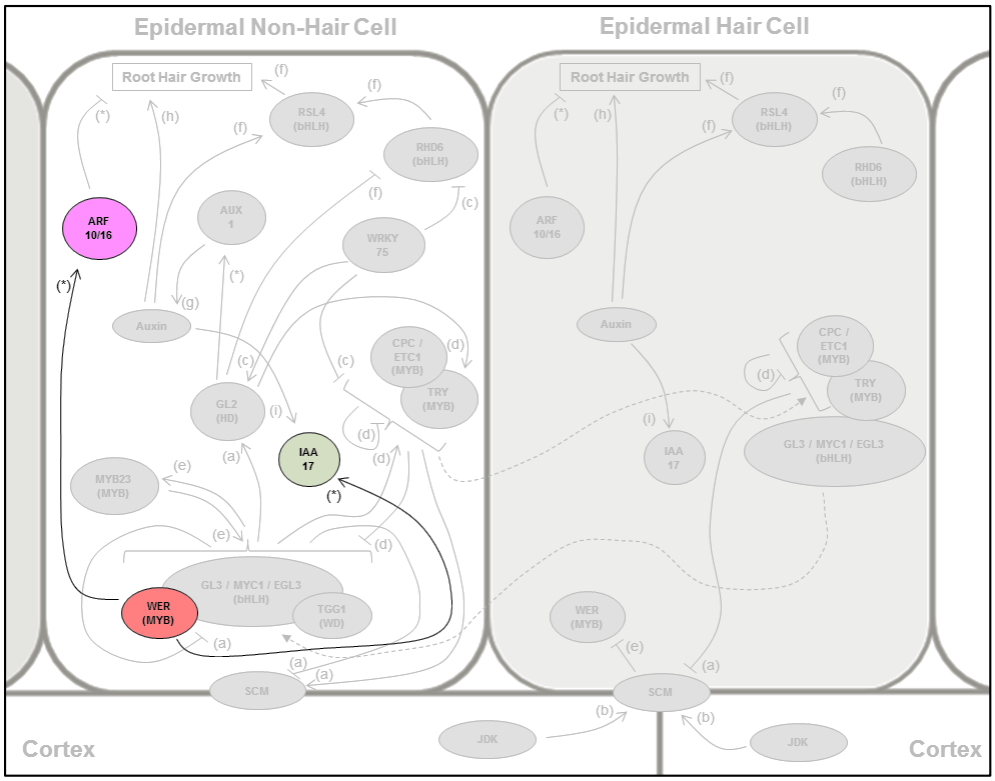

Figure 4-3: *WER* promotes the expression of *ARF10* and *IAA17* in the non-hair cells.

Results from analysis of auxin response markers in the *wer-1* mutant background were consistent with *WER* promoting the repressive auxin response regime in the root epidermis. Specifically that *WER* promotes both the expression of *ARF10* and the early expression of *IAA17*. Solid lines indicate promotion (arrow head) or inhibition (flat head), dashed lines indicate movement in the direction of the arrow head. Letters next to the arrows indicate the published source of the interaction. (a) (Kwak and Schiefelbein, 2008) (b) (Hassan et al., 2010) (c) (Rishmawi et al., 2014) (d) (Simon et al., 2007) (e) (Kang et al., 2009) (f) (Yi et al., 2010) (g) (Jones et al., 2009) (h) (Masucci and Schiefelbein, 1996) (i) Tromas and Perrot-Rechenmann 2010. (*) indicates interactions identified during this project.

4.3 Does AUX1 pattern expression of the auxin response components in the root epidermis?

Data published by Jones *et al* in 2009 indicated that in the *wer-1 myb23-1* double mutant background, expression of the auxin influx transporter *AUX1* was lost. In order to investigate if the altered auxin response expression patterns of *IAA17* in *wer-1* were due to the loss of *AUX1* expression in the root epidermis, the *wer-1 pIAA17::GFP* transcriptional cross was treated with the synthetic auxin NAA. NAA is transported into cells without the assistance of the *AUX1* influx transporter, meaning any phenotype due to the loss of *AUX1* should be negated (Delbarre, 1994). The *wer-1 pIAA17::GFP* cross and control lines were grown on increasing NAA concentrations in order to see if the wild-type expression pattern was restored (Figure 4-4). Although the level of fluorescence level did increase, which is consistent with previously published data, the expression pattern of the *IAA17* marker remained unchanged (Ouellet et al., 2001).

These results were consistent with *AUX1* not affecting the patterning of *IAA17* in the root epidermis. This was further confirmed by crossing the *ARF10* and *IAA17* transcriptional and translational markers with *aux1* mutant lines (Figure 4-5/4-6). Initially two *aux1* mutants were used, the *aux1-7* knockout mutant that produces a missense protein, which is still translated and transported but is not functionally active, and the *aux1-22* mutant, which has a null mutation whereby the protein is subject to nonsense mediated degradation (Swarup et al., 2004).

The *IAA17* transcriptional and translational markers were crossed into the *aux1-7* and *aux1-22* mutant backgrounds. Homozygote cross and control lines were selected in the manner detailed previously and the fluorescent expression pattern for *IAA17* in each of these backgrounds was observed (Figure 4-5). In the *aux1* mutant backgrounds both the transcriptional and translational markers for *IAA17* retained their wild-type expression patterns and did not differ significantly from

the control lines. These results indicated that the loss of *aux1* was not affecting the patterning of *IAA17* in the root epidermis.

In order to confirm if *AUX1* was patterning *ARF10* expression, the transcriptional *ARF10* marker was crossed into the *aux1-7* and *aux1-22* mutant backgrounds (Figure 4-6 A). Whilst the wild-type preferential expression of *ARF10* in the non-hair files was maintained in the *aux1-22* mutant, in the *aux1-7* mutant *ARF10* expression was observed to be present in all of the epidermal cells. Whilst initially confusing, further investigation indicated similar occurrences in other data that had been published. In particular a paper published by Yamel *et al* in 2010 observed *AUX1* missense mutations to affect root cap cell patterning but no effect in the *AUX1* null alleles. The authors hypothesised that the absence of AUX1 in null mutants like *aux1-22,* may trigger the redundant function of other related proteins, such as LAX1, and partially rescue the phenotype (Ugartechea-Chirino *et al*., 2010; Ugartechea-Chirino *et al*., 2010). To investigate if *AUX1* was patterning *ARF10,* but this was only apparent when other functionally redundant proteins did not rescue the phenotype, additional AUX1 mutants were crossed with the *ARF10* markers (Figure 4-6 B). These were *aux1-21,* which like *aux1-22* is a null mutation subject to nonsense mediated decay and *aux1-104,* which like *aux1-7* is a missense mutation which produces a non-functional protein (Ugartechea-Chirino *et al*., 2010). Both the *aux1-104* and the *aux1-21* mutants had a wild-type patterning of *ARF10* expression that did not differ significantly from the control lines. Indicating that the changes observed in the *aux1-7* mutant background were not typical of a missense mutation. In order to further explore this phenomenon the *AUX1* mutants were crossed with the translational *ARF10* marker (Figure 4-7). In this case the expression pattern of *ARF10* remained unaltered in all of the *AUX1* mutants including *aux1-7,* indicating that despite the unusual *aux1-7 pARF10::GFP* result, *AUX1* is unlikely to be patterning the expression of *ARF10* in the root epidermis.

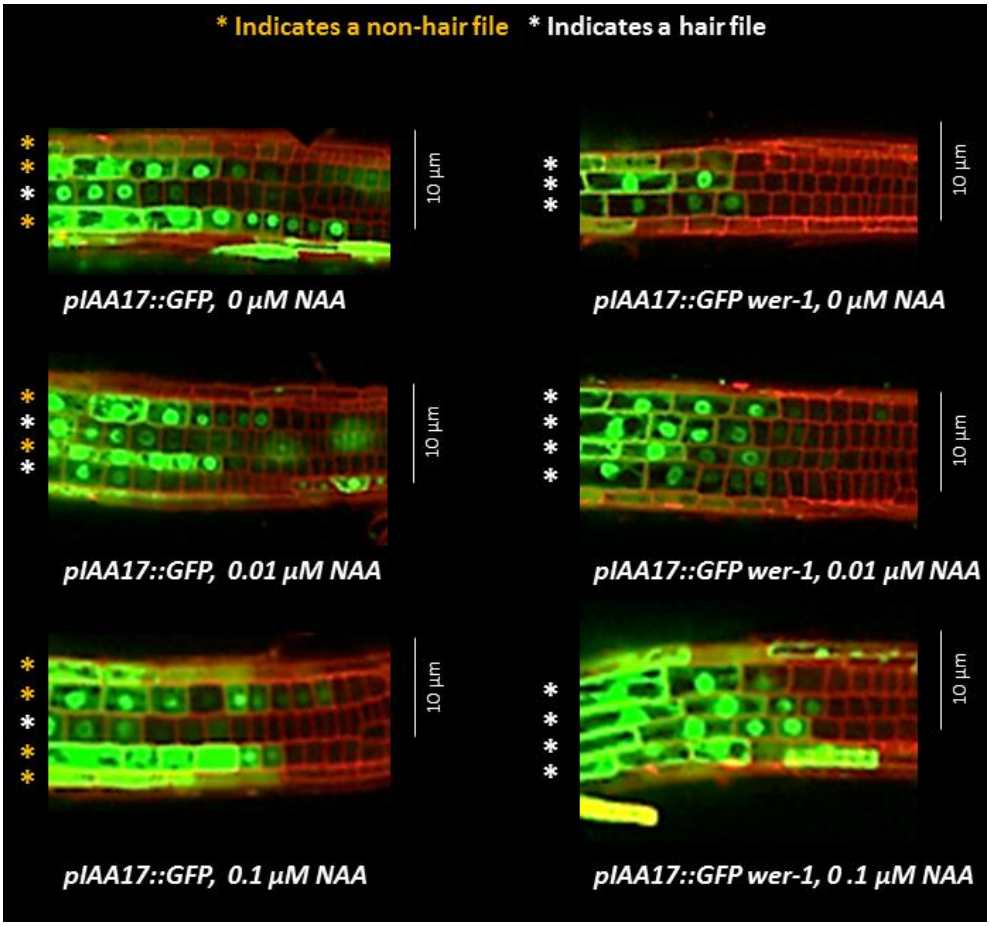

Figure 4-4: *pIAA17::IAA17-GFP* expression in the *wer-1* mutant when treated with NAA.

Homozygote lines for the transcriptional *IAA17* marker in the *wer-1* background were treated with increasing concentrations of the synthetic auxin NAA. Scale bars are labelled accordingly. White * indicate hair files whilst Orange * indicate non-hair files. Photographs: Sharpened 50%, Brightness +40%, Contrast -40%. See 2.4 Confocal Microscopy for microscope settings.

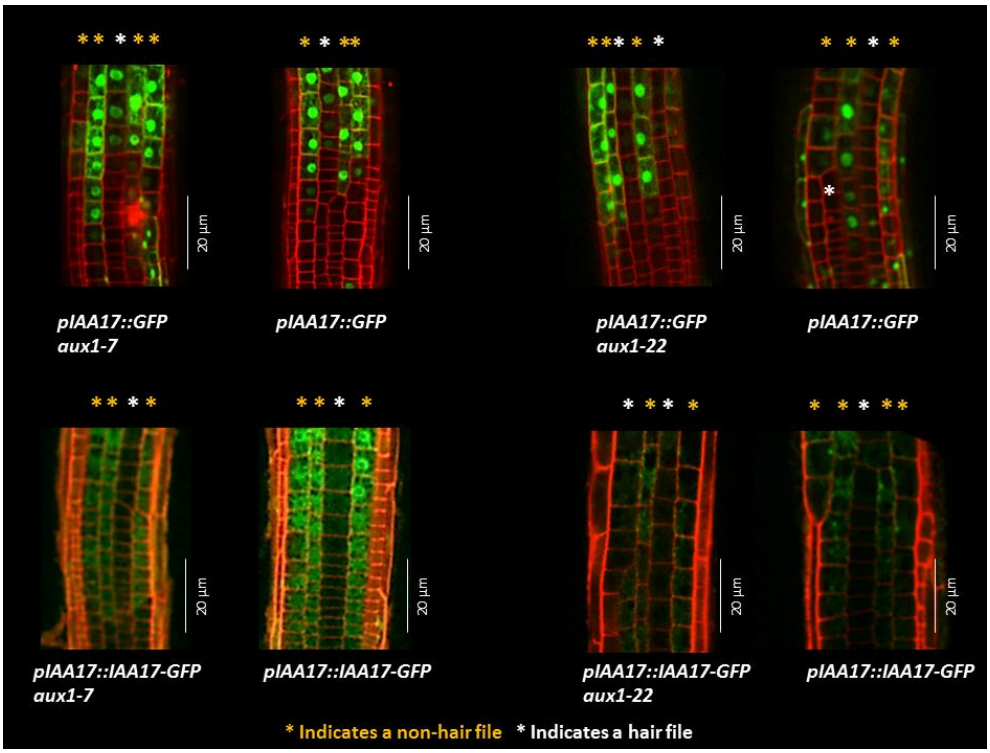

Figure 4-5: *IAA17* markers in the *AUX1* mutant backgrounds.

Translational and transcriptional markers for the Aux/IAA repressor *IAA17* were crossed into two different *AUX1* mutant backgrounds. Scale bars are labelled accordingly. White * indicate hair files whilst Orange * indicate non-hair files. Photographs: Sharpened 50%, Brightness +40%, Contrast -20%. See 2.4 Confocal Microscopy for microscope settings.

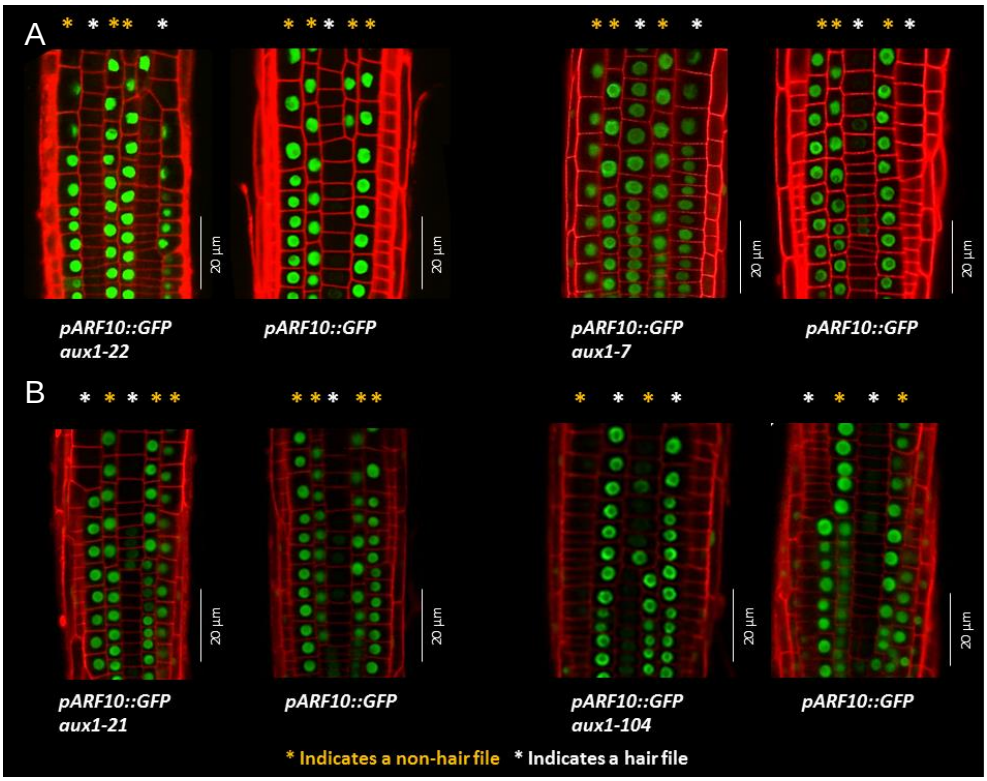

Figure 4-6: *ARF10* markers in the *AUX1* mutant backgrounds

A: The transcriptional marker for the repressive auxin response factor *ARF10* was crossed into mutants for the auxin influx transporter *AUX1.* B: The *ARF10* transcriptional marker crossed into additional null and missense *AUX1* mutants. Like *aux1-22, aux1-21* is a null mutant, whilst *aux1-104,* like *aux1-7* is a missense mutant. Scale bars are labelled accordingly. White * indicate hair files whilst Orange * indicate non-hair files. Photographs: Sharpened 50%. See 2.4 Confocal Microscopy for microscope settings.

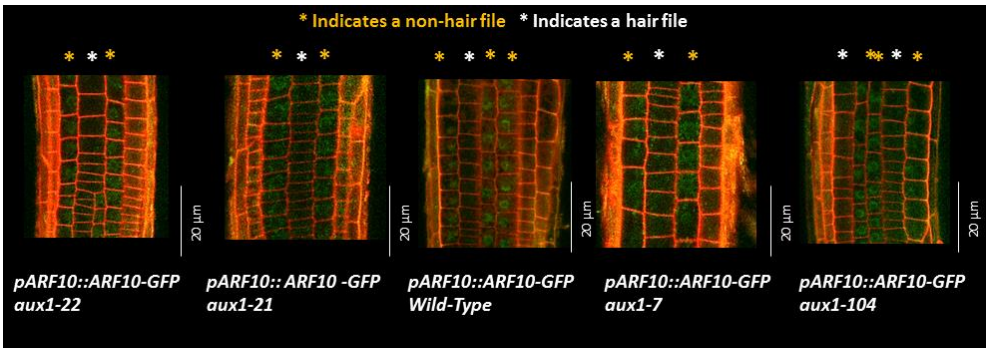

Figure 4-7: The translational *ARF10* marker in the *AUX1* mutant backgrounds.

The translational marker for *ARF10* crossed into all of the previously described *AUX1* mutants. ARF10 is patterned like the wild-type in all of these background regardless of if they are a null or missense mutations. Scale bars are labelled accordingly. White * indicate hair files whilst Orange * indicate non-hair files. Photographs: Sharpened 50%. See 2.4 Confocal Microscopy for microscope settings.

4.4 How is auxin response patterned in a *wer-1 myb23-1* double mutant?

To investigate if the *wer-1 myb23-1* double mutant patterned auxin response in the root epidermis differently to the *wer-1* single mutant, the double mutant was also crossed with the auxin response markers.

Like *WER, MYB23* is a MYB domain transcription factor (Kang *et al*., 2009). MYB domain transcription factors are involved in the regulation of growth and development in plants via many processes including; secondary metabolism, cellular morphogenesis and stress response. *WER, MYB23* and the aforementioned *GLABRA1* are all members of the same MYB sub group number 15. They share a conserved 19 amino acid motif in the putative transcription activation domain at the C-terminal end (Matsui *et al.*, 2005; Tominaga-Wada *et al*., 2012).

MYB23 is an interesting component of the epidermal patterning mechanism because it forms a positive feedback loop with itself that reinforces the non-hair cell fate (Kang *et al.*, 2009). Knockout mutants for other epidermal patterning components display variable *MYB23* transcript levels, reduced levels are observed in *WER, TTG1, GL3* and *EGL3* mutants (Kang *et al.*, 2009). In a *GL2* mutant background the *MYB23* transcript level is not significantly altered from that of the wild-type, however in a *CPC* mutant there is a significant increase, indicating that whilst MYB23 expression is promoted by *WER, TTG1, GL3* and *EGL3* it is inhibited by *CPC* and functions upstream of *GL2* (Kirik *et al*., 2001; Kang *et al*., 2009; Roeder *et al*., 2011). Conversely in a *myb23-1* mutant relative transcript levels of *GL2, WER, CPC, GL3, EGL3* and *TTG1* are not significantly altered (Kang *et al*., 2009). In addition to this GUS and GFP marker lines for these genes are not significantly altered, which is consistent with the proposed published hypothesis that *MYB23* plays a minor role in the normal establishment

of the cell pattern and gene regulatory activities in the developing root epidermis (Kang *et al*., 2009).

In a dominant negative form of *MYB23,* which utilises the modified repressor domain of *SUPERMAN (SRDX; LDLDLELRLGFA)* (Hiratsu *et al*., 2003) in frame to the 3' end of the MYB23 coding region, a significant reduction in the expression of *GL2, MYB23* and *CPC* was observed (Kang *et al*., 2009). *WER* however remains unchanged, suggesting that *MYB23* participates in the regulation of its own gene expression as well as *GL2* and *CPC* (Kang *et al*., 2009). Interestingly this construct and also a previously published *p35S::MYB23-SDRX* line both resulted in all of the epidermal cells adopting the hair cell fate (Matsui *et al*., 2005; Kang *et al.*, 2009). Published GUS reporter lines and GFP translational markers have indicated that *MYB23* is preferentially expressed in the non-hair files, and the *pWER::MYB23 wer-1* construct has indicated that MYB23 is able to functionally substitute for *WER* and rescue the *wer-1* hairy root phenotype (Kang *et al*., 2009).

Although the role of *MYB23* may be considered minor in terms of early cell patterning, the positive feedback loop that *MYB23* has with itself is proposed to reinforce the existing cell fate decision (Kang *et al*., 2009). This can be observed under conditions where the cell specification is compromised; for example where a longitudinal cell division occurs, one cell divides the wrong way resulting in the production of two new files, also known as a T junction (Figure 1-8). This occurs commonly in the root epidermis and the cells are usually robust at adopting the correct new cell fate dependent on their new position in relation to the underlying cortex. However in a *myb23-1* mutant approximately five times more of the 'new cells' adopt the incorrect cell fate (Kang *et al*., 2009). This is likely to account for the five percent increase in ectopic root hairs that are observed in this mutant, as it preferentially occurs in the non-hair files the roots appear less able to direct the non-hair cell fate (Kang *et al*., 2009).

The MYB23 mutant used during these crosses was the *myb23-1* allele from the SALK T-DNA insertion collection (Kang *et al*., 2009). The *myb23-1* mutant has a T-DNA insertion in its second intron and has no detectable *MYB23* transcripts (Kirik *et al*., 2005). As with the *wer-1* mutant the *wer-1 myb23-1* double mutant produces root hairs from all of its cells. In order to assess if knocking out *MYB23* enhances any differences in the patterning of auxin response in the root epidermis, the double mutant was crossed with the auxin response markers.

Initially crossed with the *pDR5::GFP* marker, which indicates auxin signalling output, the *wer-1 myb23-1* double mutant was observed to exhibit the same expression pattern that was present in the *wer-1* mutant (Figure 4-8).This was also true with both the *ARF10* and *IAA17* markers, indicating that knocking out *MYB23* did not result in any additive effects to the phenotype observed in the *wer*-1 single mutant, with regards to patterning auxin response in the root epidermis (Figure 4-8/Figure 4-9).

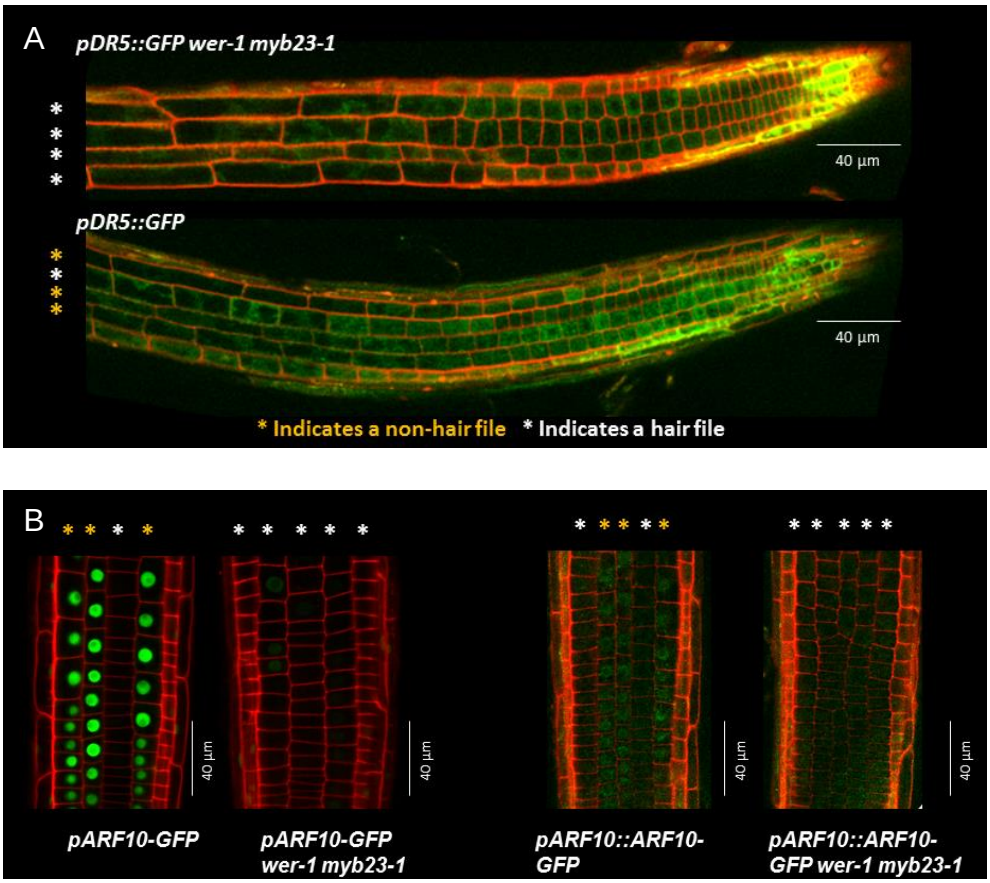

Figure 4-8: The *pDR5::GFP* and *ARF10* transcriptional and translational markers in the *wer-1 myb23-1* mutant background.

A: *pDR5::GFP* expression in the *wer-1 myb23-1* mutant background. B: In the *wer-1 myb23-1* mutant background *ARF10* expression was almost completely lost in the root epidermis. Scale bars are labelled accordingly. White * indicate hair files whilst Orange * indicate non-hair files. Sharpened 50%. See 2.4 Confocal Microscopy for microscope settings.

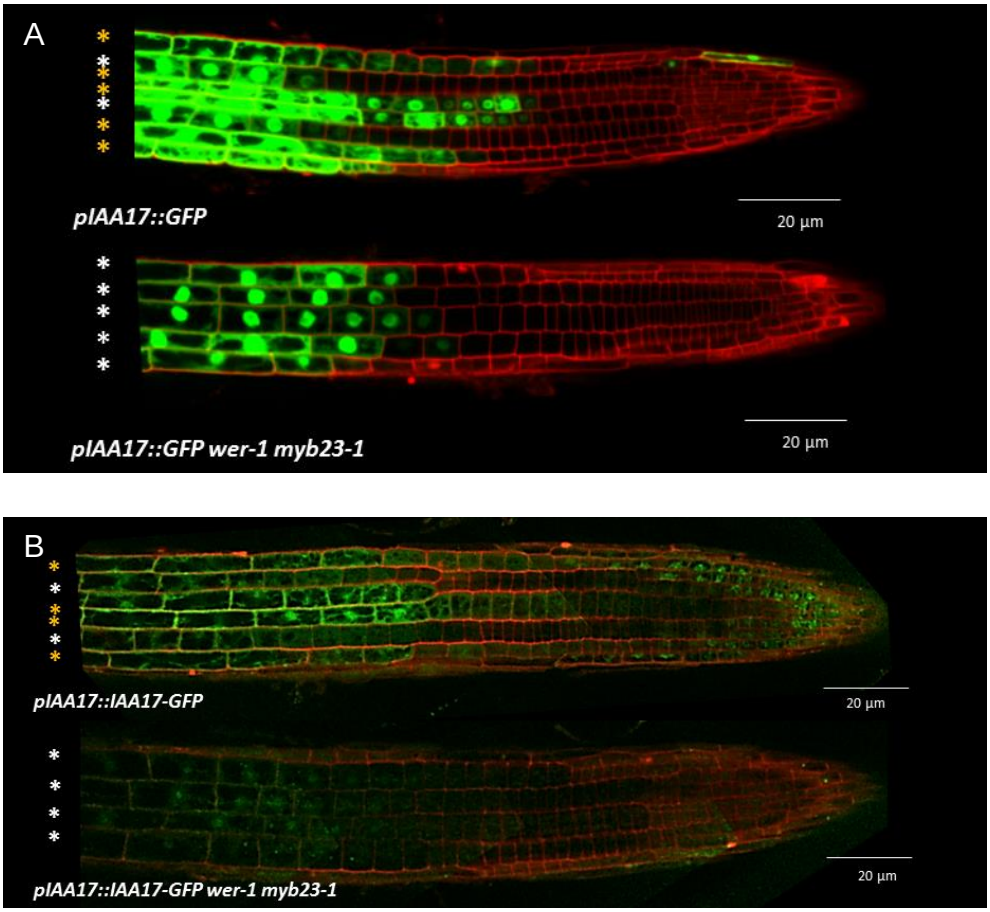

Figure 4-9: Transcriptional and Translational markers for IAA17 in the *wer-1 myb23-1* double mutant background.

A: The *pIAA17::GFP* in the *wer-1 myb23-1* mutant background. B: The *pIAA17::IAA17-GFP* translational marker In the *wer-1 myb23-1* mutant background. Scale bars are labelled accordingly. White * indicate hair files whilst Orange * indicate non-hair files. Sharpened 50%. See 2.4 Confocal Microscopy for microscope settings.

4.5 Is *MYB23* patterning auxin response in the root epidermis?

Although no additive effects were observed in the *wer-1 myb23-1* double mutant, the auxin response markers were also crossed into the single *myb23-1* mutant. As WER expression remains unchanged in both the *myb23-1* mutant background and the MYB23 SRDX line, it is possible that *MYB23* may be regulating auxin response in the root epidermis independently of *WER,* and this could not be observed in the *wer-1 myb23-1* double mutant because auxin response patterning changes in the *wer-1* background were already strong.

Initially *myb23-1* was crossed with the *pDR5::GFP* marker (Figure 4-10 A). In both the *wer-1* and *wer-1 myb23-1* mutants the patterning of *pDR5::GFP* alters so that all of the files adopt a higher level of GFP after the transition zone, as is observed in the hair files of wild-type roots. However in the *myb23-1* single mutant the expression pattern remains unchanged in comparison to the wild-type and control lines.

To see if *MYB23* was patterning *ARF10* expression, the *ARF10* transcriptional and translational markers were crossed with the *myb23-1* mutant (Figure 4-10 B). Fluorescence levels in both the transcriptional and translational makers were lower in the *myb23-1* mutant background. In order to assess if the level of fluorescence was significantly lower than the control, the fluorescence for the transcriptional marker was measured using Image J software and corrected for background levels and area. The fluorescence was measured using a circular drawing tool to specifically select the fluorescent nuclei, a minimum of ten were measured at the transition zone on each root, a minimum of ten roots were compared to get the average results. These measurements indicated that the fluorescence level for *ARF10* in the *myb23-1* background was significantly lower ($P<0.005$, T-Test) than the control lines (Figure 4-10 C). These results were

consistent with *MYB23* positively regulating *ARF10* expression in the non-hair files.

Finally the transcriptional marker for *IAA17* was crossed into the *myb23-1* mutant background (Figure 4-11). No significant changes in the expression pattern were observed in comparison to the wild-type or the control line, indicating that *MYB23* is not patterning the expression of *IAA17* in the root epidermis.

Although the majority of these auxin response markers remained unchanged in the *myb23*-1 mutant, results from the *ARF10* marker crosses were consistent with *MYB23* patterning the expression of *ARF10* in the non-hair files of the root epidermis (Figure 4-12).

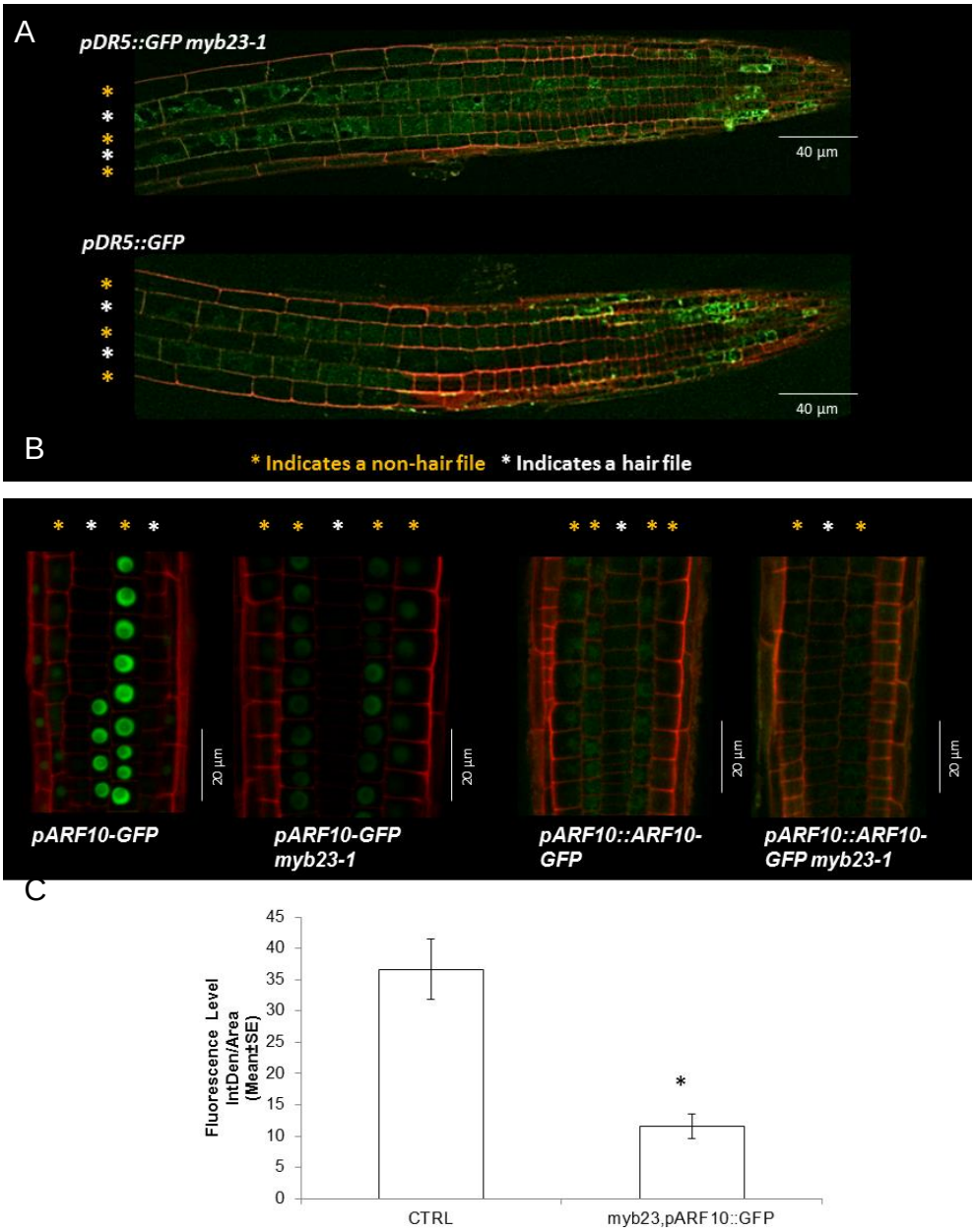

Figure 4-10: Markers for auxin response in the *myb23-1* mutant background.

A: The *pDR5::GFP* marker remained unchanged in the *myb23-1* background. B/C: Expression of both the ARF10 transcriptional and translational markers in the *myb23-1* background was significantly reduced (T-Test, P<0.005). Scale bars are labelled accordingly. White * indicate hair files whilst Orange * indicate non-hair files. See 2.4 Confocal Microscopy for microscope settings. Error bars represent standard error values.

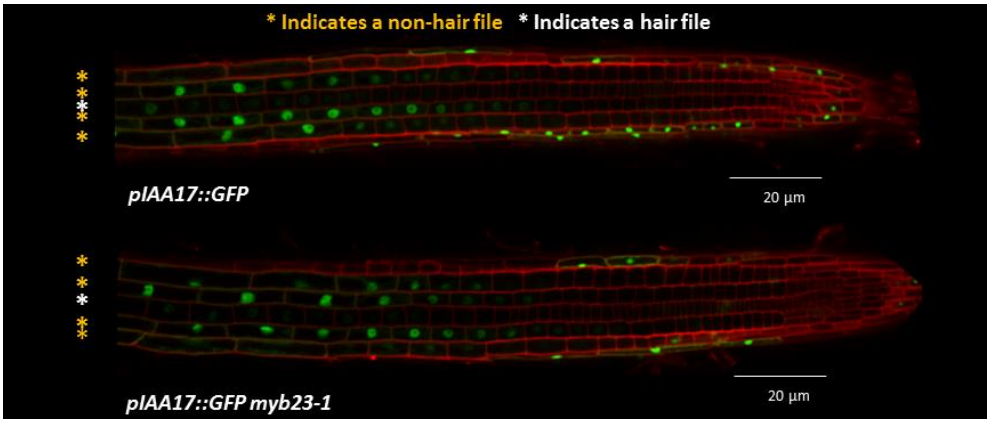

Figure 4-11: The transcriptional marker for *IAA17* in the *myb23-1* mutant background.

Scale bars are labelled accordingly. White * indicate hair files whilst Orange * indicate non-hair files. See 2.4 Confocal Microscopy for microscope settings.

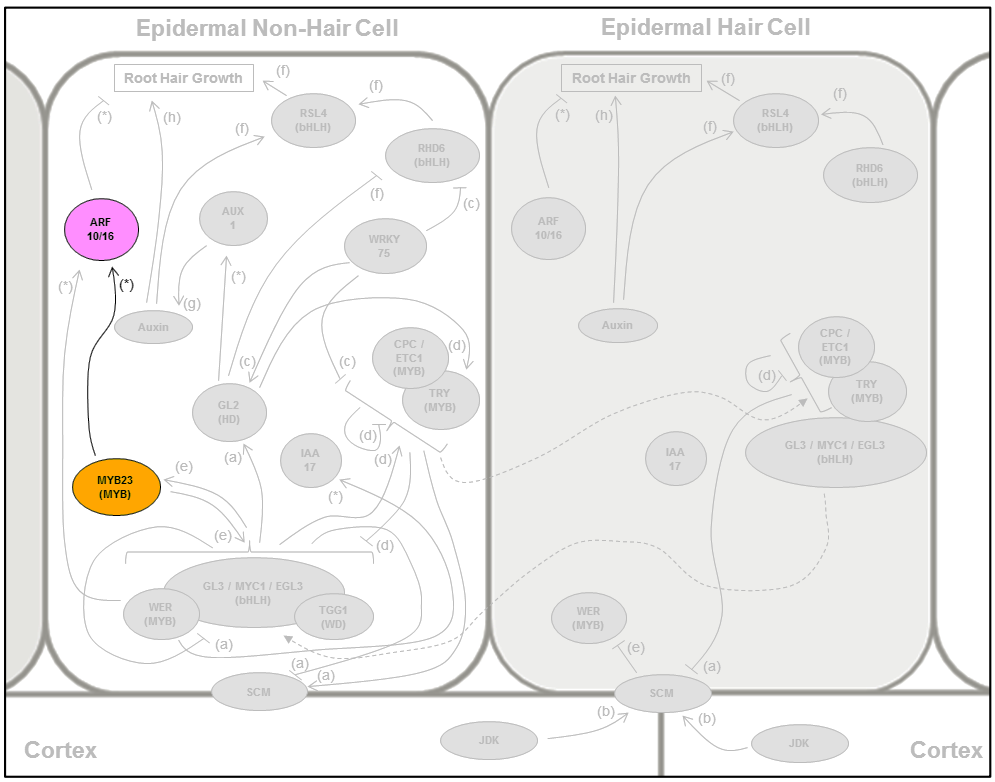

Figure 4-12: *MYB23* positively regulates the expression of *ARF10.*

Results from crossing *myb23-1* with transcriptional and translational markers for *ARF10* indicated that *MYB23* positively regulates the expression of *ARF10* in the root epidermis. Solid lines indicate promotion (arrow head) or inhibition (flat head), dashed lines indicate movement in the direction of the arrow head. Letters next to the arrows indicate the published source of the interaction. (a) (Kwak and Schiefelbein, 2008) (b) (Hassan et al., 2010) (c) (Rishmawi et al., 2014) (d) (Simon et al., 2007) (e) (Kang et al., 2009) (f) (Yi et al., 2010) (g) (Jones et al., 2009) (h) (Masucci and Schiefelbein, 1996) (i) Tromas and Perrot-Rechenmann 2010. (*) indicates interactions identified during this project.

4.6 Is *CAPRICE* patterning auxin response in the root epidermis?

So far the patterning of auxin response in the root epidermis has been studied using the knockout mutants for non-hair promoting components of the epidermal patterning mechanism. *CAPRICE (CPC)* is a hair cell promoting component (Schiefelbein *et al*., 2009). *CPC* is an interesting component of the epidermal patterning mechanism as it is involved in a complex system of lateral inhibition. Whereby it moves between different cell types in the root and negatively regulates the non-hair cell fate (Schellmann *et al*., 2002; Schiefelbein *et al*., 2009). The *CPC* gene encodes a nuclear localised R3-type MYB transcription factor which lacks a transactivation domain (Schellmann *et al*., 2002). Whilst preferentially transcribed in the non-hair and stele cells, CPC then accumulates in the nuclei of hair cells (Kang *et al*., 2013). It is hypothesised that CPC moves between cell types via the plasmodesmata in a tissue specific mode. In 2005 Kurata *et al* identified a single domain within CPC that is necessary for the cell-to cell movement. Within this domain are the N-terminal region and a section of the MYB domain (Kurata *et al.*, 2005). W76 and M78 in this MYB domain were identified as being critical for targeted transport and W76 in particular is important for CPC nuclear accumulation (Kurata *et al*., 2005).

CPC is positively regulated by WER and MYB23 (Schiefelbein *et al*., 2009), and itself inhibits *MYB23* expression in a negative feedback loop (Kang *et al*., 2009). The mutant allele used in this study was *cpc-1*, which is in the *Arabidopsis* Wassilewskija (WS) wild-type background and was first described in 1997 (Wada *et al*., 1997). The *cpc-1* mutant was isolated from a population of transfer DNA tagged lines, it was selected due to its reduced number of root hairs and named *CAPRICE* due to the irregular distribution of these root hairs *(Wada et al.*, 1997). Although there is a significant reduction in the number of root hairs produced,

those that do grow are ‘normal’ in terms of morphology in comparison to the wild-type (Wada *et al.*, 1997).

In order to see if CPC is patterning auxin response in the root epidermis, the auxin response markers were crossed into the *cpc-1* mutant background. Initially the *cpc-1* mutant was crossed with the *pDR5::GFP* marker of auxin signalling output (Figure 4-13 A). In the *cpc-1* mutant background, despite the mutant still producing some root hairs, the differential DR5 expression pattern was lost and all of the files adopted a non-hair like expression of *pDR5::GFP.* In a *cpc-1* background expression of *pDR5::GFP* is initially strong before the transition zone in all of the files, and is then reduced from that point forwards.

When the *ARF10* transcriptional and translational markers were crossed into the *cpc-1* mutant, *ARF10* expression was observed in all of the cell files (Figure 4-13 B). However the level of fluorescence was variable between cells, this was not observed in the control or wild-type backgrounds. Finally the transcriptional and translational markers for the Aux/IAA repressor *IAA17* were crossed into the *cpc-1* mutant background (Figure 4-14). The expression pattern of *IAA17* that is observed in the wild-type and control backgrounds is disrupted in the *cpc-1* mutant. Both the transcriptional and translational markers exhibit expression of *IAA17* in all the epidermal files around the earlier non-hair cell type patterning position. This is clearer in the transcriptional marker, the translational marker is still disrupted, but not as consistently.

These results were consistent with *CPC* negatively regulating the repressive auxin response components *ARF10* and *IAA17 (*Figure 4-15).

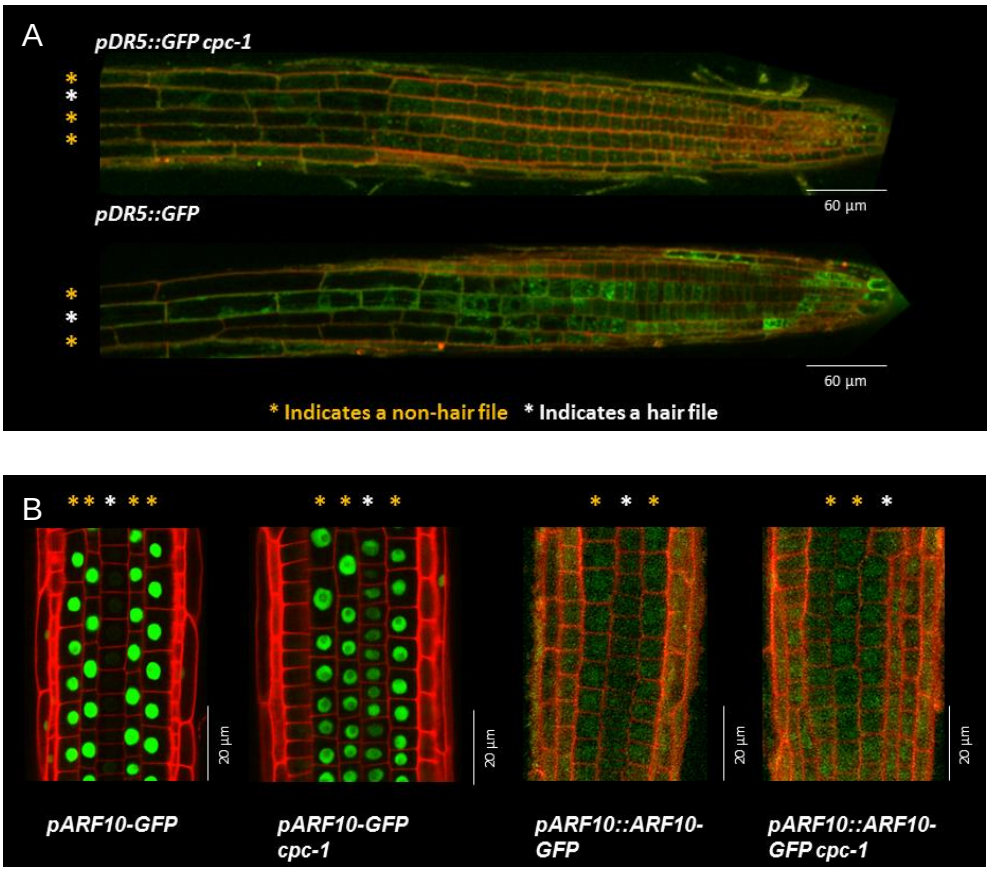

Figure 4-13: Markers for auxin response crossed into the *cpc-1* mutant background.

A: The *pDR5::GFP* marker of auxin signalling output in the *cpc-1* mutant background. B: The transcriptional and translational markers for ARF10 in the *cpc-1* mutant background. Scale bars are labelled accordingly. White * indicate hair files whilst Orange * indicate non-hair files. See 2.4 Confocal Microscopy for microscope settings.

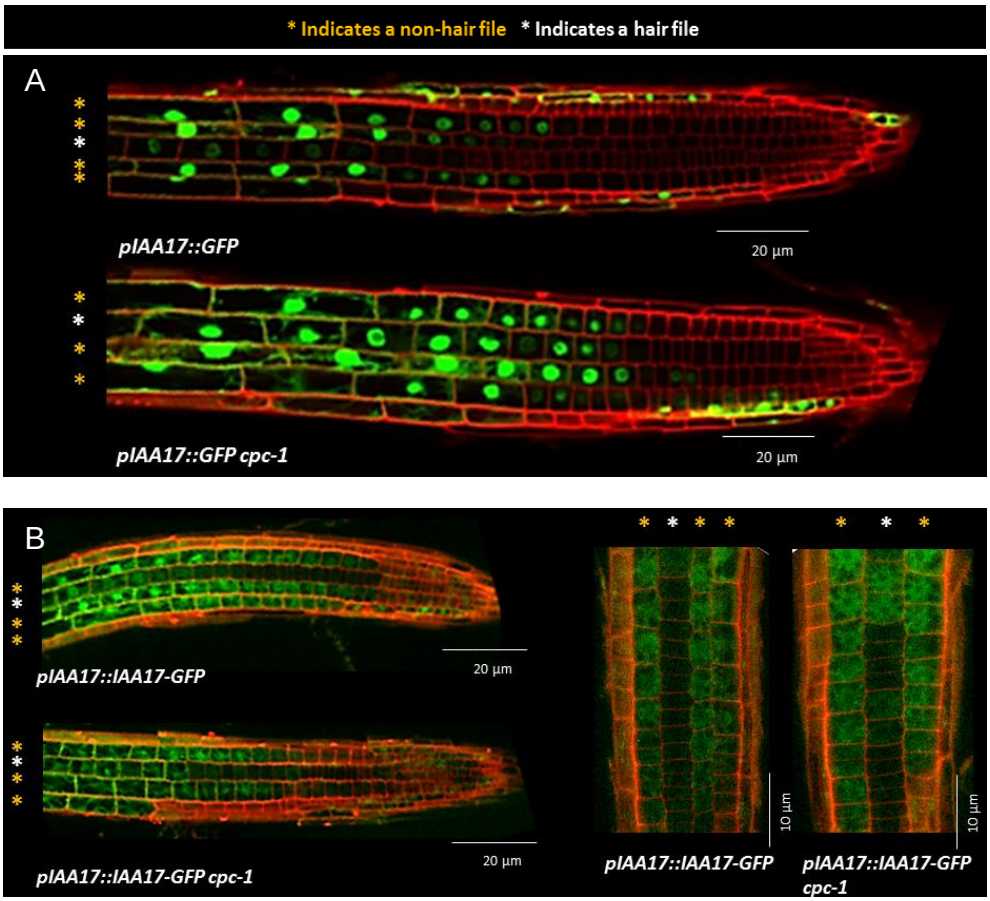

Figure 4-14: Transcriptional and translational markers for IAA17 in the *cpc-1* mutant.

A: The IAA17 transcriptional marker in the *cpc-1* mutant background. B: The IAA17 translational marker in the *cpc-1* mutant background. Scale bars are labelled accordingly. White * indicate hair files whilst Orange * indicate non-hair files. See 2.4 Confocal Microscopy for microscope settings.

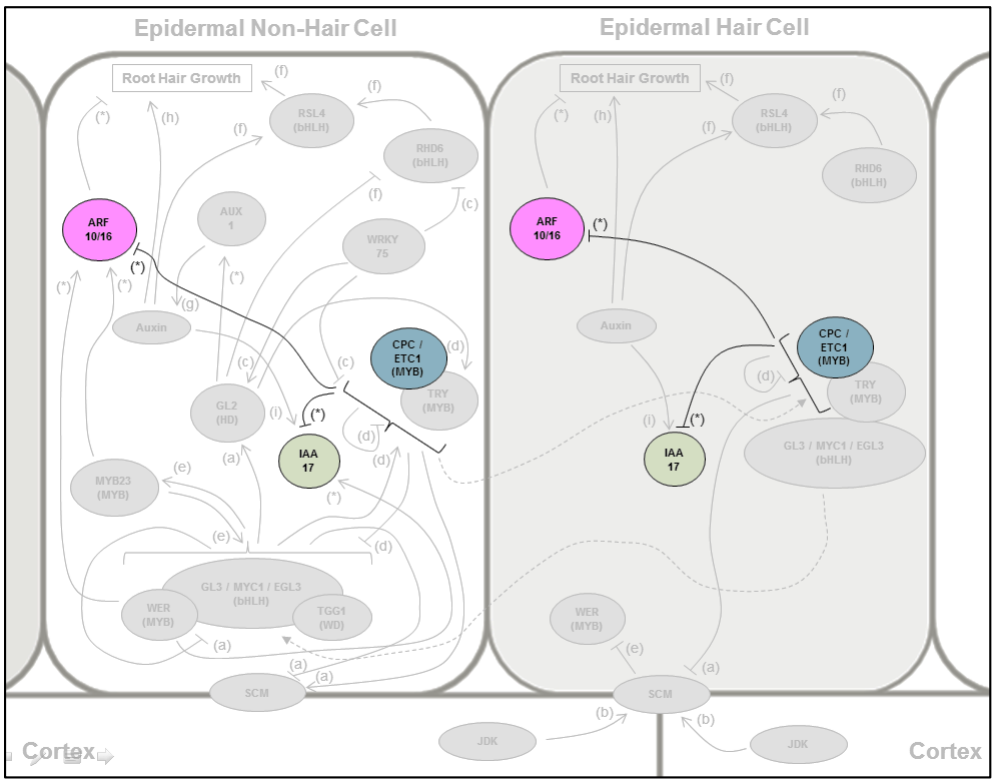

Figure 4-15: *CPC* inhibits the expression of *ARF10* and *IAA17.*

Crosses with transcriptional and translational markers for *ARF10* and *IAA17* indicated that *CPC* functions to repress *ARF10* and *IAA17* expression in the root epidermis. Solid lines indicate promotion (arrow head) or inhibition (flat head), dashed lines indicate movement in the direction of the arrow head. Letters next to the arrows indicate the published source of the interaction. (a) (Kwak and Schiefelbein, 2008) (b) (Hassan et al., 2010) (c) (Rishmawi et al., 2014) (d) (Simon et al., 2007) (e) (Kang et al., 2009) (f) (Yi et al., 2010) (g) (Jones et al., 2009) (h) (Masucci and Schiefelbein, 1996) (i) Tromas and Perrot-Rechenmann 2010. (*) indicates interactions identified during this project.

4.7 How is auxin response patterned in the *cpc-1 try-82* double mutant?

Although the patterning of auxin response is altered in a *cpc-1* mutant the changes were sometimes variable, this could be due to the fact that some of the cells are still producing root hairs. In order to look at the patterning of auxin response in a mutant where no root hairs are produced the *cpc-1 try-82* double mutant was used.

TRIPTYCHON (TRY) is a homolog of *CPC*, and like *CPC* in addition to having a role in root hair growth it is also a negative regulator of trichome development (Schellmann *et al*., 2002). Also similar to *CPC*, *TRY* encodes a R3 MYB protein that is missing a domain which activates transcription (Ishida *et al.*, 2007). Within the epidermal patterning mechanism it is proposed that CPC and TRY work to compete for binding with the basic helix-loop-helix transcription factors and thereby inhibit the formation of the non-hair transcription factor complex in the hair cells (Ishida *et al*., 2007).

The *try-82* mutant allele used in this study is a base substitution that results in a non-sense mutation (Hülskamp *et al*., 1994). The *cpc-1 try-82* mutant results in a phenotype whereby no root hairs are produced (Schellmann *et al.*, 2002). Interestingly in the shoot this same double mutant results in excessive trichome production (Kellogg, 2001; Ishida *et al*., 2008).

The makers used to asses auxin response were crossed into this double mutant background (Figure 4-16). As was observed in *cpc-1* single mutant, in the *cpc-1 try-82* double mutant the *pDR5::GFP* marker adopts the wild-type non-hair file expression pattern in all of the cell files.

Expression of the *ARF10* translational and transcriptional markers is observed in all of the epidermal cells, but the strength of the fluorescence signal is more consistent than that which was observed in the *cpc-1* single mutant. In addition to this the *IAA17* translational marker has a less variable starting point, which mirrors that of the non-hair files in the wild-type and control backgrounds (Figure 4-16).

These results are consistent with *CPC* and *TRY* acting redundantly to inhibit the expression of *ARF10* and *IAA17* in the root epidermis (Figure 4-17).

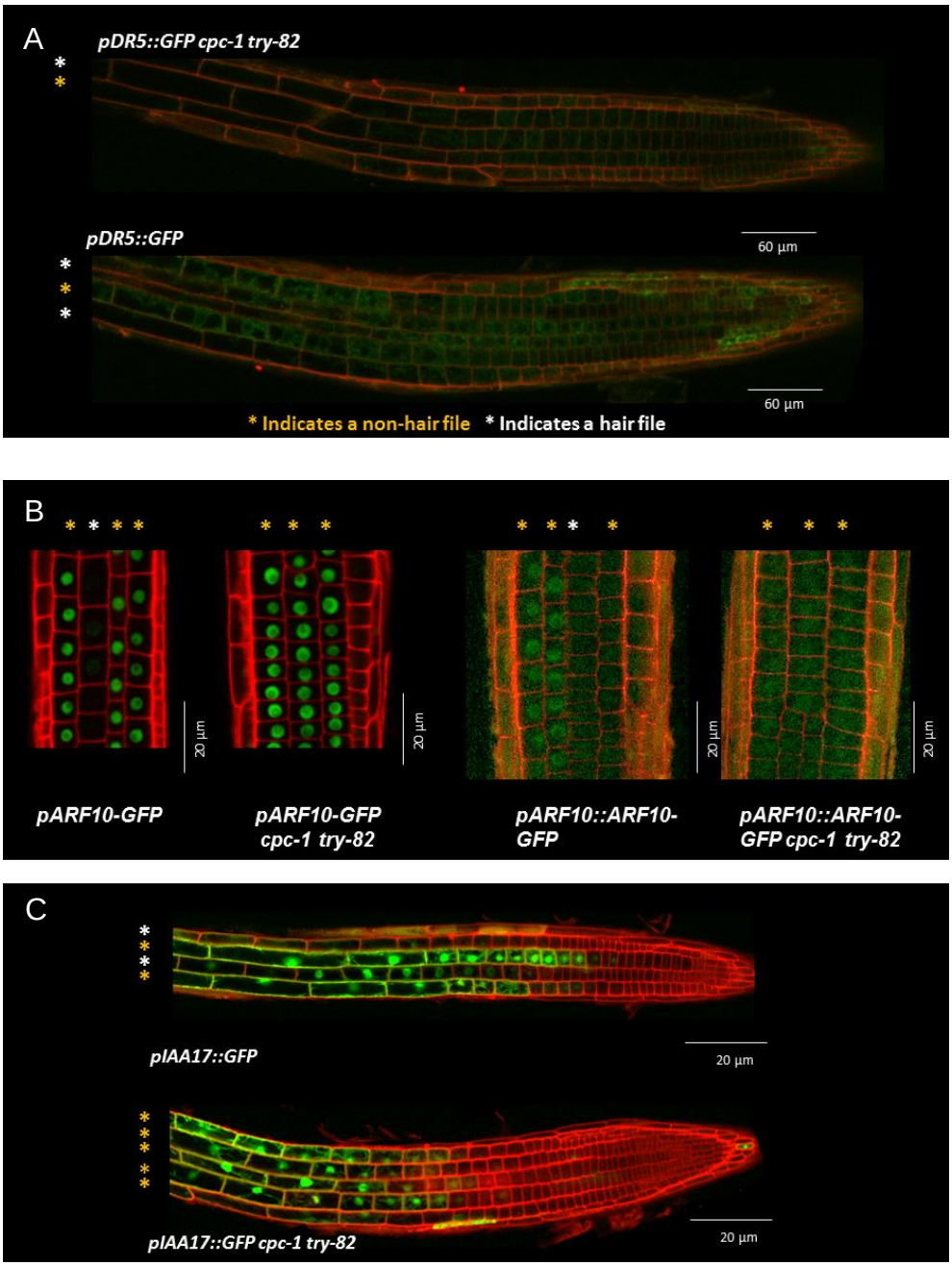

Figure 4-16: Markers of auxin response in the *cpc-1 try-82* mutant.

A: The *pDR5::GFP* marker in the *cpc-1 try-82* mutant background. B: The *ARF10* transcriptional and translational markers in the *cpc-1 try-82* mutant background. C: The *IAA17* transcriptional marker in the *cpc-1 try-82* mutant background. Scale bars are labelled accordingly. White * indicate hair files whilst Orange * indicate non-hair files Photographs: Sharpened 50%, Brightness +40%, Contrast -40%. See 2.4 Confocal Microscopy for microscope settings.

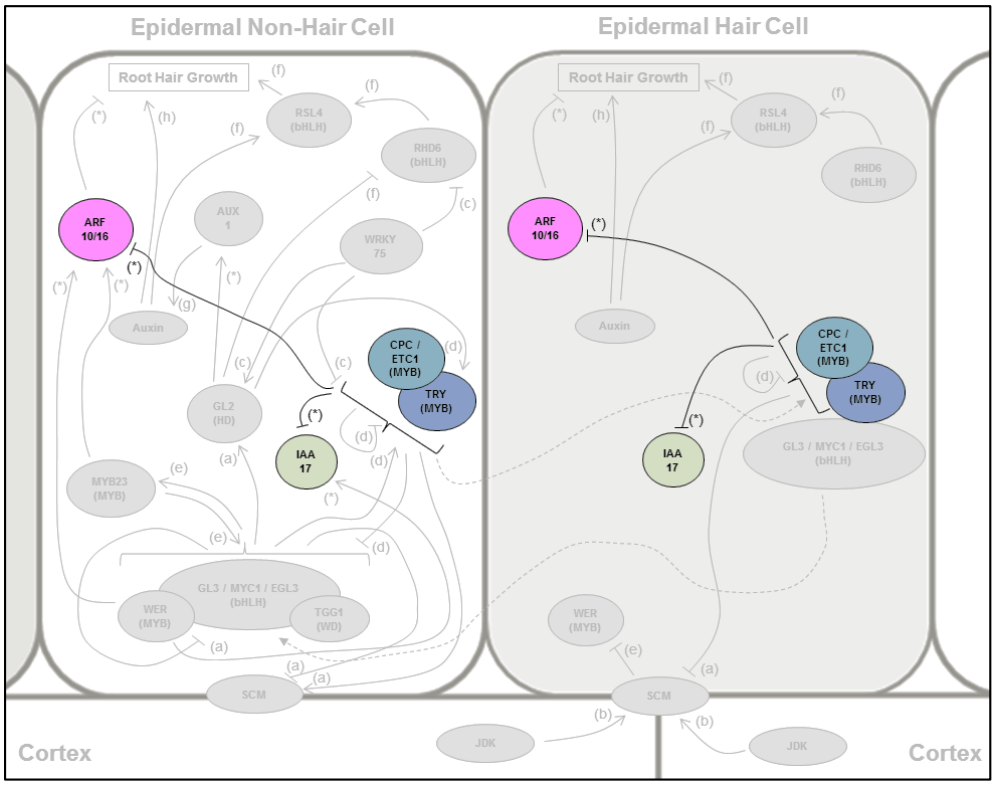

Figure 4-17: *CPC* and *TRY* act redundantly to inhibit the expression of *ARF10* and *IAA17*

Crosses indiate that *CPC* and *TRY* act redundantly to inhibit the expression of *ARF10* and *IAA17* in the *Arabidopsis* root epidermis. Solid lines indicate promotion (arrow head) or inhibition (flat head), dashed lines indicate movement in the direction of the arrow head. Letters next to the arrows indicate the published source of the interaction. (a) (Kwak and Schiefelbein, 2008) (b) (Hassan et al., 2010) (c) (Rishmawi et al., 2014) (d) (Simon et al., 2007) (e) (Kang et al., 2009) (f) (Yi et al., 2010) (g) (Jones et al., 2009) (h) (Masucci and Schiefelbein, 1996) (i) Tromas and Perrot-Rechenmann 2010. (*) indicates interactions identified during this project.

4.8 Discussion

4.8.1 Auxin signalling output

The *pDR5::GFP* marker gives an indication of auxin signalling output. It is constructed of seven auxin response elements driving the expression of a green fluorescent protein (Jones *et al*., 2009). Within the root epidermis it was initially published that DR5 expression was higher in the non-hair files, but further investigation established that this differential expression is lost around the transition zone and then persists with greater strength in the hair files from that point forward (Figure 1-9). Not only is this of interest, but it is also consistent with the fact that the root hair growth response to auxin must ultimately be affecting hair cells, rather than non-hair cells.

A variety of *pDR5::GFP* expression patterns were observed when this marker was crossed into epidermal patterning mutants with more or fewer root hairs. These are summarised schematically in Figure 4-18. In the mutants where all or none of the cells produced root hairs, all of the files adopted either the hair or non-hair wild-type expression pattern for *pDR5::GFP*, i.e. *wer-1* and *cpc-1 try-82.* These results were consistent with auxin response being patterned by a file being either a hair or non-hair file, dictated by if they do or do not produce a hair rather than their location with regards to the underlying cortex. However in the mutants with more intermediate ectopic root hair phenotypes, i.e. *gl2-1* and *myb23-1,* the overall expression pattern of *pDR5::GFP* remained unchanged, indicating that simply producing a root hair was not sufficient to alter the overall auxin response of a cell or file. The *cpc-1* mutant result was interesting because although all of the files adopted the wild-type non-hair file *pDR5::GFP* expression pattern, it still has distinct hair files which produced fewer, but 'normal' root hairs. Overall these results were consistent with the hypothesis that auxin response in the *Arabidopsis* root epidermis, quantified here as auxin

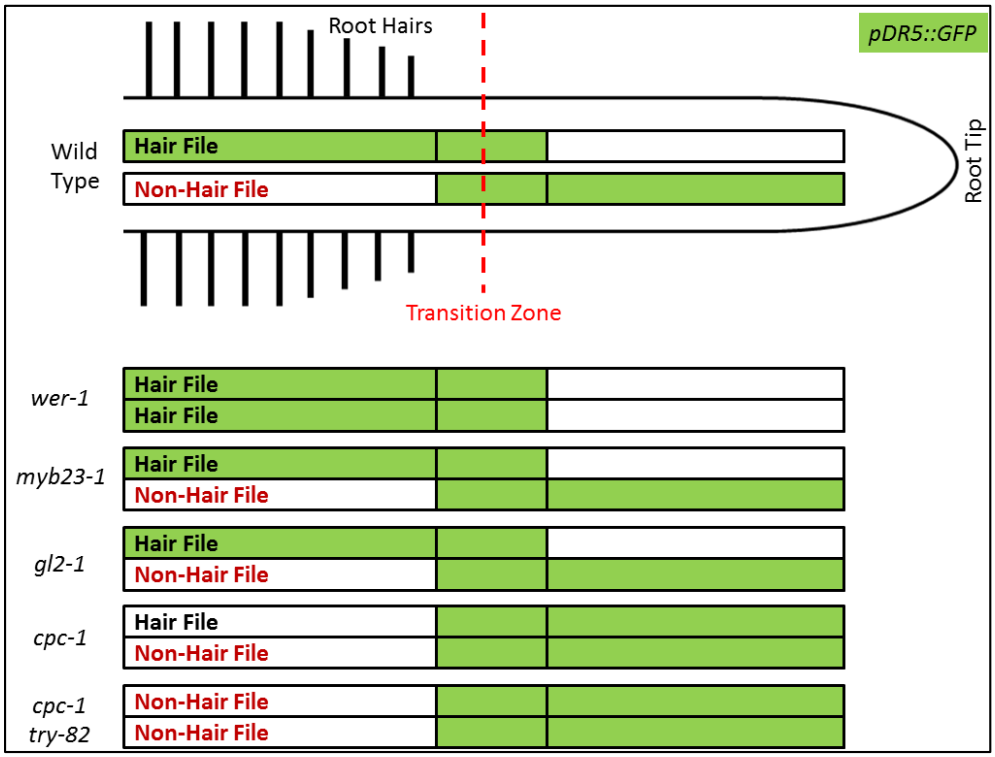

Figure 4-18: A summary of the patterning of auxin signalling output, as indicated by the *pDR5::GFP* marker, in a range of epidermal patterning mutants.

Here **hair** and **non-hair** files are identified as such due to the majority of the cells producing or not producing root hairs. The mutants with the most obvious phenotypess in which 100% or 0% of epidermal cells produce root hairs, *wer-1* and *cpc-1 try-82* respectively, saw all of the files adopting the expression pattern observed in either the hair or non-hair cells of the wild-type. The intermediate mutants which feature an increase in the amount of ectopic hairs they produce, *gl2-1* and *myb23-1,* both retain the wild-type expression pattern of *pDR5::GFP*. However the *cpc-1* mutant, which produces significantly fewer but 'normal' root hairs, adopts the non-hair *pDR5::GFP* expression pattern in all of its files.

signalling output, is patterned upstream of *GL2,* and *WER, CPC* and *TRY* are likely to play a role in determining this.

4.8.2 IAA17 expression

Transcriptomic analysis indicated that the Aux/IAA repressor protein IAA17 was expressed at a higher level in the non-hair files. This was also confirmed with transcriptional and translational GFP markers (Figure 1-10). In addition to this *IAA17* has been shown to be important for root hair growth as semi dominant domain two stabilising mutations in the *axr3-1* mutant result in a significant reduction in root hair production (Leyser *et al.*, 1996; Knox *et al*., 2003). Although the differential patterning of *IAA17* in the root epidermis may appear to be less severe than the obvious changes observed with the *ARF10* marker*,* the eight cell difference between *IAA17* expression beginning in the hair and non-hair files may be important for root hair growth.

A variety of expression patterns were observed when markers for *IAA17* were crossed into epidermal patterning mutants with more or fewer root hairs. These are summarised schematically in Figure 4-19. As was observed with the *pDR5::GFP* marker, the mutants with all or no root hairs had the strongest change in expression patterns, with a significant reduction in the number of cells between the starting points of *IAA17* expression in the different files. The *IAA17* expression began at the same point observed in either the hair or non-hair files of the wild-type, for example in a *cpc-1 try-82* double mutant *IAA17* expression began early in all of the epidermal files, this corresponded to the same position as where expression begins in the non-hair files of the wild-type and control lines. In the excessively hairy *wer-1* mutant *IAA17* expression began late, as occurs in the hair files of the wild-type and control lines. Like *pDR5::GFP,* patterning of *IAA17* in the *gl2-1* and *myb23-1* mutants remained unaltered from that of the wild-type. In *cpc-1* there was a significant drop in the differential start point of expression point between the hair and non-hair files, however not as much as was observed in *wer-1* and *cpc-1 try-82* mutants*.* These results were

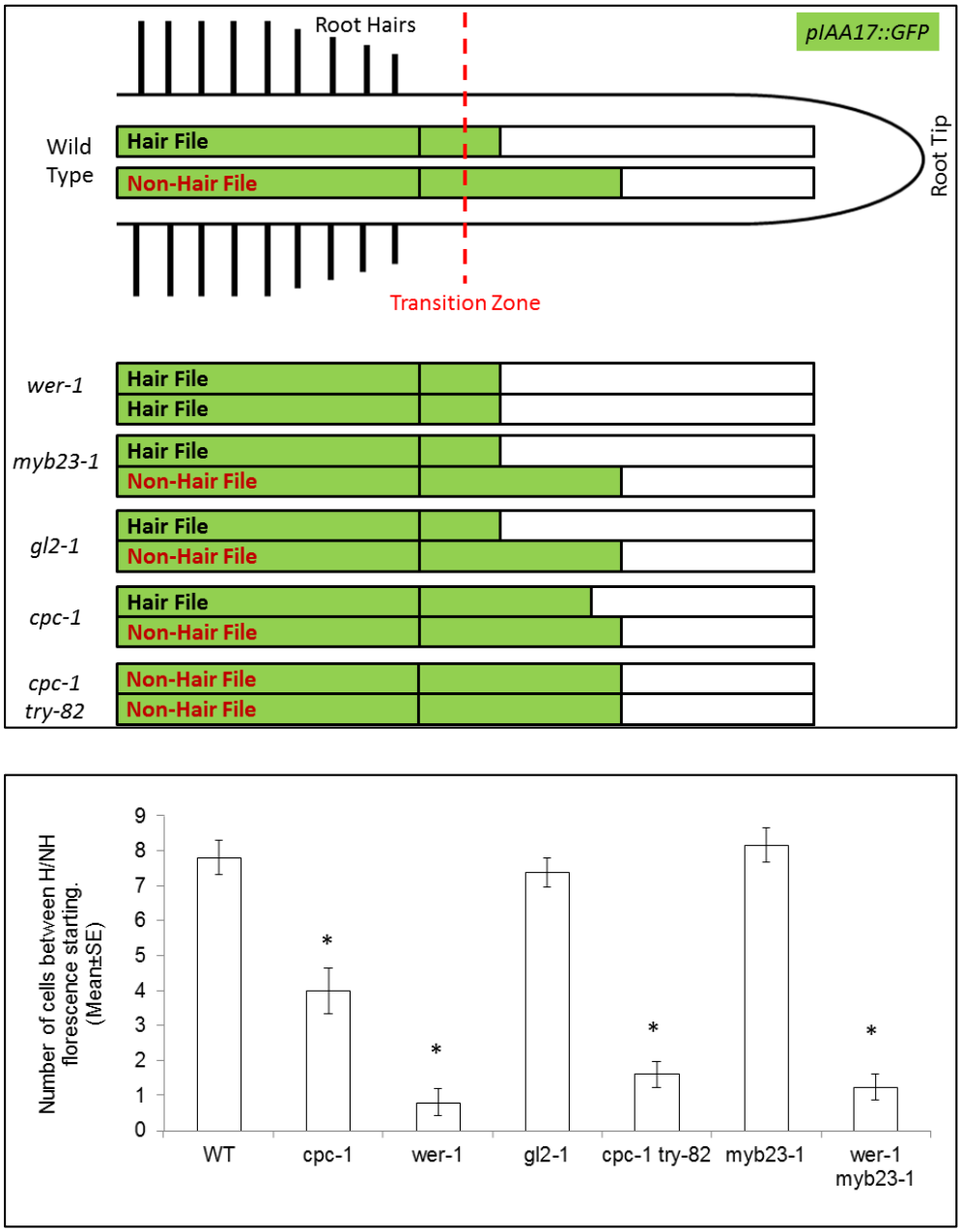

Figure 4-19: A summary of the patterning of *IAA17* in the root epidermis.

Here **hair** and **non-hair** files are identified as such due to the majority of the cells producing or not producing root hairs. The *wer-1* and *cpc-1 try-82* mutants exhibited the strongest loss in terms of differential patterning. In *gl2-1* and *myb23-1* the patterning of IAA17 remained unchanged whilst *cpc-1* showed a partial but significant reduction in the differential expression. The * indicate a significant difference in comparison to the wild-type (ANOVA, $P<0.005$). Error bars represent standard error values.

consistent with *IAA17* expression being patterned upstream of *GL2.* As with the *pDR5::GFP* marker it was clear that producing or not producing a root hair was not sufficient to alter *IAA17* expression and results indicated that whilst *CPC* and *TRY* inhibit the early expression of *IAA17* in the root epidermis, *WER* promotes it.

4.8.3 *ARF10* expression

The role of the repressing ARFs as competitors for binding sites with activating ARFs, adds an additional level of control to the already complex and finely tuned system of auxin response (Lokerse and Weijers, 2009). *ARF10* expression in the root epidermis is differential between the hair and non-hair files, initially this was identified by transcriptomic data and later confirmed with GFP marker lines (Figure 1-11). Expression of the repressing *ARF10* begins early in the non-hair files and is similar to the expression patterns of a lot of the non-hair epidermal patterning components, like *WER* and *GL2* (Kang *et al*., 2009).

A variety of expression patterns were observed when markers for *ARF10* were crossed into epidermal patterning mutants with more or fewer root hairs. These are summarised schematically in (Figure 4-20). The most obvious changes were observed in the *wer-1* and *cpc-1 try-82* mutants where all or none of the cells had strong *ARF10* expression. Like *pDR5::GFP* and *IAA17* no change was observed in the *gl2-1* mutant, but unlike the previous markers a significant reduction in *ARF10* expression was observed in the *myb23*-1 mutant. *ARF10* was also expressed everywhere in a *cpc-1* mutant, however there did appear to be greater variability in expression level between the cells in comparison to the *cpc-1 try-82* double mutant.

These results were consistent with *ARF10* expression being patterned upstream of *GL2.* As with the *pDR5::GFP* and *IAA17* markers producing or not

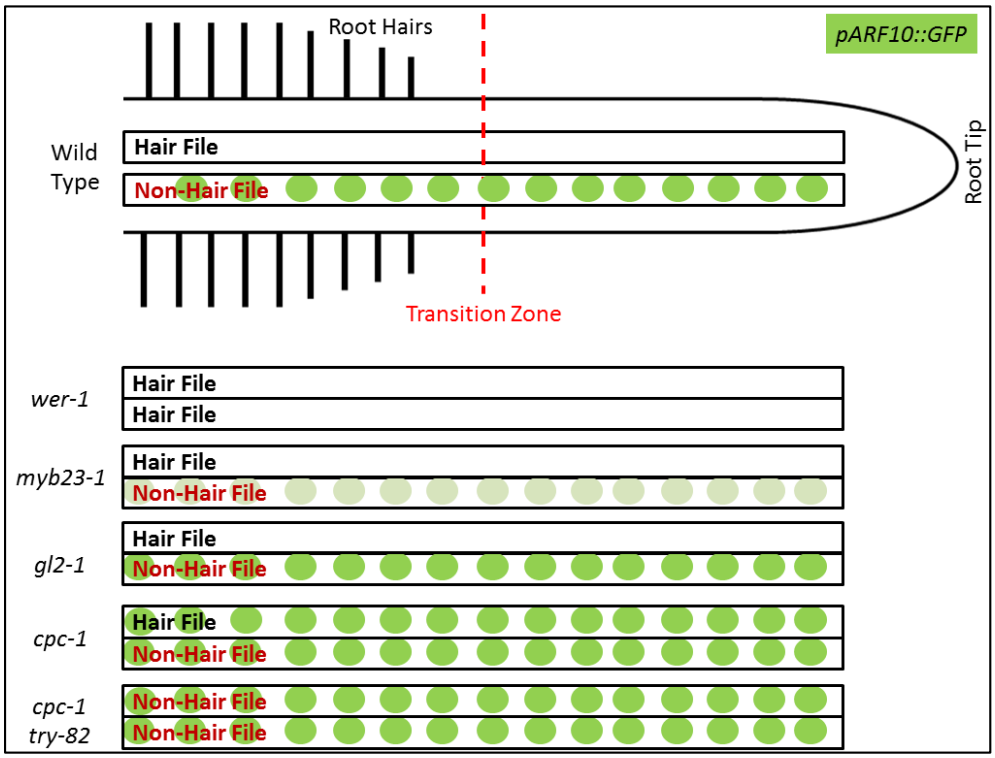

Figure 4-20: A summary of the patterning of negative auxin response, as indicated by the pARF10::GFP marker in a range of epidermal patterning mutants.

Here **hair** and **non-hair** files are identified as such due to the majority of the cells producing or not producing root hairs. The mutants with the strongest phenotypes in terms of all or no root hairs exhibited the strongest alteration in ARF10 patterning with all or none of the cells having strong *ARF10* expression. An unexpected result here was the reduction of *ARF10* expression in the *myb23-1* background.

producing a root hair alone was not sufficient to alter *ARF10* expression, the results indicated that whilst *CPC* and *TRY* inhibit the expression of ARF10, *WER* and *MYB23* promote it.

The results from these crosses indicated that in the root epidermis auxin response, specifically the expression of *IAA17* and *ARF10* are patterned upstream of the epidermal patterning component *GL2.* In addition to this they highlighted that producing or not producing a root hair was insufficient to alter the auxin response of an epidermal cell, suggesting that auxin response is not dependent on root hair producing genes. However it is important to keep in mind that the results discussed previously in Chapter 3 indicated that the auxin response profile of a particular epidermal cell or file is likely to some extent to determine the growth of a root hair from that cell.

Finally these crosses indicated that although *MYB23* does not regulate *pDR5::GFP* or *IAA17* expression it does significantly promote the expression of *ARF10*. This result was unusual in that the majority of the other changes observed in auxin response patterning, occurred alongside a change in file identity in terms of producing or not producing a root hair. For example in the *wer-1* and *wer-1 myb23-1* mutants all of the cells produce root hairs and all of the auxin response patterning mirrors that of a hair file in a wild-type root. However in the *myb23-1* background a down-regulation in *ARF10* is observed without a switch in cell file identity. To some extent this was also observed in a *cpc-1* mutant, where cells adopted the non-hair cell identity in terms of auxin response but still produced some ‘normal’ root hairs.

4.8.4 Cell size

In addition to producing or not producing root hairs epidermal hair and non-hair cells also differ in other aspects, like cell size and cytoplasmic density (Masucci *et al*., 1996). In a *gl2-1* mutant these differences are maintained between the files despite the fact that approximately 50% of the non-hair cells produce root hairs (Masucci *et al*., 1996). However in other epidermal patterning mutants, particularly those upstream of *GL2*, published data has suggested that these differences, specifically the cell size is lost (Galway *et al*., 1994).

During this chapter hair and non-hair cells have been considered in terms of if they do or do not produce a root hair. However in order to see if the changes in the patterning of auxin response may be linked to changes in cell size, the cell sizes of the hair and non-hair cells for each of the mutants were quantified (Figure 4-21).

Confocal microscopy images of the epidermal cells were stained with propidium iodide, which specifically highlights cell walls. Using these images cells sizes in hair and non-hair files were measured. In every mutant studied there was still an obvious difference in cell size between adjacent hair and non-hair files. However the roots do differ in morphology between lines, for example *wer-1* has significantly shorter (ANOVA, $P<0.005$) primary roots, whilst *cpc-1 try-82* has significantly longer (ANOVA, $P<0.005$) primary roots (Supplementary Data Figure 9-4). As the different lines were known to exhibit growth variation, measurements were taken for the first twenty cells counting up from the tip, for both the hair and non-hair files. These were then compared to get the hair to non-hair cell size ratio (Figure 4-21 B).

The calculated ratios indicated that although there was variation in the ratio values between the lines, it was not significantly different from the wild-type in any of the mutants. Indicating that every mutant maintained a difference in cell

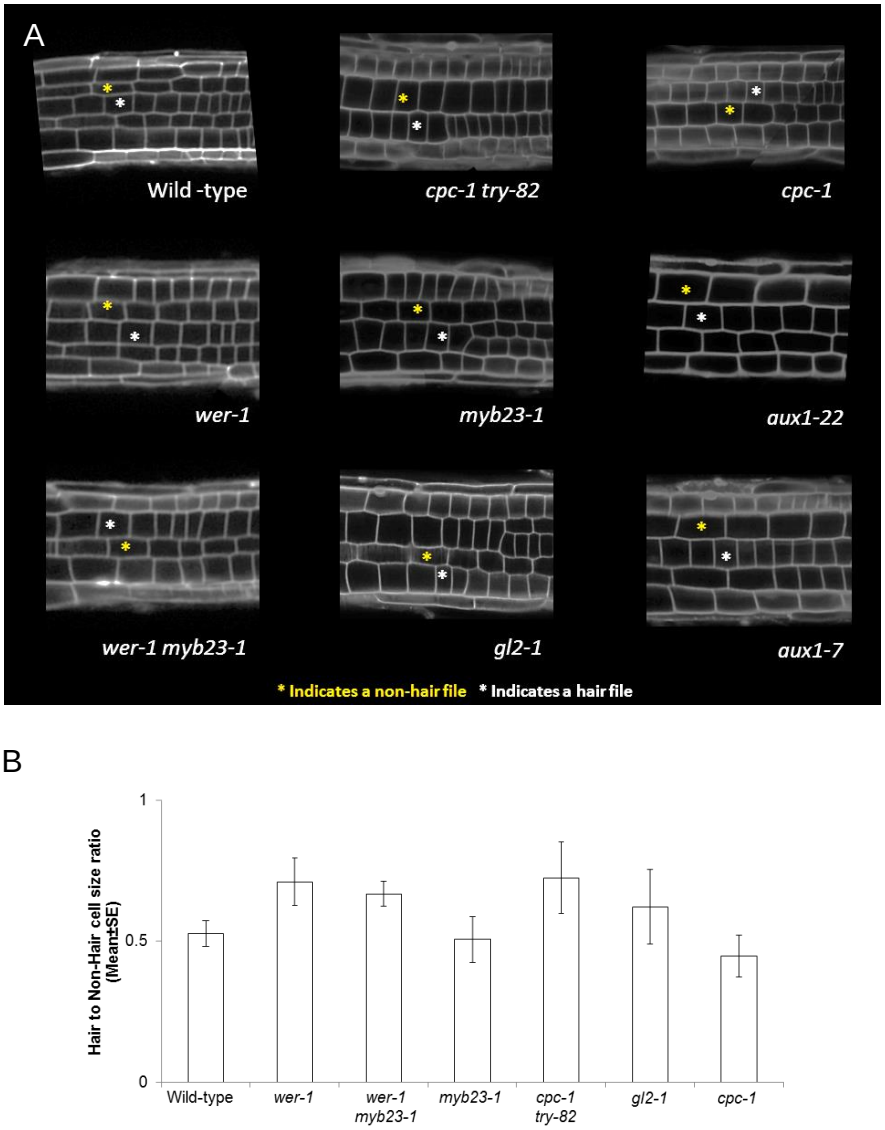

Figure 4-21: Cell size differences between hair and non-hair cells in epidermal patterning mutants.

Epidermal hair and non-hair cells differ in size in addition to making or not making a root hair. A: Confocal microscopy indicated that although there are morphological differences between the lines looked at in this study in terms of primary root growth etc, there was still a clear difference in size between the hair and non-hair cells. B: This was quantified by measuring the first twenty hair and non-hair cells and the ratio compared across several roots, indicating that although there was variation in this ratio value between lines, none were significantly different from the wild-type. Photographs: Brightness -20%, Contrast +20%. See 2.4 Confocal Microscopy for microscope settings. Error bars represent standard error values.

size between the hair and non-hair, regardless of it they did or did not produce a root hair. Therefore the patterning of auxin response in the root epidermis is likely to be independent of both cell size and of if a cell does or does not produce a root hair.

4.8.5 Summary

The results discussed during this chapter are consistent with auxin response in the root epidermis being patterned upstream of *GL2*. *WER*, which promotes the non-hair cell identity, is also likely to promote a higher level of auxin response before the transition zone, early expression of *IAA17* and high *ARF10* expression in the non-hair cells. Conversely *CPC* and *TRY*, which promote the hair cell identity, are likely to promote higher auxin response after the transition zone, late expression of *IAA17* and inhibit the expression of *ARF10*.

MYB23 is an interesting as although it does not appears to have an impact on the overall auxin response patterning as indicated by *pDR5::GFP*, or the patterning of *IAA17,* it does significantly promote the expression of *ARF10*.

Finally the cell size data indicates that the changes observed in auxin patterning are occurring independently of changes in epidermal cell size. Overall these crosses indicate that key members of the epidermal patterning mechanism are patterning auxin response in the root epidermis, by either direct or indirect regulation of certain members of the auxin response network, including but probably not limited to *IAA17* and *ARF10* (Figure 4-22).

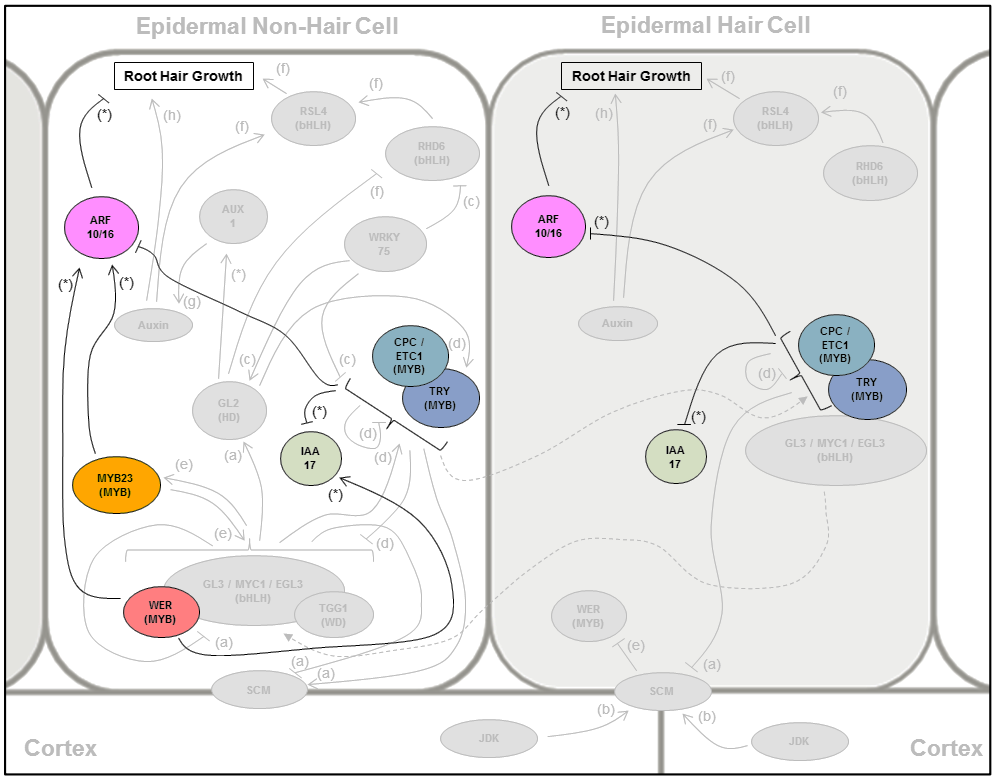

Figure 4-22: A summary of interactions brought about by the crossing of these epidermal mutants with markers of auxin response.

Epidermal patterning components that promote the non-hair fate upstream of *GL2* also promote the negative auxin response regime in the root epidermis. On the other hand epidermal patterning components that promote the hair fate upstream of *GL2* repress this repressive auxin response regime. *MYB23* is an interesting exception to this as whilst it does not affect *IAA17* or *pDR5::GFP* expression is does positively regulate the expression of *ARF10* in the non-hair files. Solid lines indicate promotion (arrow head) or inhibition (flat head), dashed lines indicate movement in the direction of the arrow head. Letters next to the arrows indicate the published source of the interaction. (a) (Kwak and Schiefelbein, 2008) (b) (Hassan et al., 2010) (c) (Rishmawi et al., 2014) (d) (Simon et al., 2007) (e) (Kang et al., 2009) (f) (Yi et al., 2010) (g) (Jones et al., 2009) (h) (Masucci and Schiefelbein, 1996) (i) Tromas and Perrot-Rechenmann 2010. (*) indicates interactions identified during this project.

5 : Establishing Feedback Loops and Direct Links between the Epidermal Patterning Mechanism and the Auxin response network

5.1 Introduction

The results detailed so far have been consistent with the hypothesis that the repressive auxin response regime in the non-hair files might contribute to the repression of root hair growth at the non-hair position. In addition to this, crosses between mutants and marker lines discussed in the previous chapter, indicated that this differential auxin response is patterned by components of the epidermal patterning mechanism upstream of *GL2*. In this chapter feedback loops between the auxin response network and the epidermal patterning mechanism are investigated. In addition to this potential direct links between the two pathways are explored further.

5.2 Does WER or MYB23 bind to the *ARF10* promoter?

A range of transcription factors direct the non-hair cell fate, these include the TTG1 WD repeat protein, GL3 and EGL3 which are basic helix-loop-helix transcription factors, the GL2 homeodomain leucine zipper transcription factor and the WER and MYB23 MYB type transcription factors (Bruex et al., 2012). Results discussed in the previous chapter indicated that the MYB type transcription factors, WER and potentially MYB23, promote the expression of *ARF10.* In order to assess if this regulation involves a direct interaction, the *ARF10* promoter was analysed for potential MYB binding sites. In order to identify these, confirmed interactions between WER, MYB23 and other epidermal patterning components were considered, one of these was *CPC. CPC* transcription is reduced in *wer-1* mutants, suggesting an interaction between the two, and in 2005 Koshino-Kimura *et al* identified two putative MYB binding sites in the *CPC* promoter, which they termed CPCMBS1 (CTCCAACT) and CPCMBS2 (ACAACCGC) (Figure 5-1 A). Base substitutions in these sites resulted in the loss of GUS expression in the CPC reporter lines, thus indicating their importance for *CPC* transcription in the non-hair cells of the root epidermis

(Koshino-Kimura *et al.*, 2005). They also examined two putative MYB binding sites in the *GL2* promoter, GL2MSB1 and GL2MSB2 (Figure 5-1 A). As a result of their analysis they identified the following octameric sequence, C(C/T)AACNG, as a WER binding consensus sequence (Koshino-Kimura *et al.*, 2005). Their conclusions were supported by the fact that this proposed consensus sequence was similar to other previously reported MYB binding sites, including those for the maize P1 protein CC(T/A)ACC (Grotewold *et al*., 1994; Williams and Grotewold, 1997) and the vertebrate MYB protein v-MYB (T/A)AACGG (Howe and Watson, 1991; Weston, 1992).

Another group identified two other putative MYB binding sites in the *CPC* promoter, called WBSI and WBSII (Figure 5-1 B) (Ryu *et al*, 2005). One of these was located nearer to the *CPC* ATG, than the binding sites described by Koshino-Kimura *et al*, and the other encompassed the CPCMBS1 site. Interestingly using in vitro assays they concluded that WER had much stronger affinity for the earlier binding site, WBSI, and proposed ANNNGTTN as a potential WER binding sequence. However Koshino-Kimura *et al* also produced promoter truncation lines, which identified a region that did not contain the WSB1 site as important for CPC expression in the root epidermis (Figure 5-2). These truncations ranged from -1252 to -394 base pairs (Figure 5-2 A), and produced a range of GUS expression patterns. The truncations with promoters larger than -681 base pairs had GUS staining in the non-hair epidermal cells, stele and trichomes but with shorter fragments, i.e -492 base pairs, staining in the epidermis was lost near the root tip. In promoters with -423 base pairs or less, GUS staining was only observed in the stele (Koshino-Kimura *et al.*, 2005). Using this data they concluded that the region between -492 and -681 base pairs of the *CPC* promoter was required for *CPC* transcription in the early stages of the root epidermis, specifically a 69 base pair region between -492 and -423 base pairs was required for transcription in the non-hair cells, Figure 5-2 B (Koshino-Kimura *et al.*, 2005).

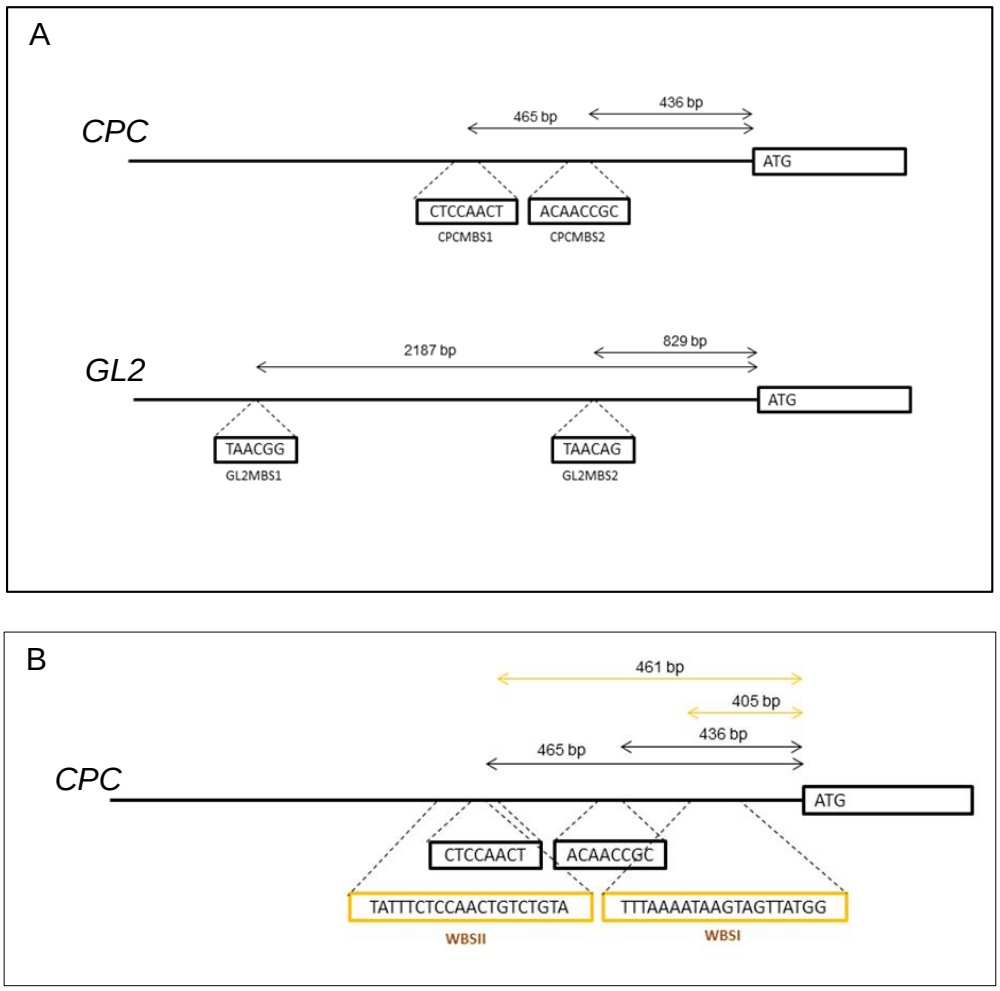

Figure 5-1: Published WER binding sites.

A: MYB binding sites identified in the promoter regions of *CPC* and *GL2*. Derived from (Koshino-Kimura *et al*., 2005). Upon analysis of these binding sites a consensus sequence was constructed, C(C/T)AACNG. B: Alternative MYB binding sites (highlighted in yellow) identified in the *CPC* promoter by Ryu *et al*., 2005. They also identified a WER binding sequence, ANNNGTTN. (Diagrams are not to scale).

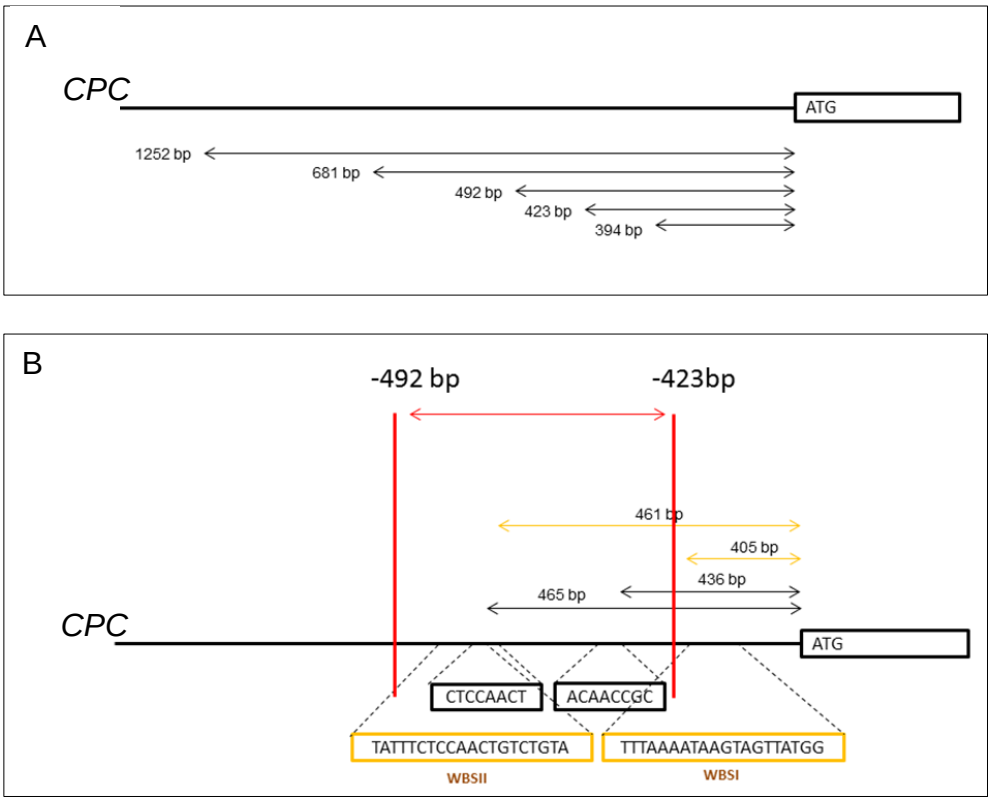

Figure 5-2: Promoter truncation analysis.

A: Several promoter truncation lines were reported by Koshino-Kimura *et al.* These ranged from 1252 bp to 394 bp. B: Lines featuring these truncations identified a 69 base pair region between -492 bp and -423 bp, which is required for epidermis specific transcription of *CPC* in the non-hair cells. This 69 base pair region does not include the WBS1 binding site identified by Ryu *et al* .

In order to confirm the function of this 69 base pair region an eight fold tandem repeat was fused to a 35S promoter to drive the reporter gene GUS, this line resulted in GUS staining in the non-hair cells. In addition to this when the same promoter was fused to the *CPC* coding region it complemented the *cpc-1* mutant phenotype (Koshino-Kimura *et al.*, 2005).

Based on these studies, 4500 base pairs of promoter sequence upstream of the *ARF10* gene translational start were analysed for potential MYB binding sites (Figure 5-3). The sequence was searched for several alternative binding sites and those identified included: the same MYB binding site sequence identified in the *GL2* promoter, similar to the WBSI binding site and also the CPCMBS1/2 binding sites, matching the Koshino-Kimura consensus sequence and finally matching the Ryu *et al* binding sequence. From this analysis several potential binding sites were established and two particular regions of interest (termed **A** and **B**) due to overlapping matches from different sources were identified (Figure 5-3). **A** exhibited the same sequence as the MYB binding site in the *GL2* promoter and was also similar to the CPCMBS binding sites, whilst **B** had the same sequence as the MYB binding site in the *GL2* promoter and matched the Koshino-Kimura consensus sequence. These points were concluded to be those most likely to interact with WER. Interestingly Kang *et al*, published a paper in 2009 where using the WSBI and CPCMBS binding sites they identified four WER binding sites (WBSI-L1, WBSI/II-L1, WBSII-L1 and WBSII-L2) within the MYB23 gene promoter. These potential binding sites were confirmed using electrophoretic mobility shift assays (EMSA) and are located -1130, -630, -570 and -430 base pairs upstream of the *MYB23* translation start (Kang *et al.*, 2009). In addition to this, using EMSA they also confirmed that MYB23 specifically binds to all four of these binding sites in the same manner as WER, indicating that the potential binding sites identified in the *ARF10* promoter may also interact with either of the MYB proteins (Kang *et al.*, 2009). In order to assess the importance of these potential binding sites Chromatin Immunoprecipitation (ChIP) and *ARF10* promoter truncation analysis was performed.

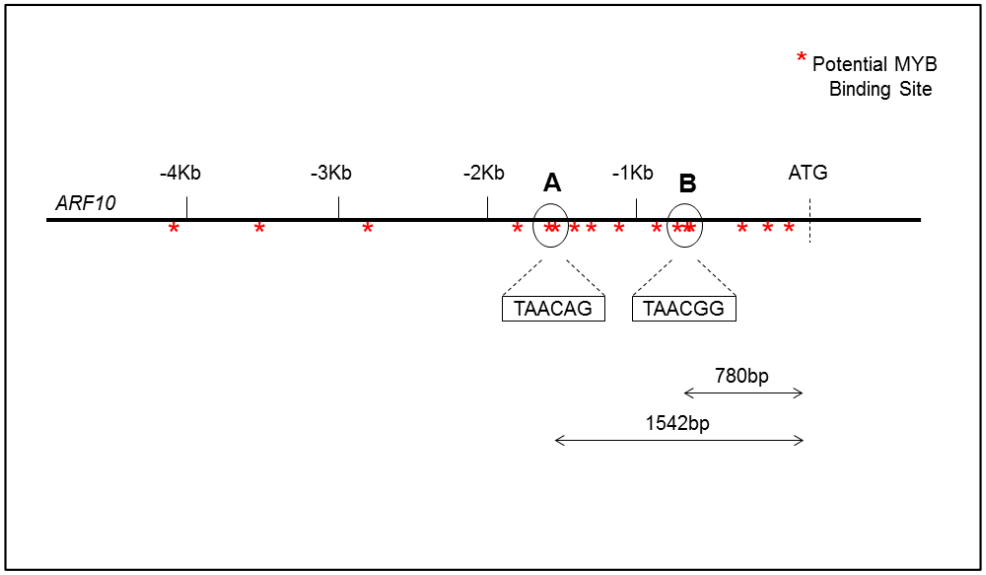

Figure 5-3: Potential MYB binding sites within the *ARF10* promoter.

Analysis highlighted two regions (A and B) where separate sources identified potential MYB binding sites, indicating that the chance of MYB transcription factors binding there was strong.

5.2.1 Chromatin immunoprecipitation

To further investigate the potential for direct interactions between the *ARF10* promoter and the WER and/or MYB23 proteins, ChIP analysis was carried out. This was done using the *pWER::WER-GFP* translational marker line that was readily available.

Using the previously identified potential MYB binding sites (Figure 5-3), in addition to data published on MYB binding sites in the *GL2* promoter (Figure 5-1), primers were designed with the aid of Dr Martin Kieffer. These primers encompassed the potential MYB binding sites in the *ARF10* promoter (Figure 5-4 A) and the published binding site GL2MBS2 in the *GL2* promoter to act as a positive control (Figure 5-4 B).

Analysis of the ChIP samples via qPCR, was unable to detect evidence of ARF10 promoter binding activity (Figure 5-5). In order to further investigate this interaction *ARF10* promoter truncation lines were also produced.

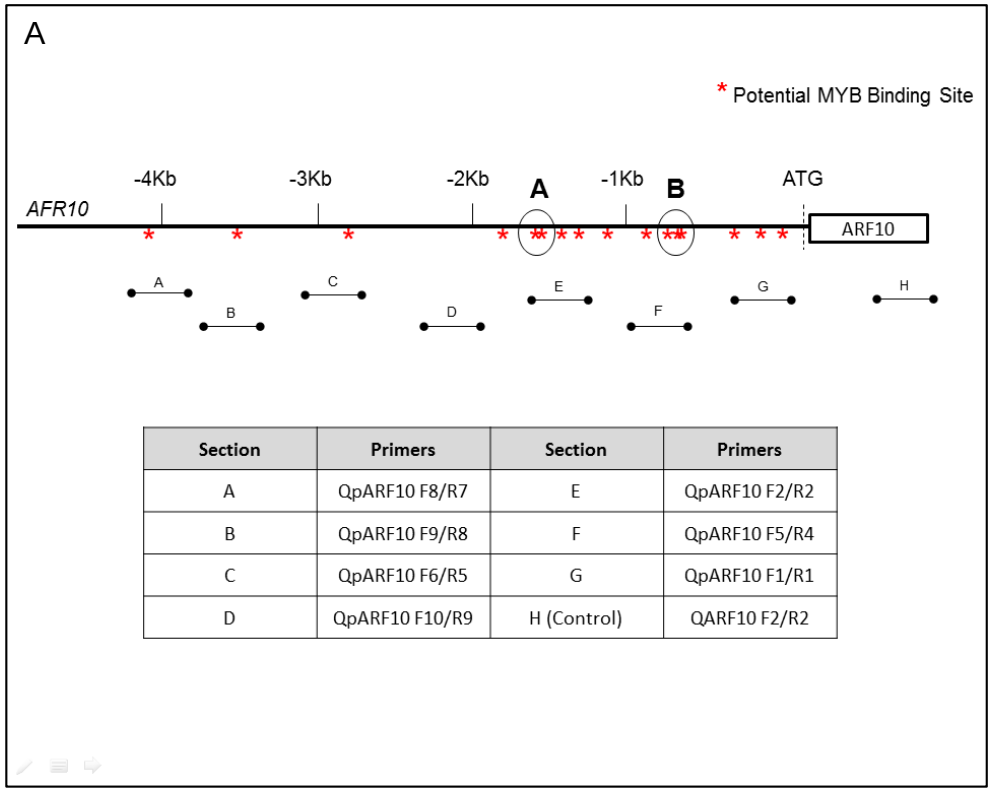

Section	Primers	Section	Primers
A	QpARF10 F8/R7	E	QpARF10 F2/R2
B	QpARF10 F9/R8	F	QpARF10 F5/R4
C	QpARF10 F6/R5	G	QpARF10 F1/R1
D	QpARF10 F10/R9	H (Control)	QARF10 F2/R2

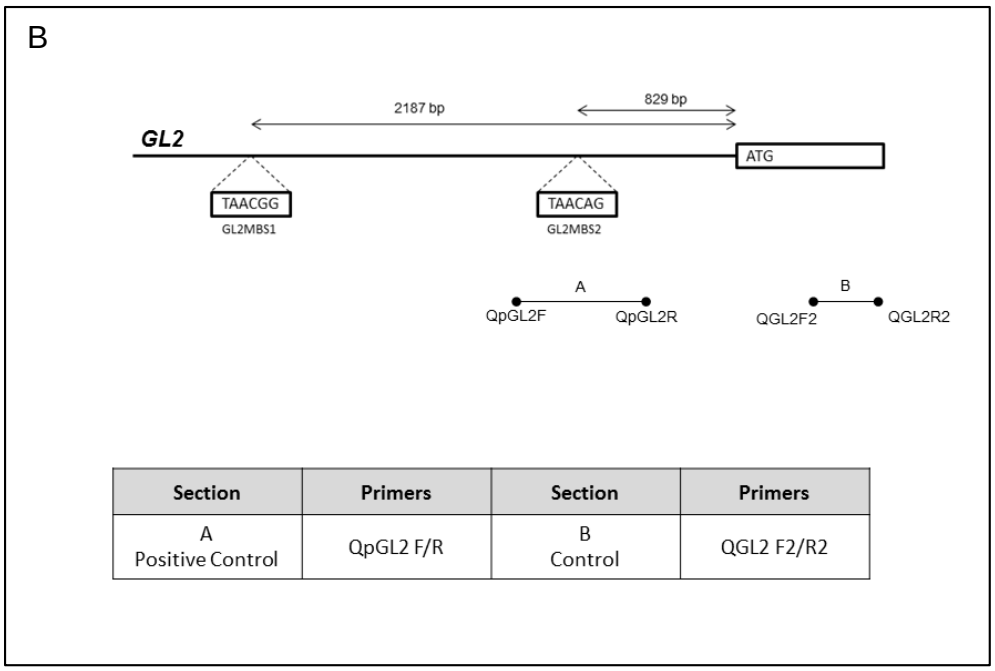

Section	Primers	Section	Primers
A Positive Control	QpGL2 F/R	B Control	QGL2 F2/R2

Figure 5-4: Primer location for ChIP analysis of the *ARF10* promoter.

A: Primer pairs were designed to encompass the previously identified potential MYB binding sites in the *ARF10* promoter, Figure 5-3. The design and the subsequent RT-qPCR analysis were carried out with the help of Dr Martin Kieffer. B: Using published data primers were also designed for the *GL2* promoter to be used as a positive control of *WER* binding.

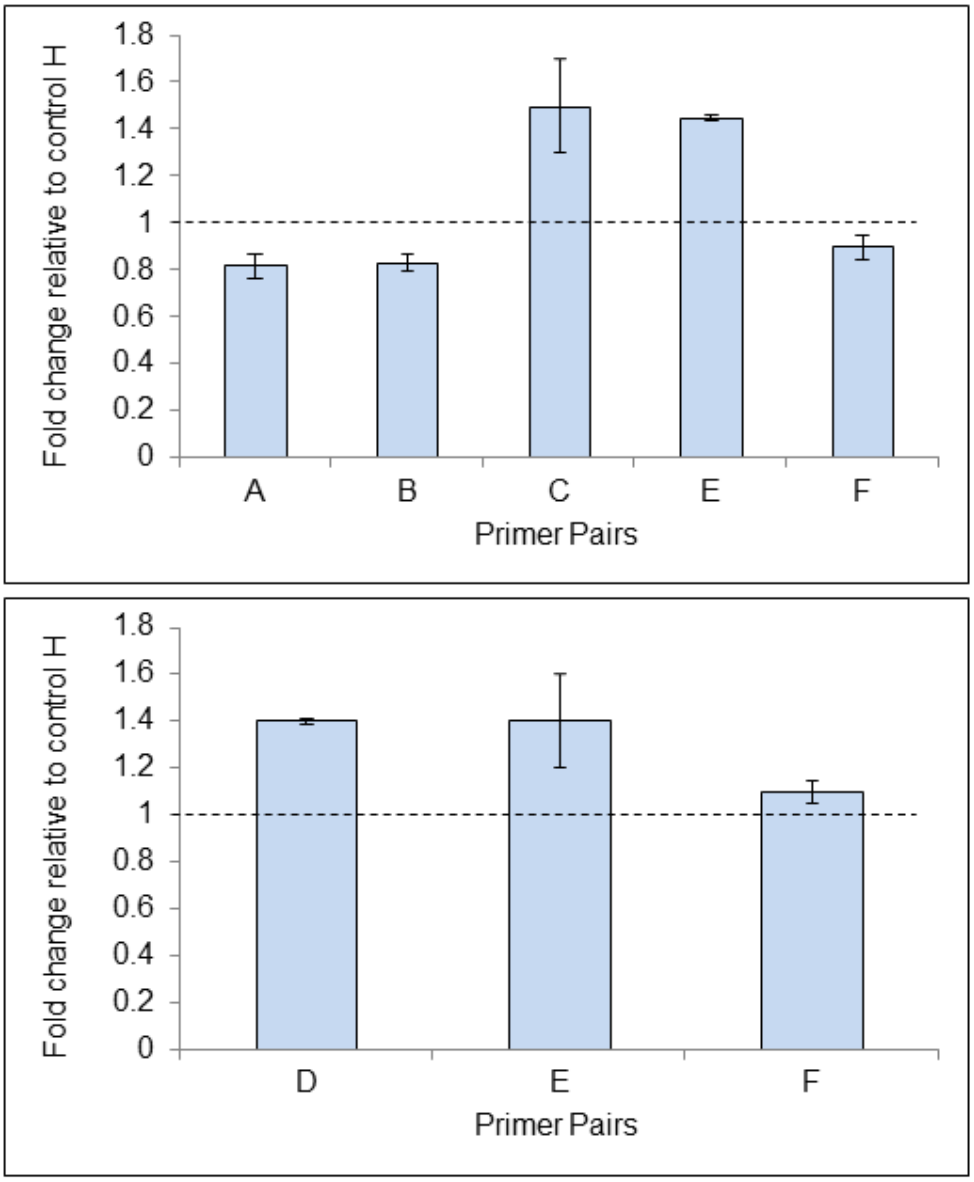

Figure 5-5: ChIP analysis of the *ARF10* promoter.

Various primer pairs were tested as detailed in Figure 5-4 A. The fold change was relative to control primer pair H. These results indicated no evidence of ARF10 promoter binding activity. Error bars represent standard error values.

5.2.2 ARF10 promoter truncations

Three *ARF10* promoter truncation constructs were made using the pGTJ01 vector following the Invitrogen® GATEWAY® approach. Starting from the 2078 base pair promoter sequence that was used to construct the *pARF10::ARF10-GFP* line, the largest truncation, truncation 1, encompassed both of the predicted binding sites **A** and **B.** Truncation 2 encompassed only binding site **B** alone, whilst the final truncation, truncation 3 omitted both **A** and **B** (Figure 5-6 A).

Analysis of these promoter truncation lines indicated that the differential expression of *ARF10* in the hair and non-hair cells of the root epidermis persisted in all of the lines (Figure 5-6 B). Thus indicating that the potential MYB binding sites **A** and **B** are unlikely to be of importance for *ARF10* expression in the root epidermis, regardless of if they do or do not interact with either WER and/or MYB23. An additional interesting pattern of expression observed was in the smallest truncation line, truncation 3, *ARF10* expression was lost at the very tip of the root epidermis (Figure 5-6 C).

These results were consistent with the first 710 base pairs of the *ARF10* promoter being important for the differential expression of *ARF10* in the late root epidermis development. Unfortunately the ChIP analysis did not confirm or dismiss the hypothesis that the positive regulation of *ARF10* by *WER* and *MYB23* was direct. A reliable homozygote line for *pMYB23::MYB23-GFP* was not produced before the submission of this thesis, however the ChIP analysis will be performed as soon as sufficient homozygous seed is obtained.

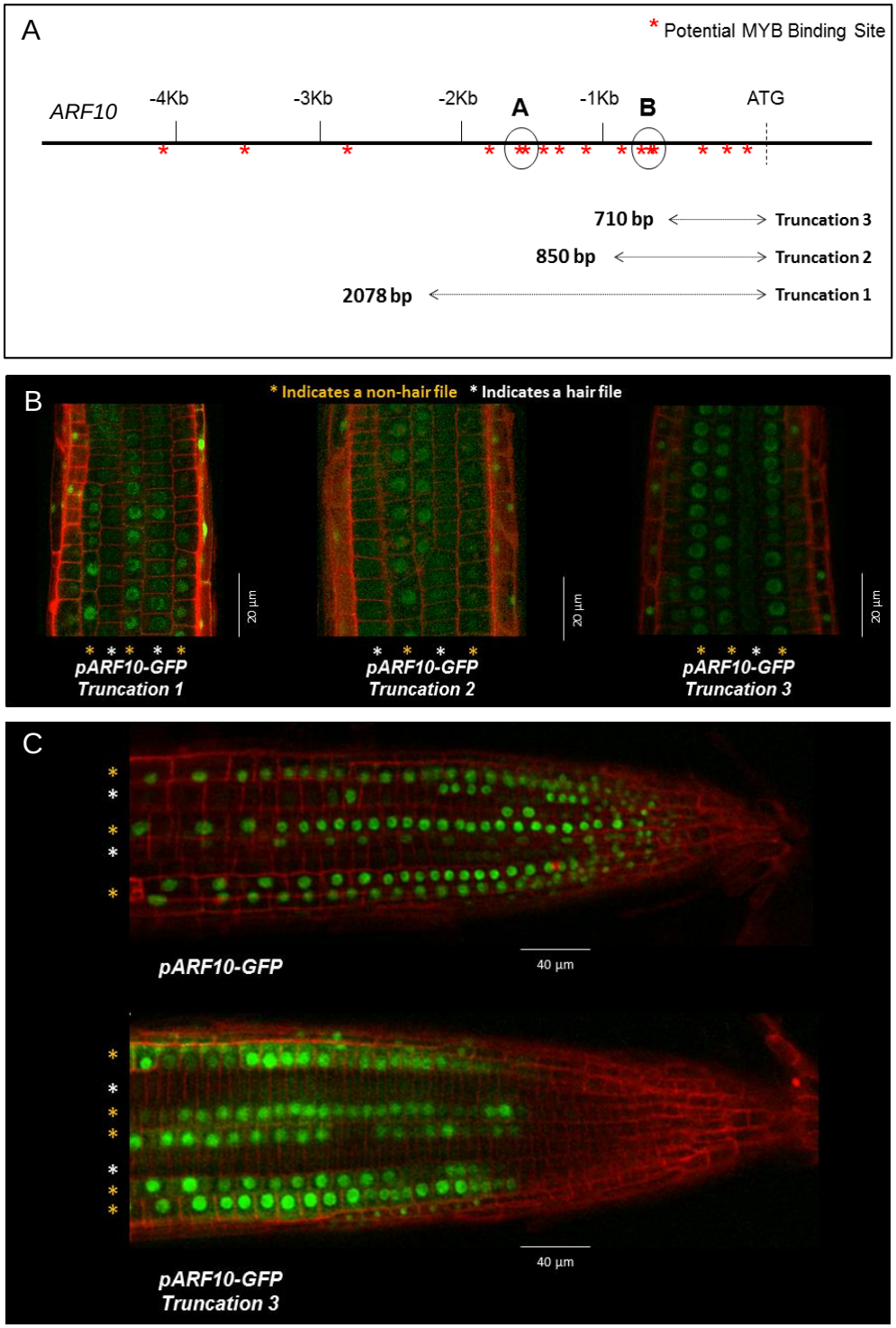

Figure 5-6: *ARF10* promoter truncation analysis.

A: Promoter truncations were generated to include both, **A** and **B, B** alone or neither **A** or **B,** potential MYB binding sites in the *ARF10* promoter. B: All of the truncation lines retained their differential hair/non-hair expression patterns. C: The smallest truncation, Truncation 3, did lose *ARF10* expression in the tip of the epidermis. Photographs:

Sharpened 50%, Brightness +40%, Contrast -40%. See 2.4 Confocal Microscopy for microscope settings.

5.3 Do feedback loops exist between the epidermal patterning mechanism and the auxin response network?

It was not possible to establish if there was a direct interaction between *ARF10,* MYB23 and WER results detailed in the previous chapter indicated that epidermal patterning components upstream of *GL2,* pattern both auxin response, and the auxin response network members in the root epidermis. In particular the expression of *ARF10* is promoted by two non-hair inducing epidermal patterning components, *WER* and *MYB23*, and inhibited by two hair cell promoting components, *CPC* and *TRY*.

Multiple feedback loops are apparent in both the epidermal patterning mechanism and the auxin response network. For example, in the auxin response network whilst the majority of the Aux/IAA proteins are degraded in an auxin dependent manner, for many, like IAA17, their expression is also up-regulated by auxin treatment, thus resulting in a feedback loop that enables tight regulation of this pathway (Ouellet *et al.*, 2001; Tromas and Perrot-Rechenmann, 2010; Kieffer *et al.*, 2010).

The epidermal patterning mechanism in particular is heavily dependent on feedback loops, for example *MYB23* is involved in both positive and negative feedback loops (Kang *et al*., 2009). Whilst *MYB23* promotes the expression of *CPC*, in turn *CPC* represses the expression of *MYB23*, thereby creating a negative feedback loop (Kang *et al.*, 2009). In contrast to this *MYB23* promotes

the expression of itself, thereby forming a positive feedback loop (Kang *et al.*, 2009).

5.3.1 Do ARF10 and/or ARF16 regulate *WER* expression?

In order to assess possible feedback regulation between the auxin response network and the epidermal patterning mechanism, transcriptional and translational markers for *WER* were crossed into the *arf10-3 arf16-2* double mutant (Figure 5-7). *WER* was selected because there was a loss of *ARF10* expression in the *wer-1* background and it is upstream of *GL2,* which is where interactions were observed in the previous crosses.

The *arf10-3 arf16-2* double loss of function mutant encompasses two repressing ARFs within the same clade (Finet *et al.*, 2013). In this clade, *ARF10* and *ARF16*, along with *ARF17* all share high amino acid sequence similarities and all contain an additional stretch of amino acids in the DNA binding domain (Wang *et al.*, 2005). The *arf10-3 arf16-2* double mutant was used in this study because of the known genetic redundancy in *Arabidopsis* implying a functional redundancy (Wang *et al*., 2005). Both the *arf10-3* and *arf16-2* mutants carry T-DNA insertions, the double mutant exhibits a severely agravitropic phenotype (Wang *et al.*, 2005). In addition to this a high number of ectopic root hairs are observed (Figure 5-7 B).

In the *arf10-3 arf16-2* mutant background the expression level of the *pWER::GFP* transcriptional marker was significantly reduced (T-Test, $P<0.005$) (Figure 5-7 C). This result indicates that in addition to *WER* positively regulating *ARF10 (*Figure 4-3), *ARF10* and/or *ARF16* are positively regulating *WER* expression in the root epidermis (Figure 5-8). These results are consistent with *ARF10* and *WER* being part of a positive feedback loop. This result was confirmed by analysis of the

pWER::WER-GFP translational marker in the *arf10-3 arf16-2* double mutant background (Figure 5-9). Again the fluorescence level was significantly reduced in this background (T-Test, P<0.005) (Figure 5-9 B).

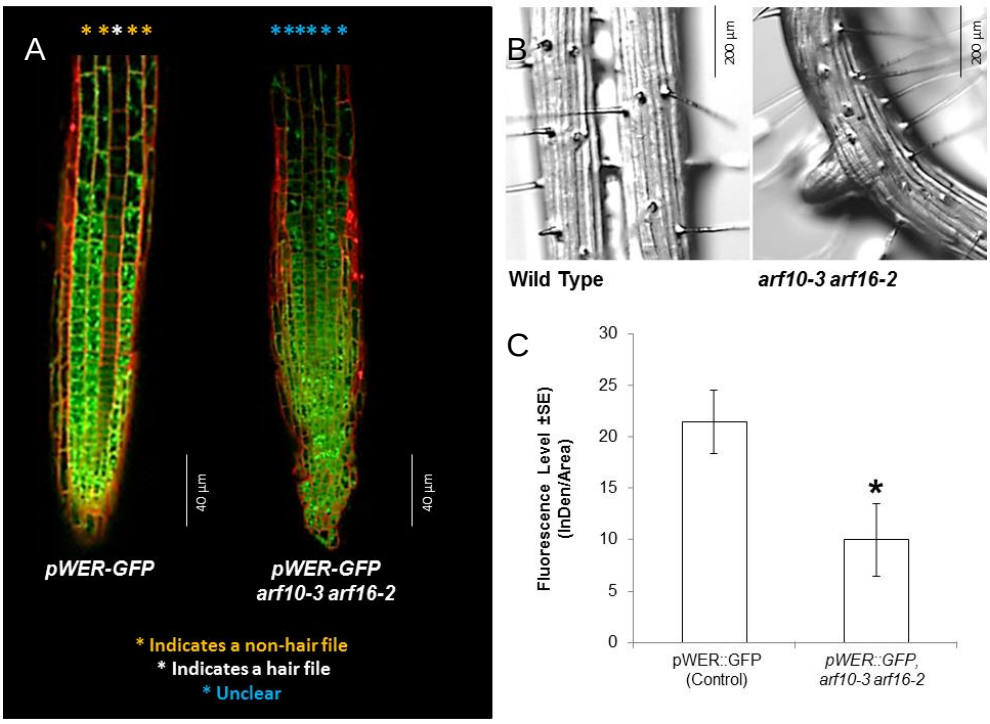

Figure 5-7: Expression of the transcriptional marker for *WER* in the *arf10-3 arf16-2* mutant background.

A: *pWER::GFP* expression in the *arf10-3 arf16-2* background. B: In the *arf10-3 arf16-2* mutant background the epidermal patterning is abnormal, root hair cells arise in adjacent files and a large frequency of ectopic root hairs are observed. C: The fluorescence level for the *pWER::GFP* line in the *arf10-3 arf16-2* mutant background is significantly lower (T-TEST, P<0.005) than the control. *pWER::GFP* was measured in the transition zone. Scale bars are labelled accordingly. White * indicate hair files, Orange * indicate non-hair files, Blue * indicate that the file identity is unclear. Photographs: Sharpened 50%, Brightness +40%, Contrast -20%. See 2.4 Confocal Microscopy for microscope settings. Error bars represent standard error values.

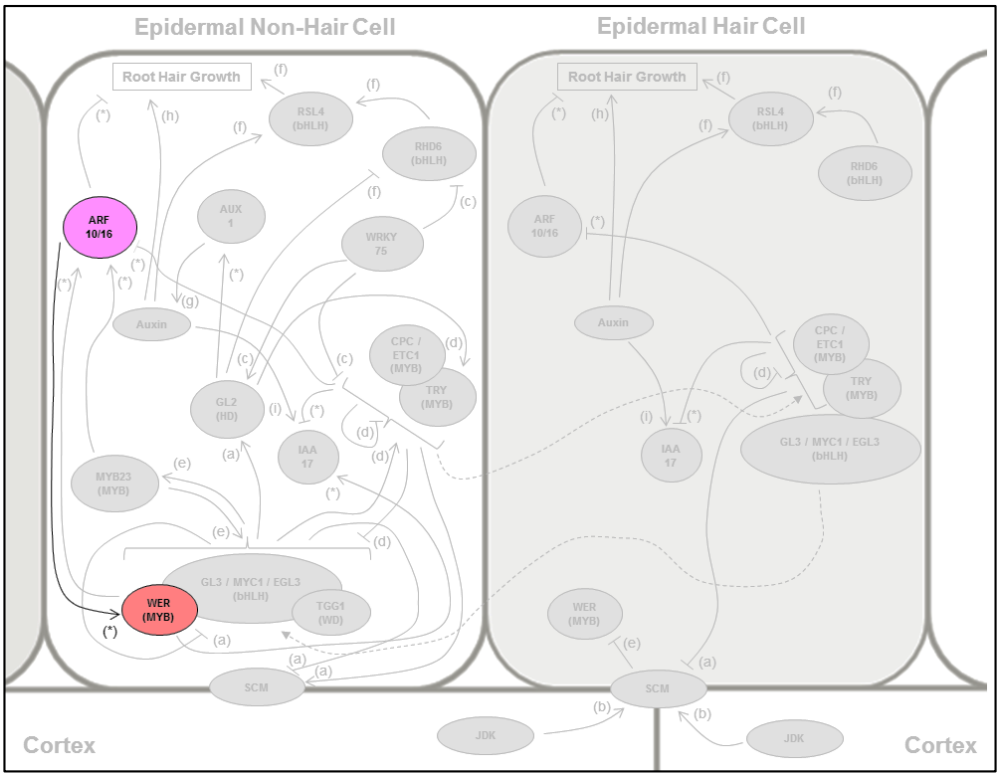

Figure 5-8: *ARF10* and/or *ARF16* promote the expression of *WER.*

Analysis of the *pWER::GFP* and pWER::WER-GFP markers in the *arf10-3 arf16-2* double mutant indicated that *ARF10* and/or *ARF16* promote the expression of *WER.* Solid lines indicate promotion (arrow head) or inhibition (flat head), dashed lines indicate movement in the direction of the arrow head. Letters next to the arrows indicate the published source of the interaction. (a) (Kwak and Schiefelbein, 2008) (b) (Hassan et al., 2010) (c) (Rishmawi et al., 2014) (d) (Simon et al., 2007) (e) (Kang et al., 2009) (f) (Yi et al., 2010) (g) (Jones et al., 2009) (h) (Masucci and Schiefelbein, 1996) (i) Tromas and Perrot-Rechenmann 2010. (*) indicates interactions identified during this project.

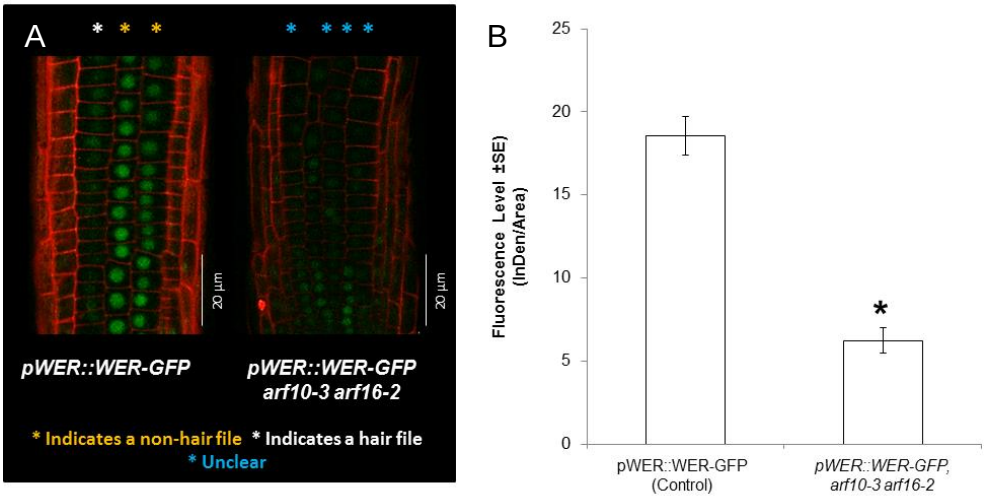

Figure 5-9: The translational marker for WER in the *arf10-3 arf16-2* background.

The translational marker for WER crossed into the *arf10-3 arf16-2*mutant background is weaker, and the differential expression between the files is lost. A: *pWER::WER-GFP* expression in the *arf10-3 arf16-2* mutant background. B: The fluorescence level in the *arf10-3 arf16-2* mutant was significantly lower than the control (T-Test, P<0.05). Scale bars are labelled accordingly. White * indicate hair files, Orange * indicate non-hair files, Blue * indicate that the file identity is unclear. See 2.4 Confocal Microscopy for microscope settings. Error bars represent standard error values.

In the cross involving the translational fusion marker it was also apparent that the differential expression of WER, which in the wild-type is preferentially expressed in the non-hair cells, was lost in the *arf10-3 arf16-2* mutant. This indicates a potential role for *ARF10* and *ARF16* in epidermal patterning.

5.3.3 Do ARF10 and/or ARF16 regulate *GL2* expression?

Thus far all of the interactions between the epidermal patterning mechanism and the auxin response network has been restricted to those occurring upstream of *GL2;* In order to check if *ARF10* also regulates *GL2* expression, the *pGL2::GFP* marker was crossed into the *arf10-3 arf16-2*mutant (Figure 5-10).

The fluorescence level of *pGL2::GFP* was significantly reduced in the *arf10-3 arf16-2* mutant background (Figure 5-10 C). Indicating that *ARF10* is a positive regulator of *GL2* expression*,* this is likely to be via effects on *WER* expression (Figure 5-11 A). In addition to this, as observed with the *WER* marker*,* it was also clear that the differential *pGL2::GFP* expression in the non-hair files is lost (Figure 5-10 B).

5.3.4 Do ARF10 and/or ARF16 regulate *MYB23* expression?

RT-qPCR analysis carried out by Dr Martin Kieffer confirmed that WER and GL2 expression levels are significantly reduced in the *arf10-3 arf16-2* double mutant background, Supplementary Data (Figure 9-5). Interestingly this data also indicated that MYB23 expression levels are significantly increased in *an arf10-3 arf16-2* mutant. A result that is consistent with *ARF10* and/or *ARF16* repressing *MYB23* expression (Figure 5-11 B).

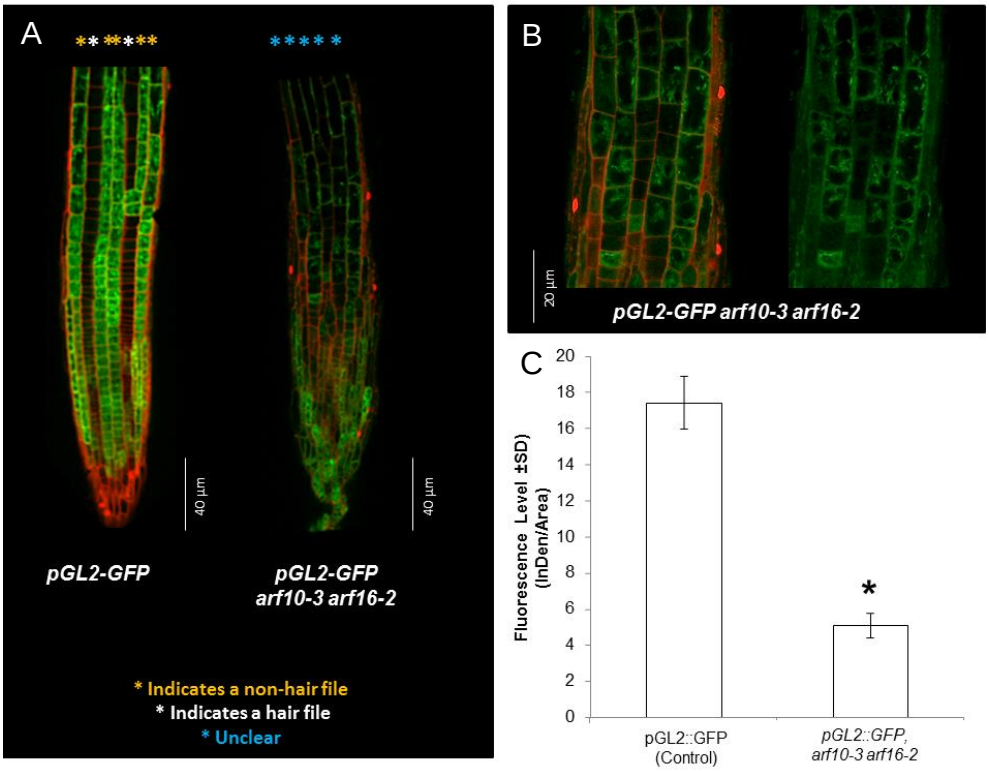

Figure 5-10: Expression of *pGL2::GFP* in the *arf10-3 arf16-2* mutant background.

A: The transcriptional maker *pGL2::GFP* crossed into the *arf10-3 arf16-2* mutant background. B: In the *arf10-3 arf16-2* mutant background the differential expression of *GL2* is lost. C: The expression of *pGL2::GFP* in the *arf10-3 arf16-2* mutant background is significantly lower (T-TEST, P<0.005) than the control. Scale bars are labelled accordingly. White * indicate hair files, Orange * indicate non-hair files, Blue * indicate that the file identity is unclear. Photographs: Brightness +40%, Contrast -20%. See 2.4 Confocal Microscopy for microscope settings. Error bars represent standard error values.

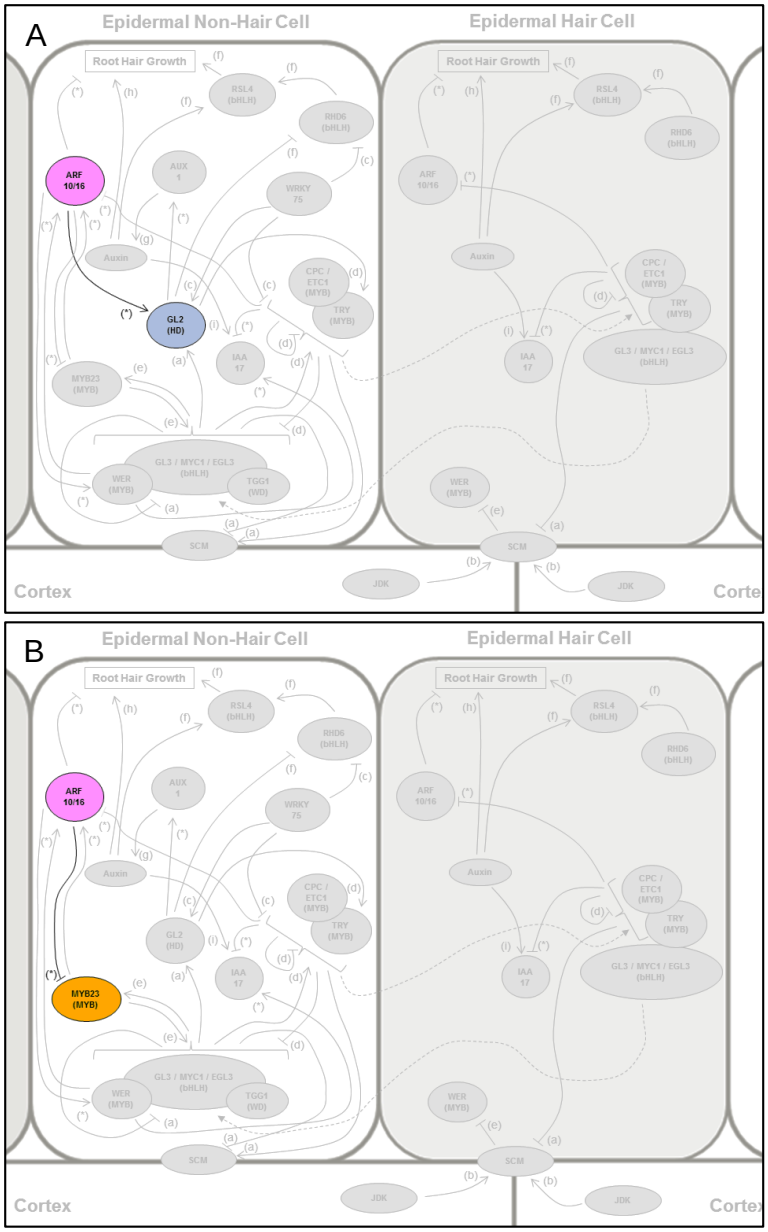

Figure 5-11: *ARF10* and/or *ARF16* promote the expression of *GL2* and inhibit the expression of *MYB23.*

A: Analysis of the *pGL2::GFP* marker in the *arf10-3 arf16-2* mutant indicated that *ARF10* and/or *ARF16* promote the expression of *GL2*. B: RT-qPCR data also indicated that *ARF0* and/or *ARF16* down-regulate *MYB23* expression. Solid lines indicate promotion (arrow head) or inhibition (flat head), dashed lines indicate movement in the direction of the arrow head. Letters next to the arrows indicate the published source of the interaction. (a) (Kwak and Schiefelbein, 2008) (b) (Hassan et al., 2010) (c) (Rishmawi et al., 2014) (d) (Simon et al., 2007) (e) (Kang et al., 2009) (f) (Yi et al., 2010) (g) (Jones et al., 2009) (h) (Masucci and Schiefelbein, 1996) (i) Tromas and Perrot-Rechenmann 2010. (*) indicates interactions identified during this project.

5.4 Does ARF10 directly bind to the *MYB23* promoter?

Results thus far have indicated that both *WER* and *MYB23* are part of a feedback loop with *ARF10* and/or *ARF16*. Whilst *WER* and *MYB23* both promote the expression of *ARF10*, *ARF10* and/or *ARF16* promote the expression of WER, forming a positive feedback loop, and inhibit the expression of *MYB23,* thereby forming a negative feedback loop. In order to assess if this negative regulation of *MYB23* is direct, the promoter region of *MYB23* was analysed for Auxin Response Elements (AuxRE's). AuxREs have been characterised by various sequences, including, TGTCNC, TGTCGG and TGTCNN (Tiwari *et al*., 2003; Guilfoyle and Hagen, 2007; Tromas and Perrot-Rechenmann, 2010). Analysis of the *MYB23* promoter region indicated several potential AuxRE's. Primers were designed to encompass these potential AuxRE binding sites and ChIP assays carried out using the *pARF10::ARF10-GFP* marker line (Figure 5-12 A). The ChIP assay indicated there was no evidence of promoter binding activity (Figure 5-12 B).

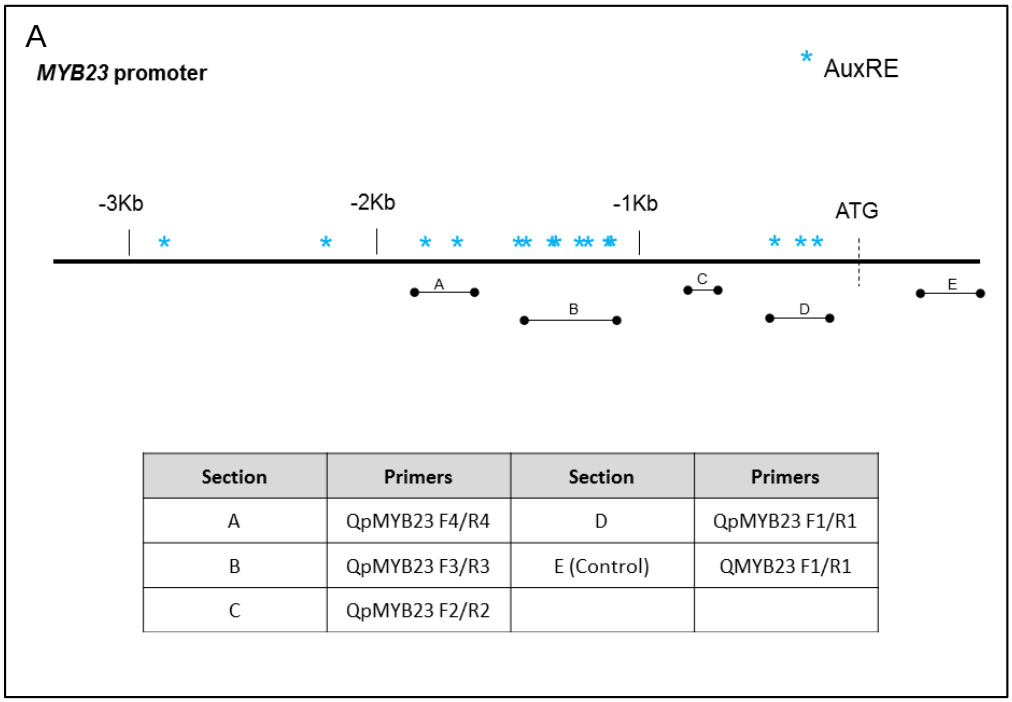

Section	Primers	Section	Primers
A	QpMYB23 F4/R4	D	QpMYB23 F1/R1
B	QpMYB23 F3/R3	E (Control)	QMYB23 F1/R1
C	QpMYB23 F2/R2		

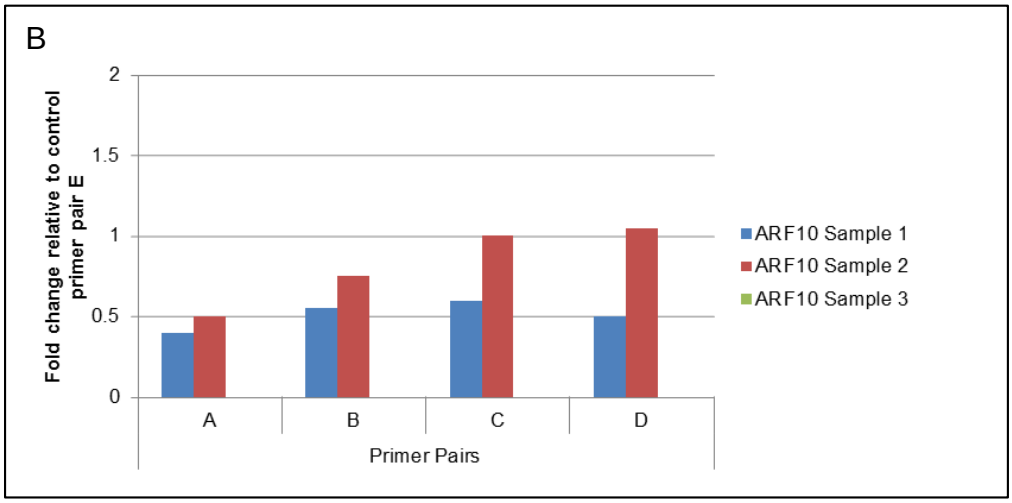

Figure 5-12: ChIP analysis of the *MYB23* promoter.

A: Primers were designed to encompass the potential AuxRE's in the *MYB23* promoter. B: Fold change enrichment relative to control DNA region E. These results show no evidence of ARF10 promoter binding.

5.5 Discussion

The results presented in this chapter indicated that *ARF10* and/or *ARF16* promote and inhibit the expression of several epidermal patterning mechanism components, thereby facilitating the formation of both positive and negative feedback loops between these two important aspects of plant growth (Figure 5-13).

Despite a well-designed experiment, due to the positive control failing to show any evidence of promoter binding activity, it was not possible to reliably conclude if there was or was not a direct interaction between the components in the ChIP assays. However results from the promoter truncation assays were consistent with the first 710 base pairs of the *ARF10* promoter being important for the differential expression of *ARF10* in the root epidermis.

A reliable homozygote line for *pMYB23::MYB23-GFP* was not produced before the submission of this thesis, however ChIP analysis will be performed as soon as sufficient homozygous seed is obtained.

Future work including; further promoter truncations, a more reliable positive control and ChIP analysis of the *pMYB23::MYB23-GFP* marker line, would give a better understanding of the direct and/or indirect nature of the regulation between these epidermal patterning mechanism and auxin response network members.

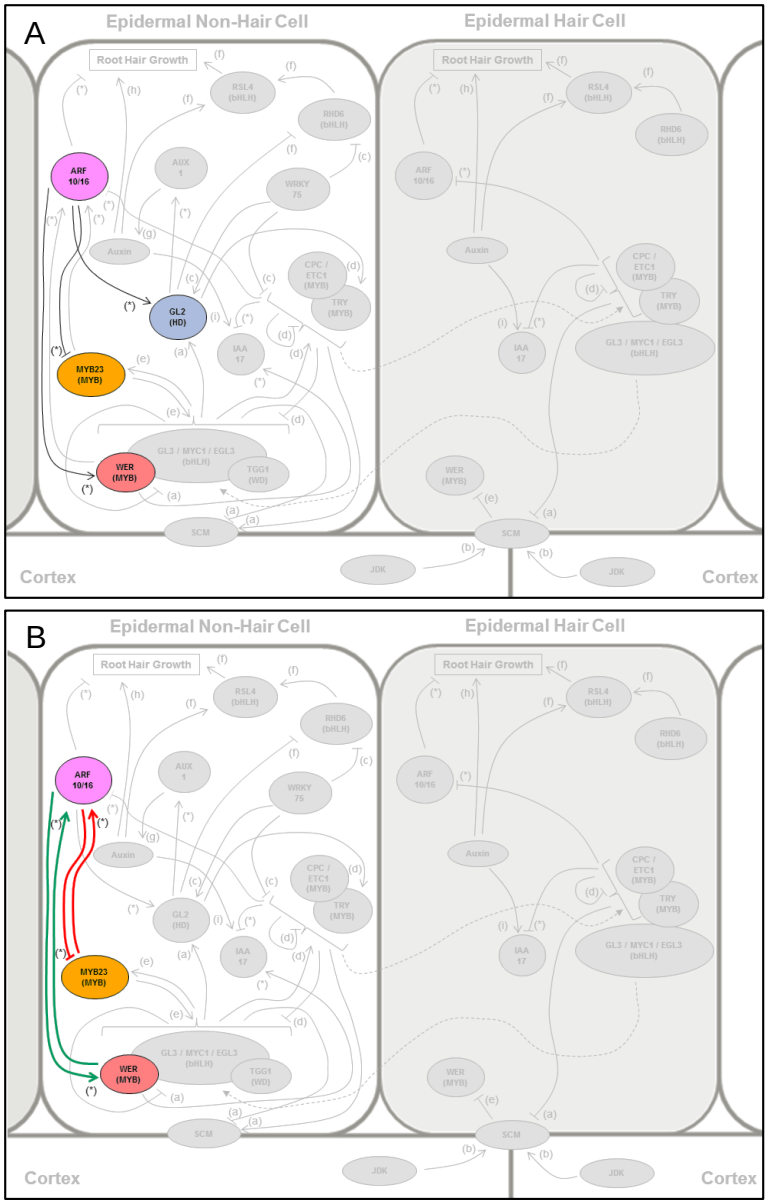

***Figure* 5-13: Interactions identified during this chapter.**

A: A summary of the interactions discussed and identified in this chapter. B: The positive (green) and negative (red) feedback loops identified during this chapter. Solid lines indicate promotion (arrow head) or inhibition (flat head), dashed lines indicate movement in the direction of the arrow head. Letters next to the arrows indicate the published source of the interaction. (a) (Kwak and Schiefelbein, 2008) (b) (Hassan et al., 2010) (c) (Rishmawi et al., 2014) (d) (Simon et al., 2007) (e) (Kang et al., 2009) (f) (Yi et al., 2010) (g) (Jones et al., 2009) (h) (Masucci and Schiefelbein, 1996) (i) Tromas and Perrot-Rechenmann 2010. (*) indicates interactions identified during this project.

6 : The Role of the Auxin Mediated Down-Regulation of *GL2* and *MYB23* on Root Hair Growth

6.1 Introduction

Before this project began microarray data indicated that two epidermal patterning components, *GL2* and *MYB23,* are down-regulated by auxin treatment. During the course of this project this was confirmed by Dr Martin Kieffer using RT-qPCR assays (Supplementary Data Figure 9-5). The functional significance of auxin-mediated down-regulation of *GL2* and *MYB23* on root hair growth is not clear. Whilst *GL2*'s role in the production of root hairs has long been well established, *MYB23* affecting root hair growth hasn't been previously considered.

GL2 functions primarily in the non-hair cells and downstream of the epidermal patterning components *WER* and *CPC*. *GL2* encodes a homeodomain leucine-zipper transcription factor protein, and negatively regulates key root hair growth related genes like *RHD6* (Bruex *et al.*, 2012). Downstream of GL2, proteins controlling cell wall biosynthesis, cytoskeletal activities and production and trafficking of extracellular material influence later morphogenesis events in the epidermal cells (Bruex *et al.*, 2012).

MYB23's role appears to be very different. Via positive regulation of its own promoter, *MYB23* is proposed to stabilise the epidermal establishment of hair and non-hair cells (Figure 1-7) (Kang *et al*., 2009). In addition to this whilst the *gl2-1* knockout mutant results in excessive root hair production, the *myb23-1* knock out mutant results in only a small increase in ectopic root hairs (Figure 3-1). Thus indicating that a significant role for *MYB23* in root hair growth may be unlikely (Kang *et al*., 2009). As it has long been established that auxin plays an important role in root hair growth, the impact of the down-regulation of these two epidermal patterning components was considered further.

6.2 Further clarification of auxin down-regulation of epidermal patterning components

In order to clarify this apparent regulation of *GL2* and *MYB23* further, visualisation of the proposed auxin down-regulation was carried out using the *pGL2::GFP* marker. The *pGL2::GFP* marker was treated with auxin and PEO-IAA, an auxin antagonist (Figure 6-1) (Hayashi *et al*., 2008). A significant decrease (ANOVA, $P<0.005$) in fluorescence was observed when treated with auxin and a significant increase (ANOVA, $P<0.005$) when treated with PEO-IAA. The existing microarray and RT-qPCR data measured mRNA whilst the *pGL2::GFP* marker measured promoter activity, thus indicating that auxin is not regulating *GL2* expression in a post transcriptional manner.

6.2.1 Does auxin down-regulate GL2 and MYB23 independently of one another?

Having further clarified this relationship, experiments were carried out to establish if *GL2* was down-regulated independently of *MYB23. GL2* expression is located downstream of the epidermal patterning mechanism and therefore downstream of *MYB23.* In order to establish if *GL2* expression was decreased as a result of *MYB23* levels decreasing, the *pGL2::GFP* marker was crossed into the *myb23-1* mutant (Figure 6-2).

In the *myb23-1* mutant background the fluorescence pattern of *pGL2::GFP* does not differ significantly from that observed in the wild-type (Figure 6-2 B). This result is consistent with transcriptomic data published by Kang *et al*, 2009, which shows no significant change in *GL2* transcript levels in a *myb23-1* mutant background. In addition, when treated with auxin the *pGL2::GFP* fluorescence level in the *myb23-1* mutant is still significantly reduced (ANOVA, $P<0.005$) (Figure 6-2 B). Indicating that auxin down regulates *GL2* and *MYB23,* at least partly, independently of one another (Figure 6-3).

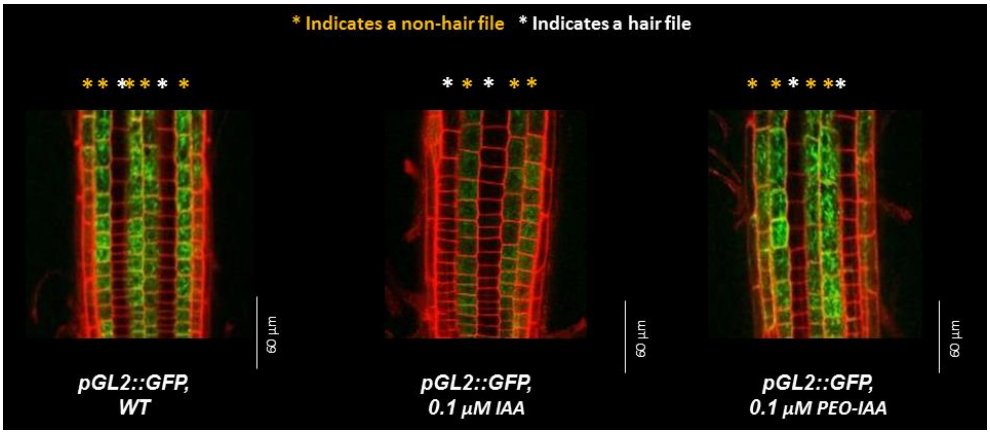

Figure 6-1: *pGL2::GFP* marker treated with IAA and PEO-IAA.

The *pGL2::*GFP marker was treated with 0.1 µM IAA and 0.1 µM PEO-IAA. See 2.4 Confocal Microscopy for microscope settings. Scale bars are labelled accordingly.

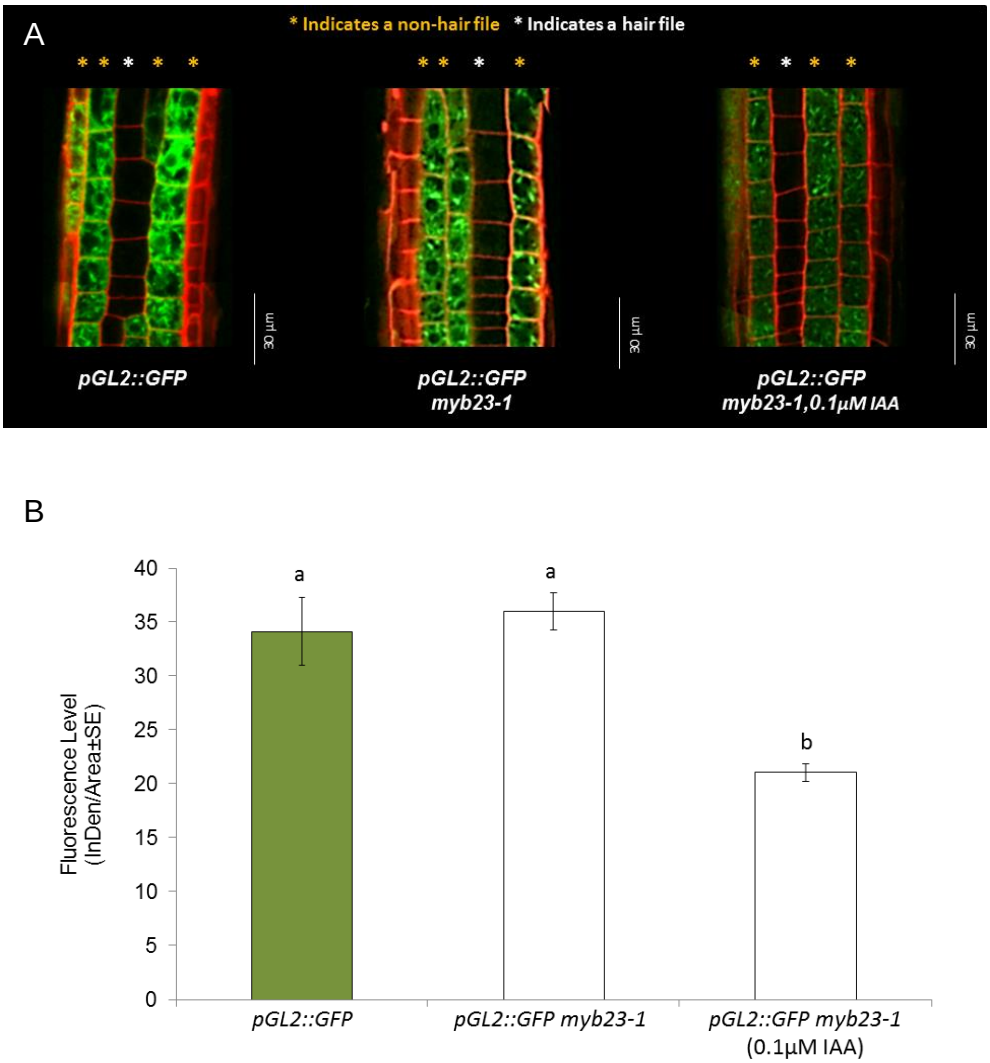

Figure 6-2: Analysis of the *pGL2::GFP* marker in the *myb23-1* background.

The *pGL2::GFP* marker was crossed into the *myb23-1* mutant background. A: The clear differential pattern of *pGL2::GFP* between the hair and non-hair files was retained in the *myb23-1* background. B: Measured fluorescent levels with and without auxin treatment indicated a significant decrease in the *pGL2::GFP myb23-1* line when it was treated with auxin (ANOVA, $P<0.005$). See 2.4 Confocal Microscopy for microscope settings. Error bars represent standard error values. Scale bars are labelled accordingly.

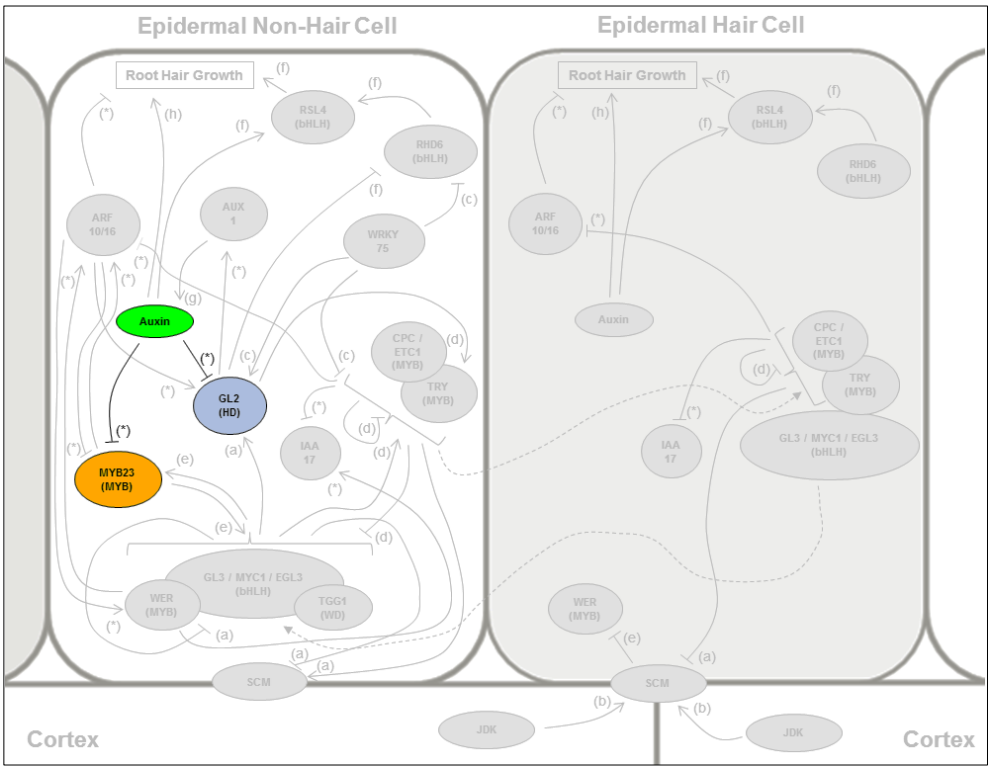

Figure 6-3: Auxin down-regulates *MYB23* and *GL2.*

Analysis of the *pGL2::GFP* marker in both the wild-type and *myb23-1* mutant backgrounds indicated that auxin down-regulates *MYB23* and *GL2* independantly of one another. Solid lines indicate promotion (arrow head) or inhibition (flat head), dashed lines indicate movement in the direction of the arrow head. Letters next to the arrows indicate the published source of the interaction. (a) (Kwak and Schiefelbein, 2008) (b) (Hassan et al., 2010) (c) (Rishmawi et al., 2014) (d) (Simon et al., 2007) (e) (Kang et al., 2009) (f) (Yi et al., 2010) (g) (Jones et al., 2009) (h) (Masucci and Schiefelbein, 1996) (i) Tromas and Perrot-Rechenmann 2010. (*) indicates interactions identified during this project.

6.3 Does *MYB23* and/or *GL2* down-regulation by auxin affect root hair initiation?

Adding auxin to a wild-type plant does not result in increased root hair initiation. The non-hair cell is very resistant to auxin and other repression mechanisms may hide the effect of a reduction in *MYB23* and/or *GL2* transcript. Therefore to assess if the down-regulation of *MYB23* or *GL2* by auxin could increase root hair initiation an epidermal patterning system, which was already compromised and highly favouring the non-hair cell fate was selected. The *cpc-1* and *cpc-1 try-82* mutants, producing fewer or no root hairs respectively, were treated with auxin (Figure 6-4).

When these non-hair favouring mutants were treated with 0.01 μM of auxin no significant increase in root hair production was observed (Figure 6-4 A). Initially the auxin concentration was kept low to avoid any significant changes in the primary root length, (Alarcón *et al.*, 2014), which can affect the reliability of root hair density measurements (Figure 6-4 B). To assess if no response was observed because the auxin concentration was too low, both the *cpc-1* and *cpc-1 try-82* mutants were then grown on increasing auxin concentrations up to a final concentration of 1 μM IAA (Figure 6-4 C). Again no significant change in root hair density was observed in either background. These results were consistent with the down-regulation of *GL2* and *MYB23* in these backgrounds being insufficient to result in increased root hair production.

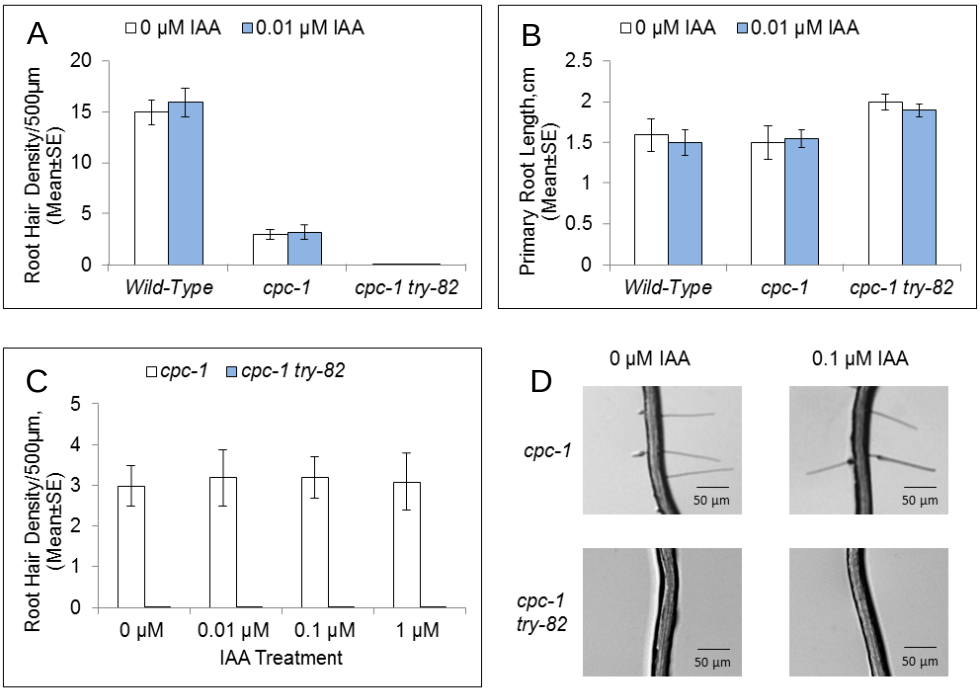

Figure 6-4: Analysis of root hairs in the *cpc*-1 and *cpc-1 try-82* mutants.

A: No significant change in root hair density was observed when the *cpc-1* and *cpc-1 try-82* mutants were treated with auxin. B: No significant change in primary root length was observed upon treatment with low concentrations of auxin. The primary root length was measured to assess if increases in density may be due to a shortening of the primary root. C: The *cpc*-1 and *cpc-1 try-82* double mutants were treated with higher concentrations of auxin, none of the treatments resulted in any root hair density increases. D: Regardless of increasing auxin concentrations the *cpc-1 try-82* double mutant did not produce any root hairs. Photographs: Sharpened 50%, Brightness +40%, Contrast +20%. Error bars represent standard error values. Scale bars are labelled accordingly.

6.3.1 *Does auxin down-regulation of MYB23 in the gl2-1* mutant have an effect on root hair initiation?

The experiments above indicated that down-regulation of *MYB23* and/or *GL2* by auxin did not result in increased root hair production in a mutant background where the hair cell identity was compromised. In order to assess if the down-regulation of *MYB23* can result in increased root hair production in a mutant where the non-hair cell identity is compromised, the *gl2-1* knockout mutant was used (Figure 6-5).

In the *gl2-1* mutant approximately 50% of non-hair cells produce root hairs, meaning there is still the potential for further increase (Masucci and Schiefelbein, 1996). As the *gl2-1* knockout does not result in 100% root hair production, as is observed in the *wer-1* mutant, it is logical to assume that other factors may also be controlling root hair initiation. Although the down-regulation of *MYB23* and/or *GL2* in the hairless mutants was insufficient to result in increased root hair production, it was hypothesised that in a system which was already compromised in terms of hair production a different result may be observed.

The root hair density of the *gl2-1* mutant was observed consistently and reproducibly to significantly increase by approximately 12 root hairs per 500 μm on plants treated with auxin. As with the previous assay the auxin concentration was kept low in order to avoid any significant shortening of the primary root (Figure 6-5). Whilst it is reasonable to hypothesise that this increase in root hair density could be due to the down-regulation of *MYB23,* it was also possible that the changes could be caused by a disruption of the auxin response machinery. To test this hypothesis the *pARF10::GFP, gl2-1* and *pIAA17::GFP, gl2-1* lines initially discussed in Chapter 3, were treated with auxin in order to assess if any significant changes in expression patterns or levels was observed (Figure6-6) .

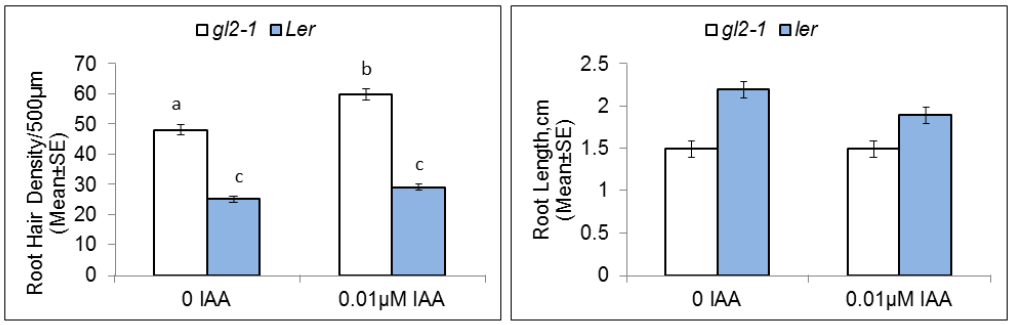

Figure 6-5: Root hair density in the *gl2-1* mutant.

A small but significant increase in root hair density was observed in the *gl2-1* mutant when it was treated with auxin (ANOVA, $P<0.005$). There was no significant change in primary root length, therefore the significant increase in root hair density was due to the production of more root hairs, rather than a shortening of the primary root. Error bars represent standard error values.

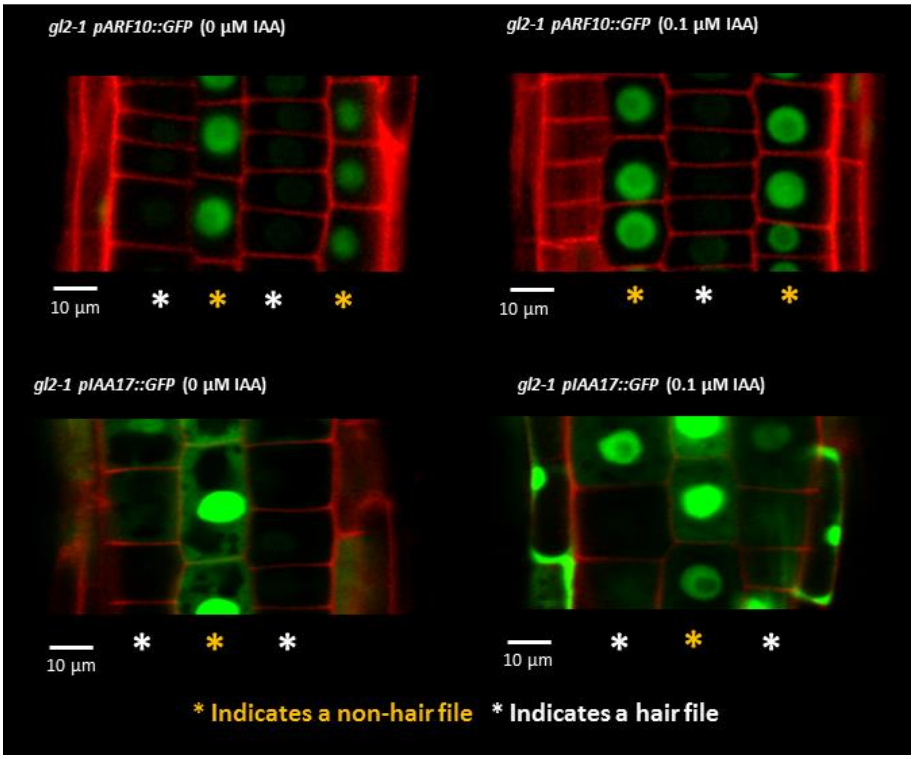

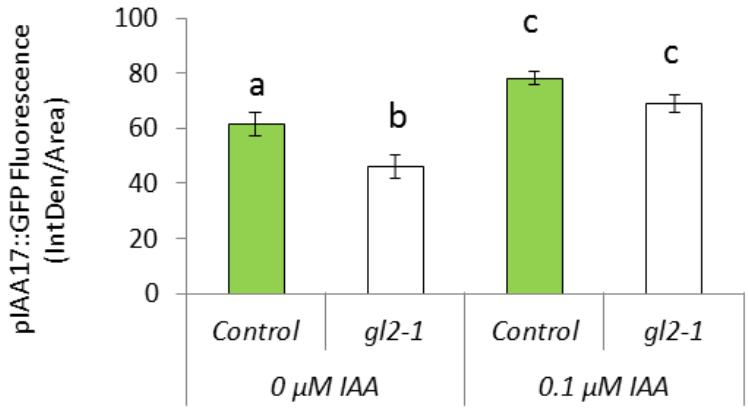

Figure 6-6: Changes in *ARF10* and *IAA17* expression in the *gl2-1* mutant when treated with auxin.

When treated with auxin a significant increase (ANOVA, P<0.005) in fluorescence was observed in the *pIAA17::GFP* marker in both the wild-type (not pictured) and the *gl2-1* mutant background. No significant changes were observed in *ARF10* fluorescence in the *gl2-1* mutant background when treated with auxin. Error bars represent standard error values. Scale bars are labelled accordingly. Significant differences in data sets are indicated by different letters.

When treated with auxin a significant increase (ANOVA, P<0.005) in the fluorescence level for the *IAA17* marker was observed in the *gl2-1* mutant background, a response consistent with published data (Tromas and Perrot-Rechenmann, 2010). In addition to this, no significant change in the expression level of *ARF10* was observed in the *gl2-1* mutant when it was treated with auxin. As the auxin response machinery in *gl2-1* did not differ significantly from that of the wild-type, these results were consistent with the hypothesis that altered *ARF10* or *IAA17* expression in the *gl2-1* mutant due to auxin treatment was not a factor in this small but significant increase in root hair density.

6.3.2 Root hair initiation in the myb23-1 gl2-1 double mutant

In order to confirm if this increase in root hair density was due to the down-regulation of *MYB23* by auxin, the *myb23-1 gl2-1* double mutant was created by crossing the two single mutant lines together (Figure 6-7). When treated with auxin the *myb23-1 gl2-1* double mutant did not exhibit the significant increase in root hair density that was observed in the *gl2-1* single mutant. A result consistent with the hypothesis that the down-regulation of *MYB23* by auxin plays a role in root hair initiation, thus indicating the possibly of a parallel pathway to *GL2.*

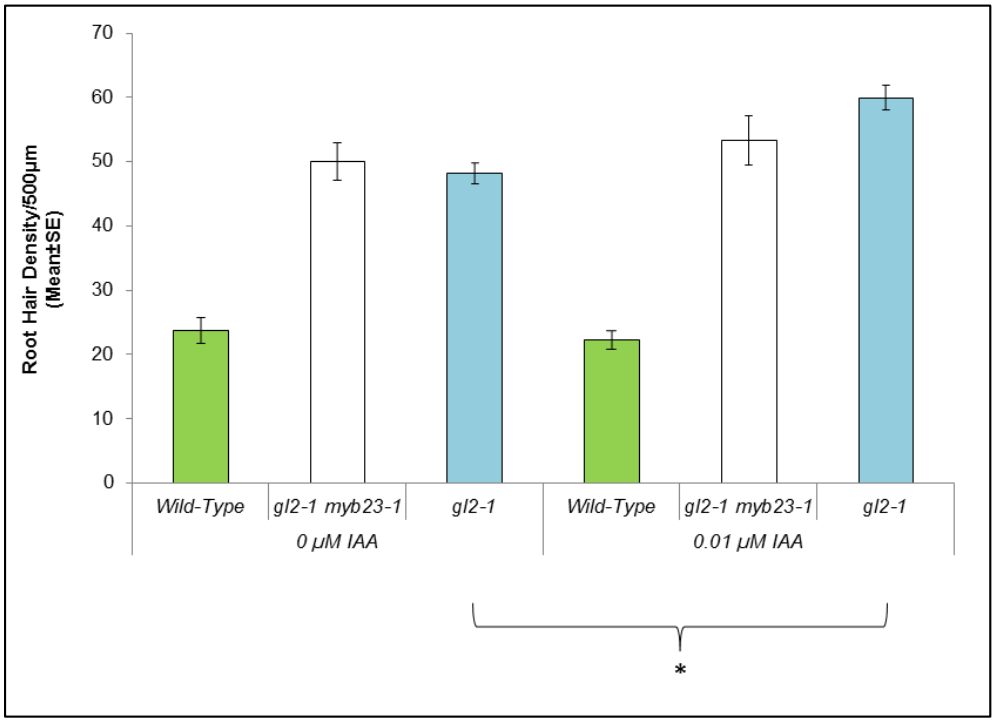

Figure 6-7: Analysis of root hairs in the *gl2-1 myb23-1* double mutant.

The *gl2-1 myb23-1* double mutant did not exhibit the significant increase in root hair density when treated with auxin that was observed in the *gl2-1* single mutant (ANOVA, $P<0.005$). Error bars represent standard error values. * Indicates a significant difference between the two identified data sets before and after auxin treatment.

6.4 Does *MYB23* and/or *GL2* down-regulation by auxin affect root hair elongation?

During this project all of the epidermal patterning mutants and some *AUX1* mutants were assessed for auxin responsiveness in several ways, these included primary root length and root hair elongation (Supplementary Data Figure 9-4). During these assays it was found that some of the mutants had root hairs that elongated more in response to auxin treatment, whilst others had root hairs that elongated less (Figure 6-8). For example the *wer-1* and *myb23-1* mutants had root hairs that elongated significantly more (ANOVA, $P<0.005$) than the wild-type, whilst the root hairs in *cpc-1* elongated significantly less (ANOVA, $P<0.005$). The *gl2-1* mutant had an average root hair length that was significantly shorter than the wild-type without auxin treatment, previously discussed in Chapter 3 (Figure 3-6), but this was not significantly different from the wild-type after treatment with 0.1 µM IAA.

The possibility that the mutants with more hair cells may be more responsive to auxin was considered. However this idea was quickly dismissed as repeated assays indicated that the *myb23-1* mutant consistently and reproducibly displayed one of the strongest increased elongation phenotypes, despite retaining the majority of its non-hair cells (Kang *et al*., 2009). In addition to this, there is no immediate logical reason to expect the auxin responsiveness of hair cells to be affected by neighbouring non-hair cells. Therefore other differences in the mutant backgrounds were considered.

As both the *myb23-1* and *wer-1* mutants had root hairs that consistently elongated more in response to auxin treatment than the wild-type, and it is well documented that these two components work closely to promote the non-hair cell fate, relative transcript levels of these two components were considered in

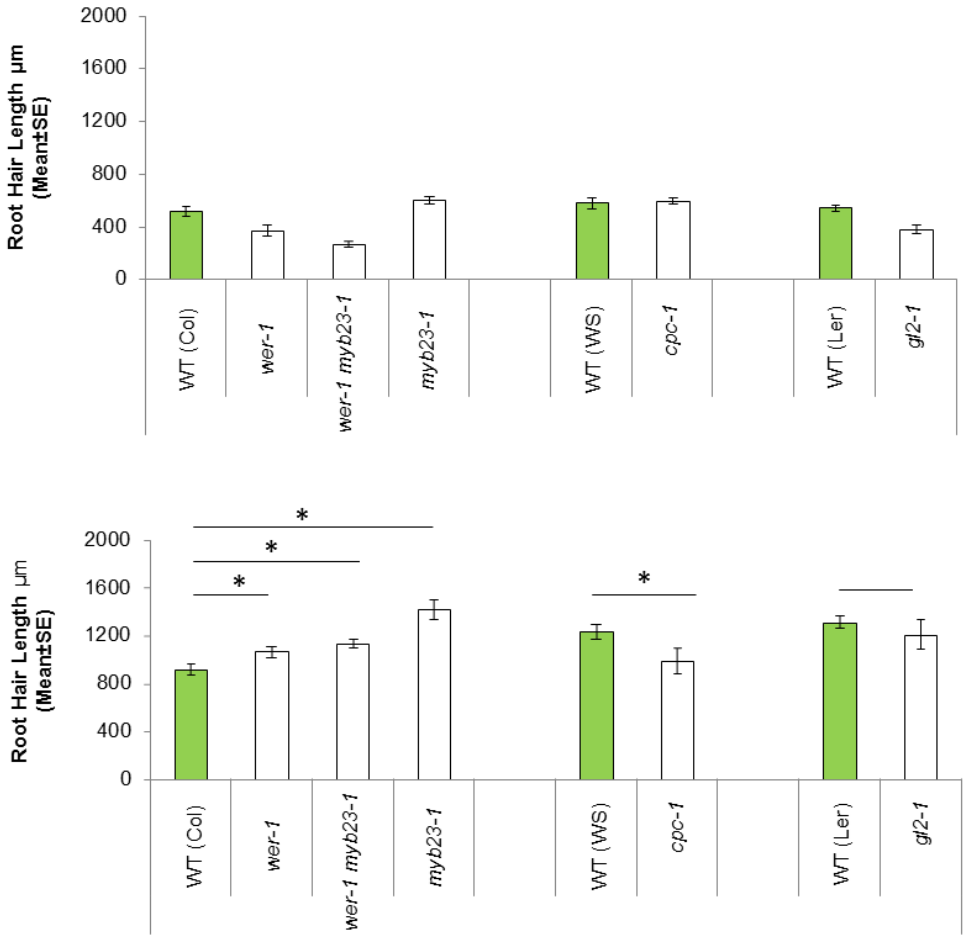

Figure 6-8: Root hair elongation in response to auxin treatment.

When treated with 0.1 µM of auxin *wer-1* and *myb23-1* elongated significantly more than the wild-type (WT) (ANOVA, P<0.005), whilst the root hairs in the *cpc-1* mutant elongated significantly less than the wild-type (T-Test, P<0.005). Previously the *gl2-1* mutant has been shown to have a population of shorter root hairs that do not elongate in response to auxin, however with 0.1 µM IAA treatment the average root hair length is not considered to be significantly different to the wild-type, although a broader standard error value was observed. * Indicate significant differences between mutant and wild-type lines after treatment with 0.1 µM IAA. Error bars represent standard error values.

all of the affected backgrounds. In 2009 Kang *et al* confirmed that whilst *WER* levels are significantly reduced in the *wer-1* mutant they were not significantly changed in the *myb23-1* single mutant, thus indicating that *WER* expression is unlikely to be affecting root hair elongation in this instance. However in both the *wer-1* and *myb23-1* backgrounds, they found that the *MYB23* transcript level was significantly reduced. In addition to that, in the *cpc-1* mutant, where the root hairs elongate significantly less than the wild-type, the *MYB23* transcript level is 156% of that observed in the wild-type (Kang *et al*., 2009). These data indicated a potential role for *MYB23* in root hair elongation in response to auxin treatment; a hypothesis further strengthened by previous results showing that auxin down-regulation of *MYB23* has a significant role in root hair initiation.

6.4.1 Does blocking down-regulation of MYB23 by auxin have an impact on root hair elongation?

Using the *pWER::MYB23* construct in the *wer-1* line, originally published and kindly supplied by Professor John Schiefelbein (Table 2-1), the effect of blocking the auxin transcriptional down-regulation of *MYB23* could be examined (Figure 6-9). The microarray data analysed before this project, indicated that auxin's effect on *WER* expression is minimal (Supplementary Data Figure 9-5). Therefore by driving *MYB23* from the *WER* promoter some of auxin's repression of *MYB23* expression was removed. Confirmation that the protein was functional came from the rescue of the *wer-1* hairy root phenotype, a result that had been previously reported (Kang *et al*, 2009).

When the auxin repression of *MYB23* transcription was reduced, root hair elongation in response to auxin was significantly reduced in comparison to the wild-type *Arabidopsis* line Colombia (ANOVA, $P<0.005$) (Figure 6-9). Without auxin treatment there was

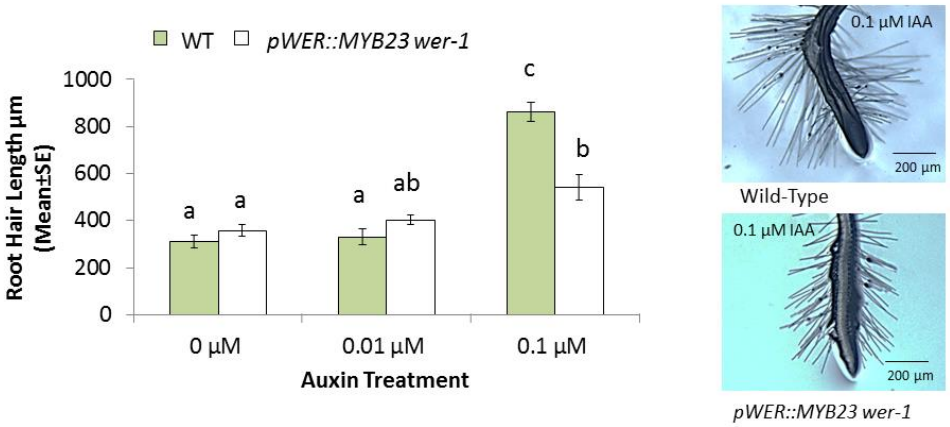

Figure 6-9: Analysis of the *pWER::MYB23 wer-1* construct.

Driving the MYB23 protein from the *WER* promoter blocks the down-regulation of *MYB23* by auxin. Under these conditions root hairs in the *pWER::MYB23, wer-1* line were still able to elongate significantly (ANOVA, $P<0.005$) compared to root hairs with no auxin treatment but this elongation was significantly less (ANOVA, $P<0.005$) than the wild-type. Photographs: Sharpened 50%, Contrast -40%. Error bars represent standard error values. Scale bars are labelled accordingly. Different letters indicate a significant difference between data sets.

no significant difference in root hair length between the mutant line and the wild-type. Although these results were consistent with the hypothesis that the auxin down-regulation of *MYB23* may be affecting root hair elongation, a further possibility with this line was that by driving *MYB23* from the *WER* promoter it was being expressed in the hair cells at a much higher level than it usually would. Given that MYB23 is known to promote the non-hair cell fate, this ectopic expression of *MYB23* in the hair cells, may be affecting root hair growth in general, rather than by blocking any auxin mediated down-regulation.

6.4.2 Is the ectopic expression of MYB23 in the hair cells affecting root hair elongation in response to auxin?

In order to establish if blocking the auxin down-regulation of *MYB23,* or the ectopic expression of *MYB23* in the hair cells, was responsible for the reduced root hair elongation response, two new constructs were produced, *pEXP7::MYB23* and *pCOBL9::MYB23 (*Figure 6-10*).* The *EXPANSIN7 (EXP7)* and *COBRA LIKE 9 (COBL9)* promoters were chosen because of their specific expression in the hair cells of the root epidermis (Cho, 2002; Jones *et al*., 2006; Schiefelbein *et al*., 2009). In addition to this whilst *COBL9* is down-regulated by auxin treatment, *EXP7* is up-regulated (Supplementary Data Figure 9-5). This experiment addressed three questions. Firstly does ectopic expression of *MYB23* in the hair cells affect root hair growth? Secondly if *MYB23* is up-regulated by auxin how does this affect root hair elongation? Finally if *MYB23* is down-regulated by auxin how does this affect root hair elongation?

With no auxin treatment the root hairs in both the *pEXP7::MYB23* and *pCOBL9::MYB23* lines are significantly shorter (ANOVA, $P<0.005$) than those observed in the wild-type (Figure 6-10 A/B). This was observed consistently across multiple homozygote lines selected for both constructs. This result is

consistent with ectopic expression of *MYB23* in the hair cells resulting in reduced root hair growth.

Furthermore when the *pEXP7::MYB23* line was treated with auxin, therefore up-regulating the *MYB23* transcription, the root hairs did elongate significantly more compared to untreated plants, but they were still significantly shorter than the root hairs observed in the wild-type. In comparison to this when the *pCOBL9::MYB23* line was treated with auxin and therefore MYB23 expression was down-regulated, the root hairs elongated to a length that was not significantly different to the wild-type (Figure 6-10 B). These results were consistent with auxin down-regulation of *MYB23* playing a role in root hair elongation in response to auxin.

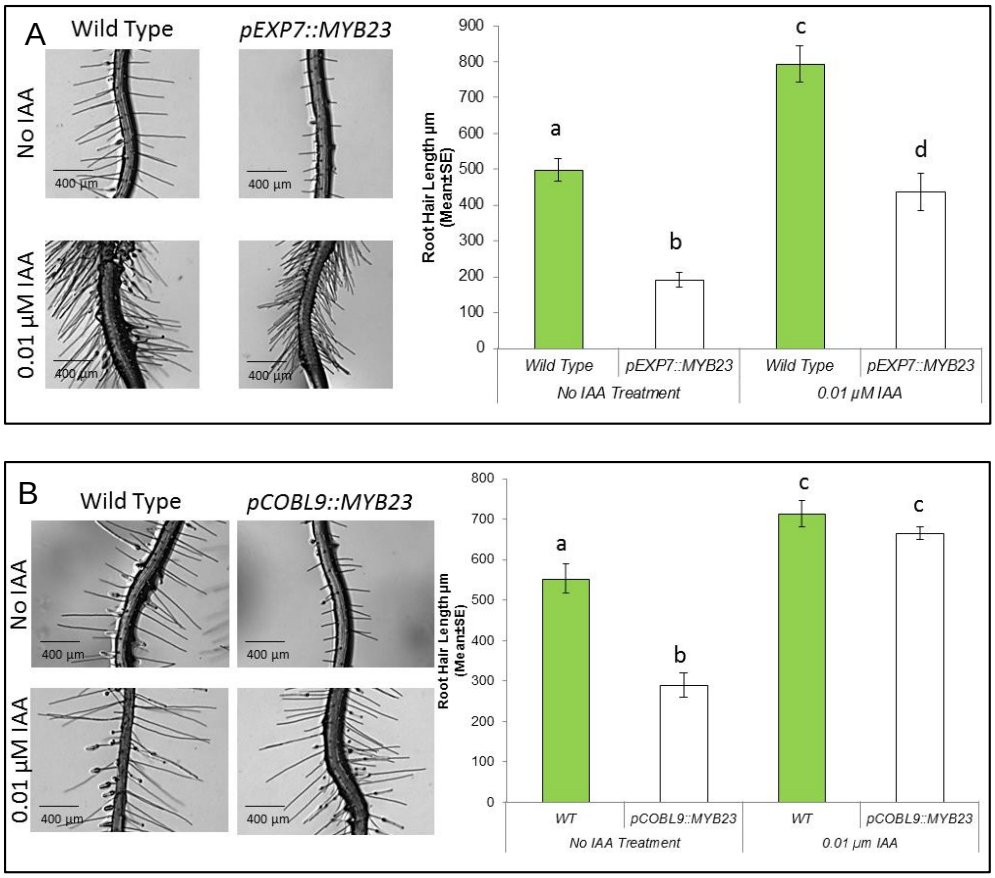

Figure 6-10: Root hair phenotypes in the *pCOBL9::MYB23* and *pEXP7::MYB23* constructs.

A: Without auxin treatment root hairs in the *pEXP7::MYB23* line are significantly shorter (ANOVA, P<0.005) than the wild-type. Although the root hairs in the *pEXP7::MYB23* lines do elongate in response to auxin treatment, they are still signifiantly shorter than the wild-type (ANOVA, P<0.005). B: Without auxin treatment root hairs in the *pCOBL9::MYB23* line are significantly shorter (ANOVA, P<0.005) than the wild-type. When treated with auxin the root hairs in the *pCOBL9::MYB23* lines elongate to a length that is not signifiantly different to the wild-type (ANOVA, P<0.005). Different letters indicate a significance difference between data sets. Photographs: Sharpened 50%, Brightness +20%. Error bars represent standard error values. Scale bars are labelled accordingly.

6.5 Discussion

Analysis of the *pGL2::GFP* marker in the *myb23-1* mutant background indicated that *GL2* and *MYB23* are down-regulated by auxin independently of one another. Whilst this down-regulation was insufficient to result in increased root hair production in the *cpc-1* or *cpc-1 try-82* mutants, a significant increase in root hair density was observed in the *gl2-1* mutant. Published data indicates that in the *cpc-1* mutant background the *MYB23* transcript level may be as high as 156% of that observed in the wild-type, potentially indicating why an increase in root hair production in this mutant was not observed (Kang *et al.*, 2009).

6.5.1 The role of MYB23 on root hair initiation

The hypothesis that the down-regulation of *MYB23* is playing a role in root hair initiation is consistent with a number of published results. The small but significant increase in root hair density observed in the *gl2*-1 mutant when treated with auxin was consistent with the small but significant increase in ectopic root hairs observed in a *myb23-1* mutant (Kang *et al.*, 2009). In addition to this whilst the *cpc-1* mutant has around 21% of the hairs observed in a wild-type line, in the *cpc-1 myb23-1* double mutant root hair initiation is partially rescued, with the phenotype developing 40% of the hairs observed in the wild-type (Kang *et al*., 2009).

Two dominant negative forms of *MYB23*, which utilise the modified repressor domain of *SUPERMAN (SRDX; LDLDLELRLGFA)* in frame to the 3' end of the *MYB23* coding region: *pMYB23::MYB23SRDX* produced by Kang *et al.*, 2009 and *p35S::MYB23SRDX* produced by Matsui *et al*., 2005, both resulted in root hairs being produced from all of the epidermal cells. Interestingly expression of *MYB23* from the cauliflower mosaic virus (CaMV) 35S promoter, which is published to result in expression of the associated gene everywhere, resulted in little change in root hair density in comparison to the wild-type, indicating that

potentially the location of *MYB23* expression may not play an important role in root hair initiation (Kirik *et al*., 2001; Kang et al., 2009). This was further supported by subsequent analysis of the *pEXP7::MYB23* line, which promoted up to a 30 fold increase in *MYB23* expression in the hair cells, but did not result in a significant change in root hair density in comparison to the wild-type (Supplementary Data Figure 9-8).

6.5.2 Root hair elongation

Some of the epidermal patterning mutants had root hairs that elongated significantly more, or significantly less than the wild-type. Whilst *wer-1* and *myb23-1* elongated significantly more in response to auxin treatment, *cpc-1* and a population of root hairs in the *gl2-1* mutant elongated significantly less. When auxin down-regulation of *MYB23* was blocked in the *pWER::MYB23 wer-1* line, root hair elongation in response to auxin treatment was significantly reduced.

The results discussed during this chapter were consistent with several hypotheses; firstly that auxin down-regulation of *MYB23* has the potential to play a role in both root hair initiation and elongation. Root hair elongation in response to auxin treatment was significantly reduced in both the *pWER::MYB23 wer-1* line*,* which is not down regulated by auxin, and the *pEXP7::MYB23* line*,* which is up-regulated by auxin. In addition to this root hair elongation in response to auxin treatment was strong in the *pCOBL9::MYB23* line, whose promoter induces down-regulation of *MYB23* by auxin. Secondly these results indicated that the ectopic expression of *MYB23* in the hair cells does not have a significant impact on root hair initiation, but does result in significantly shorter root hairs in comparison to the wild-type with no auxin treatment.

Interestingly these shorter root hairs were not observed in the *pWER::MYB23 wer-1* line. This could be due to the fact that in the hair cells *WER* expression is

subject to significant inhibition from the cortex layer via *SCM*. In comparison both *COBL9* and *EXP7* are actively promoted in the hair cells. Therefore *MYB23* expression may be much higher in the hair cells in these two constructs. If this is the case it is interesting that the *pWER::MYB23 wer-1* line still has significantly reduced root hair elongation in response to auxin treatment in the hair cells, even if potentially it is not expressed there. Indicating that *MYB23* may mediate this response from the non-hair cells position, maybe via promotion or inhibition of a component that can travel between the two cells types? Considering the results discussed in previous chapters a potential candidate for this may be ARF10.

6.5.3 The role of MYB23 on root hair elongation

In order to assess if loss of *MYB23* expression alone was sufficient to restore root hair elongation in the mutants where a significant reduction in elongation in response to auxin treatment occurred, single mutants were crossed to create the *cpc-1 myb23-1* and *gl2-1 myb23-1* double mutants.

Analysis of the double *cpc-1 myb23-1* mutant indicated that although the root hair density was partially rescued, a result consistent with data previously published by Kang *et al*, 2009, the root hair elongation in response to auxin treatment was not (Figure 6-11). Analysis of the *gl2-1 myb23-1* double mutant indicated that the distinct population of short root hairs observed in the *gl2-1* single mutant was lost (Figure 6-12). In addition to this all of the root hairs in the *gl2-1 myb23-1* double mutant were able to elongate normally, with no significant difference from the wild-type in response to auxin treatment. These results indicated that removing *MYB23* expression alone was insufficient to fully rescue the reduced root hair elongation in response to auxin treatment phenotype.

The results presented during this chapter have indicated a role for auxin mediated regulation of *MYB23* expression in both root hair initiation and elongation.

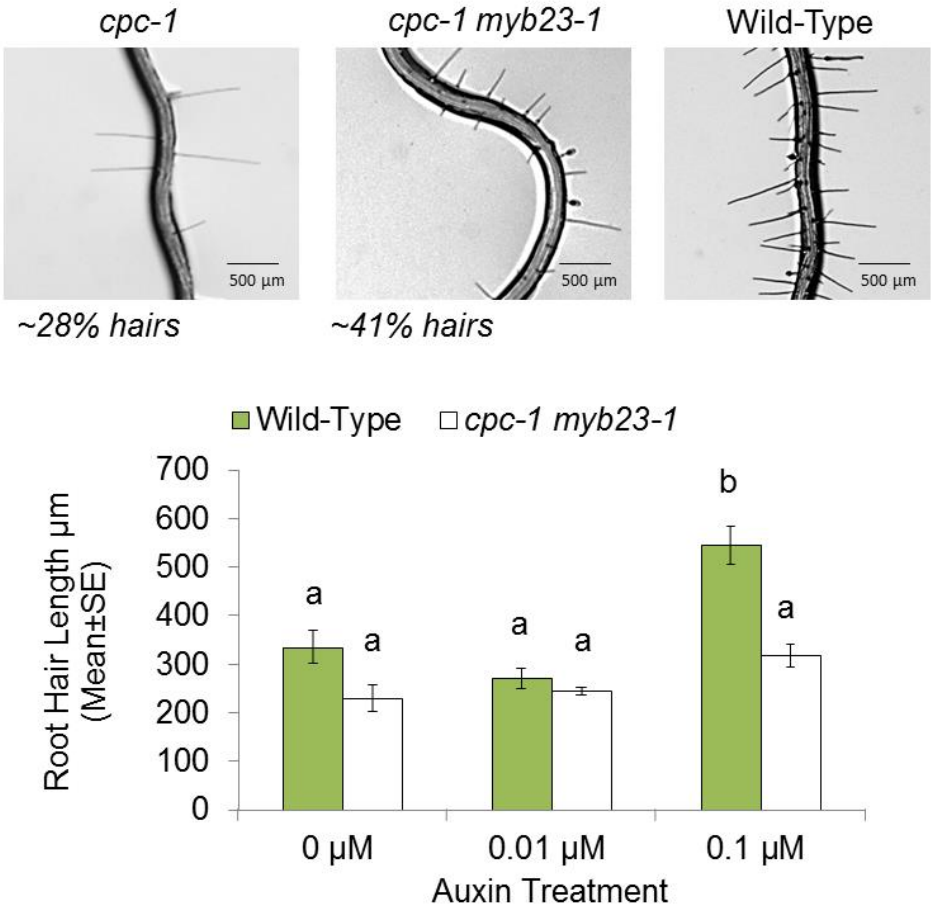

Figure 6-11: Analysis of the *cpc-1 myb23-1* double mutant.

The *cpc-1 myb23-1* mutant partially rescues the single *cpc-1* hair loss phenotype. However it does not rescue the reduced root hair elongation in response to auxin treatment. Photographs: Sharpened 50%, Brightness +20%, Contrast +20%. Error bars represent standard error values. Different letters indicate a significant difference between data sets (ANOVA, $P<0.005$). Scale bars are labelled accordingly.

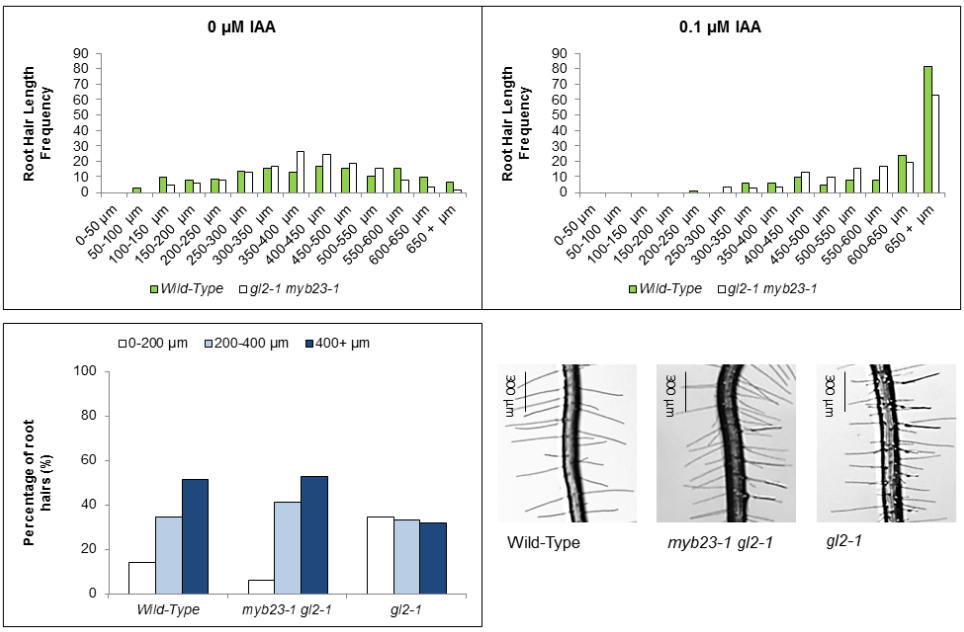

Figure 6-12: Analysis of root hair length in the *gl2-1 myb23-1* double mutant.

Unlike the *gl2-1* single mutant (Figure 3-6), the *gl2-1 myb23-1* double mutant does not possess a population of shorter root hairs that do not elongate as much as the wild-type in response to auxin. In addition to this the *gl2-1 myb23-1* double mutant does not have significantly more shorter root hairs than the wild-type. Photographs: Sharpened 50%, Brightness +20%, Contrast +20%. Scale bars are labelled accordingly.

7 : General Discussion

During this project the root epidermis of the model species Arabidopsis was used to develop our understanding of auxin's role in the developmental patterning and growth of root hairs. According to data published before this project began, the epidermal patterning mechanism and the auxin response network were seen as two independent components of development (Masucci and Schiefelbein, 1996). However the data presented in this thesis have shown that the transcription factor networks mediating epidermal patterning and auxin response interact at multiple levels (Figure 7-1).

7.1.1 The functional significance of the repressive auxin response regime in the non-hair cells

Research carried out in the Kepinski lab before this project began introduced the concept of a differential auxin response between the hair and non-hair cells of the root epidermis, with differentiating hair cells having a greater inherent capacity to respond to auxin. This contrasts with published data highlighting differential auxin transport between the hair and non-hair files of the root epidermis, which suggested auxin response was higher in the meristematic non-hair cells (Jones *et al.*, 2009). Here, the identification and detailed analysis of *ARF10* and *IAA17* expression patterns revealed an apparent repressive auxin response regime in non-hair cells, which is consistent with the data on auxin responsiveness from both Jones *et al.*, 2009 and the Kepinski lab.

Investigation of the functional significance of this repressive auxin response regime in the non-hair cells was carried out using the *gl2-1* loss of function mutant (Koornneef, 1981; Ohashi *et al*., 2003). The concept of auxin and the root epidermal patterning mechanism working together was first considered by Masucci *et al* in 1996. Their paper concluded that auxin response and the epidermal patterning mechanism were two independent aspects of plant growth, and that auxin acts downstream of the non-hair promoting component *GL2* (Masucci and Schiefelbein, 1996). A combination of background data and data

collected during this project has indicated that this view is too simplistic. In order to clarify the relationship between these two mechanisms and place the spatial control of auxin response in the current knowledge of the epidermal patterning mechanism, the auxin response marker lines were crossed with several epidermal patterning mutants. By crossing the *gl2-1* mutant with auxin response markers it was possible to confirm that the repressive auxin response regime was still functional in the non-hair cells, despite up to 50% of them producing root hairs (Masucci *et al*., 1996). Subsequent root hair analysis indicated that the *gl2-1* mutant had significantly more shorter root hairs, and these shorter root hairs were those produced by the non-hair cells (Figure 3-3). Treatment with the synthetic auxin NAA and the naturally occurring auxin IAA, showed that the *gl2-1* mutant also had a population of root hairs that were less responsive to auxin, (Figure 3-5). These results were consistent with the repressive auxin response regime in the non-hair cells functioning as part of the mechanism that restricts root hair growth. This result was further corroborated by the analysis of the *gl2-1 arf10-3 arf16-2* triple mutant (Figure 3-8). The disruption of these key repressing ARFs in conjunction with the *gl2-1* mutation, resulted in all of the root hairs elongating, without auxin treatment, to a length that was not significantly different from the wild-type. In addition to this all of the root hairs elongated significantly in response to auxin treatment.

When considering these results it was important to keep in mind the *arf10-3 arf16-2* double mutant phenotype. The double mutant is severely agravitropic and the root tip is misshaped, therefore analysis of these mutants on media is challenging (Wang *et al*., 2005). In addition to this analysis of the *pGL2::GFP arf10-3 arf16-2* line (Figure 5-10) highlighted that the hair and non-hair patterning of the epidermal cells is disrupted. Another important factor to consider is that the *gl2-1 arf10-3 arf16-2* triple mutant produces significantly fewer root hairs than the *gl2-1* single mutant (Supplementary Data Figure 9-7 B). It is therefore possible that the excessive short root hair production in this background was lost because in the triple mutant there is less ectopic root hair production overall. Although the triple mutant does have significantly fewer

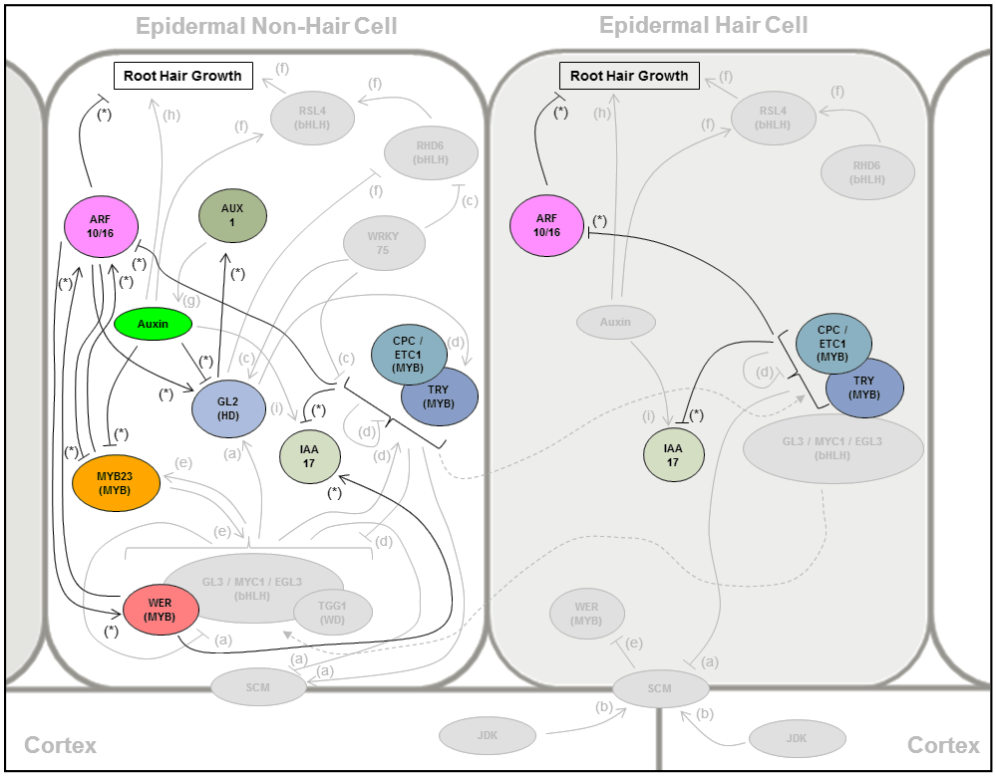

Figure 7-1: A summary of the interactions identified between the epidermal patterning mechanism and the auxin response network during this project.

Solid lines indicate promotion (arrow head) or inhibition (flat head), dashed lines indicate movement in the direction of the arrow head. Letters next to the arrows indicate the published source of the interaction. (a) (Kwak and Schiefelbein, 2008) (b) (Hassan et al., 2010) (c) (Rishmawi et al., 2014) (d) (Simon et al., 2007) (e) (Kang et al., 2009) (f) (Yi et al., 2010) (g) (Jones et al., 2009) (h) (Masucci and Schiefelbein, 1996) (i) Tromas and Perrot-Rechenmann 2010. (*) indicates interactions identified during this project.

ectopic root hairs than *gl2-1,* it still has significantly more than both the wild-type and the *arf10-3 arf16-2* double mutant (Supplementary Data Figure 9-7 A). Whilst these data indicate that the triple mutant is still producing ectopic root hairs, the fact that the epidermal patterning is disrupted, means that although root hairs may appear ectopic, i.e produced in a non-hair cell position, the cell identity may be essentially 'hair' in terms of all but position. In order to clarify the hair cell identity under these circumstances the use of a marker like *pGL2::GFP* would be informative. Unfortunately in an *arf10-3 arf16-2* mutant background the expression of this marker is significantly reduced (Figure 5-10), therefore although visualisation on the confocal microscope is possible, analysis with the GFP microscope suitable for collecting root hair data would be very challenging.

With regards to the repressive auxin response regime functioning as part of the mechanism that inhibits root hair growth, the results presented in Chapter 3 were consistent with this hypothesis. Considered alone data from the *gl2-1 arf10-3 arf16-2* triple mutant could not reliably indicate a role for the repressing auxin response regime in root hair growth. However, when considered in conjunction with additional data detailed in subsequent chapters, for example, the significant decrease in root hair elongation in response to auxin in mutants with more *ARF10* present (Figure 6-8), and the lack of root hair elongation when *ARF10* is expressed ectopically in the hair cells (Supplementary Data Figure 9-6), a strong argument for the repressing ARFs playing an important role in root hair growth repression in the non-hair cells is evident. Potential for the repressing auxin response regime functioning in parallel to *GL2* is also apparent.

7.1.2 Spatial control of auxin response in the epidermal patterning mechanism

To analyse further the position of the auxin response repression regime in relation to the epidermal patterning mechanism, several auxin response maker lines were crossed into epidermal patterning mutants.

Crossing epidermal patterning mutants with the *pDR5::GFP* marker gave an indication of auxin signalling output, (Figure 4-18). In the wild-type the *pDR5::GFP* expression pattern initially begins stronger in the non-hair files, at the transition zone the fluorescence level evens out across all of the files and then persists with greater strength in the hair files. In mutants where all or none of the cells produced root hairs, all of the files adopted either the hair or non-hair wild-type *pDR5::GFP* pattern. These results initially appeared to be consistent with auxin response being patterned by a file being either a hair or non-hair file, dictated by if they did or did not produce root hairs. However as was discussed in Chapter 3, in the *gl2-1* mutant, which produces root hairs from approximately 50% of it's non-hair cells, the expression pattern of *pDR5::GFP* remains unchanged (Figure 3-2). This was also true of the *myb23-1* background discussed in Chapter 4 (Figure 4-10). This indicates that the production of a root hair does not alter the overall auxin response of a cell or file. Expression of *pDR5::GFP* in the *cpc-1* mutant was also interesting, although all of the files adopted the wild-type non-hair file *pDR5::GFP* expression pattern, this line retains distinct hair files which produce root hairs. Indicating an apparent uncoupling of *DR5* patterning and root hair production.

A range of expression patterns were also observed when the transcriptional and translational *IAA17* markers were crossed into the same epidermal patterning mutants. In summary, the expression of *IAA17* in these backgrounds mirrored the changes observed in the *pDR5::GFP* marker. The mutants producing all hair or all non-hair cells lost the differential start point of *IAA17* expression, and expression began in all of the files at a point either corresponding to the wild-type hair or non-hair file position, (Figure 4-19). Expression in *myb23-1* and *gl2-1* again did not differ significantly from the wild-type or control lines, but a slight variability in the starting position of *IAA17* expression was observed in the *cpc-1*

mutant. These results were consistent with *WER* promoting the early expression of *IAA17* in the root epidermal cell files, and *CPC* and *TRY* inhibiting it.

Analysis of the *ARF10* transcriptional and translational markers in these epidermal patterning mutants indicated that *ARF10* expression was almost completely lost in mutants with all hair cells, and expressed in all of the epidermal cells in mutants with no hair cells, (Figure 4-20). In the *gl2-1* mutant the expression did not differ significantly from the wild-type, and although *ARF10* was expressed in all of the cells in the *cpc-1* mutant, the expression level was variable between cells. One of the most interesting results from this marker was the cross with the *myb23-1* mutant, which indicated a significant reduction in *ARF10* expression in this background, (Figure 4-12). These results were consistent with *ARF10* expression being promoted by *WER* and *MYB23,* and inhibited by *CPC* and *TRY.*

Analysis of these markers in the *myb23-1* and *cpc*-1 mutant backgrounds indicated that expression of repressive auxin response components like *ARF10*, could be up or down-regulated in the root epidermis without a switch in cell identity. However results discussed subsequently in Chapter 6 highlighted that this does have an impact on root hair elongation.

Quantification of the epidermal cell size in all of the epidermal mutant backgrounds, indicated that the ratio of hair to non-hair cell size did not differ significantly from the wild-type (Figure 4-21). Therefore the patterning of auxin response in the root epidermis is likely to be independent of both cell size and of if a cell does or does not produce a root hair.

The results from these crosses were consistent with auxin response, specifically the expression of *IAA17* and *ARF10,* being patterned upstream of the epidermal patterning component *GL2,* but downstream of *WER* and *CPC. WER*, which

promotes the non-hair cell identity, also promotes the repressive auxin response regime in the root epidermis. As *WER* is primarily expressed in the non-hair files, this is consistent with the repressive auxin response regime also being present there. Conversely *CPC* and *TRY*, which promote the hair cell identity, inhibit the expression of the repressive auxin response components like *IAA17* and *ARF10*. Mutants with the more intermediate phenotypes indicated that the relationship between auxin response and epidermal cell type can be complex, and that the production of hairs from cells at non-hair positions is not always accompanied by a reduction in auxin response repression at that location and *vice versa*.

7.1.3 Feedback loops and direct links between the epidermal patterning mechanism and the auxin response network

Positive and negative feedback loops are common in both the epidermal patterning mechanism and the auxin response network. For example, the expression of the activating ARF, *ARF19*, is itself up-regulated by auxin while the auxin-induced expression of Aux/IAA repressor proteins creates a negative feedback loop thereby enforcing tight regulation of auxin-induced gene expression (Tromas and Perrot-Rechenmann, 2010; Kieffer *et al*., 2010). Within the epidermal patterning mechanism *MYB23* promotes the expression of *CPC,* whilst *CPC* inhibits the expression of *MYB23* (Kang *et al*., 2009). *MYB23* also promotes the expression of itself and *WER*, thereby forming two positive feedback loops (Kang *et al*., 2009).

In order to establish if feedback regulation exists between the epidermal patterning mechanism and the auxin response network, GFP markers for *WER* and *GL2* were crossed into the *arf10-3 arf16-2* double mutant, (Figure 5-9 / 5-10). These crosses indicated that in this background both *WER* and *GL2* expression was significantly reduced, a result which implies that *ARF10* and/or

ARF16 may be promoting the expression of *WER* and *GL2.* Whilst this interaction, taken in conjunction with the *wer-1 pARF10-GFP* cross result discussed in Chapter 4 (Figure 4-1) was consistent with a positive feedback loop existing between *ARF10* and *WER,* the relationship between *ARF10* and *GL2* was more unexpected, as relationships identified previously had all occurred upstream of *GL2.*

The interactions initially identified in these genetic experiments were later confirmed by a RT-qPCR analysis of *GL2* and *WER* expression in the *arf10-3 arf16-2* double mutant carried out with Dr Martin Kieffer (Supplementary Data Figure 9-5). This experiment also revealed a possible negative feedback loop between *ARF10*, *ARF16* and *MYB23.* A result that will be investigated further upon completion of a *pMYB23::MYB23-GFP* marker line, by introducing it in the *arf10-3 arf16-2* background.

Taken together with the genetic data presented in Chapter 4, the results reported in Chapter 5 support the idea that feedback loops between the auxin response network and the epidermal patterning mechanism might contribute to the control for developmental patterning and auxin response in the root epidermis. In order to establish if this control was achieved via direct interactions between the auxin response network and epidermal patterning mechanism components, ChIP and promoter truncation analysis was carried out. Initially ChIP analysis was carried out using the *pWER::WER-GFP* translational marker, to see if WER bound directly to any of the potential MYB binding sites identified in the *ARF10* promoter. This assay was unable to detect any promoter binding activity, (Figure 5-5). There were several potential reasons this may have occurred. Firstly, there is the possibility that WER does not bind directly to the *ARF10* promoter. Secondly, since the *GL2* positive control did not show enrichment following *pWER::WER:GFP* ChIP, it is possible that there were technical problems with the assay or else, the published data about the MYB binding sites in the *GL2* promoter may be incorrect. Thirdly, it is also possible that assays were focused on the wrong region of the *ARF10* promoter. Subsequent analysis of a number of

different ARF10 promoter truncation lines indicated that the first 710 base pairs in the promoter region were sufficient to drive expression of *ARF10* in the root epidermis, (Figure 5-6) the majority of the ChIP assays were focused upstream of this region. Finally, it is also possible that MYB23 binds to some of the identified MYB binding sites while WER does not. In order to test this interaction the *pMYB23::MYB23-GFP* marker was also produced during this project. Unfortunately a reliable homozygote line was not generated before the submission of this thesis, however ChIP analysis will be performed as soon as sufficient homozygous seed is obtained.

Analysis of the *myb23-1 pARF10::GFP* cross in Chapter 4 indicated that *MYB23* may promote the expression of *ARF10,* and the RT-qPCR data indicated that *ARF10* and/or *ARF16* may inhibit the expression of *MYB23.* Therefore the *MYB23* promoter was analysed for potential AuxREs and ChIP analysis was carried out using the *pARF10::ARF10-GFP* translational marker. As with the previous ChIP assays there was no evidence of direct promoter binding, (Figure 5-12) indicating that the ChIP assay may not be functioning correctly or *ARF10* may regulate the expression of *MYB23* indirectly. A number of results support this latter hypothesis: the disruption of the hair and non-hair cell epidermal patterning in the *arf10-3 arf16-2* double mutant, may result in the function of other epidermal patterning components that would usually repress *MYB23* expression, like *CPC*, being disrupted. Further support for this hypothesis is evident in the *cpc-1* mutant, where strong *ARF10* expression was observed in every epidermal cell, (Figure 4-13) however there is also a significant increase in *MYB23* transcript levels (Kang *et al*., 2009). Thus indicating that CPC is likely to be regulating *MYB23* expression independently of ARF10*,* and potentially more significantly than *ARF10.* Another apparent paradox arises in the idea that *MYB23* might be directly regulated by a repressing ARF while also being down-regulated in response to auxin treatment (Figure 6-3). If ARF10 is binding directly to the *MYB23* promoter then this down-regulation by auxin could be achieved via an up-regulation of the repressive *ARF10,* however observations from assays during this project have not found any evidence of a regulation of *ARF10* expression by auxin.

Overall the results presented in Chapter 5 indicated that whilst positive and negative feedback loops are apparent between the epidermal patterning mechanism and the auxin response network, the specific interactions occurring in order to achieve these relationships are complex. Further clarification could be achieved via analysis of *pMYB23::MYB23-GFP* ChIP assays, production of additional promoter truncation lines within the first 710 base pair region of the *ARF10* promoter and identification of putative intermediate components that facilitate the complex relationship between *MYB23, ARF10* and auxin using yeast two hybrid studies. Whilst to some extent inconclusive, the results detailed during Chapter 5 highlighted that the complex and tight regulation observed individually within the auxin response network and the epidermal patterning mechanism extends beyond these to link these two important aspects of plant growth together.

7.1.4 Auxin mediated down-regulation of GL2 and MYB23

Analysis of the *pGL2::GFP* marker in the *myb23-1* mutant background indicated that *GL2* and *MYB23* are down-regulated by auxin independently of one another, (Figure 6-2). Results indicated that the down-regulation of *MYB23* was important for both root hair initiation and elongation.

Treatment of the *gl2-1* mutant with auxin resulted in a small but significant increase in root hair density, a result which was not observed in the *gl2-1 myb23-1* double mutant, (Figure 6-5 / 6-7). This indicates that the down-regulation of *MYB23* by auxin may play a role in root hair initiation. Published data supports the hypothesis of a role for *MYB23* in root hair initiation. In a *cpc-1 myb23-1* double mutant the reduced root hair phenotype is partially restored, and in the dominant negative *MYB23-SRDX* lines, root hairs are produced from every epidermal cell (Matsui *et al*., 2005; Kang *et al.*, 2009). Interestingly, ectopic

expression of *MYB23* in the *p35S::MYB23* and *pEXP7::MYB23* lines did not result in significant changes in root hair density in comparison to the wild-type, indicating that ectopic expression of *MYB23* does not significantly impact root hair initiation (Supplementary Data Figure 9-8), (Kirik *et al*., 2001).

Root hair elongation in response to auxin treatment was significantly reduced by expressing *MYB23* from promoters that were not down-regulated by auxin. Expressing *MYB23* ectopically in the hair cells resulted in two phenotypes. Firstly, without auxin treatment the root hairs in these constructs were significantly shorter than the wild-type, (Figure 6-10). This phenotype persisted in changing environmental conditions, such as alterations in temperature and humidity (Supplementary Data Figure 9-10). Although the root hairs were able to elongate in response to these conditions they were always significantly shorter than the wild-type. These results were consistent with *MYB23* functioning to inhibit root hair elongation in the hair cells without auxin treatment.

Secondly when treated with auxin, in lines where *MYB23* was up-regulated by auxin (*pEXP7::MYB23,)* root hair elongation was significantly less than in the wild-type, and in lines where *MYB23* was down-regulated by auxin (*pCOBL9::MYB23,)* root hair elongation did not differ significantly from the wild-type, (Figure 6-10). These results are consistent with the idea that the down-regulation of *MYB23* by auxin is playing an important role in root hair elongation in response to increased auxin levels.

Interestingly the shorter root hairs observed in both the *pEXP7::MYB23* and *pCOBL9::MYB23* constructs without auxin treatment, were not observed in the *pWER::MYB23 wer-1* line, despite the root hair elongation in response to auxin also being inhibited, (Figure 6-9). This could be due to the fact that in the hair cells *WER* expression is subject to significant inhibition from the cortex layer via *SCM*. In comparison both *COBL9* and *EXP7* are actively promoted. Therefore *MYB23* expression in the hair cells could be higher in these two constructs. If this

is the case it is interesting that the *pWER::MYB23 wer-1* line still has significantly reduced root hair elongation in response to auxin treatment in the hair cells, since it may not be expressed in these cells. This result highlighted the concept that *MYB23* may be able to mediate this reduced elongation in response to auxin treatment from the non-hair cell position, via promotion or inhibition of a component that can travel between the two cells types. Considering the results discussed in previous chapters a potential candidate for this is ARF10.

The *myb23-1, pARF10::GFP* cross discussed in Chapter 4 (Figure 4-10) indicated that MYB23 promotes the expression of *ARF10. ARF10* is a key component of the repressive auxin response regime present in the non-hair cells and results discussed in Chapter 3 indicated that this repressive auxin response regime functions as part of the mechanism that restricts root hair growth. The key indicators of this were the populations of short ectopic root hairs and less responsive to auxin root hairs, observed in the *gl2-1* mutant (Figure 3-3). This can be compared to the short root hair phenotype observed when *MYB23* was expressed ectopically in the hair cells using the *EXP7* and *COBL9* promoters. In the *gl2-1* mutant when some of the repressive auxin response regime was alleviated in the *gl2-1 arf10-3 arf16-2* triple mutant these short root hairs were lost, (Figure 3-8). The same phenotype was observed in the *gl2-1 myb23-1* double mutant (Figure 6-7), a result consistent with this potential relationship between *ARF10* and *MYB23* functioning to repress root hair growth.

In addition to *ARF10* playing a role in root hair growth without auxin treatment, in the epidermal patterning mutants, which have root hairs that elongate significantly more or less than the wild-type in response to auxin treatment, they also have a corresponding high or low level of *ARF10* expression. For example *myb23-1* elongates significantly more than the wild-type (Figure 6-8) and has significantly lower levels of ARF10 expression (Figure 4-10). Whilst *cpc-1* elongates significantly less than the wild-type (Figure 6-8) but has significantly more *ARF10* expression (Figure 4-13). In addition to this the *arf10-3 arf16-2*

mutant also has root hairs that elongate significantly more than the wild-type in response to auxin treatment (Figure 3-9).

Considered together, these results indicate that there is potential for *MYB23* and *ARF10* to be working together to regulate root hair elongation both with and without auxin treatment. However, RT-qPCR analysis has indicated that *ARF10* and *ARF16* expression are not significantly up-regulated in the *pEXP7::MYB23* construct (Supplementary Data Figure 9-11). Therefore the short root hairs observed in the *pEXP7::MYB23* and *pCOBL9::MYB23* constructs are not likely to be due to an increase in *ARF10* levels in the hair cells. This indicates that these root hair are likely to be subject to a different mechanism of regulation, in comparison to the short root hairs observed in the *gl2-1* mutant.

Overall these results demonstrate the existence of two new mechanisms of root hair growth regulation in addition the established pathway acting via *GL2.* The work presented here has highlighted the complex regulation mechanism of root hair growth upstream of *GL2* which involves members of the auxin response network. Although a simple pathway in which *MYB23* regulates root hair growth via promotion of *ARF10* must be considered, the fact that root hair elongation is not restored in the *cpc-1 myb23-1* double mutant, and without auxin treatment the *cpc-1* single mutant has root hairs that grow to a length that do not differ significantly from the wild-type despite having high *MYB23* and *ARF10* levels indicates that the regulation at work here is complex and still not fully understood.

7.2 Conclusions

The aim of this project was to define the link between developmental patterning and auxin response in the *Arabidopsis thaliana* root epidermis. The root epidermis was used as a model to understand the interaction of patterning

mechanisms, such as those that define the hair and non-hair producing epidermal cells, and auxin. Having established the presence of a putative repressive auxin response regime in the non-hair cells of the root epidermis, analysis of the *gl2-1* mutant allowed us to further understand the functional significance of this repressive response regime. Data from the *gl2-1 arf10-3 arf16-2* triple mutant, the *gl2-1 myb23-1* double mutant, and analysis of the *pCOBL9::ARF10* line, supported the hypothesis that the repressive auxin response regime in the non-hair files functions as part of the control mechanism for root hair growth. These results were consistent with *ARF10* and/or *ARF16* functioning to restrict root hair growth.

Subsequent analysis of crosses between mutants and markers for both the epidermal patterning mechanism and the auxin response network, indicated a complex relationship of promotion and inhibition between these two key components of plant growth. Positive and negative feedback loops between these two mechanisms were identified and the patterning of auxin response was placed upstream of *GL2*, with non-hair promoting components like *WER* and *MYB23* promoting and reinforcing the repressive auxin response regime present in the non-hair files.

The analysis of a potential differential auxin response between different epidermal patterning mutants, indicated a relationship between the presence of *ARF10, MYB23* and the ability of root hairs to elongate both with and without auxin treatment. This identified a previously unknown mechanism whereby auxin mediated root hair elongation, occurs to some extent via the auxin mediated down-regulation of the epidermal patterning mechanism component, *MYB23.*

The data presented during this thesis has been consistent with the relationship between the auxin response network and the epidermal patterning mechanism being much more complex than was originally thought. It has highlighted two additional potential mechanisms of control for root hair growth, via *MYB23* and

ARF10, potentially both working together and independently, in addition to the known pathway downstream of *GL2.* The fact that the *gl2-1* mutant only has 50% of its non-hair cells producing root hairs, indicates that the suppression of hair growth at the non-hair position depends upon more than the regulation of GL2 levels. The results discussed here have shed light on what is an incredibly complex, robust, and tightly regulated system of control, which almost certainly also encompass components downstream of *GL2* such as *RHD6* and *RSL4,* which are also regulated by auxin (Yi et al., 2010). In addition to this the versatility of the root epidermis in terms of response to other phytohormones, nutrients, environmental conditions and different species hasn't yet been considered, thus there is broad scope for this area of research to expand further, (Savage *et al*., 2013; Kazan, 2013; Marzec *et al*., 2014; Tominaga-Wada and Wada, 2014; Cheng *et al*., 2014; Bishopp and Bennett, 2014).

The results presented in this thesis have increased our understanding of auxin's role in the developmental patterning of the root epidermis. It is now apparent that the relationship is much more complex than the originally proposed hypothesis of auxin functioning solely downstream of *GL2* (Figure 7-2). Whilst the cell type of a root epidermal cell is patterned by components of the epidermal patterning mechanism, the results presented during this thesis have indicated that this is reinforced via interactions with members of the auxin response network. For example, the positive feedback loop between *WER* and *ARF10* promote both the non-hair cell fate and the repressive auxin response regime present in this cell type. Whilst *WER* functions to promote *GL2* thus inhibiting root hair growth, the repressive auxin response regime functions to inhibit root hair growth via *ARF10. ARF10* in turn also promotes *GL2* expression in addition to inhibiting root hair growth independently of *GL2.* This level of complexity indicates the tight regulation of root hair growth and hints at how the root epidermis may be able to achieve such a range of plasticity when responding to environmental conditions such as nutrient shortage (Farquharson, 2008).

Auxin-mediated root hair elongation functioning via the down-regulation of *MYB23* has highlighted a potentially novel role for an epidermal patterning component as a regulator of hair growth per se. In addition to this, the results presented have shed further light on the potential functions of repressing ARFs, the regulatory roles of which are still is not fully understood (Tromas and Perrot-Rechenmann, 2010; Overvoorde *et al.*, 2010; Del Bianco and Kepinski, 2011).

Published data indicated *WER* as the primary controller of the non-hair cell identity, with *GL2* functioning to inhibit the growth of root hairs after the cell fate decision had been made, and *MYB23* playing a minor role in patterning stabilisation via its positive feedback loops (Kang et al., 2009). *ARF10* hadn't been previously considered in any non-hair cell identity or root hair growth role. However the results presented during this thesis have highlighted that establishment of the non-hair cell identity is likely to occur via the parallel and co-ordinated action of *WER, MYB23, ARF10* and *GL2.* They have also indicated the potential for these components to control root hair development at different time points and possibly other developmental aspects like cell size and vacuolation.

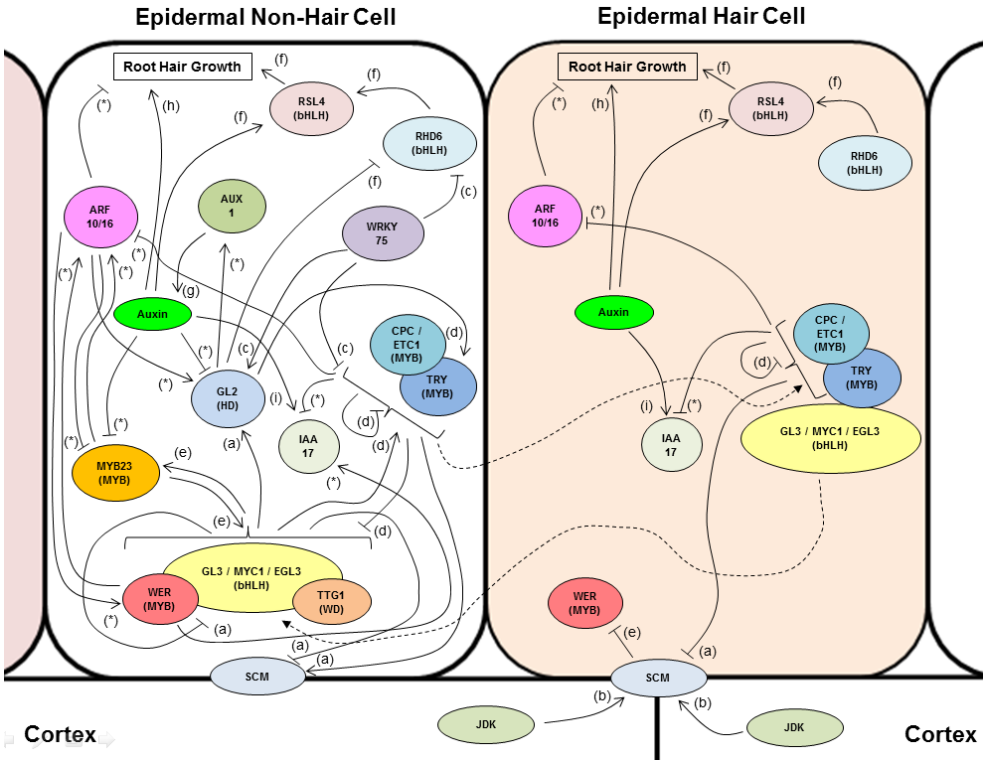

Figure 7-2: A summary of the current published knowledge of the epidermal patterning mechanism in conjunction with the additional interactions identified during this project.

The results presented during this thesis have identified multiple interactions between components of the epidermal patterning mechanism and the auxin response network. Epidermal patterning components that promote the non-hair cell fate, for example *WER* and *MYB23,* also promote the expression of repressive auxin response components such as *IAA17* and *ARF10.* Conversely components that promote the hair cell fate, like *CPC* and *TRY* inhibit the expression of *IAA17* and *ARF10.* Overall, the data presented demonstrates a much more complex relationship between these two important regulatory systems in plant growth than was previously thought. Solid lines indicate promotion (arrow head) or inhibition (flat head), dashed lines indicate movement in the direction of the arrow head. Letters next to the arrows indicate the published source of the interaction. (a) (Kwak and Schiefelbein, 2008) (b) (Hassan et al., 2010) (c) (Rishmawi et al., 2014) (d) (Simon et al., 2007) (e) (Kang et al., 2009) (f) (Yi et al., 2010) (g) (Jones et al., 2009) (h) (Masucci and Schiefelbein, 1996) (i) Tromas and Perrot-Rechenmann 2010. (*) indicates interactions identified during this project.

The impact of this work has the potential to extend beyond this specific tissue to encompass many areas of plant growth and developmental patterning, an example could be the patterning of trichome production in the shoots (Wang and Chen, 2014). In addition to this, from an agricultural prospective auxin is already widely used, a better understanding of the relationship between this phytohormone and plant growth can only be advantageous (Mithila *et al*., 2011; Brown *et al*., 2013). Further benefit can also be gained from the potential for improvement of root function, particularly in terms of nutrient uptake with the aim of reducing fertiliser input. With an ever expanding population, harvests worldwide are threatened by numerous factors. The scientific challenges in ensuring sufficient food supply are substantial, and in order to achieve this, continuing to increase our knowledge and understanding of plant growth, as has been presented here, is vital.

8 : References

Abel, S. and Theologis, A. (2010). Odyssey of auxin. *Cold Spring Harb. Perspect. Biol.* **2**, a004572.

Alarcón, M. V., Lloret, P. G. and Salguero, J. (2014). Synergistic action of auxin and ethylene on root elongation inhibition is caused by a reduction of epidermal cell length. *Plant Signal. Behav.* **9**,.

Baluska, F., Volkmann, D. and Barlow, P. W. (1996). Specialized zones of development in roots: view from the cellular level. *Plant Physiol.* **112**, 3–4.

Baluska, F., Vitha, S., Barlow, P. W. and Volkmann, D. (1997). Rearrangements of F-actin arrays in growing cells of intact maize root apex tissues: a major developmental switch occurs in the postmitotic transition region. *Eur. J. Cell Biol.* **72**, 113–21.

Baluska, F., Mancuso, S., Volkmann, D. and Barlow, P. W. (2010). Root apex transition zone: a signalling-response nexus in the root. *Trends Plant Sci.* **15**, 402–8.

Baluška, F., Kubica, S. and Hauskrecht, M. (1990). Postmitotic “isodiametric” cell growth in the maize root apex. *Planta* **181**, 269–74.

Bensmihen, S., To, A., Lambert, G., Kroj, T., Giraudat, J. and Parcy, F. (2004). Analysis of an activated ABI5 allele using a new selection method for transgenic Arabidopsis seeds. *FEBS Lett.* **561**, 127–131.

Bishopp, A. and Bennett, M. J. (2014). Hormone crosstalk: directing the flow. *Curr. Biol.* **24**, R366–8.

Brown, L. K., George, T. S., Dupuy, L. X. and White, P. J. (2013). A conceptual model of root hair ideotypes for future agricultural environments: what combination of traits should be targeted to cope with limited P availability? *Ann. Bot.* **112**, 317–30.

Bruex, A., Kainkaryam, R. M., Wieckowski, Y., Kang, Y. H., Bernhardt, C., Xia, Y., Zheng, X., Wang, J. Y., Lee, M. M., Benfey, P., et al. (2012). A gene regulatory network for root epidermis cell differentiation in Arabidopsis. *PLoS Genet.* **8**, e1002446.

Chapman, E. J. and Estelle, M. (2009). Mechanism of auxin-regulated gene expression in plants. *Annu. Rev. Genet.* **43**, 265–85.

Cheng, Y., Zhu, W., Chen, Y., Ito, S., Asami, T. and Wang, X. (2014). Brassinosteroids control root epidermal cell fate via direct regulation of a MYB-bHLH-WD40 complex by GSK3-like kinases. *Elife*.

Cho, H.-T. (2002). Regulation of Root Hair Initiation and Expansin Gene Expression in Arabidopsis. *PLANT CELL ONLINE* **14**, 3237–3253.

Cho, M., Lee, S. H. and Cho, H.-T. (2007). P-glycoprotein4 displays auxin efflux transporter-like action in Arabidopsis root hair cells and tobacco cells. *Plant Cell* **19**, 3930–43.

Costa, S. and Shaw, P. (2006). Chromatin organization and cell fate switch respond to positional information in Arabidopsis. *Nature* **439**, 493–6.

Costa, S. and Shaw, P. (2007). “Open minded” cells: how cells can change fate. *Trends Cell Biol.* **17**, 101–6.

Datta, S., Kim, C. M., Pernas, M., Pires, N. D., Proust, H., Tam, T., Vijayakumar, P. and Dolan, L. (2011). Root hairs: development, growth and evolution at the plant-soil interface. *Plant Soil* **346**, 1–14.

Del Bianco, M. and Kepinski, S. (2011). Context, specificity, and self-organization in auxin response. *Cold Spring Harb. Perspect. Biol.* **3**, a001578.

Delbarre, A. (1994). Uptake, accumulation and metabolism of auxins in tobacco leaf protoplats. *Planta* 159–167.

Dreher, K. A., Brown, J., Saw, R. E. and Callis, J. (2006). The Arabidopsis Aux/IAA protein family has diversified in degradation and auxin responsiveness. *Plant Cell* **18**, 699–714.

Eckardt, N. A. (2014). A useful model of auxin transport in the root apex. *Plant Cell* **26**, 843.

Farquharson, K. L. (2008). Phosphate-deprived roots are hypersensitive to auxin. *Plant Cell* **20**, 3183.

Finet, C., Berne-Dedieu, A., Scutt, C. P. and Marlétaz, F. (2013). Evolution of the ARF gene family in land plants: old domains, new tricks. *Mol. Biol. Evol.* **30**, 45–56.

Fischer, U., Ikeda, Y. and Grebe, M. (2007). Planar polarity of root hair positioning in Arabidopsis. *Biochem. Soc. Trans.* **35**, 149–51.

Foreman, J. (2001). Root Hairs as a Model System for Studying Plant Cell Growth. *Ann. Bot.* **88**, 1–7.

GAHOONIA, T. S. and NIELSEN, N. E. (2003). Phosphorus (P) uptake and growth of a root hairless barley mutant (bald root barley, brb) and wild type in low- and high-P soils. *Plant, Cell Environ.* **26**, 1759–1766.

Galway, M. E., Masucci, J. D., Lloyd, A. M., Walbot, V., Davis, R. W. and Schiefelbein, J. W. (1994). The TTG gene is required to specify epidermal cell fate and cell patterning in the Arabidopsis root. *Dev. Biol.* **166**, 740–54.

Goh, T., Voβ, U., Farcot, E., Bennett, M. J. and Bishopp, A. (2014). Systems biology approaches to understand the role of auxin in root growth and development. *Physiol. Plant.* **151**, 73–82.

Grebe, M., Friml, J., Swarup, R., Ljung, K., Sandberg, G., Terlou, M., Palme, K., Bennett, M. J. and Scheres, B. (2002). Cell Polarity Signaling in Arabidopsis Involves a BFA-Sensitive Auxin Influx Pathway. *Curr. Biol.* **12**, 329–334.

Grossmann, K. (2007). Auxin herbicide action: lifting the veil step by step. *Plant Signal. Behav.* **2**, 421–3.

Grotewold, E., Drummond, B. J., Bowen, B. and Peterson, T. (1994). The myb-homologous P gene controls phlobaphene pigmentation in maize floral organs by directly activating a flavonoid biosynthetic gene subset. *Cell* **76**, 543–53.

Guilfoyle, T. J. and Hagen, G. (2007). Auxin response factors. *Curr. Opin. Plant Biol.* **10**, 453–60.

Hassan, H., Scheres, B. and Blilou, I. (2010). JACKDAW controls epidermal patterning in the Arabidopsis root meristem through a non-cell-autonomous mechanism. *Development* **137**, 1523–9.

Hayashi, K.-I., Tan, X., Zheng, N., Hatate, T., Kimura, Y., Kepinski, S. and Nozaki, H. (2008). Small-molecule agonists and antagonists of F-box protein-substrate interactions in auxin perception and signaling. *Proc. Natl. Acad. Sci. U. S. A.* **105**, 5632–7.

Hayashi, K., Hasegawa, J. and Matsunaga, S. (2013). The boundary of the meristematic and elongation zones in roots: endoreduplication precedes rapid cell expansion. *Sci. Rep.* **3**, 2723.

Hiratsu, K., Matsui, K., Koyama, T. and Ohme-Takagi, M. (2003). Dominant repression of target genes by chimeric repressors that include the EAR motif, a repression domain, in Arabidopsis. *Plant J.* **34**, 733–9.

Howe, K. M. and Watson, R. J. (1991). Nucleotide preferences in sequence-specific recognition of DNA by c-myb protein. *Nucleic Acids Res.* **19**, 3913–9.

Hua, Z. and Vierstra, R. D. (2011). The cullin-RING ubiquitin-protein ligases. *Annu. Rev. Plant Biol.* **62**, 299–334.

Hülskamp, M., Misŕa, S. and Jürgens, G. (1994). Genetic dissection of trichome cell development in Arabidopsis. *Cell* **76**, 555–66.

Ichikawa, M., Hirano, T., Enami, K., Fuselier, T., Kato, N., Kwon, C., Voigt, B., Schulze-Lefert, P., Baluška, F. and Sato, M. H. (2014). Syntaxin of

Plant Proteins SYP123 and SYP132 Mediate Root Hair Tip Growth in Arabidopsis thaliana. *Plant Cell Physiol.* **55**, 790–800.

Ikeda, Y., Men, S., Fischer, U., Stepanova, A. N., Alonso, J. M., Ljung, K. and Grebe, M. (2009). Local auxin biosynthesis modulates gradient-directed planar polarity in Arabidopsis. *Nat. Cell Biol.* **11**, 731–8.

Ishida, T., Hattori, S., Sano, R., Inoue, K., Shirano, Y., Hayashi, H., Shibata, D., Sato, S., Kato, T., Tabata, S., et al. (2007). Arabidopsis TRANSPARENT TESTA GLABRA2 is directly regulated by R2R3 MYB transcription factors and is involved in regulation of GLABRA2 transcription in epidermal differentiation. *Plant Cell* **19**, 2531–43.

Ishida, T., Kurata, T., Okada, K. and Wada, T. (2008). A genetic regulatory network in the development of trichomes and root hairs. *Annu. Rev. Plant Biol.* **59**, 365–86.

Ishikawa, H. and Evans, M. L. (1995). Specialized zones of development in roots. *Plant Physiol.* **109**, 725–7.

Jones, M. A., Raymond, M. J. and Smirnoff, N. (2006). Analysis of the root-hair morphogenesis transcriptome reveals the molecular identity of six genes with roles in root-hair development in Arabidopsis. *Plant J.* **45**, 83–100.

Jones, A. R., Kramer, E. M., Knox, K., Swarup, R., Bennett, M. J., Lazarus, C. M., Leyser, H. M. O. and Grierson, C. S. (2009). Auxin transport through non-hair cells sustains root-hair development. *Nat. Cell Biol.* **11**, 78–84.

Kang, Y. H., Kirik, V., Hulskamp, M., Nam, K. H., Hagely, K., Lee, M. M. and Schiefelbein, J. (2009). The MYB23 gene provides a positive feedback loop for cell fate specification in the Arabidopsis root epidermis. *Plant Cell* **21**, 1080–94.

Kang, Y. H., Song, S.-K., Schiefelbein, J. and Lee, M. M. (2013). Nuclear trapping controls the position-dependent localization of CAPRICE in the root epidermis of Arabidopsis. *Plant Physiol.* **163**, 193–204.

Kazan, K. (2013). Auxin and the integration of environmental signals into plant root development. *Ann. Bot.* **112**, 1655–65.

Kellogg, E. A. (2001). Root hairs, trichomes and the evolution of duplicate genes. *Trends Plant Sci.* **6**, 550–2.

Kepinski, S. (2007). The anatomy of auxin perception. *Bioessays* **29**, 953–6.

Kepinski, S. and Leyser, O. (2002). Ubiquitination and auxin signaling: a degrading story. *Plant Cell* **14 Suppl**, S81–95.

Ketelaar, T. (2002). Positioning of Nuclei in Arabidopsis Root Hairs: An Actin-Regulated Process of Tip Growth. *PLANT CELL ONLINE* **14**, 2941–2955.

Ketelaar, T. (2014). Live cell imaging of Arabidopsis root hairs. *Methods Mol. Biol.* **1080**, 195–9.

Kieffer, M., Neve, J. and Kepinski, S. (2010). Defining auxin response contexts in plant development. *Curr. Opin. Plant Biol.* **13**, 12–20.

Kirik, V., Schnittger, A., Radchuk, V., Adler, K., Hülskamp, M. and Bäumlein, H. (2001). Ectopic expression of the Arabidopsis AtMYB23 gene induces differentiation of trichome cells. *Dev. Biol.* **235**, 366–77.

Kirik, V., Lee, M. M., Wester, K., Herrmann, U., Zheng, Z., Oppenheimer, D., Schiefelbein, J. and Hulskamp, M. (2005). Functional diversification of MYB23 and GL1 genes in trichome morphogenesis and initiation. *Development* **132**, 1477–85.

Kleine-Vehn, J., Ding, Z., Jones, A. R., Tasaka, M., Morita, M. T. and Friml, J. (2010). Gravity-induced PIN transcytosis for polarization of auxin fluxes in gravity-sensing root cells. *Proc. Natl. Acad. Sci. U. S. A.* **107**, 22344–9.

Knox, K., Grierson, C. S. and Leyser, O. (2003). AXR3 and SHY2 interact to regulate root hair development. *Development* **130**, 5769–77.

Koornneef, M. (1981). The complex syndrome of ttg mutants. *Arab. Inf. Serv* **18**, 45–51.

Koornneef, M., Dellaert, L. W. and van der Veen, J. H. (1982). EMS- and radiation-induced mutation frequencies at individual loci in Arabidopsis thaliana (L.) Heynh. *Mutat. Res.* **93**, 109–23.

Koshino-Kimura, Y., Wada, T., Tachibana, T., Tsugeki, R., Ishiguro, S. and Okada, K. (2005). Regulation of CAPRICE transcription by MYB proteins for root epidermis differentiation in Arabidopsis. *Plant Cell Physiol.* **46**, 817–26.

Kurata, T., Ishida, T., Kawabata-Awai, C., Noguchi, M., Hattori, S., Sano, R., Nagasaka, R., Tominaga, R., Koshino-Kimura, Y., Kato, T., et al. (2005). Cell-to-cell movement of the CAPRICE protein in Arabidopsis root epidermal cell differentiation. *Development* **132**, 5387–98.

Kwak, S.-H. and Schiefelbein, J. (2007a). The role of the SCRAMBLED receptor-like kinase in patterning the Arabidopsis root epidermis. *Dev. Biol.* **302**, 118–31.

Kwak, S.-H. and Schiefelbein, J. (2007b). The role of the SCRAMBLED receptor-like kinase in patterning the Arabidopsis root epidermis. *Dev. Biol.* **302**, 118–31.

Kwak, S.-H. and Schiefelbein, J. (2008). A feedback mechanism controlling SCRAMBLED receptor accumulation and cell-type pattern in Arabidopsis. *Curr. Biol.* **18**, 1949–54.

Lee, M. M. and Schiefelbein, J. (1999). WEREWOLF, a MYB-related protein in Arabidopsis, is a position-dependent regulator of epidermal cell patterning. *Cell* **99**, 473–83.

Leyser, H. M. O., Pickett, F. B., Dharmasiri, S. and Estelle, M. (1996). Mutations in the AXR3 gene of Arabidopsis result in altered auxin response including ectopic expression from the SAUR-AC1 promoter. *Plant J.* **10**, 403–413.

Ljung, K. (2014). Auxin - a simple compound with a profound effect on plant development. *Physiol. Plant.* **151**, 1–2.

Lokerse, A. S. and Weijers, D. (2009). Auxin enters the matrix--assembly of response machineries for specific outputs. *Curr. Opin. Plant Biol.* **12**, 520–6.

Marchant, A. and Bennett, M. J. (1998). The Arabidopsis AUX1 gene: a model system to study mRNA processing in plants. *Plant Mol. Biol.* **36**, 463–71.

Marchant, A., Kargul, J., May, S. T., Muller, P., Delbarre, A., Perrot-Rechenmann, C. and Bennett, M. J. (1999). AUX1 regulates root gravitropism in Arabidopsis by facilitating auxin uptake within root apical tissues. *EMBO J.* **18**, 2066–73.

Marzec, M., Melzer, M. and Szarejko, I. (2014). The evolutionary context of root epidermis cell patterning in grasses (Poaceae). *Plant Signal. Behav.* **9**,.

Masucci, J. D. and Schiefelbein, J. W. (1994). The rhd6 Mutation of Arabidopsis thaliana Alters Root-Hair Initiation through an Auxin- and Ethylene-Associated Process. *Plant Physiol.* **106**, 1335–1346.

Masucci, J. D. and Schiefelbein, J. W. (1996). Hormones act downstream of TTG and GL2 to promote root hair outgrowth during epidermis development in the Arabidopsis root. *Plant Cell* **8**, 1505–17.

Masucci, J. D., Rerie, W. G., Foreman, D. R., Zhang, M., Galway, M. E., Marks, M. D. and Schiefelbein, J. W. (1996). The homeobox gene GLABRA2 is required for position-dependent cell differentiation in the root epidermis of Arabidopsis thaliana. *Development* **122**, 1253–60.

Matsui, K., Hiratsu, K., Koyama, T., Tanaka, H. and Ohme-Takagi, M. (2005). A chimeric AtMYB23 repressor induces hairy roots, elongation of leaves and stems, and inhibition of the deposition of mucilage on seed coats in Arabidopsis. *Plant Cell Physiol.* **46**, 147–55.

Mithila, J., Hall, J. C., Johnson, W. G., Kelley, K. B. and Riechers, D. E. (2011). Evolution of Resistance to Auxinic Herbicides: Historical Perspectives, Mechanisms of Resistance, and Implications for Broadleaf Weed Management in Agronomic Crops. *Weed Sci.* **59**, 445–457.

Müller, B. and Bartelheimer, M. (2013). Interspecific competition in Arabidopsis thaliana: root hairs are important for competitive effect, but not for competitive response. *Plant Soil* **371**, 167–177.

Ohashi, Y., Oka, A., Rodrigues-Pousada, R., Possenti, M., Ruberti, I., Morelli, G. and Aoyama, T. (2003). Modulation of phospholipid signaling by GLABRA2 in root-hair pattern formation. *Science* **300**, 1427–30.

Ouellet, F., Overvoorde, P. J. and Theologis, A. (2001). IAA17/AXR3: biochemical insight into an auxin mutant phenotype. *Plant Cell* **13**, 829–41.

Overvoorde, P., Fukaki, H. and Beeckman, T. (2010). Auxin control of root development. *Cold Spring Harb. Perspect. Biol.* **2**, a001537.

Park, E. and Nebenführ, A. (2013). Myosin XIK of Arabidopsis thaliana accumulates at the root hair tip and is required for fast root hair growth. *PLoS One* **8**, e76745.

Peer, W. A., Jenness, M. K. and Murphy, A. S. (2014). Measure for measure: determining, inferring and guessing auxin gradients at the root tip. *Physiol. Plant.* **151**, 97–111.

Pencík, A., Simonovik, B., Petersson, S. V, Henyková, E., Simon, S., Greenham, K., Zhang, Y., Kowalczyk, M., Estelle, M., Zazímalová, E., et al. (2013). Regulation of auxin homeostasis and gradients in Arabidopsis roots through the formation of the indole-3-acetic acid catabolite 2-oxindole-3-acetic acid. *Plant Cell* **25**, 3858–70.

Péret, B., De Rybel, B., Casimiro, I., Benková, E., Swarup, R., Laplaze, L., Beeckman, T. and Bennett, M. J. (2009). Arabidopsis lateral root development: an emerging story. *Trends Plant Sci.* **14**, 399–408.

Pesch, M., Schultheiß, I., Digiuni, S., Uhrig, J. F. and Hülskamp, M. (2013). Mutual control of intracellular localisation of the patterning proteins AtMYC1, GL1 and TRY/CPC in Arabidopsis. *Development* **140**, 3456–67.

Pitts, R. J., Cernac, A. and Estelle, M. (1998). Auxin and ethylene promote root hair elongation in Arabidopsis. *Plant J.* **16**, 553–60.

Rerie, W. G., Feldmann, K. A. and Marks, M. D. (1994). The GLABRA2 gene encodes a homeo domain protein required for normal trichome development in Arabidopsis. *Genes Dev.* **8**, 1388–99.

Riechmann, J. L., Heard, J., Martin, G., Reuber, L., Jiang, C., Keddie, J., Adam, L., Pineda, O., Ratcliffe, O. J., Samaha, R. R., et al. (2000).

Arabidopsis transcription factors: genome-wide comparative analysis among eukaryotes. *Science* **290**, 2105–10.

Rishmawi, L., Pesch, M., Juengst, C., Schauss, A., Schrader, A. and Huelskamp, M. (2014). Non-cell-autonomous regulation of root hair patterning genes by WRKY75 in Arabidopsis thaliana. *PLANT Physiol.*

Robert, H. S. and Friml, J. (2009). Auxin and other signals on the move in plants. *Plant Biotechnol.* **5**, 325–332.

Roeder, A. H. K., Tarr, P. T., Tobin, C., Zhang, X., Chickarmane, V., Cunha, A. and Meyerowitz, E. M. (2011). Computational morphodynamics of plants: integrating development over space and time. *Nat. Rev. Mol. Cell Biol.* **12**, 265–73.

Rosinski, J. A. and Atchley, W. R. (1998). Molecular evolution of the Myb family of transcription factors: evidence for polyphyletic origin. *J. Mol. Evol.* **46**, 74–83.

Rouse, D. (1998). Changes in Auxin Response from Mutations in an AUX/IAA Gene. *Science (80-.).* **279**, 1371–1373.

Růzicka, K., Ljung, K., Vanneste, S., Podhorská, R., Beeckman, T., Friml, J. and Benková, E. (2007). Ethylene regulates root growth through effects on auxin biosynthesis and transport-dependent auxin distribution. *Plant Cell* **19**, 2197–212.

Ryu, K. H., Kang, Y. H., Park, Y., Hwang, I., Schiefelbein, J. and Lee, M. M. (2005). The WEREWOLF MYB protein directly regulates CAPRICE transcription during cell fate specification in the Arabidopsis root epidermis. *Development* **132**, 4765–75.

Savage, N. Saint, Walker, T., Wieckowski, Y., Schiefelbein, J., Dolan, L. and Monk, N. A. M. (2008). A mutual support mechanism through intercellular movement of CAPRICE and GLABRA3 can pattern the Arabidopsis root epidermis. *PLoS Biol.* **6**, e235.

Savage, N., Yang, T. J. W., Chen, C. Y., Lin, K.-L., Monk, N. A. M. and Schmidt, W. (2013). Positional signaling and expression of ENHANCER OF TRY AND CPC1 are tuned to increase root hair density in response to phosphate deficiency in Arabidopsis thaliana. *PLoS One* **8**, e75452.

Schellmann, S., Schnittger, A., Kirik, V., Wada, T., Okada, K., Beermann, A., Thumfahrt, J., Jürgens, G. and Hülskamp, M. (2002). TRIPTYCHON and CAPRICE mediate lateral inhibition during trichome and root hair patterning in Arabidopsis. *EMBO J.* **21**, 5036–46.

Schiefelbein, J., Kwak, S.-H., Wieckowski, Y., Barron, C. and Bruex, A. (2009). The gene regulatory network for root epidermal cell-type pattern formation in Arabidopsis. *J. Exp. Bot.* **60**, 1515–21.

Scott, A. C. and Allen, N. S. (1999). Changes in cytosolic pH within Arabidopsis root columella cells play a key role in the early signaling pathway for root gravitropism. *Plant Physiol.* **121**, 1291–8.

Seo, E., Yu, J., Ryu, K. H., Lee, M. M. and Lee, I. (2011). WEREWOLF, a Regulator of Root Hair Pattern Formation, Controls Flowering Time through the Regulation of FT mRNA Stability. *Plant Physiol.*

Simon, M., Lee, M. M., Lin, Y., Gish, L. and Schiefelbein, J. (2007). Distinct and overlapping roles of single-repeat MYB genes in root epidermal patterning. *Dev. Biol.* **311**, 566–78.

Swarup, R., Kargul, J., Marchant, A., Zadik, D., Rahman, A., Mills, R., Yemm, A., May, S., Williams, L., Millner, P., et al. (2004). Structure-function analysis of the presumptive Arabidopsis auxin permease AUX1. *Plant Cell* **16**, 3069–83.

Szemenyei, H., Hannon, M. and Long, J. A. (2008). TOPLESS mediates auxin-dependent transcriptional repression during Arabidopsis embryogenesis. *Science* **319**, 1384–6.

Tanaka, N., Kato, M., Tomioka, R., Kurata, R., Fukao, Y., Aoyama, T. and Maeshima, M. (2014). Characteristics of a root hair-less line of Arabidopsis thaliana under physiological stresses. *J. Exp. Bot.* **65**, 1497–512.

Tian, Q. and Reed, J. W. (1999). Control of auxin-regulated root development by the Arabidopsis thaliana SHY2/IAA3 gene. *Development* **126**, 711–21.

Tiwari, S. B., Wang, X. J., Hagen, G. and Guilfoyle, T. J. (2001). AUX/IAA proteins are active repressors, and their stability and activity are modulated by auxin. *Plant Cell* **13**, 2809–22.

Tiwari, S. B., Hagen, G. and Guilfoyle, T. (2003). The roles of auxin response factor domains in auxin-responsive transcription. *Plant Cell* **15**, 533–43.

Tiwari, S. B., Hagen, G. and Guilfoyle, T. J. (2004). Aux/IAA proteins contain a potent transcriptional repression domain. *Plant Cell* **16**, 533–43.

Tominaga-Wada, R. and Wada, T. (2014). Regulation of root hair cell differentiation by R3 MYB transcription factors in tomato and Arabidopsis. *Front. Plant Sci.* **5**, 91.

Tominaga-Wada, R., Nukumizu, Y., Sato, S., Kato, T., Tabata, S. and Wada, T. (2012). Functional divergence of MYB-related genes, WEREWOLF and AtMYB23 in Arabidopsis. *Biosci. Biotechnol. Biochem.* **76**, 883–7.

Tromas, A. and Perrot-Rechenmann, C. (2010). Recent progress in auxin biology. *C. R. Biol.* **333**, 297–306.

Ugartechea-Chirino, Y., Swarup, R., Swarup, K., Péret, B., Whitworth, M., Bennett, M. and Bougourd, S. (2010). The AUX1 LAX family of auxin influx carriers is required for the establishment of embryonic root cell organization in Arabidopsis thaliana. *Ann. Bot.* **105**, 277–89.

Van den Berg, C., Willemsen, V., Hage, W., Weisbeek, P. and Scheres, B. (1995). Cell fate in the Arabidopsis root meristem determined by directional signalling. *Nature* **378**, 62–5.

Wada, T., Tachibana, T., Shimura, Y. and Okada, K. (1997). Epidermal cell differentiation in Arabidopsis determined by a Myb homolog, CPC. *Science* **277**, 1113–6.

Walsh, T. A., Neal, R., Merlo, A. O., Honma, M., Hicks, G. R., Wolff, K., Matsumura, W. and Davies, J. P. (2006). Mutations in an auxin receptor homolog AFB5 and in SGT1b confer resistance to synthetic picolinate auxins and not to 2,4-dichlorophenoxyacetic acid or indole-3-acetic acid in Arabidopsis. *Plant Physiol.* **142**, 542–52.

Wang, S. and Chen, J.-G. (2014). Regulation of cell fate determination by single-repeat R3 MYB transcription factors in Arabidopsis. *Front. Plant Sci.* **5**, 133.

Wang, J.-W., Wang, L.-J., Mao, Y.-B., Cai, W.-J., Xue, H.-W. and Chen, X.-Y. (2005). Control of root cap formation by MicroRNA-targeted auxin response factors in Arabidopsis. *Plant Cell* **17**, 2204–16.

Wang, S., Kwak, S.-H., Zeng, Q., Ellis, B. E., Chen, X.-Y., Schiefelbein, J. and Chen, J.-G. (2007). TRICHOMELESS1 regulates trichome patterning by suppressing GLABRA1 in Arabidopsis. *Development* **134**, 3873–82.

Wang, S., Hubbard, L., Chang, Y., Guo, J., Schiefelbein, J. and Chen, J.-G. (2008). Comprehensive analysis of single-repeat R3 MYB proteins in epidermal cell patterning and their transcriptional regulation in Arabidopsis. *BMC Plant Biol.* **8**, 81.

Weston, K. (1992). Extension of the DNA binding consensus of the chicken c-Myb and v-Myb proteins. *Nucleic Acids Res.* **20**, 3043–9.

Williams, C. E. and Grotewold, E. (1997). Differences between plant and animal Myb domains are fundamental for DNA binding activity, and chimeric Myb domains have novel DNA binding specificities. *J. Biol. Chem.* **272**, 563–71.

Yan, X., Liao, H., Beebe, S. E., Blair, M. W. and Lynch, J. P. (2004). QTL mapping of root hair and acid exudation traits and their relationship to phosphorus uptake in common bean. *Plant Soil* **265**, 17–29.

Yi, K., Menand, B., Bell, E. and Dolan, L. (2010). A basic helix-loop-helix transcription factor controls cell growth and size in root hairs. *Nat. Genet.* **42**, 264–7.

Yu, N.-I., Lee, S. A., Lee, M.-H., Heo, J.-O., Chang, K. S. and Lim, J. (2010). Characterization of SHORT-ROOT function in the Arabidopsis root vascular system. *Mol. Cells* **30**, 113–9.

Yu, H., Moss, B. L., Jang, S. S., Prigge, M., Klavins, E., Nemhauser, J. L. and Estelle, M. (2013). Mutations in the TIR1 auxin receptor that increase affinity for auxin/indole-3-acetic acid proteins result in auxin hypersensitivity. *Plant Physiol.* **162**, 295–303.

Zhao, Q., Wu, Y., Gao, L., Ma, J., Li, C.-Y. and Xiang, C.-B. (2014). Sulfur nutrient availability regulates root elongation by affecting root IAA levels and the stem cell niche. *J. Integr. Plant Biol.*

9 : Supplementary Data

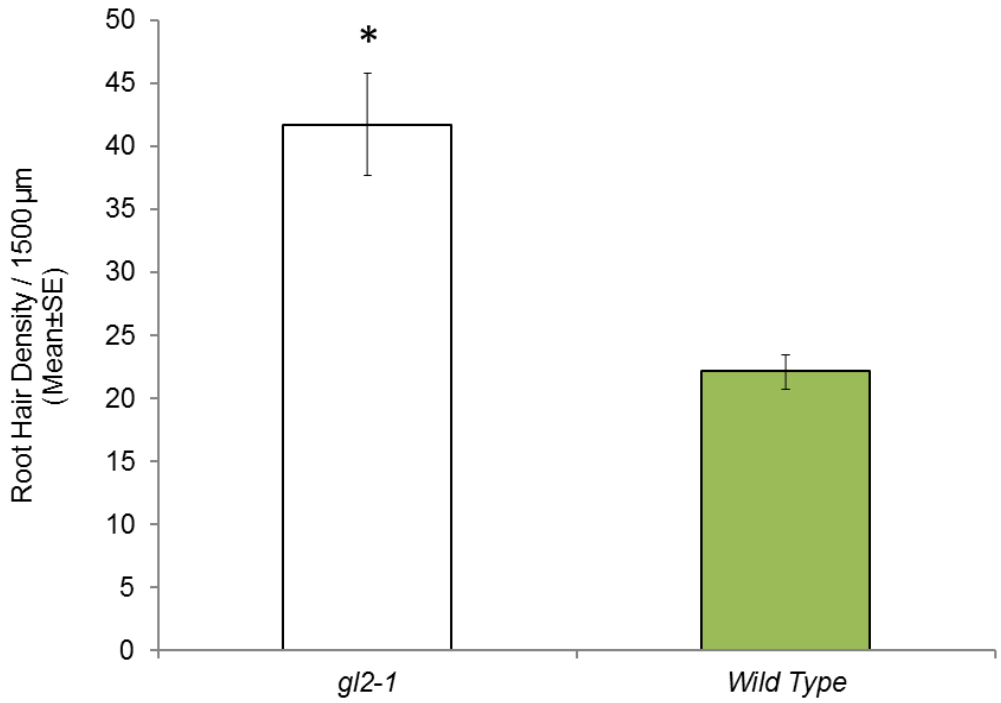

Figure 9-1: Root hair density in the *gl2-1* single mutant.

The *gl2-1* mutant has a significantly higher root hair density compared to the wild-type ($P<0.005$, T-Test).

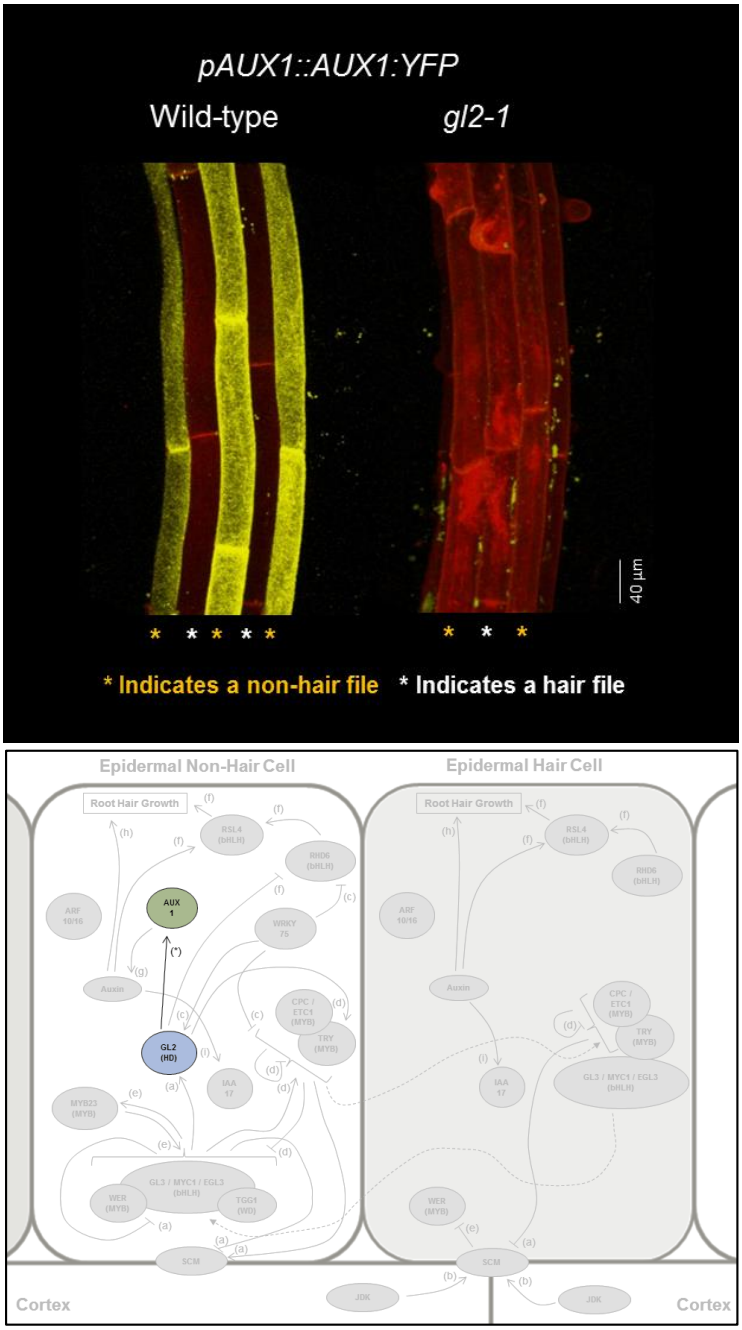

Figure 9-2: Analysis of the *pAUX1::AUX1-YFP* marker in the *gl2-1* background.

Analysis of the *pAUX1::AUX1-YFP* marker in the *gl2-1* background indicated that *AUX1* expression was lost when the *GL2* gene function was knocked out. This result was consistent with the published report of *pAUX1::AUX-YFP* expression also being lost in the *wer-1 myb23-1* double mutant, Jones et al, 2009. These results were consistent with *GL2* functioning to promote the expression of *AUX1* in the non-hair cells of the root epidermis. Data and pictures provided by Dr Martin Kieffer.

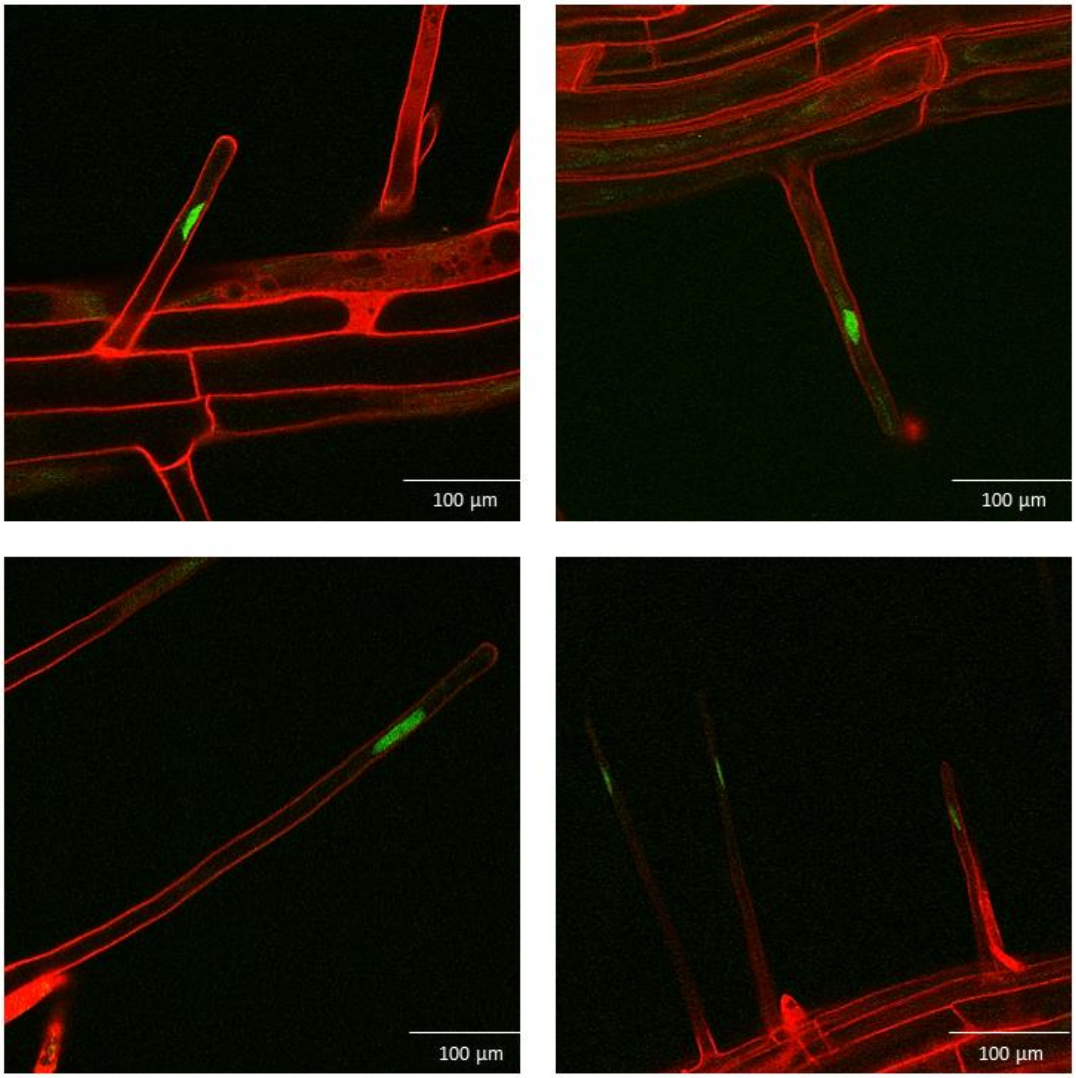

Figure 9-3: *pARF10::GFP* expression in ectopic root hairs.

Initially the *pARF10::GFP* marker was used to identify ectopic root hairs produced by the non-hair cells in the *gl2-1* mutant. However whilst these were identifiable, it could only be reliably done using the confocal microscope and by layering multiple images so the entire root hair was in focus. Therefore this was not a practical or reliable method of measuring the length of these root hairs.

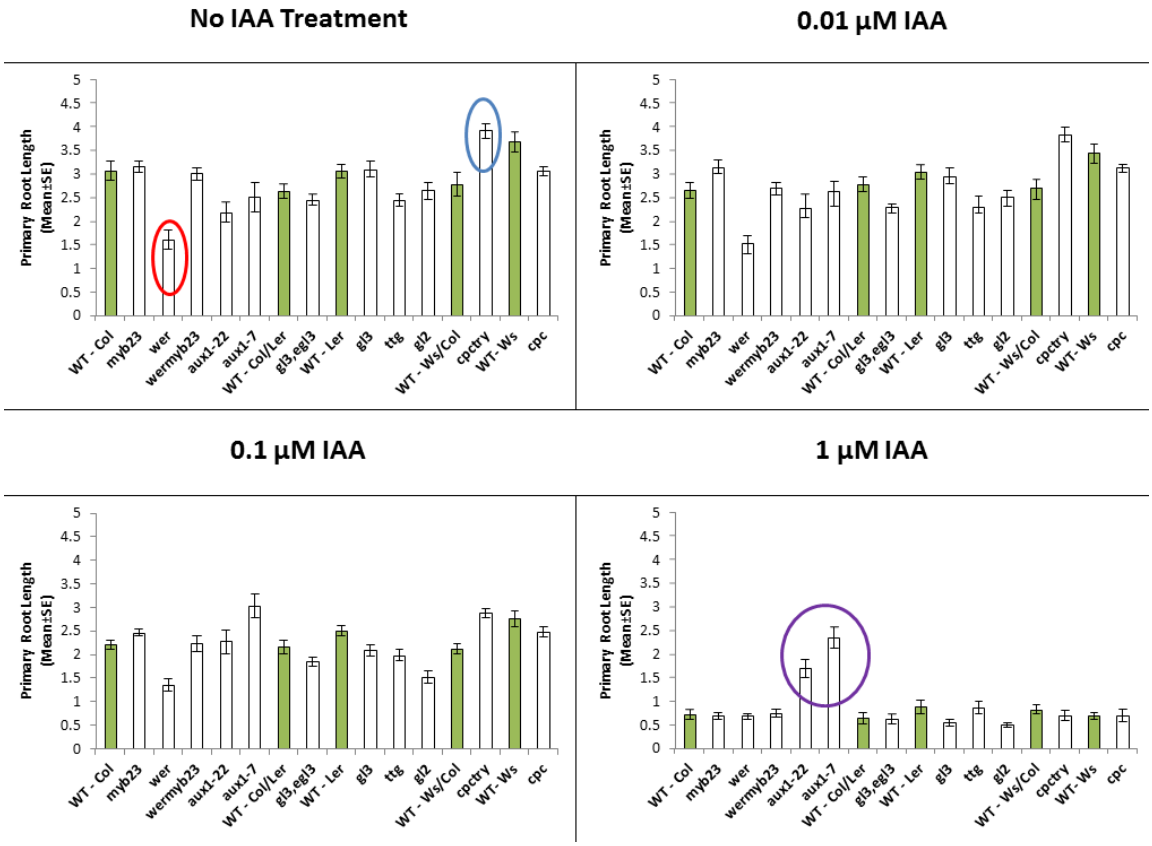

Figure 9-4: Primary root length analysis of epidermal patterning mutants when treated with auxin.

High concentrations of exogenous auxin result in shorter primary roots. Each mutant is positioned alongside its associated *Arabidopsis* wild-type line on the left hand side. Wild-type lines are coloured green, whilst mutants are coloured white. Particularly interesting results are circled. The red circle indicates that the *wer-1* mutant has a short root length phenotype without any auxin treatment, possibly indicating an increased sensitivity to auxin. Conversely the *cpc-1 try-82* mutant, circled in blue has a much longer primary root that it's associated wild-type. The *aux1-22* and *aux1-7* mutants primary root does not shorten as much as the wild-type when treated with exogenous auxin, purple circle. This is not particularly surprising as the loss of AUX1 would mean that the IAA was not readily transported into the cells.

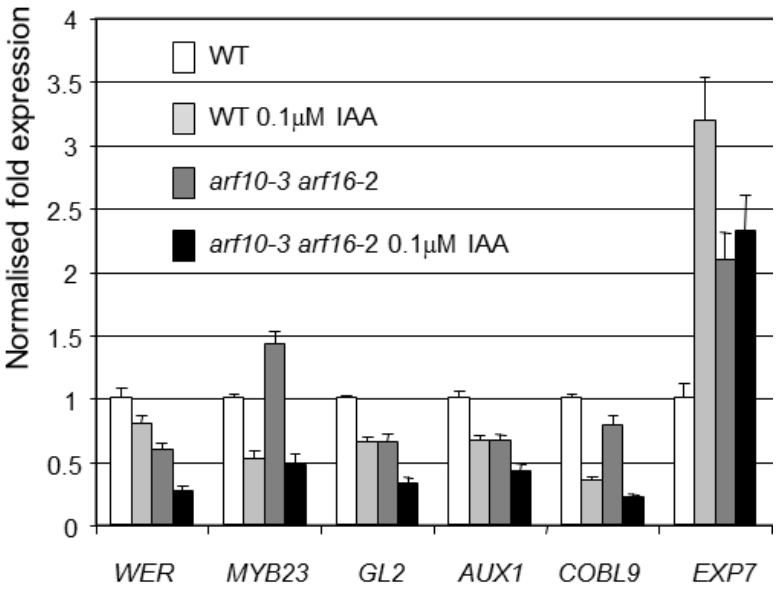

Figure 9-5: RT-qPCR analysis.

RT-qPCR analysis carried out by Dr Martin Kieffer confirmed that *WER* and *GL2* expression levels were significantly reduced in the *arf10-3 arf16-2* double mutant background. It also confirmed that both *MYB23* and *GL2* expression levels were significantly reduced upon auxin treatment. Interestingly this data also indicated that *MYB23* expression levels are significantly increased in an *arf10-3 arf16-2* mutant background, a result that is consistent with *ARF10* and *ARF16* repressing *MYB23* expression. Importantly this data also confirmed that *EXP7* is significantly up-regulated with auxin treatment whilst *COBL9* is significantly down-regulated by auxin.

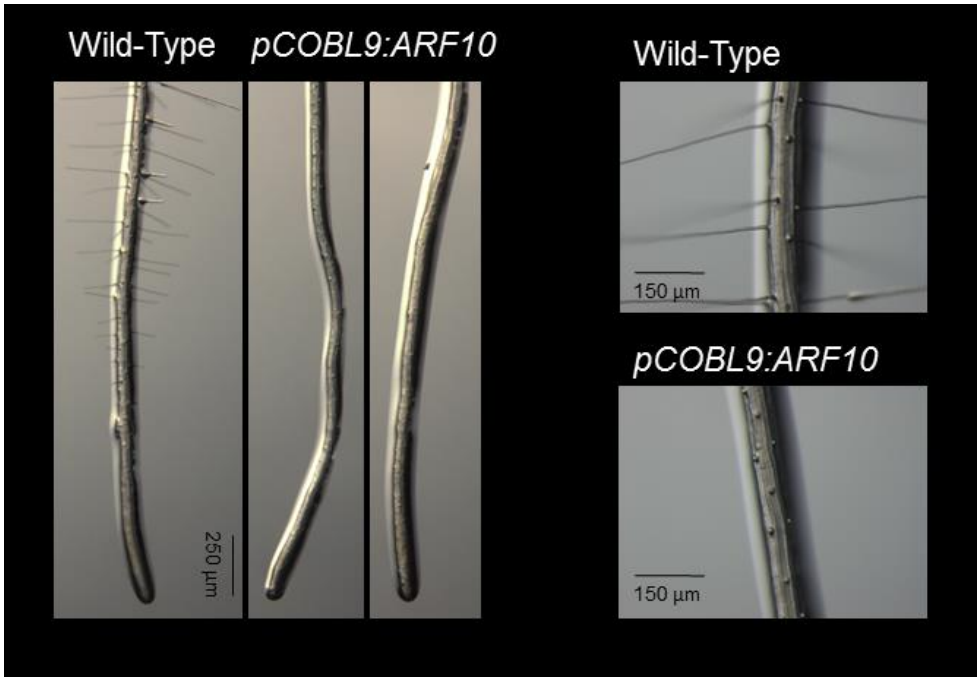

Figure 9-6: Analysis of root hairs in the *pCOBL9::ARF10 construct.*

Expressing *ARF10* ectopically in the hair cells using the *pCOBL9* promoter results in a loss of root hair elongation. Root hair initiation bumps are still apparent.

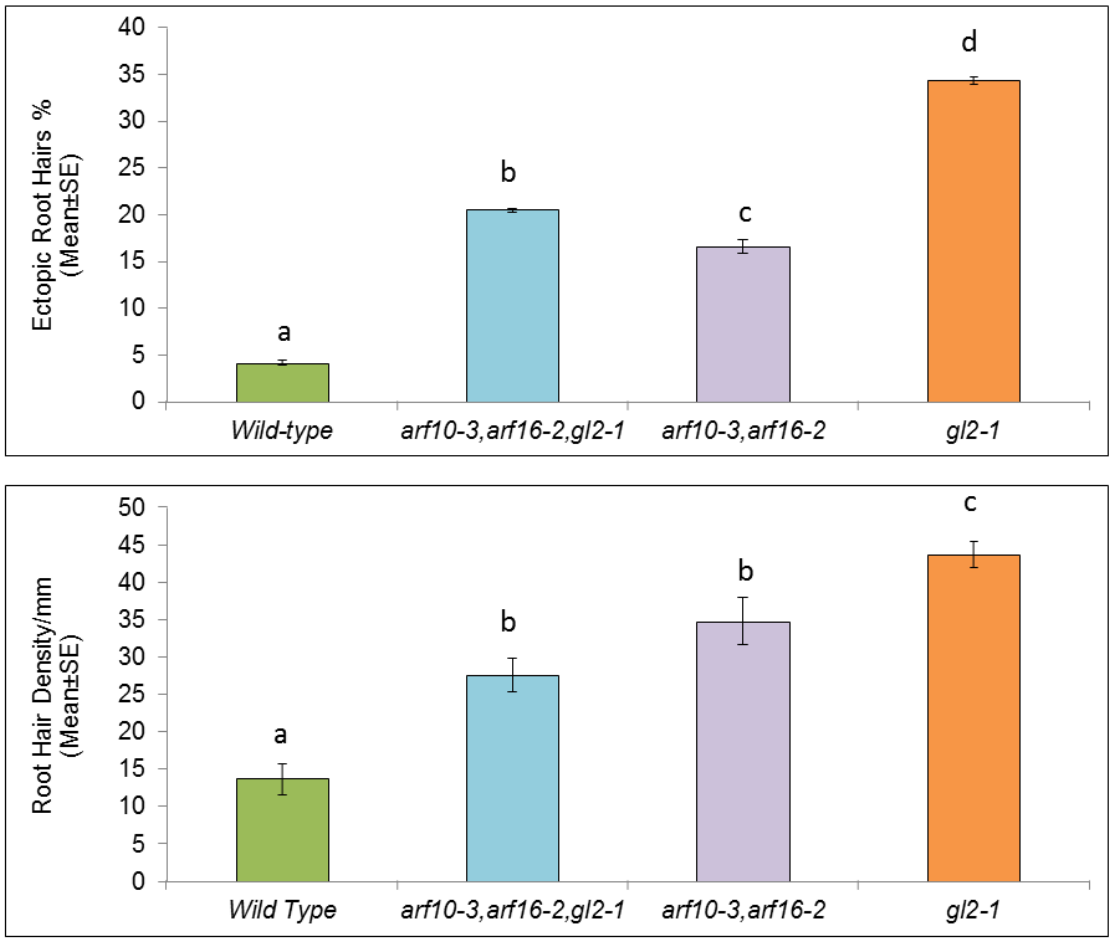

Figure 9-7: Analysis of root hair density and ectopic root hairs in the *arf10-2,arf16-2,gl2-1* mutant in comparison to the wild-type and single mutants.

A: The *arf10-3 arf16-2 gl2-1*, *arf10-3 arf16-2* and *gl2-1* mutants all have significantly more (ANOVA, P<0.005) ectopic root hairs than the wild-type. B: The *arf10-3 arf16-2 gl2-1*, *arf10-3 arf16-2* and *gl2-1* mutants all have a significantly higher (ANOVA, P<0.005) density than the wild-type.

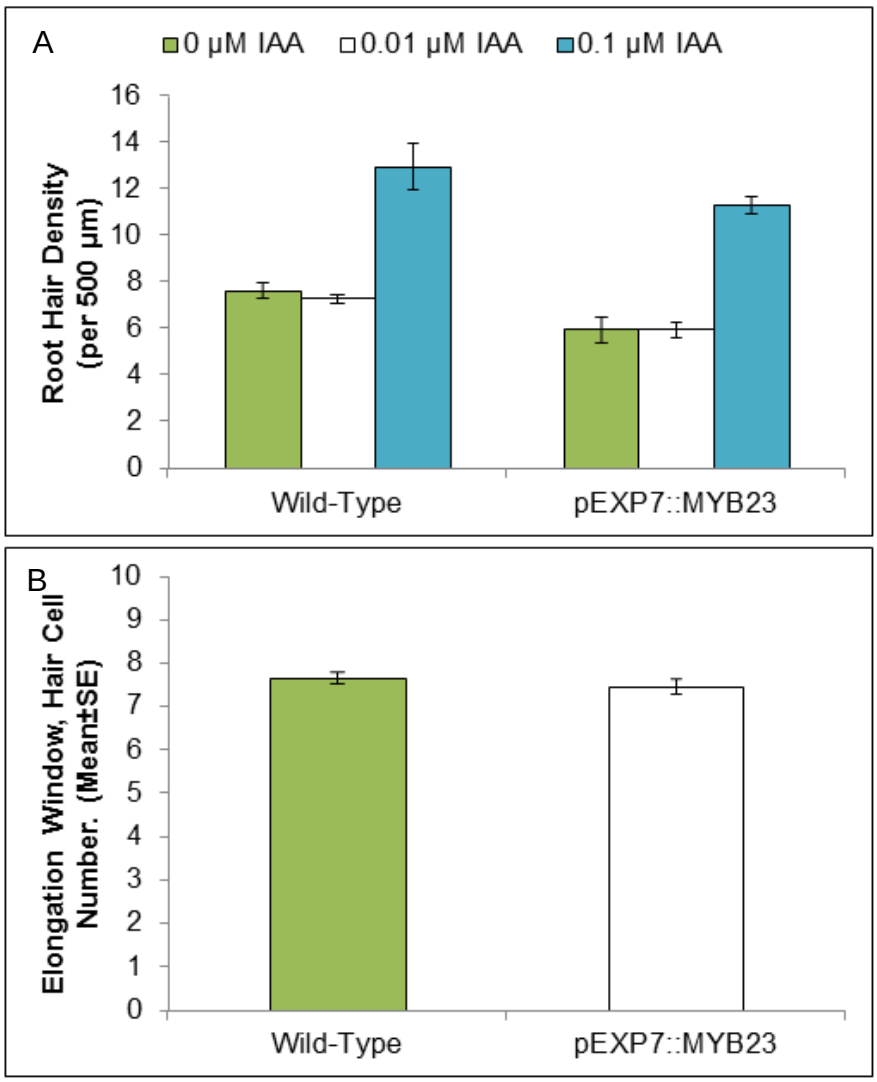

Figure 9-8: Root hair density in the *pEXP7::MYB23* construct.

A: The root hair density in the *pEXP7::MYB23* construct did not differ significantly from the wild-type, with or without auxin treatment. B: Analysis of the root hair elongation window indicated no significant difference between the *pEXP7::MYB23* line and the wild-type.

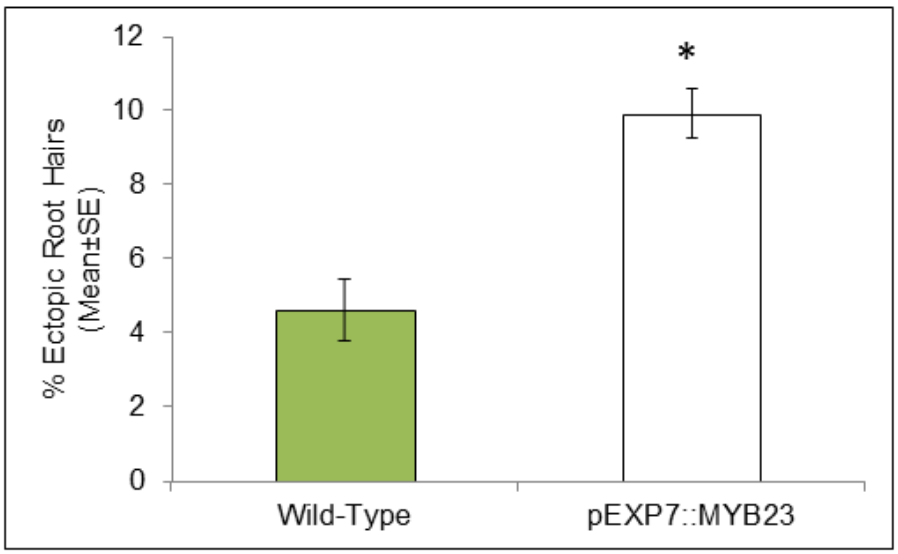

Figure 9-9: Ectopic root hairs in the *pEXP7::MYB23* construct.

The *pEXP7::MYB23* construct has a small but significant increase in ectopic root hair production in comparison to the wild-type. (T-Test, P<0.005).

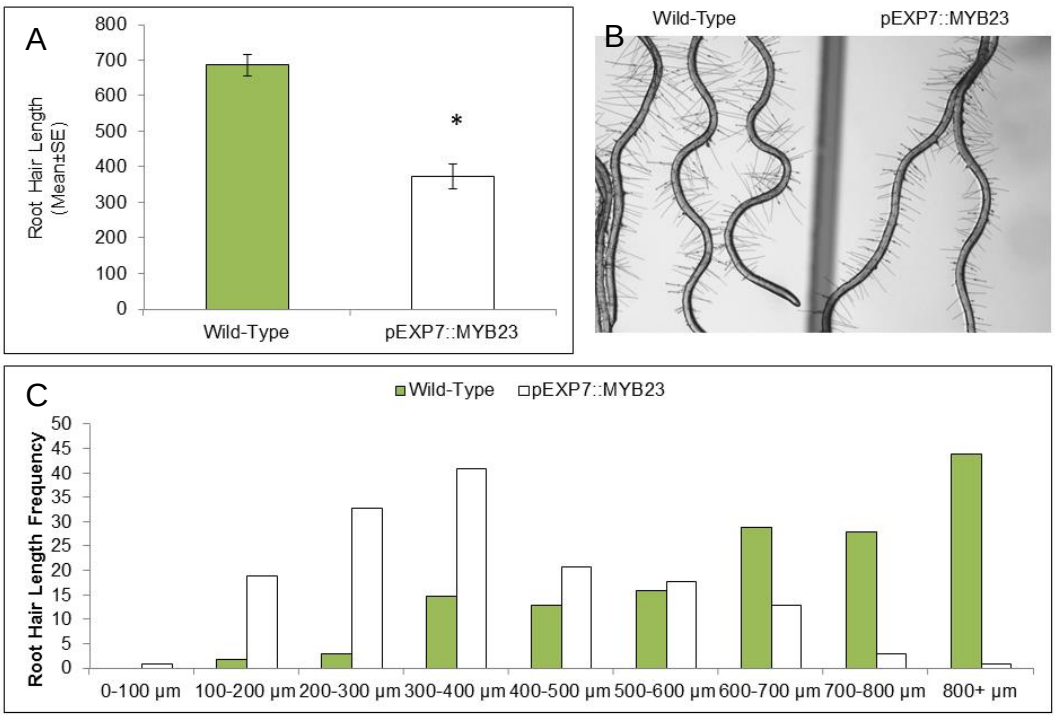

Figure 9-10: Root hair length frequencies in the *pEXP7::MYB23* construct.

A/B Root hairs in the *pEXP7::MYB23* line were able to elongate to reasonably long lengths under differing environmental conditions, i.e temperature/humidity etc, however they were always significantly shorter (T-TEST, $P<0.005$) than the wild-type. C: Analysis of the root hair length frequency profile indicated that the *pEXP7::MYB23* line had an overall population of shorter root hairs in comparison to the wild-type, rather than some very short individuals bringing the average length down.

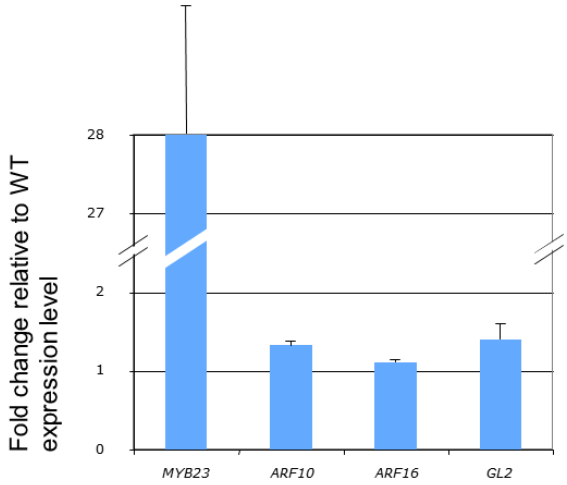

QPCR analysis based on three biological replicates normalised against *GAPDH*.

Figure 9-11: Changes in expression level of putative *MYB23* target genes in *pEXP7::MYB23* plants.